SYNTHESIS AND CHARACTERIZATION OF NOVEL GROUP 13 TRIDECAMERIC INORGANIC NANOCLUSTERS

by

JASON TREVOR GATLIN

A DISSERTATION

Presented to the Department of Chemistry
and the Graduate School of the University of Oregon
in partial fulfillment of the requirements
for the degree of
Doctor of Philosophy

December 2007

"Synthesis and Characterization of Novel Group 13 Tridecameric Inorganic Nanoclusters," a dissertation prepared by Jason Trevor Gatlin in partial fulfillment of the requirements for the Doctor of Philosophy degree in the Department of Chemistry. This dissertation has been approved and accepted by:

Prof. Dr. Michael M. Haley, Chair of the Examining Committee

12/3/2007
Date

Committee in Charge: Prof. Dr. Michael M. Haley, Chair
Prof. Dr. Darren W. Johnson
Prof. Dr. Kenneth M. Doxsee
Prof. Dr. J. Andrew Berglund
Prof. Dr. Scott D. Bridgham

Accepted by:

Dean of the Graduate School

An Abstract of the Dissertation of

Jason Trevor Gatlin for the degree of Doctor of Philosophy

in the Department of Chemistry to be taken December 2007

Title: SYNTHESIS AND CHARACTERIZATION OF NOVEL GROUP 13 TRIDECAMERIC INORGANIC NANOCLUSTERS.

Approved: _____
Prof. Dr. Darren W. Johnson

Tridecameric inorganic hydroxo/aquo nanoclusters comprise a very small fraction of compounds under the large and varied umbrella of inorganic clusters. The Anderson-Evans cluster is a subset of these larger polymetallic tridecameric clusters. A novel synthesis of M_{13} nanoclusters containing the Anderson-Evans cluster as cores has been discovered. This synthesis proceeds with the aid of a key organic reagent, which reacts with the nitrate counter anions of the starting material removing them from the solution. This forces the formation of a higher nuclearity species. Research continues to focus on the generality of the reaction as it applies to both inorganic and organic synthesis, as well as on extensive characterization of the novel clusters by a variety of analytical methods. These nanoclusters have proven to be useful as single-source precursors for the preparation of thin film oxides due to their high purity and crystallinity.

Chapter I is a literature review of Anderson-Evans clusters in the context of how they comprise the core substructure in the reported tridecameric nanoclusters. Attention is also given to the numerous clusters or complexes that are absent from this series. Chapter II chronicles the discovery and synthesis of $[Ga_{13}(\mu_3\text{-}OH)_6(\mu_2\text{-}OH)_{18}(H_2O)_{24}](NO_3)_{15}$, a nanocluster previously thought to be unstable. Chapter III describes the modification of the reaction to prepare other tridecameric inorganic nanoclusters with increases in yield and purity. Chapter IV reports the isolation of a series of new heterometallic tridecameric nanoclusters and a potential predictive strategy for tuning the metal ratios in the crystalline products. Chapter IV also highlights the application of the nanoclusters as precursors to thin film oxides. Initial characterization of tridecameric inorganic nanoclusters using powder and single crystal XRD, NMR, ToF-SIMS, EPMA and SEM instrumentation is explained in Chapter V. Finally, Chapter VI is a summary and a report of the current standing of a different project aimed at developing a template-assisted self-assembly of organic nanocages using two different ligand classes that were explored.

This dissertation includes previously published and co-authored material.

CURRICULUM VITAE

NAME OF AUTHOR: Jason Trevor Gatlin

PLACE OF BIRTH: Lexington, KY

DATE OF BIRTH: December 21st, 1976

GRADUATE AND UNDERGRADUATE SCHOOLS ATTENDED:

University of Oregon, Eugene OR
Colby College, Waterville ME

DEGREES AWARDED:

Doctor of Philosophy, 2007, University of Oregon
Master of Science, 2003, University of Oregon
Bachelor of Arts, 2000 Chemisty-Biochemisty, Colby College

AREAS OF SPECIAL INTEREST:

Supramolecular Chemistry
Single Crystal XRD
Organic synthesis

PROFESSIONAL EXPERIENCE:

Ph.D. Summer Intern, Invitrogen. June 2007 – September 2007

Graduate Research Assistant, University of Oregon, July 2002 – December 2007

Research Assistant – Encoding Specialist, Harvard Institute of Chemistry and Cell Biology, June 2000 – June 2002

Research Assistant – Summer Intern, Harvard Institute of Chemistry and Cell Biology, May 1999 – August 1999

Undergraduate Research Assistant, Colby College, February 1999 – May 2000

Research Intern, Biogen Inc., January 1999

PUBLICATIONS:

Gatlin, J. T.; Mensinger, Z. L.; Zakharov, L. N.; MacInnes, D.; Johnson, D. W. "Facile Synthesis of $Aluminum_{13}$ Keggin-like Nanocluster." I*norg. Chem. manuscript accepted.*

Rather, E.; Gatlin, J. T.; Nixon, P. G.; Tsukamoto, T.; Kravtsov, V.; Johnson, D. W. "A Simple Organic Reaction Mediates the Crystallization of the Inorganic Nanocluster $[Ga_{13}(\mu_3\text{-}OH)_6(\mu_2\text{-}OH)_{18}(H_2O)_{24}](NO_3)_{15}$." *J. Am. Chem. Soc.* **2005**, *127*, 3242.

ACKNOWLEDGMENTS

Support from the ARL-ONAMI Nanoarchitectures for Enhanced Performance Center and the University of Oregon is gratefully acknowledged. The purchase of the X-ray diffractometer was made possible by a grant from the National Science Foundation (CHE-0234965). I am grateful to my committee for their continued support and helpful discussions. I am grateful to my advisor – Prof. Dr. Darren W. Johnson – for his support and the freedom to explore new chemistry. I am grateful to my reviews: Julie Larios, Melanie A. Pitt, and Dr. Nathan Lien. I am grateful to my lab mates for their help throught this research. I am very grateful to my parents, Larry and Carol Gatlin, for this support and belief. Most of all I am extremely grateful for all the support and patience from my wife Mary C. Gatlin.

To Mary C. Gatlin and Jackson T. Gatlin

TABLE OF CONTENTS

LIST OF FIGURES

Figure Page

LIST OF SCHEMES

LIST OF TABLES

LIST OF GRAPHS

CHAPTER I

ANDERSON AND ANDERSON-CORED TRIDECAMERIC INORGANIC NANOCLUSTERS

Section 1 Background

Polyoxometalate, hydroxyl/aqua bridged clusters and their variations have been known for quite some time.[1, 2] There are a wide range of reported polyoxometalate clusters as well as many reviews covering them.[3-16] The spectrum of clusters ranges from the Anderson-Evans cluster, which consists of small repeating units of the brucite lattice, to much larger 100+ metal discrete clusters.[17-22] This review will focus on the small metal clusters that are based upon the Anderson-Evans, Wells-Dawson, Keggin and tridecameric clusters. Background on Wells-Dawson clusters, Keggin clusters and their dimers will be presented. A focus on Anderson-Evans clusters will follow. Emphasis will be placed on how each of these clusters relates to the tridecameric cluster, with special attention given to the Anderson-Evans core. The polyhedron cartoons of these clusters are shown (**Figure 1.01**), where the vertices are bridging atoms and the metal center is in the middle of the each solid polyhedron.

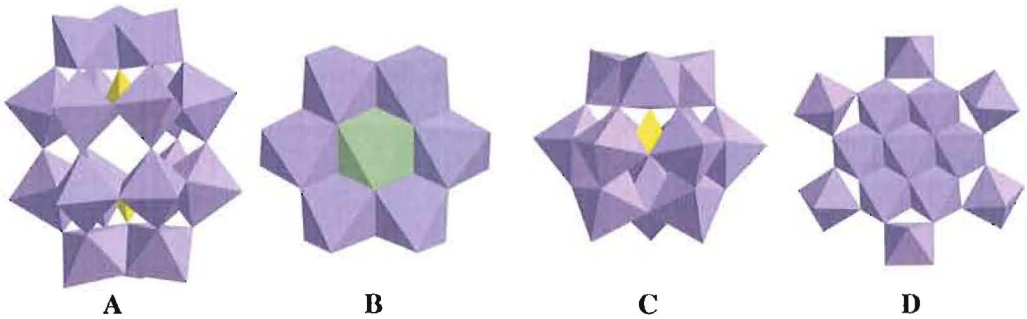

A **Wells-Dawson** | **B** **Anderson-Evans** | **C** **α Keggin (M_{13}^{t})** | **D** **"Flat"-M_{13} (M_{13}^{o})**

Figure 1.01. Survey of Inorganic Clusters. A. Wells-Dawson ($M_{18}M'_2$), B. Anderson-Evans (M_7), C. Keggin (M_{13}^{t}), and D. Flat M_{13}^{o}.

The Wells-Dawson cluster (**Figure 1.01A**) is an M_{18} cluster that consists of eighteen octahedral metals encapsulating two tetrahedral atoms, that may not always be transition metals. Twelve metal centers form a "belt" made up of two rings of six that stack over each other to form a mirror plane along the equator of the molecule with an empty central space much like the ring of six from Anderson-Evans cluster (**Figure 1.01B**). Half of the belt is made up of a $M_6(\mu_2\text{-}O)_6$ ring that is isostructural to the first ring of the Anderson-Evans structure (**Figure 1.01B**). In addition, the cluster contains three metal centers at each end that comprise a trimeric cap. This trimer is very similar to one of the faces of a Keggin cluster.

Anderson-Evans clusters contain an inorganic M_7 core that has a hexagonal close packing arrangement. The core position can be substituted with a variety of transition metals or non-transition metals such as the main group, alkaline earth, lanthanide or actinide metals.[5] Both the first reported Anderson cluster as a Mo_7O_{24} cluster, with its most-studied derivative bearing central iodine substitution (IMo_6O_{24}), have been studied extensively.[2, 23] Anderson-Evans clusters make up a large percentage of known inorganic

clusters while the tridecameric congers are rare in relation and can be considered as a subset of the Anderson-Evans cluster family.

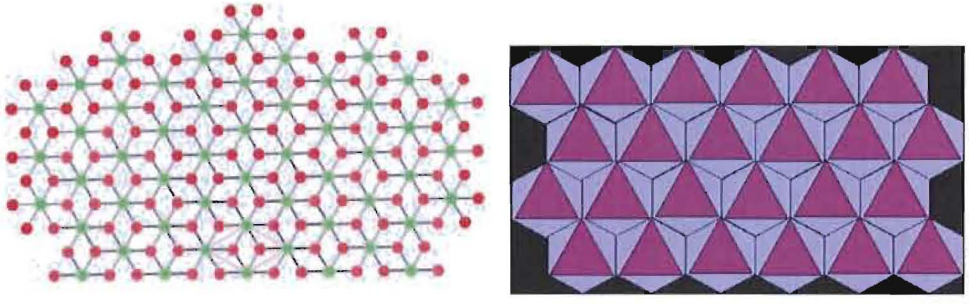

Figure 1.02. Ball and stick and polyhedron view of Brucite lattice of the same array.[24]

The brucite lattice could be described as a series of hexagonal close packed metal clusters that form a planar lattice of edge-sharing octahedra with the six perpheral metal centers of the cluster. That is, it is a series of interlocking Anderson core clusters that are offset when a peripheral metal center becomes the central metal of an adjacent cluster of seven metal ions. A Mn_{19} cluster reported by Pohl et al. contains a similar connectivity (**Figure 1.09D**) compared to a Fe_{19} cluster reported by Heath and coworkers which is more "layered" (**Figure 1.09C**).[25, 26] Counter-anions act as bridges between the planes of the brucite lattice.[27, 28]

Keggin clusters contain four trimers of octahedral metal centers arranged around a central tetrahedral metal center core.[1, 29] The tetrahedral metal center of the Keggin clusters can be a variety of metals as well.[3, 4, 30] There are five different isomers of the Keggin cluster, α through ε (**Figure 1.03**). The difference between the Keggin isomers is

in their successive rotations, 60° for each trimer surrounding the central metal (α^{31}, β^{32}, γ^{33}, δ^{34}, ε^{35}).[3, 36] The rotations changes the orientation of the timers from vertex-sharing to edge-sharing octahedra. There are different notations for different tridecameric clusters to differentiate the central metal coordination. The notation for a Keggin cluster is M_{13}^{t}, while Anderson-Evans-like expanded tridecameric flat clusters are denoted M_{13}^{o}, where *o* and *t* refer to the coordination geometry of the central metal, octahedral or tetrahedral. Keggin clusters are also seen as units of larger clusters (**Figure 1.04**).[3] Two M_{13}^{t} Keggin clusters appear to dimerize with an M_4 bridge of octahedral metals between the two units to yield a M_{30} cluster.[3] Similar "trimers" are also formed where the clusters share a face of three octahedral metals.[36, 37]

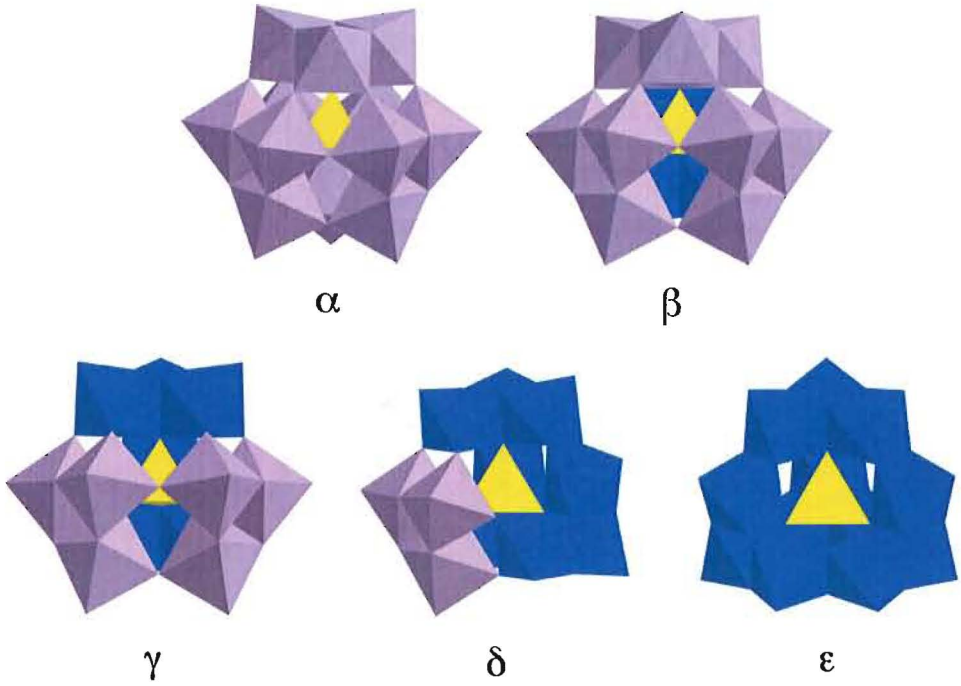

Figure 1.03. Rotations of the M_{13}^{t} Keggin cluster [3] to produce the α to ε isomers.

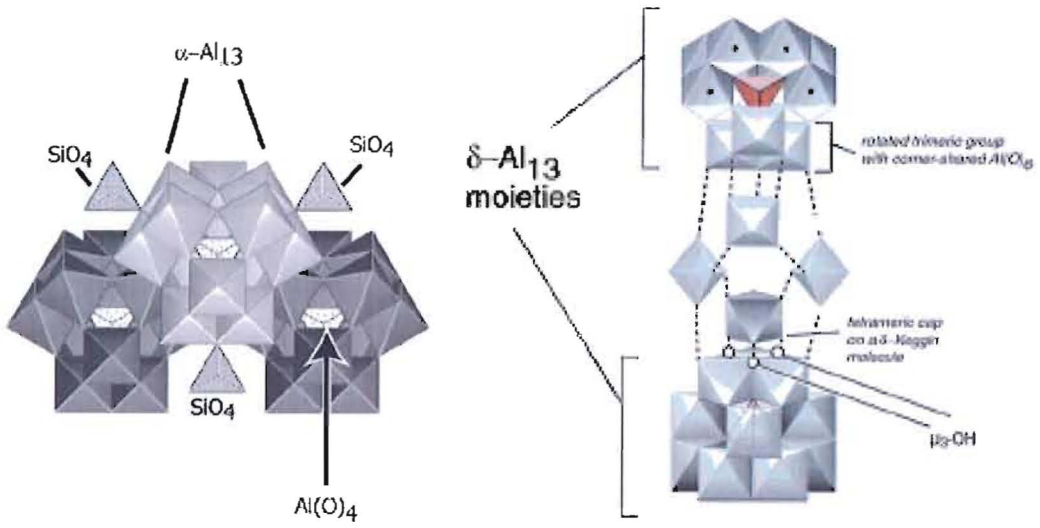

Figure 1.04 Keggin M_{30} and other "aggregates"[3, 36]

There is also a class of clusters that falls between the Keggin and Anderson-Evans type clusters, the M_{13}^{o} clusters. Anderson-Evans structures are only a two-dimensional array of metal sheets that are bridged in the same manner as the small repeating unit of the brucite lattice. This larger class shares the same core of seven octahedral metal centers arranged in a hexagonal close packed array. The M_{13}^{o} cluster contains an Anderson-Evans-type planar $M_1(\mu_3\text{-OH})_6M_6(\mu_2\text{-OH})_6$ core fragment that forms a central plane.[38] Six $M(H_2O)_4$ groups are connected to this core *via* two alkoxo (μ_2-OH) bridges; the groups alternate above and below the central plane.[39-41] The Anderson-type core of the flat M_{13}^{o} clusters contains octahedral metals arranged in planar sheets, similar to the arrangement of seven concentric metal centers in a brucite lattice.

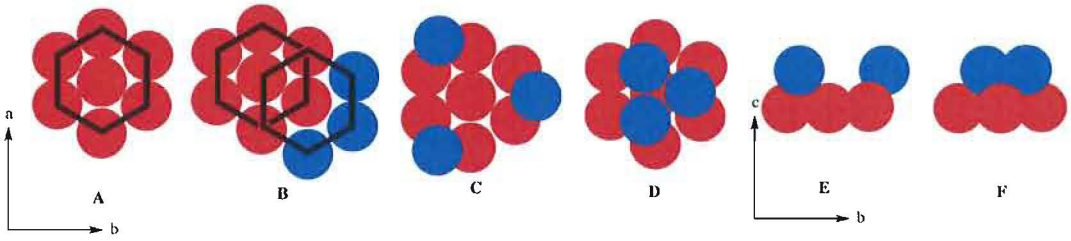

Figure 1.05. Hexagonal close packed metal centers of a brucite lattice

These new types of clusters have been called "flat" -M_{13}, clusters, to distinguish them from the more spherical M_{13}^{t} Keggin clusters. The term "flat" is somewhat misleading, because these clusters are not flat like the Anderson-Evans core and brucite lattices; instead, they have outer metal centers that lie above and below the central planar core of seven metals. However, these flat clusters are not Keggin or "Keggin-like", as they lack a central tetrahedral metal ion. Furthermore, Keggin clusters are more spherical than planar, with a diameter of 5.5Å. The flat M_{13}^{o} clusters themselves are more disc-like with a diameter of 12Å and a cylindrical height of about 8Å. As the Anderson-Evans cluster continues to grow*, new metal centers are not added in the plane, producing more concentric rings or growing in the *a* or *b* directions.[43] While the M_{13}^{o} cluster has more metals that are not in the same plane as the core, they grow off in the *c* direction. A hexagonal close packed array is seen from above as just an Anderson-Evans cluster **(Figure 1.05A)**. When more metals are added in the plane to expand into a brucite

* The term "grow" may be a misnomer as it implies that there is a known mechanism for cluster formation, a discrete growth pattern. The term is only used here to describe the addition of new metal centers to an existing cluster or stable fragments. There have been a few predictions on how clusters grow.42. Goodwin, J. C.; Teat, S. J.; Heath, S. L., How do clusters grow? The Synthesis and Structure of Polynuclear Hydroxide Gallium(III) Clusters. *Angew. Chem. Int. Ed.* **2004,** 43, 4037-4041. Work is continuing to determine stable fragments under mass spectrometry conditions in order to extrapolate back to nucleation sites, (Chapter V).

lattice, an original metal is now the center of the new adjacent unit (**Figure 1.05B**). Instead if the three new metals are added above the plane of the original seven, they can either be packed tightly in the center or offset to the outside. The same cluster is shown from both the top and the side to show stacking (**Figure 1.05C** & **E**).

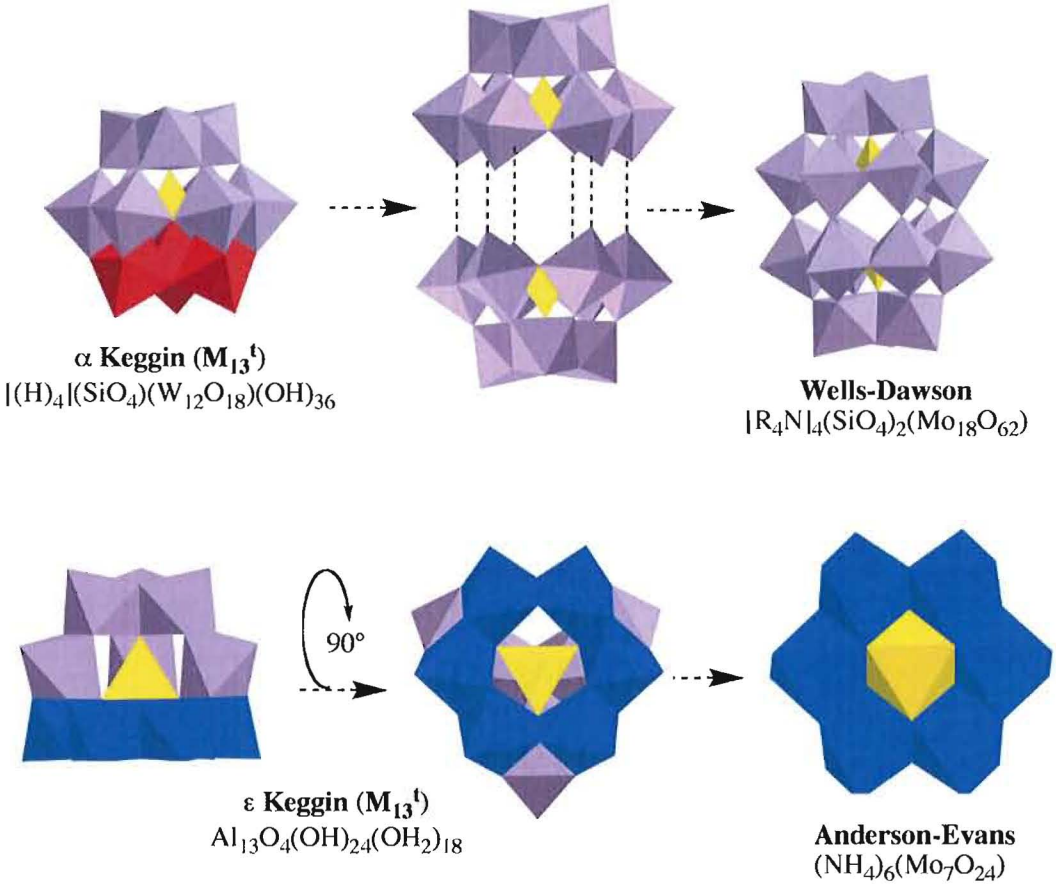

Figure 1.06. Interconversion of Keggin clusters to yield Wells-Dawson and Anderson clsters.

When the Anderson-Evans core begins to grow* in the *c* direction, the clusters stop at 13, 15 or 19 metal centers. Smaller all-octahedral metal clusters that look like the Anderson core precursor have been synthesized.[44] The vast majority of these clusters

contain Group 13 metals. The Anderson core that is contained in the M_{13}^{o}, M_{15}^{o} and M_{19}^{o} clusters are homometallic while the Anderson-Evans cluster often contains substitutions at the central metal. There have been several reported single substitutions of the central position.[5, 24] New additions to the variation of the central metal and an improved synthesis of these cores (personal communication) have recently been discovered. Metals of smaller radii are seen quite often in these hexagonal close packed arrays using oxo bridges while larger radii metals are almost exclusively seen in a bridging fashion between complexes where they are not as sterically confined.[27, 45, 46] The larger radii metals are also seen using acetate bridges. The difference in ionic radii may play an important factor in cluster stability, which depends on both the charge of the metal and the high/ low spin of electron configuration.[47, 48] It must be noted that data from the ionic radii on group 13 metals and their bond distances in metal clusters is missing in the Orpen paper.[47]

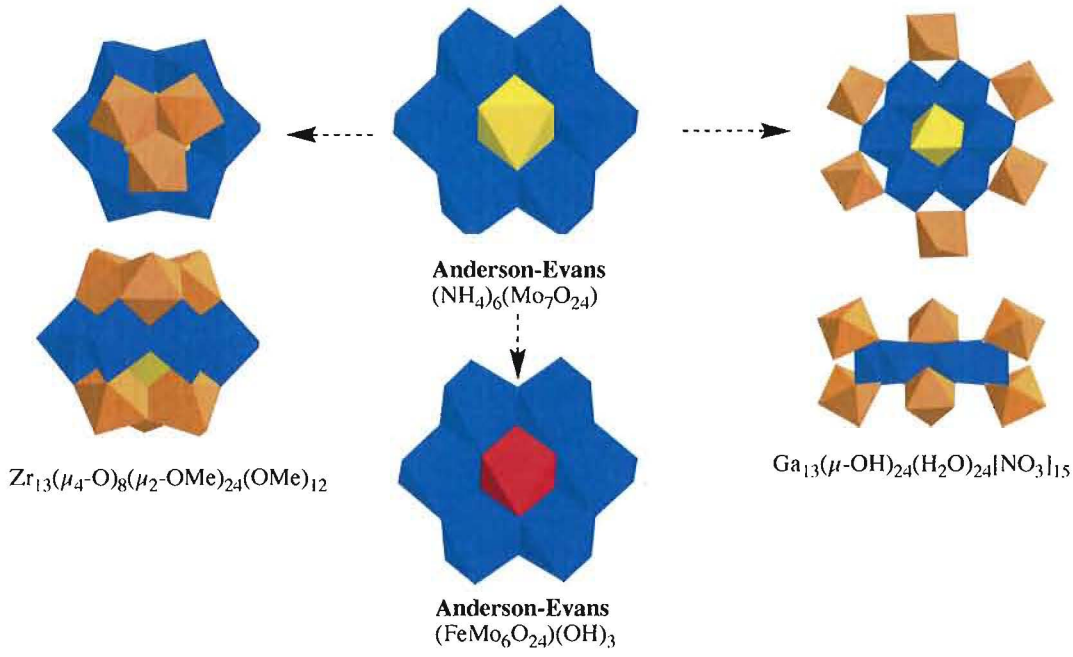

Figure 1.07. Anderson Core as a critical substructure for M_{13} clusters.

The Lorenzo-Luis review of Anderson-Evans clusters is slightly dated and needs some updating. It does not mention larger inorganic clusters, while Casey's review describes briefly the flat M_{13}^{o} cluster.[3, 5] These reviews do not describe how some clusters are fragments of larger clusters; for example, the Anderson-Evans cluster is a fragment of the "flat" M_{13}^{o} cluster. The following sections describe how the Anderson-Evans cluster is a component of the larger M_{13}^{o} metal clusters and show relevant structural data.

Section 2 Searches and Criteria

There are two main databases to search for inorganic compounds, the Cambridge Structure Database (CSD) and the Inorganic Chemical Database (ICD).[49] The structures found in the ICD are purely inorganic, while entries into the CSD database must have at

least one carbon atom per unit cell. Therefore, it is ironic that something as small as a disordered methanol in an inorganic cluster would allow for submission into the organic CSD.

The CSD allows for the drawing of desired components and substructures, while the ICD is text driven with a choice of elements, but not their arrangement in space nor connectivity to each other. The results from the two databases are not easily compared because the search criteria are so different. Hits from data are not always accurate for searches being conducted. However, there is a way to combine multiple searches using Boolean operators to allow for better searching of the ICD.

Searches were done with the CSD using stick compounds where "4M" represents any metal and O is any oxygen-containing bridging group (**Figure 1.08**). This ambiguity of the oxygen allows for the bridging ligand to be oxide, hydroxide or an oxo from an alkoxy group (O can be OH, OH_2, or OR). The same goes for the acetate bridge where it can be any R group from formic acid on up. The search does not state that the bridging motifs are not connected to each other; this allows for multidentate ligands to be included in the results. The search can also be restricted to transition metals. The 4M was purposely used in order to allow for the greatest potential of metal variety, including the alkali earth metals. Some clusters require organic stabilizing ligands as an external shell. Some are inorganic clusters, which only need organic additives to from (in some cases) in the solid state. The CSD searches yield only limited connectivity allowing for large variation in the types of structures found. The inclusion of OR and RCOO in the search

criteria yielded too many results, therefore constraints were added for geometry and rigidity of larger polymetallic clusters.

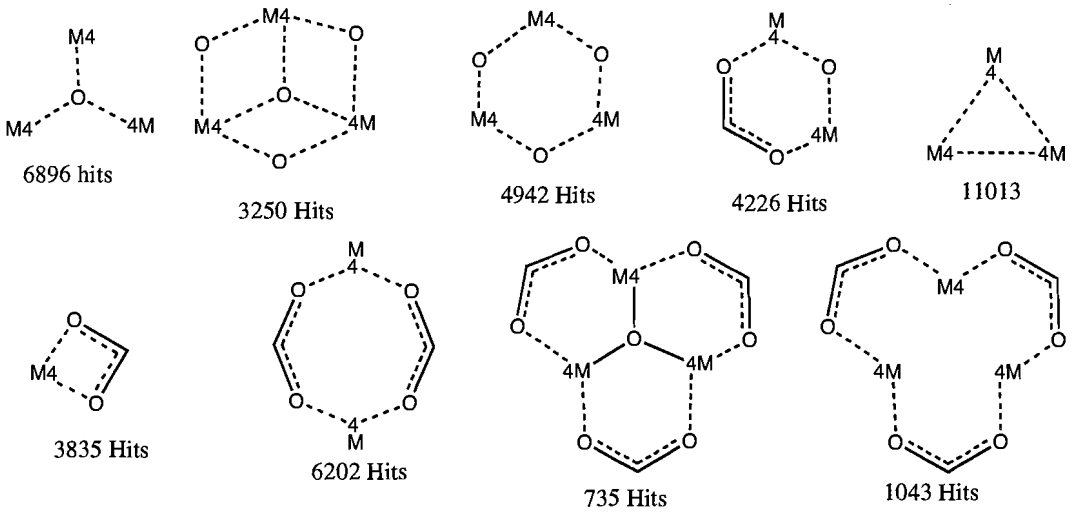

Figure 1.08. Search criteria for various metal-oxo bindings from the CSD.

Multiple searches were performed with the CSD that had varying degrees of rigidity. Each search contained a fragment of the tridecameric cluster; each successive search increased the rigidity. The first was the M_6 fragment, while subsequent searches were contained as subsets of previous searches. It was extremely difficult to perform the same search in the ICD. Specific elements and their stoichiometry could be chosen but no connectivity or structural data could be selected. When searching for any metal, the number of metals in a cluster could not be chosen. The ICD proved to be useful only if the exact composition or unit cell parameters are known. Specific clusters could be found, but a general search for a topology was difficult. The user interface is more text driven in nature than GUI as in the CSD. Screening hits was also more difficult because the data was tabular; to visualize the structure, a second program had to be launched for

each view. Previous queries made in the ICD could not be modified for future searches by utilizing the back function. A new query needed to be built each time, which increases the possibility of user input error from search to search. What took thirteen searches with the ICD could be done in one search with the CSD, where M = Mo, Ni, Mn, Ga, Al, In, Fe, W, Te, Cu, Co, Cr, which would allow it to fall under the CSD designation 4M. The ICD does allow for metal counts to be include but only with individual metals not with a wild card for all metals, therefore mixed metal clusters were not found. There were far too many hits with the first three searches, but with increased structural rigidity the specificity improved (**Figure 1.09**). Major omissions in the data were possible when looking for specific compositions.

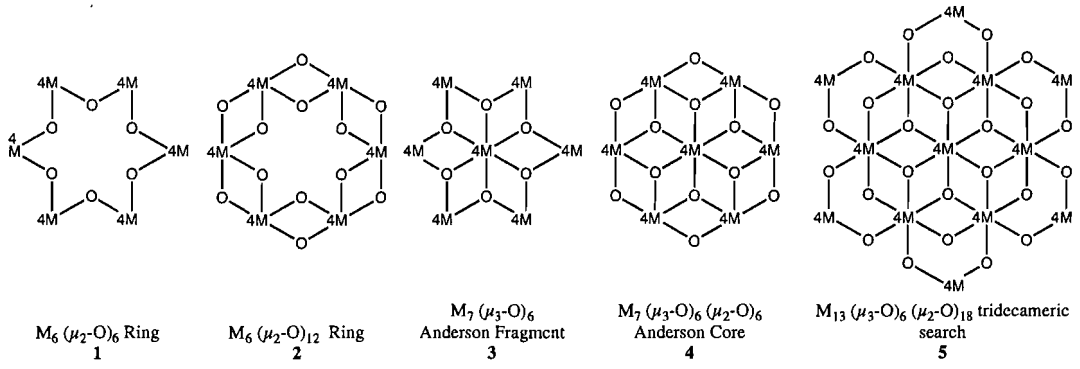

Figure 1.09. Substructures searched on the CSD.

For this review a ligand is bound to at least one metal of the cluster while an additive is co-crystallized out with the metallic cluster. The ligands found in the CSD search are shown in **Figure 1.10**. A summary of the hits from search 3 that are not in Search 5 of the M_{13} clusters are shown in **Table 1.1**.

Table 1.1. All hits from the $M_7(\mu_3\text{-}O)_6$ ring that are not in $M_{13}{}^{o}$ search

CCDC Ref.	Central Metal	First ring	Second Ring/Bridges	Ligand	Additive	Reference
AGICUO	Zn	Mo		L[9]		Hasenknopf[50]
AGIDEZ	Ni	Mo		L[10]		Hasenknopf[50]
AQOKAS	Fe	V		L[11]		Khan[51]
AQOKAS01	Fe	V		L[11]		Khan[52]
BEDBES	Mn	Mo		L[12]		Favette[53]
BEHJUU	V	V		none		Kurata[54]
BETFIQ	Cr	Mo		none		An[55]
CASXEA	Cr	Mo		none		An[56]
CUDGEN	Co	Mo	As	None		He[57]
CUMSEI	Na	V		L[11]		Chen[58]
CUMSEI01	Na	V		L[11]		Chen[59]
DAHYUH	Mn	Mo		none		Zhange[60]
DAQNUE	CU	Mo	As	None		He[61]
DAWBAE	Cr	Cu	Nd	TFA		Cui[62]
DAWBOS	Cl	Cu	La	TFA		Cui[62]
EMUJOL	Al	Mo	Cu	none		Shivaiah[63]
ESAXUR	Li	Fe		L[13] & MeOH		Affronte[64]
ESUWOE	Cr	Mo	La	none		An[65]
HAVSAZ	As	Mo	V	none		Li[66]
HEFXUL	Cr	Mo		none		Wery[46]
HEGBUQ	Cr	Mo		none		Wery[46]
HOQHEA	Mn	Mn		L[14]		Janas[67]
HUHNED	Ni	Ni	Ni	L[15]		Ochsenbein [68]
HUHNIH	Ni	Ni	Ni	L[15]		Ochsenbein [68]
IBAXUF	Cr	Mo		none	piperazine	Kaziev[69]
INIMOH	Cr	Mo			BEDT-TTF	Ouahab[70]
IPUKEJ	Mn	Mn	Mn	L[16]		Jones[71]
IPUKEJ01	Mn	Mn	Mn	L[16]		Jones[71]
IPULUA	Mn	Mn		L[17]		Harden[72]
JAPQOH	Cr	Mo	Ce	L[18]		An[73]
JAPQUN	Cr	Mo	La	L[18]		An[73]
JAPRAU	Cr	Mo	Pr	L[18]		An[73]
JAPREY	Cr.	Mo	Nd	L[18]		An[73]
JINKAS	Ca	Ca	Ca	L[6]		Goel[74]
JOZCAC	Cd	Cd	Cd	L[6]		Boulmaaz[75]
KUPDII	V	V	As	aniline		Kahn[76]
LAHWIB	Na	V		L[11]		Shivaiah[77]
LAHWOH	Li	V		L[11]		Shivaiah[77]
MAYNEG	AI	Mo	Cu	none		Shivaiah[77]
MAYNIK	Cr	Mo	Cu	none		Shivaiah[77]
NECDUU	Li	Fe		L[13]		Abbati[78]
NEWRAI	Na	Fe		L[11]		Saalfrank[79]
NEWROW	Li	Fe		L[11]		Saalfrank[79]
NITBEX	Mn	Mn		L[16]		Bolcar[80]
NOCJEU	Na	Mn		L[13]		Abbati[81]
NOCKUL	Cr	Mo	Na	none		Golhen[82]
NOCLAS	Cr	Mo		none	ferrocene	Golhen[82]
NOCLEW	Cr	Mo		none	ferrocene	Golhen[82]

OCEZUS	Mn	In		L^{19}		Saalfrank[83]
OCIBAE	Mn	In		L^{19}		Saalfrank[83]
OCIBEI	Fe	Mn		L^{19}		Saalfrank[83]
OJEHEQ	Mn	Mo		L^{20}		Marcoux[84]
OJEHIU	Fe	Mo		L^{20}		Marcoux[84]
OJEHUG	Mn	Mo		L^{12}		Marcoux[84]
PADPOA	Cl	Cu	Sm	AcOH		Zhang[85]
PAKPAT	Mn	Mn		L^{19}		Saalfrank[86]
PAKPEX	Mn	Mn		L^{21}		Saalfrank[86]
PAKPIB	Mn	Mn		L^{21}		Saalfrank[86]
PAZVER	Mn	Mn		L^{13}		Abbati[87]
PAZVOB	Mn	Mn		L^{13}		Abbati[87]
POZRAX	Mn	Mn	Mn	L^{22}		Brechin[88]
QAYNEJ	V	V	V	none	TBAOH	Hayashi[89]
QUDBEW	Na	Ga		L^{13}		Abbati[90]
RAPDES	Cr	Mo		none		An[91]
RAPDIW	Cr	Mo	La	none		An[91]
RAQGOG	Mn	Mn		L^{19}		Koizumi[92]
RASMEE	Mn	Mo		L^{10}	BEDT-TTF	Liu[93]
RASMII	Mn	Mo		L^{10}	BEDT-TTF	Liu[93]
RASMOO	Mn	Mo		L^{20}	BEDT-TTF	Liu[93]
TUMSUP	Na	Fe		L^{13}		Caneschi[94]
TUNYIK	Mn	Mn	Mn	benzoic acid		Sun[95]
TUQJAQ	Zn	Zn		L^{17}		Tesmer[96]
TUSFOC	Fe	FE		L^{23}		Oshio[97]
UDAZUU	Al	Al	Al	L^{24}		Schmitt[98]
UDEBAG	Al	Al	Al	L^{24}		Schmitt[98]
UDEBEK	Al	Al	Al	L^{24}		Schmitt[98]
VEFQON	Na	Bi		L^{7}		Mehring[99]
WADKOC	Co	Mo		none	guanidine	Lee[100]
WATGUU	Cr	Mo	Na	L^{18}		An[101]
XALKOL	V	Mo		none		Duan[102]
XALXOY	Fe	Fe		L^{25}		Labat[103]
XEZFIR	Ni	Ni	Ni	L^{15}		Murrie[104]
XUTSIO	Mn	V		L^{11}		Khan[105]
XUTSIO01	Mn	V		L^{11}		Khan[105]
XUYRAK	Pt	W		none	guanidine	Lee[106]
YAMHAW	Cr	Mo	Ce	none	18	An[107]
YAMHEA	Cr	Mo	La	none	18	An[107]

Table 1.2. All hits from the $M_{13}(\mu_3\text{-}O)_6(\mu_2\text{-}O)_{18}$ ring
Data table from Search 5, The M_{13} Fragment

CCDC Ref.	Metal	Ligand	Reference
BETCOT	Mn	L^1	Murugesu[108]
JIDNIT	Zn	MeOH	Morosin[109]
JONWUE	Fe	L^2	Heath[110]
MEQZOX	Ta	L^3	Morgensem[111]
OFURAI	Mn	L^4	Brockman[112]
PAFKAJ	Ga	L^2	Goodwin[42]
QAVDAT	Mn	L^5	Zaleski[113]
SUZPUY	Al	L^2	Heath[39]
TAWWUK	Zr	MeOH	Day[114]
TAWWUK01	Zr	MeOH	Day[114]
TAWWUK02	Zr	MeOH	Day[114]
UCOTUB	Mn	L^6	Pohl[26]
UKUMIW	Mn	L^5	Denrinou-Samara[115]
VEFPIG	Bi	L^7	Mehring[99]
VEFQIH	Bi	L^7	Mehring[99]
WESTOD	Fe	L^2	Goodwin[25]
WESWUM	Fe	L^2	Goodwin[25]
WETCON	Fe	L^2	Goodwin[25]
WETFOQ	Fe	L^8	Goodwin[25]

The CSD data set was current as of November 2006, and validity of the data can only be confirmed through that edition. Additional data has been provided via personal communication and research done by the author and co-workers that is included in this dissertation. A question remains as to how useful the CSD and ICD can be due to the number of false positives and false negatives found, since the data found is only accurate to the parameters entered but not always accurate for what is actually needed. Each structure that is out put from the search as a hit should be evaluated carefully to confirm its accuracy to the criteria.

Section 3 Ligands and Stability

The searches outlined in section 2 yield a large variety of clusters which contain organic supporting ligands or that co-crystallize with organic additives. Smaller monodentate ligands like pyridine seem only form monometal complexes. The Ga_{13}^{o}

cluster had previously been synthesized using stabilizing aminocarboxlate ligands, such as HEIDI.[42] The only example of an unstabilized Al_{13}^{o} cluster was produced in low yields requiring both caustic conditions and long reaction times.[40] A very similar M_{15} cluster was synthesized using HDTP as s stabilizing ligand.[98] There were also a variety of multidentate ligands like HEIDI and HDTP used to stabilize metal cluster.[25, 39, 42, 50, 98, 110] This led the way for researchers to explore even larger ligands like EDTA or DTPA.

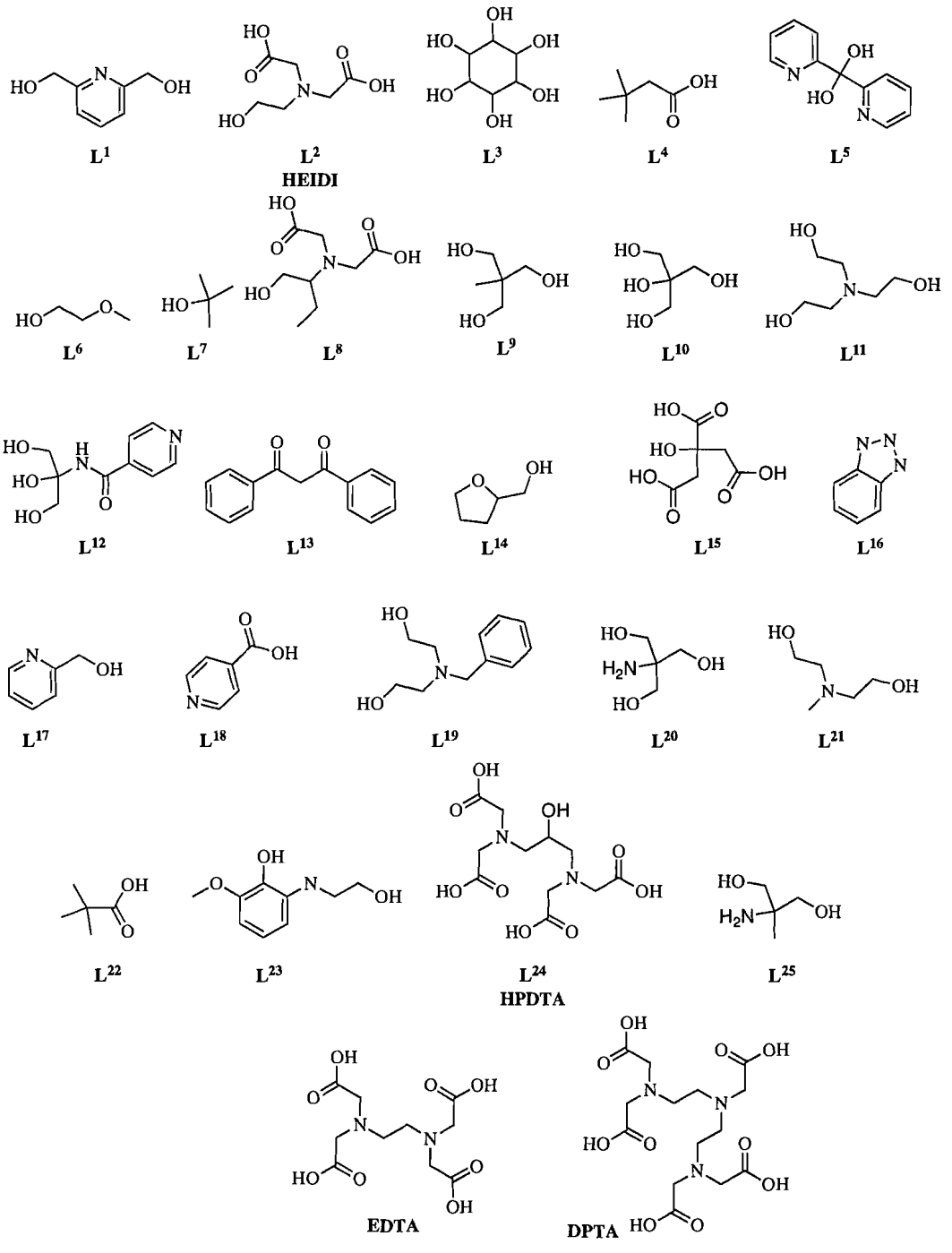

Figure 1.10. Organic binding ligands commonly found in inorganic cluster crystal structures.

The coordination chemistry of gallium is of interest because of its similar ionic radii to iron.[48] Gallium also poses an interesting target because of its use in PET scanning.[116, 117] The majority of the ligands for Ga are catechol[118-120] or aminocarboxolate derivatives.[39] Recently, an unstabilized Ga_{13} cluster was synthesized.[41] Since then, a faster and cleaner synthesis of both the Ga_{13} cluster and other M_{13} clusters has been reported in Chapters II-V.[121]

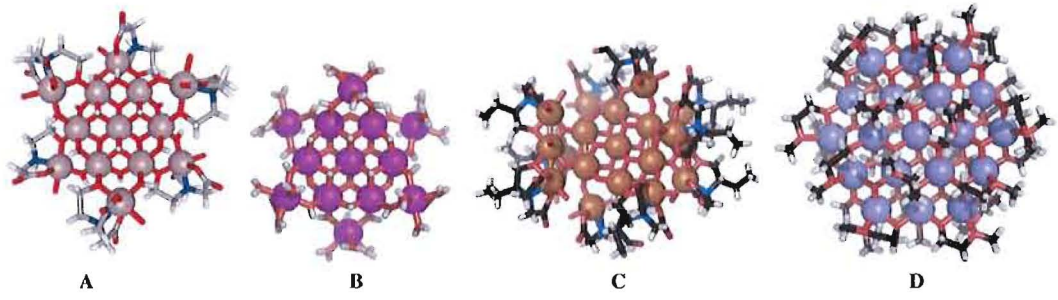

Figure 1.11. Ball and stick representations of common clusters A. HEIDI bridged M_{13}^{o}, B. unbridged M_{13}^{o}, C. HEIDI-bridged M_{19}, D. unbridged M_{19}

The actual number of discrete tridecameric clusters is much smaller than the twenty hits from the CSD. In fact, there are only about eight that count as containing the M_{13}^{o} core, a few are M_{15} or M_{19} clusters.[25, 98] These are distinct from the Pohl M_{19} cluster (**Figure 1.11D**), which is more Anderson-Evans like because of the pattern of growth from the central core.[26] The Pohl M19 cluster is filling in between the existing outer shell metals with more centers to make a continuous array of planar metals.[42]

We have synthesized a series of heterometallic M_{13}^{o} clusters. We now have the complete set of $Ga_{13-x}In_x$, where $0 \geq x \geq 6$. Two of the corresponding aluminum and indium series have been synthesized, Al_{13} and Al_8In_5. Analogous heterometallic clusters

were not observed in the results from either the CSD or the ICD. Despite the lack of substitution in the central ring, the second ring substitutions may help determine cluster growth and stability of precursor fragments in how the clusters form.[42] Elemental analysis will only tell the relative abundance of metals present. A problem with x-ray structural analysis of heterometallic clusters is their high symmetry (D_{3d}), which often leads to disorder within the heterometallic cluster. However, the ratio of metals can be determined based on occupancy factors by counting the electrons of the metals in the symmetrically equivalent positions (**Figure 1.12**).

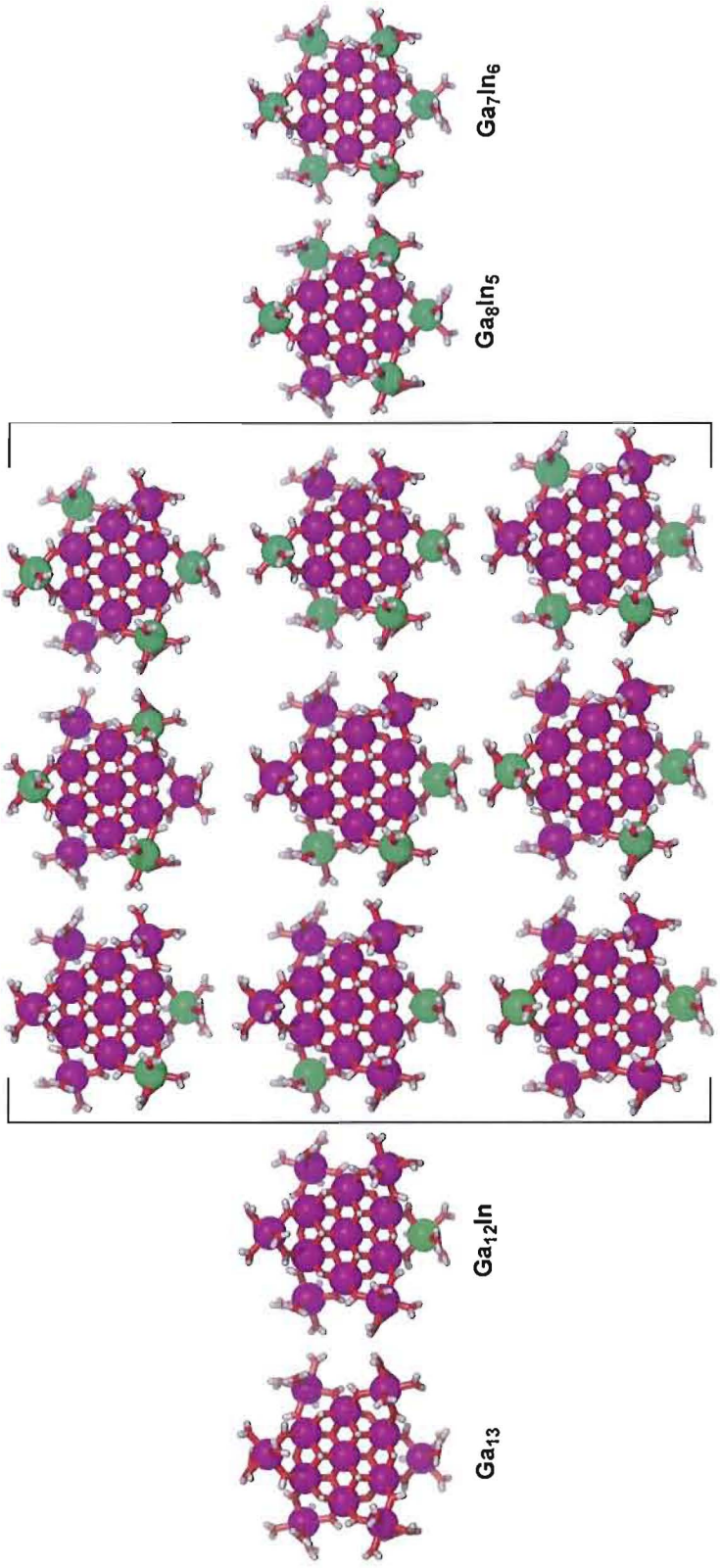

Figure 1.12. The distribution of the heterometallic series of $Ga_{13-x}In_x$ clusters.

Section 4 Results of Cluster Synthesis

Anderson-Evans clusters are quite stable, which is why the original Mo_7 Anderson cluster can easily be used as a starting material for substitution at the central position; many examples are known in which the core metal has been exchanged.[5] This review is quite old though, and there are more examples that have been discovered since its publication, in fact more than 70 new Anderson-Evans and cored clusters have been synthesized (**Table 1.1 & 1.2**) . The Mo_7 cluster now seems quite easy to alter. The stability of the Anderson-Evans cluster, as well as larger structures built off of it, may offer some insight into how these clusters form.[42]

New work has augmented the field of inorganic nanoclusters by the use of organic reagents and additives to form nanoclusters. The use of organic reagents, such as nitrosobenzene, can allow the synthesis of multiple metal (Chapter II).[41] The same clusters and new analogs have been synthesized by using DBNA, however the organic by-product has not been isolated.[121] Other additives have also been used to induce crystallization and/or to help to nucleate the cluster. Fedin's work with Cucurbit[6]uril (CB[6]) is an excellent example of organic additives serving as nucleation sites (**Figure 1.13**).[122, 123] The same additive has not always yielded the analogous cluster with different metals. Fedin used CB[6] in an attempt to make the flat Al_{13}^{o} cluster[3] but instead obtained the Al_{13}^{t} Keggin cluster.[123] It is surprising that there are no reports using the analogous additives CB[7] or CB[8] to co-crystallize similar clusters. The use of bis(ethylenedithio)tetrathiafulvalene (BEDT-TTF) as an additive has also been in the crystallization of these clusters (IBAXUF[69], INIMOH[70], NOCLAS[82], NOCLEW[82],,

RASMEE[93], RASMII[93], RASMOO[93], WADKOC[100], XUYRAK[106]).[106] However, some additives may not be entirely innocuous, in that they in fact modulate the electronics of the inorganic cluster.[124-126]

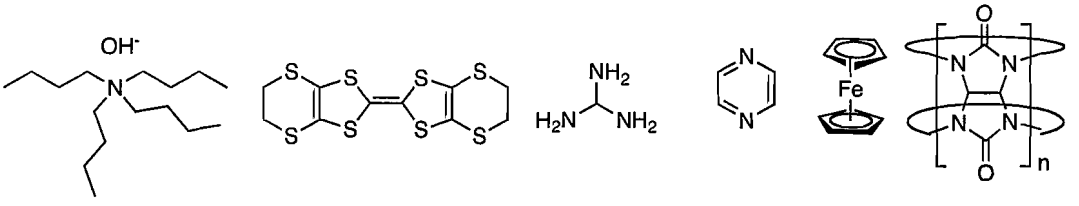

Figure 1.13. Additives that co-crystalize with metal clusters

Metals of different oxidation states can be contained in the same cluster. This is quite common for manganese.[80, 81, 87, 112, 127] These clusters have a potential use as single molecule magnets.[18, 26, 51, 62, 108, 115, 128-135] For these mixed oxidation state clusters it appears that the oxidation state of one of the reagents changes throughout the reaction from starting material to crystal. Hydroxyl oxygens are the most common heteroatoms used as bridges. The only heterometallic clusters observed in the literature of Anderson-Evans cord clusters are the Anderson-Evans clusters themselves.[5] The very large clusters seem to have different metals involved in different roles as bridges between smaller subunits.

Section 5 – Results, Series that are present or Missing

The data obtained from the CSD is significant, but there were many other structures of interest that were found that were not found in the CSD search. A search of the ICD found the original Al_7 Anderson-Evans cluster; however the analogous Ga_7 and In_7 clusters are not present in the database. We expected to see the Ga_7 cluster, as that

fragment was observed in our heterometallic series. The large ionic radius of indium explains why we did not see the In_7 Anderson-Evans cluster.[48] A very interesting structure that appears in the M_6 core but not in the M_7 Anderson-Evans or M_7 Anderson-Evans fragment searches is an In_6 ring that is the same as the core of the tridecameric clusters, **Figure 1.14C,** (BEQRAR[136]). Additionally, there is the same ring but with manganese or iron inserted into the central position (OCEZUS, OCIBAE, OCIBEI[83]). This is also true of both the Anderson core and the Anderson fragment search. From the M_7 Anderson-Evans core CSD search we do find a M_{15} isomer that is not included in the tridecameric search (UDAZUU[98]).

Other clusters of interest were found which contain thirteen or more metals that have the same binding as the $M_{13}{}^{o}$ cluster, but the three metals that are above and below the M_7 core are now offset from the outer rim but instead are packed directly above the core. There are a few examples of cluster that are still $M_{13}{}^{o}$ but spherical (**Figure 1.14A**), in this case the metals added are in the voids above the plane between the central and two adjacent ring metals (**Figure 1.05D & F**). The Anderson-Evans core forms an equator; this plane contains the most metals per plane, additional parallel to the core. There can be three additional metals added to the top and bottom of the ring to make a sphere (CUDGEN[57], DAQNUE[61], DAWBAE[62], DAWBOS[62], JIDNIT[109], MEXZOX[111], PADPOA[85], TUNYIK[95]). The second layer above the equatorial plane does not need to continue in the hexagonal close packed array. Similar to the $M_{13}{}^{O}$ clusters where additional metals are added outside the Anderson-Evans core the addition metals can be added in a column above the first ring only offset by 30°. Typically, this layer contains

six co-planar metals (KUPDII,[76]), though sometimes only four metals are present in the second layer with vacancies at 180° (POZRAX[108], YEBLIB[137]). Three more metals can be added to the second layer in distal positions with the third layer offset on top for a M_{25} cluster, which stacks in layers of 3,6,7,6 and3 metal centers, **Figure 1.14B**. (BETCOT[108]) There is one example where the growth is not symmetric: additional layers are only on top of the Anderson-Evans core (**Figure 1.14B**) (UKUMIW[115]).

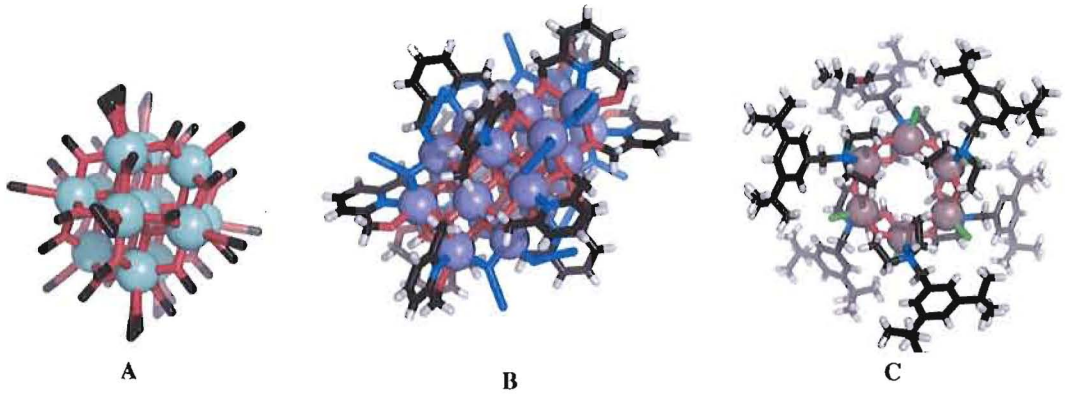

Figure 1.14. Interesting clusters discovered in the search. A. M_{13}° Sphericical 3,6,3 metals, B. 3,6,7,6 and 3 array of Mn centers, C. In_6 ring.

Two M_8 clusters were discovered through other searches of the literature. The clusters Al_8 [44] and Ga_8 (PAFJUC[42]), though not Anderson-Evans or M_{13} clusters, have portions that are structurally similar in about half of the complex. The M_8 cluster has six metals that closely resemble the M_7 core of the indium Anderson-Evans cluster. If one of the six metals from the first ring of the core is removed, the two adjacent metals will twist out of the plane to relieve the torsional strain imposed by the planarity of the seven metals. These clusters may help to explain the stability of other clusters like the M_{13} as

well as fragments that are observed from ToF-SIMS experiments to be discussed later (Chapter V).

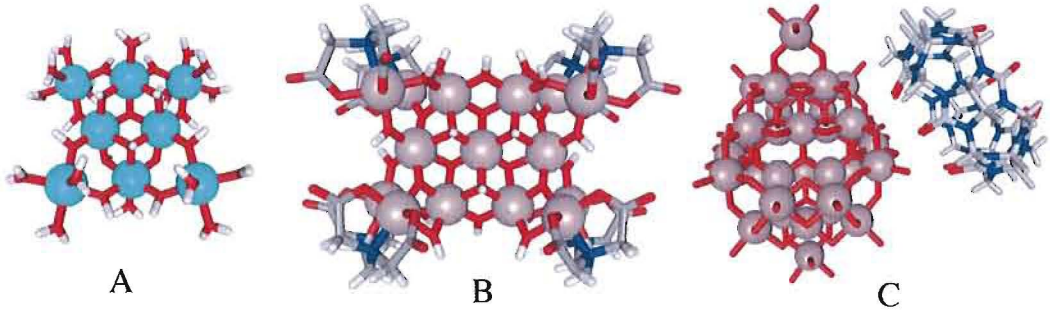

Figure 1.15. Ball and stick representations of A. M_8, B. M_{15} and C. M_{32} Clusters

The original search for tridecameric and Anderson-Evans clusters and component fragments only looked for a ring of six metals. The CSD does not allow definition of cyclic or repeating units. Follow-up searches copied the $M_6(\mu_2\text{-}O)_{12}$ fragment for the larger $Mn(\mu_2\text{-}O)_{2n}$ rule. The same 2N+2 rule for organic degrees of unsaturation applies to inorganic rings as well. A ring has one degree of unsaturation, which subtracts two bridges from the corresponding chain. These other ring structures may be of interest to help explain the stability of the clusters. There are clusters containing up to twelve metals, which would begin to resemble the second metal shell in a brucite lattice. These larger ring systems have a cavity size the same as the smaller Anderson-Evans clusters and could be used as templates or nucleation sites for the formation of these smaller clusters.

The identical search was performed for n = 7, 8, 9, 10, 11 and 12. The search in the CSD that yielded hits was the n = 8 ring.[138, 139] A structure was found that has a single oxo bridge between ring one and ring two, opening up a position on each metal of

ring one and therefore changing the bonding geometry between the Anderson core and the second ring of metals.[71] There might need to be an additional review of metallic ring structures that are not solid in the middle such as those given in (**Figure 1.16A**).[131, 140, 141]

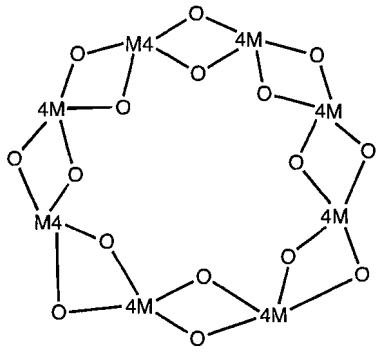

M_8 (μ_2-O)$_{16}$ Ring

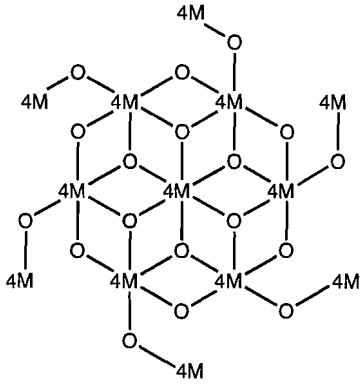

M_{13} (μ_3-O)$_6$ (μ_2-O)$_{12}$ tridecatmeric search

Figure 1.16. Secondary CSD searches criteria

The modified M_{13} structure should yield structures that fall between the previous searches of the Anderson-Evans cluster and the rigid tridecameric cluster. It also presents the possibility of other heteroatoms acting as bridging or coordinating ligands. The single bridged M_{13} cluster yielded thirty nine hits. The previous tridecameric search hits are included in this data set. Some new observations include the incorporation of larger metal ions in the other ring, as well as much larger ligands that contain functionalized pyridine rings. There are fifteen analogous M_8 ring clusters found in searching the CSD, **Figure 1.17A**. Eleven of them did not require a larger ligand to force the formation of the larger ring, however most encapsulate an ion such as oxolate (AWEWEE[142], AXEPAU[143], DAWYAB[144], EDUNOG[145], FAFQOT01[146], PAQFAO[147], SAKPID[148],

SWJYOV & SEJYUB[149], TASMIK[150], XOVPED[151]). The remaining four used the functionalized *p-tert*-butylsulfonylcalix[4]arene and large diameter lanthanides to form the cluster, **Figure 1.17B** and **C**.[152]

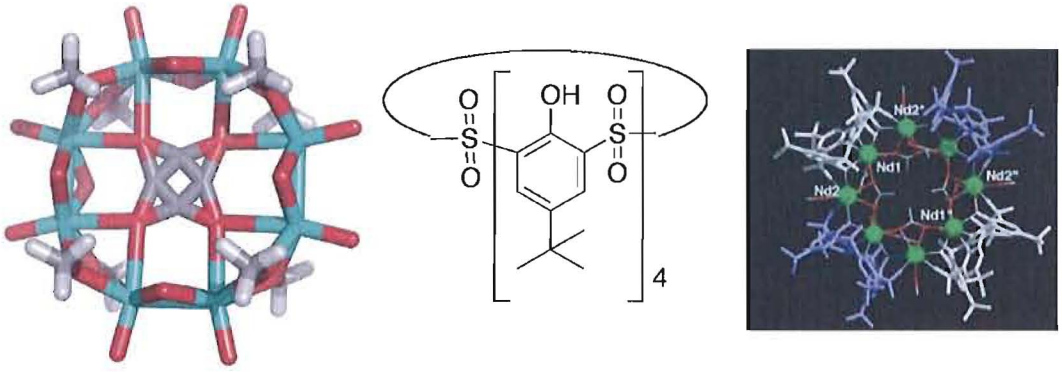

Figure 1.17 A M_8 ring with a disordered oxolate cation, and calix[4]arene ligand supported clusters

SUMMARY

Recent searches of the CSD and ICD show there are numerous clusters that contain the Anderson cluster as a fragment in their full structure. Despite the wide variety of metal substitution seen at the central metal substitution of the Anderson-Evans and Keggin clusters, there are few other heterometallic structures found. Database updates are far behind the research, and the interfaces are not always friendly. It is crucial that databases provide an option to combine a completely inorganic search with a full CSD search. Prior to this, the M_{13}^{o} clusters have typically been called tridecameric clusters, though an extensive review by Casey distinguishes them from a classical Keggin cluster by calling them "flat-M_{13}" clusters. We have contributed to this field with new substitution at the core position and with our expansion of the M_{13}^{o} chemistry as well.[41,

[121] The dilemma presented by this research is in the naming of the flat tridecameric clusters because of their different expansion on the Anderson-Evans core. These cluster are already showing their potential use as synthons. These clusters will need their own name and naming scheme as more of these clusters are synthesized and used.

CHAPTER II

A SIMPLE ORGANIC REACTION MEDIATES THE CRYSTALLIZATION OF THE INORGANIC NANOCLUSTER $[Ga_{13}(\mu_3\text{-}OH)_6(\mu_2\text{-}OH)_{18}(H_2O)_{24}](NO_3)_{15}$

I initially identified the novel cluster and performed the collection of the Single Crystal XRD data. I was the primary contributor to the optimization of the synthetic conditions including the determination of the active functional group and developed the purification procedure. Dr. Elisabeth Rather was helpful in solving the crystal structure. Dr. Victor Kravtsov was helpful in verifying the charge state of the cluster. Dr. Paul G. Nixon and Dr. Takuji Tsukamoto contributed to this publication by providing the original organic reagents. This work was published in Volume 125 of the *Journal of the American Chemical Society* in February of 2005. Dr. Prof. Darren W. Johnson was the principle investigator for this work.

A series of NMR titration experiments were run to determine the binding of Ga(III) with proprietary organic ligands developed by Chemica Technologies, Inc. The NMR reaction was allowed to evaporate and yielded large crystals (**Figure 2.1**). Evaporation of the solvent from the experiment solutions yielded crystallographic grade single crystals of the $[Ga_{13}(\mu_3\text{-}OH)_6(\mu_2\text{-}OH)_{18}(H_2O)_{24}](NO_3)_{15}$ nanocluster (**Figure 2.2A**). However, the crystal structure does not contain the organic ligand from the titration. The isostuctural unstabilized $[Al_{13}(\mu_3\text{-}OH)_6(\mu_2\text{-}OH)_{18}(H_2O)_{24}](NO_3)_{15}$ nanocluster has been previously reported (**Figure 2B**),[1] and Goodwin et al. had theorized that the $[Ga_{13}(\mu_3\text{-}OH)_6(\mu_2\text{-}OH)_{18}(H_2O)_{24}](NO_3)_{15}$ was unstable.[2] The $[Ga_{13}(\mu_3\text{-}OH)_6(\mu_2\text{-}OH)_{12}(HEIDI)_6(H_2O)_6](NO_3)_{15}$ and $[Al_{13}(\mu_3\text{-}OH)_6(\mu_2\text{-}OH)_{12}(HEIDI)_6(H_2O)_6](NO_3)_{15}$ organic ligand-stabilized clusters have also been isolated (**Figure 2.2C and D**).[2, 3]

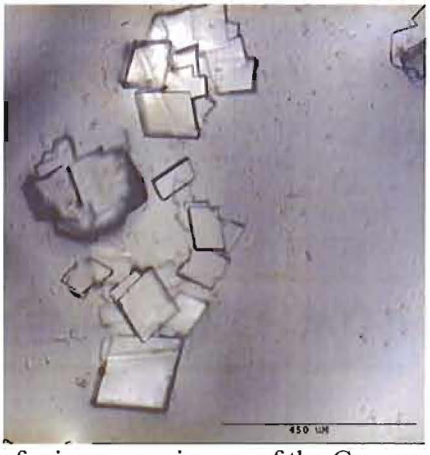

Figure 2.1.Screen capture of microscope image of the Ga_{13} crystals

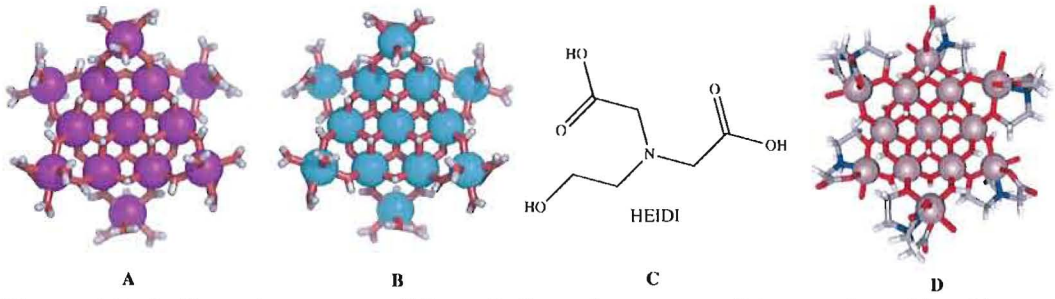

Figure 2.2. A. Crystal structure of Ga_{13}; B Crystal structure of the pervious Al_{13}; C. HEIDI ligand; D. Crystal structure of HEIDI Stabilized Ga_{13}.

Since there were no organic binding ligands in the structures, and $Ga(NO_3)_3$ recyrstallized on its own will not form $[Ga_{13}(\mu_3\text{-}OH)_6(\mu_2\text{-}OH)_{18}(H_2O)_{24}](NO_3)_{15}$ clusters like this, the organic additives must have had some effect. Follow-up experiments to determine the active functionality of the proprietary ligand yielded the discovery that the nitroso functionality is necessary for the formation of the Ga nanocluster. Nitrosobenzene acts as an organic reductant by reducing the nitrate counter ions; this forces the formation of the multiple metal $[Ga_{13}(\mu_3\text{-}OH)_6(\mu_2\text{-}OH)_{18}(H_2O)_{24}](NO_3)_{15}$ inorganic nanocluster. The other functionalities from the proprietary ligand yielded ligand substituted products or starting materials. A functional group testing approach was taken to determine the active functional group. Each functionality of the ligand was tried individually. Multiple combinations of functional groups were tested also for reactivity.

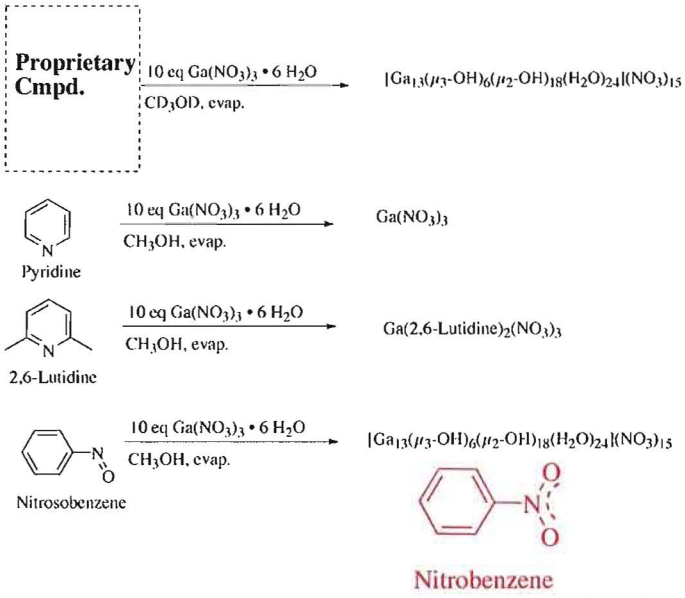

Scheme 2.1.Organic reductants or ligands used to determine the functional group responsible for the formation of the Ga_{13} cluster.

After the publication of our method utilizing the nitroso functionality as an organic reductant, another group published research yielding the same $[Ga_{13}(\mu_3\text{-}OH)_6(\mu_2\text{-}OH)_{18}(H_2O)_{24}](NO_3)_{15}$ inorganic nanocluster. However, their cluster co-crystallized with cucurbit[6]uril (CB[6]) and an oxo bridged Ga_{32} species.[4] The Fedin group was not sure how their additive aided in the formation of the flat Ga_{13} clusters. Their group continues to use CB[6] as an organic additive to make other clusters in the same manner, allowing our two routes to diverge.[5, 6] They were able to visually sort their crystals based on their physical morphology from just CB[6] and the Ga_{32} cluster .

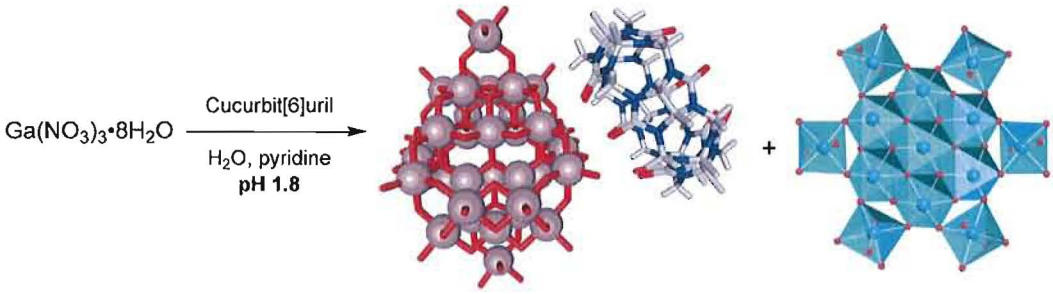

Scheme 2.2. Synthesis of Ga_{13} using CB[6] as an organic additive.[4]

The following pages summarize our initial publication of the synthesis, isolation and characterization of the flat Ga_{13} nanocluster. Other work on these types of clusters is in the chapters which follow. Included is an in-depth characterization chapter and a discussion of future works.

Developing predictive design strategies to prepare inorganic cluster compounds has attracted much research interest, due in part to the potential applications of these novel materials.[2, 7-11] We present a potentially new synthetic strategy for preparing discrete inorganic clusters, and we use this strategy to prepare the first crystalline example of an inorganic tridecameric Ga cluster. By using $Ga(NO_3)_3(H_2O)_6$ as a nitrate source for the conversion of nitrosobenzene to nitrobenzene — which is known to proceed using nitric acid — robust crystals of the nitrate-deficient gallium cluster $[Ga_{13}(\mu_3\text{-}OH)_6(\mu\text{-}OH)_{18}(H_2O)_{24}](NO_3)_{15}$ form. To the best of our knowledge, this is the first synergistic use of a simple organic reaction to mediate the formation of a polynuclear inorganic cluster compound.

Studies on polycationic metal oxo- and hydroxo- aggregates of gallium and aluminum have centered around understanding their environmental impact (*e.g.* soil

science, water treatment),[10, 12-14] determining their biological relevance (*e.g.* toxicity and transport of metallic species),[14, 15] and preparing new materials (*e.g.* catalysis, magnetism, porous solids).[16-18] In this context, aqueous complexes of gallium(III) have received less attention than their aluminum counterparts, largely due to difficulties in preparing stable single crystal forms of these clusters.[13] Solid state and solution investigations on the formation of inorganic gallium clusters reveal that the majority of the compounds are polyoxycations based upon the modified-Keggin structure, which possesses octahedral peripheral gallium cations bridged to a central tetrahedral Ga(III).[17, 18] While the presence of chelating organic ligands stabilizes a range of polynuclear clusters and allows for their crystallization,[2, 3, 7, 19] the structural characterization of purely inorganic Ga(III) clusters analogous to the Al_{13} clusters is lacking.[1, 13] We report the single crystal structure of an inorganic Ga_{13} cluster **1**[*] prepared using a simple *organic* reaction to drive the formation of the crystalline *inorganic* cluster.

Robust crystals up to 15 mm^3 in volume of $[Ga_{13}(\mu_3\text{-}OH)_6(\mu\text{-}OH)_{18}(H_2O)_{24}](NO_3)_{15}\cdot 6H_2O$, **1**, (Figure 1) were obtained from slow evaporation at room temperature of a methanolic solution of hydrated $Ga(NO_3)_3$ in the presence of nitrosobenzene. In this process the nitrosobenzene acts as a scavenger of nitrate ions and facilitates the nucleation of Ga_{13} clusters *via* a redo process in which the nitrosobenzene is oxidized into nitrobenzene with concomitant reduction of some of the nitrate counter ions. High-Pressure Liquid Chromatography-Mass Spectrometry (HPLC-MS) and ^1H NMR spectroscopic data prove that nitrobenzene is indeed formed in the crystallization

[*] Crystal data for **1**: Trigonal, *R*-3, $a = 20.214(3)$, $c = 18.353(4)$ Å, volume = 6494.7(19) Å^3, $Z = 3$, $D_c = 2.127$ g cm^{-3}, $\mu = 4.128$ mm^{-1}, $F(000) = 4116$, $2\theta_{max} = 52.80°$ ($-24 = h = 25$, $-25 = k = 25$, $-22 = l = 22$). Final residuals (for 228 parameters) were $R1 = 0.0310$ for 2500 reflections with $I > 2\sigma(I)$, and $R1 = 0.0349$, $wR2 = 0.0988$, GooF = 1.035 for all 2831 data. Residual electron density was 0.949 and 0.567 e.Å^{-3}.

process.[†] Furthermore, it is known that nitric acid can oxidize nitroso derivatives into the corresponding nitro compounds; this procedure simply represents a milder form of this reaction, in which nitrate oxidizes nitrosobenzene at a slightly acidic pH.[20-22] In effect, as a result of consumption of some of the nitrate counter ions of $Ga(NO_3)_3$, the remaining gallium-containing species must form a higher nuclearity cluster where the ratio of nitrate to gallium(III) is less than 3:1. In this case, the stoichiometry descends to 15:13. In this redox process one Ga_{13} cluster must be produced *per* 24 nitrosobenzene oxidized.

[†] ^{1}H NMR and LC-MS spectra of the mother liquor remaining after crystallization of **1** showed peaks characteristics of both nitrosobenzene and nitrobenzene.

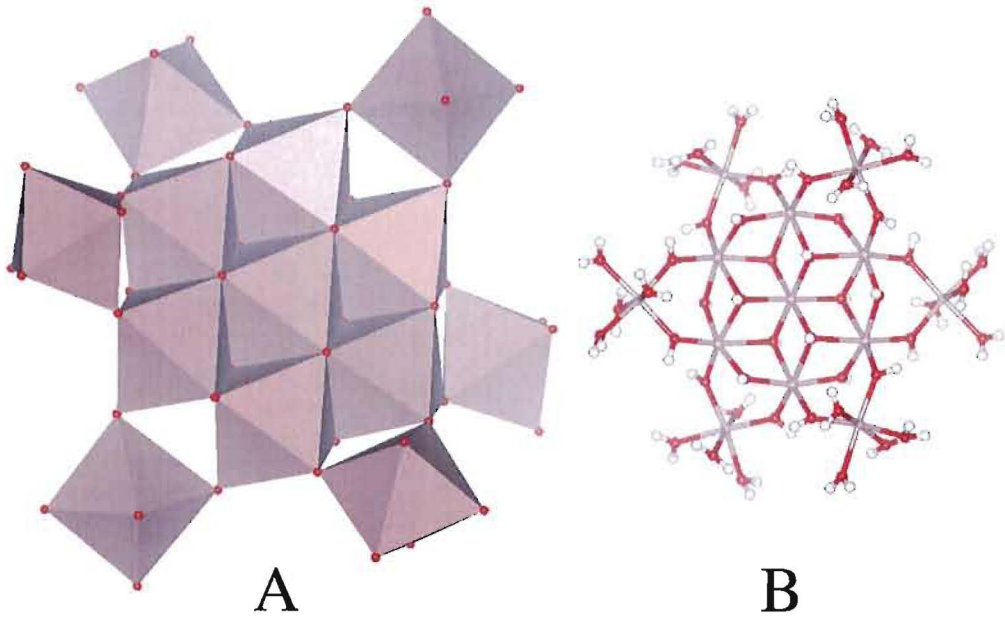

Figure 2.3 Polyhedral (a) and ball and stick (b) representations of the crystal structure of the polycationic $[Ga_{13}(\mu_3\text{-}OH)_6(\mu\text{-}OH)_{18}(H_2O)_{24}]^{15+}$.

The crystal structure of the mixed hydroxo/aquo cluster **1** reveals the compound does not crystallize as the modified Keggin structure seen in the related Al_{13} or MAl_{12} clusters,[23, 24] but rather is similar to Ga_{13} clusters stabilized by supporting ligands, where the central gallium is octahedral, not tetrahedral.[‡] Each tridecamer consists of a central Ga(III) bridged *via* hydroxyl groups to six surrounding gallium cations forming an inner core of seven edge-shared $Ga(O)_6$ polyhedra. The six inner polyhedra are further vertex-shared to six peripheral tetrahydrated Ga(III) ions generating a disk-like compound with an effective diameter of *ca.* 1.81 nm and a thickness of *ca.* 1.03 nm. The central, inner

[‡] In the structure of the related aluminium tridecamer reported by Seichter *et al.*,1. Seichter, W.; Mogel, H.-J.; Brand, P.; Salah, D., Crystal Structure and Formation of the Aluminum Hydroxide Cloride $[Al_{13}(OH)_{24}(H_2O)_{24}]Cl_{15} \cdot 13\ H_2O$. *Eur. J. Inorg. Chem.* **1998**, 795-797.[16] not all hydrogen atoms positions could be determined. Therefore, charge balance considerations based on the number of chloride counterions were used to determine the number of hydroxo versus aqua ligands, and it was assumed that only the hydroxo ligands were bridging. The structure of **1**, in which all hydrogens atoms from the coordinated O-H groups were located in the Fourier difference map, corroborates this.

Ga(III) lies at a special position on the $\bar{3}$ axis of the unit cell and is coplanar with respect to the six surrounding edge-shared $Ga(O)_6$ polyhedra (mean plane deviation of 0.06 to 0.07 Å). The distances between edge-shared gallium cations and the corresponding oxygen atoms d(Ga-μ_3-OH) are in a range of 1.96 to 2.15 Å. The six external $Ga(O)_6$ polyhedra are bonded to the inner core of seven Ga(III) each *via* two vertices with corresponding distances d(Ga-μ_2-OH) of 1.91 to 1.92 Å. The peripheral Ga(III) are each coordinated to four water ligands with distances d(Ga-OH_2) in a range of 1.98 to 2.01 Å.

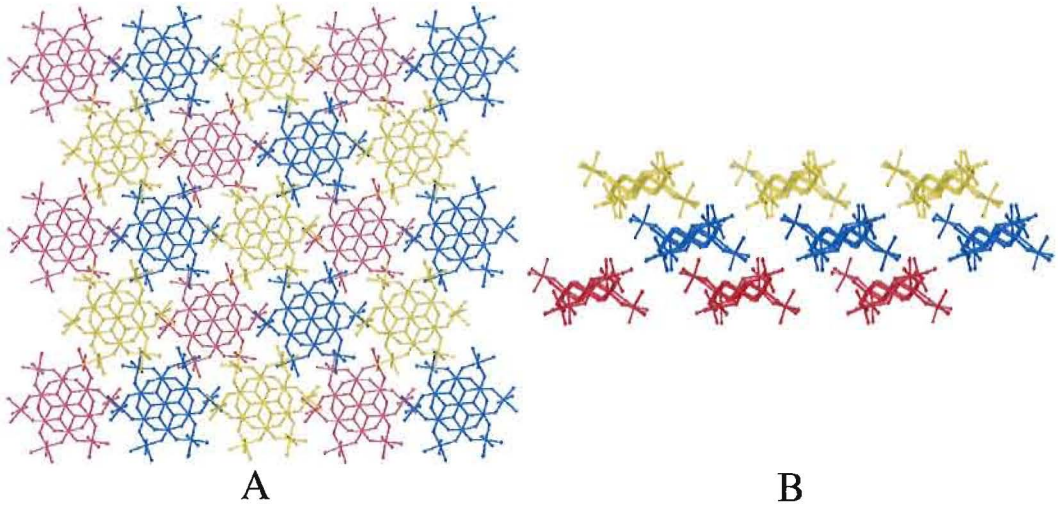

Figure 2.4 Crystal packing of the polycations $[Ga_{13}(\mu_3\text{-}OH)_6(\mu\text{-}OH)_{18}(H_2O)_{24}]^{15+}$ in **1** representing the stacking of sheets in an ABCABC mode orthogonal to the *z*-axis (a) and orthogonal to the *y*-axis (b), hydrogen atoms, counter-anions NO_3^- and water molecules have been omitted for clarity.

The peripheral tetrahydrated gallium centers deviate from the mean plane of the inner core formed by the seven edge-sharing cations by *ca.* 30° and they are positioned alternatively above and below the plane of the Ga_7 core. The main difference with respect to the structure of $[Al_{13}(OH)_{24}(H_2O)_{24}]Cl_{15}\cdot 13H_2O$ lies in the crystal packing adopted by

1 (Figure 2.1.2): the Ga_{13} clusters crystallize in a hexagonal array. The polycationic units arrange in layers parallel to [001] and repeat in an ABCABC mode along the *z*-axis with an interlayer separation of 6.12 Å. Cluster **1** is a highly hydrophilic compound with a surface rising with hydrogen bond donors and acceptors. These particles are completely surrounded by counteranions forming shells around the polycations through an intricate hydrogen bonding network in which interstitial NO_3^- and uncoordinated guest water molecules interact with coordinated water and hydroxide ligands with distances d(O···O) in a range of 2.57 to 3.00 Å.

In summary, a straightforward method to generate mixed aquo/hydroxo gallium clusters in the form of large robust single crystals has been presented and provides an alternative to the hydrolysis of the cations in the presence of base, which usually results in the formation of poor quality crystals. Further work is currently underway to investigate the properties in solution of the Ga_{13} clusters. These purely inorganic aggregates might be relevant as starting materials for the generation of a wider range of particles *via* exchange of the water ligands with appropriate organic species. We are exploring the generality of our synthetic route to see if treatment of other metal nitrate salts with nitrosobenzene provides higher nuclearity metal clusters as well.

Supporting Information Available: Crystallographic data for **1** in .CIF format is available as CSD 414322. These data can be obtained from the Fachinformationzentrum (FIZ) Karlsruhe, D-76344 Eggenstein-Leopoldshafen (Germany) www.fiz-informationsdienste.de. This material, details of the synthetic procedure and x-ray

powder diffraction patterns are also available free of charge *via* the Internet at http://pubs.acs.org.

CHAPTER III

NOVEL SYNTHESIS OF ALUMINUM 13 INORGANIC NANOCLUSTERS

The synthetic procedure in this chapter was developed by a number of lab members including Jason T. Gatlin and Zachary L. Mensinger. Zachary L. Mensinger contributed substantially to this chapter by participating in the development of a standard synthetic procedure. I was the primary contributor to the optimization of the synthetic conditions and developed the purification procedure. Dr. Lev N. Zakharov was helpful in solving the crystal structure. Dr. David MacInnes was helpful in reviewing and editing the manuscript. This work has not yet been published but will be submitted in the summer of 2007 to the journal *Inorganic Chemistry*. Zachary L. Mensinger initially identified the alternate nitroso reductant for cluster synthesis, which yields the identical cluster to the Nitrosobenzene synthesis. Dr. Prof. Darren W. Johnson was the principle investigator for this work.

Since the synthesis of our first "flat"-$\mathbf{Ga_{13}}^{o}$ cluster[1], we sought to explore the generality of the reaction. There were two different directions of experiments to explore; the organic side and the inorganic side. The first was to determine if the identical unstabilized $\mathbf{Ga_{13}}^{o}$ cluster can be made with other reductants and determine the importance of the nitroso functionality. The second was to determine if other similar clusters could be synthesized via the same reaction conditions. Chapter 2 will discuss the results of the organic experiments, and Chapter 3 will address the synthesis of other M_{13}^{o} nanoclusters via the same reaction.

We began changing the conditions of the crystallization in hopes of increasing the isolated yield of the nanocluster. We were hoping to see what drove the crystallization of the nanocluster and to determine if it was the observed oxidation of nitrosobenzene and, therefore removal of the nitrate counter ions or if it was the evaporation of the solvent. Crystallizations set up in the refrigerator or freezer yielded large, stable, colorless crystals very quickly. However the only crystalline product isolated was the dimer of nitrosobenzene which can be isolated by lowering the temperature or by chromatography of the reaction mixture before completion. This structure was already know and was present in the CSD (reference code: CAZBZO10 and JTG46.)[2, 3]

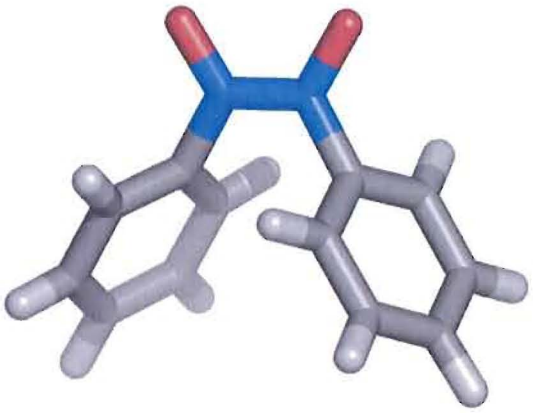

Figure 3.1. Known crystal structure the nitrosobenzene dimer. (Orthorhombic P, *Pbcn*, *a* = 10.292(1)Å, *b* = *13.796(1) Å*, *c* = *15.005(1) Å*, $\alpha = \beta = \gamma = 90$ °*V* = *2137.8 Å*^{3}, *Z* = *8)*

Since determining that the nitroso functionality was the active functional group, commercial suppliers were searched for other nitroso-containing organic compounds as well as potential reductants with similar electrochemical potentials **Figure 3.2**. Typically, it is difficult to determine reduction potentials for organic compounds and only a few have been determined (**Scheme 3.1**).[4]

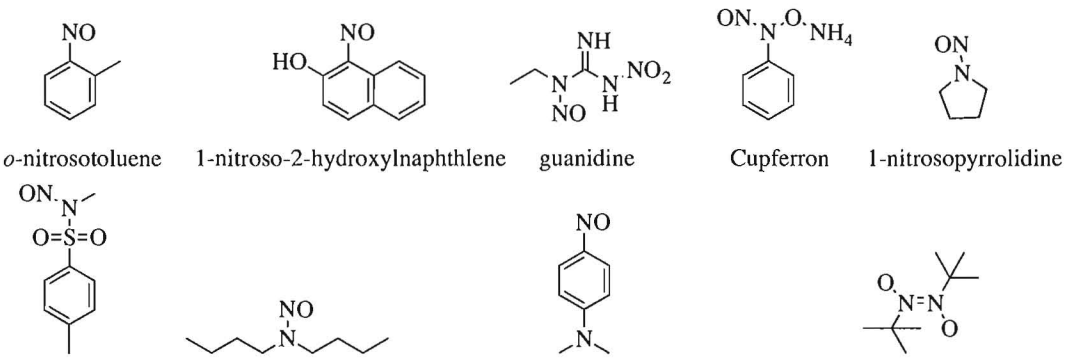

Figure 3.2.Some of the commercially available nitroso group containing compounds

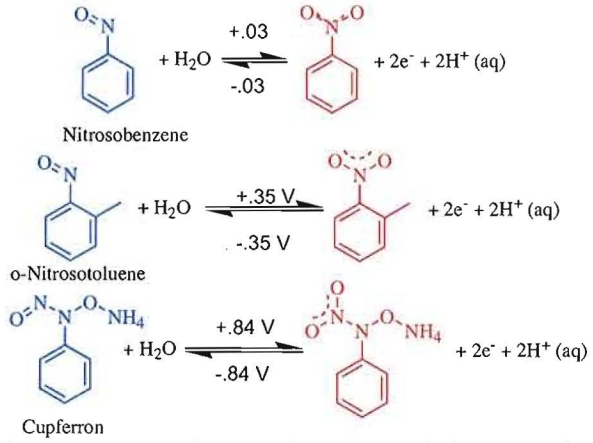

Scheme 3.1. Reduction potentials of three nitroso containing organic compounds versus a SCE.[4]

All the reactions were set up following the same procedure as the synthesis with nitrosobenzene, except for the exchange of organic reductants in the same stoichiometry. **Scheme 3.2** shows the crystalline products isolated from the reactions of the alternate reductants with $Ga(NO_3)_3$. Cuperferron has been known to bind copper and iron in a similar manner, hence the name, as well as aluminum.[5] The nitroso functionality of the guanidine and the diazald are not stable: both compounds denitrosolate under reaction conditions, with or without metal being present. From the series of organic compounds in **Figure 3.2**, only one, N,N-Dibutyl-N-nitrosoamine (DBNA), yielded the same flat Ga_{13}° nanocluster. **Figure 3.3** shows a side-by-side comparison of the two reactions with the different nitroso compounds: nitrosobenzene (on the left) and DBNA (on the right), both of which yield the nanocluster in respectable yields.

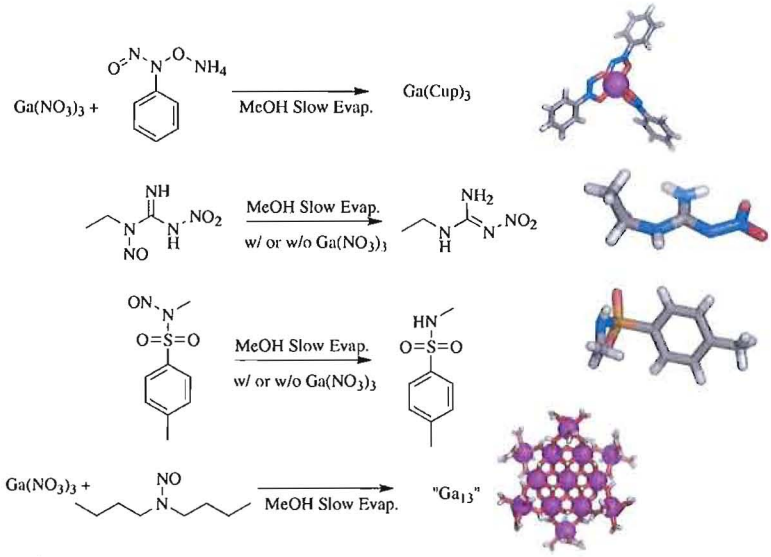

Scheme 3.2. Nitroso compounds that show activity and the isolated crystalline products yielded.

The difference in the two reactions is very clear. The yields are higher in the DBNA reaction, most likely because of the great ease in which we can isolate crystals by just decanting the oil byproduct. The new organic additive DBNA can also be recycled and reused for further reactions making this synthesis greener than using the nitrosobenzene. This suggests that the organic byproduct of the cluster synthesis with DBNA is not as stable as the nitrobenzene product of the nitrosobenzene reductant. Current works to track down the oxidized product of the DBNA reductant have not been successful. We hope to determine if the reaction can be used in the future as gentle organic oxidant.

Figure 3.3. The decomposition of the organic reductants post oxidation. Nitrosobenzene product and DBNA product (left to right)

Tweaking the conditions for Ga_{13}° cluster formation allowed us to synthesize the analogous Al_{13}° cluster. This new organic reductant allows for the formation of our previous Ga_{13}° cluster in a higher yield and allowed for the isolation of the previously known Al_{13}° nanocluster as well with the same reaction conditions. The Fedin group also tried to use their CB[6] strategy to synthesize the flat Al_{13}° nanocluster, which they reported to Casey[6] as a personal communication, but their later published results indicate that they in fact synthesized the Keggin Al_{13}^{t} cluster not the "flat"-Al_{13}° cluster.[7] Due to the other stability issues the use of nitrosobenzene will be discontinued in favor of DBNA.

We tested a variety of other organic compounds that we believed were easily oxidized and that do not contain the nitroso functionality as possible reductants for the formation of the flat Ga_{13}^{0} nanocluster **Figure 3.4**. As of yet none of them have yielded a metal cluster.

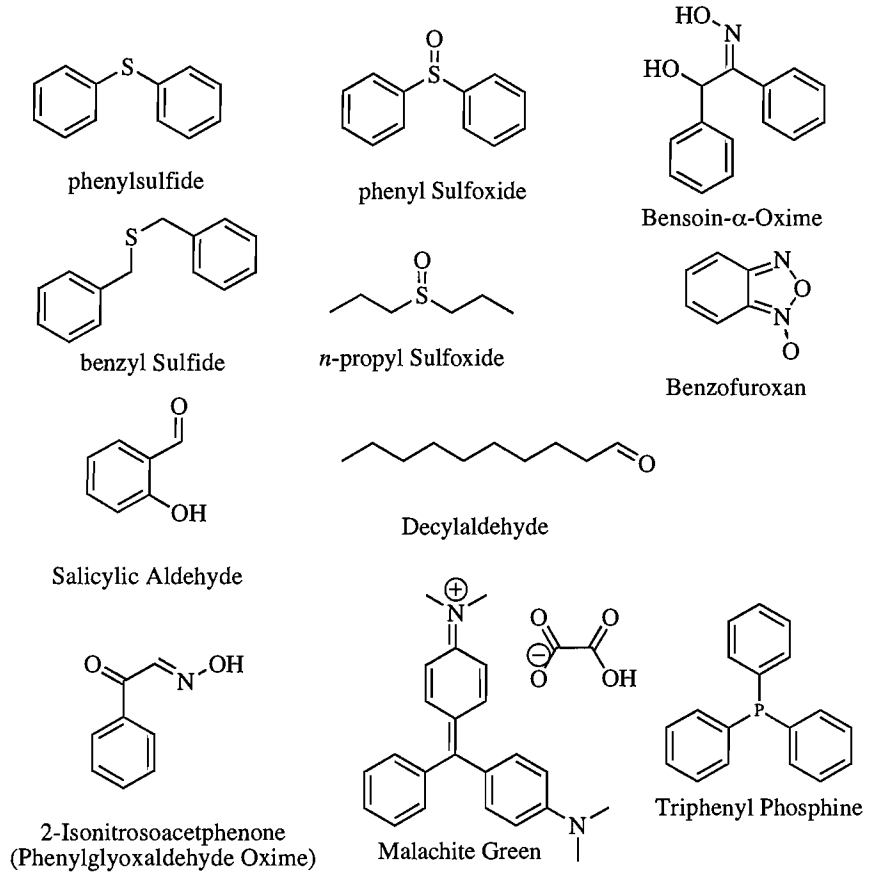

Figure 3.4. Other potential organic reductants screened

One conversion of interest with low oxidation potential is the oxidation of a phosphine or an arsine to its oxide.[4] The ease of oxidation of the pnictogens follows the established trend (P>Sb>As), with P the easiest to oxidize. It is clear that phosphines are easily oxidized to phosphine oxides while arsines are more stable to oxidation. Triphenyl

phosphine, triphenyl arsine and their oxides are used extensively for initiating polymerization reactions and as ligands in transition metal complexes and catalysis.[8] The thermodynamically stable pentavalent oxides are generally made from phosphines and arsines either with strong oxidants or activating with a transition metal, followed by oxidization by a less powerful reagent.[9-14] Some preliminary results have been achieved with the use of triphenyl pnictogens as reductants.

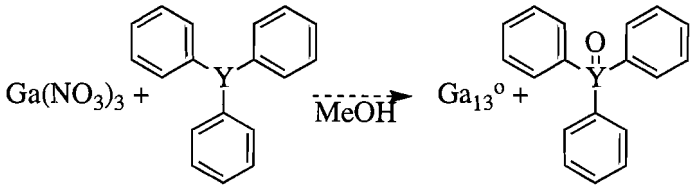

Y = P, As, Bi, and Sb

Scheme 3.3. The oxidation with formation of pnictogen oxides for the reactions.

The use of gallium nitrate was explored in oxidizing both triphenyl phosphine and arsine while concomitantly producing a $\mathbf{Ga_{13}^{o}}$ nanocluster. Allowing a solution of gallium nitrate and triphenyl phosphine to incubate at room temperature for 5 days resulted in isolation of only the starting materials. Only after heating for one to two hours at 69°C did a reaction occur, giving the known $[(C_6H_5)_3As{=}O{-}H{-}O{=}As(C_6H_5)_3]$ complex which contains a hydrogen bond between two triphenyl arsenic oxides entities. This complex contains a $[NO_3]$ counter ion, as oppossed compared to other previously formed clusters.[15-18] A $Ph_4P^+ NO_3^-$ species was also crystallized. Triphenyl phosphine can also be oxidized by $Fe(NO_3)_3$ but it appears that the analogous Fe_{13} cluster is not formed; instead, a $Fe(NO_3)_2 (Ph_3PO)_3$ salt is formed. A control reaction run without metal salts showed no oxidization of the pnictogens.

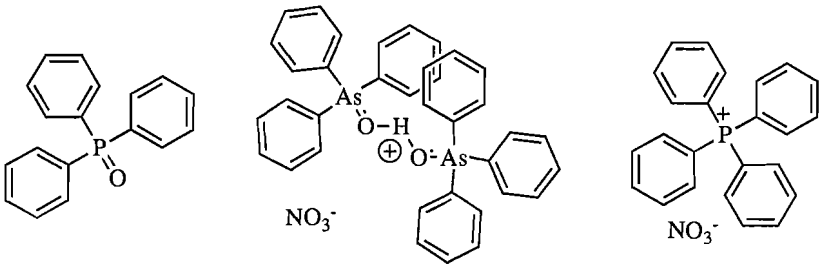

Figure 3.5. The isolated products from the pnictogen oxidation.

Although the preliminary results for non-nitroso reductants are encouraging, it is problematic that the Ga_{13}° cluster was not isolated in addition to the organic reagent nor was any other multiple metal complex, **Figure 3.5**. A balanced equation cannot be written; therefore, this reaction is not useful to the project until a new inorganic product can be isolated. There is a solved crystal structure of the triphenyl arsenic oxide dimer and the tetraphenyl phosphine cation, but only IR confirmation of the triphenyl phosphine oxide. This set of experiments needs to be repeated because a metal product could not be isolated, not even as the starting salt, which is important to demonstrate the generality of the reaction for forming M_{13}° clusters.

A functional group of great interest was oximes because they tautomerize to nitroso functionality, but the tautomerization equilibrium lies heavily to the oxime isomer, **Scheme 3.4**. This tautomerization is not possible for nitrosobenzene because the α carbon is tied up in the aromatic ring and fully substituted. Unfortunately, the oxime reactions only yielded the recrystallization of the starting materials, with no nanocluster formation.

oxime Nitroso

Scheme 3.4. Oxime-Nitroso tautomerization

We preformed a series of experiments of the group 13 metals (Al, Ga and In) with DBNA at different pH's by adding KOH or HNO_3. Not surprisingly the yields of cluster were lower with decreased pH by addition of HNO_3 addition because we were driving the reaction the wrong way with addition of the nitrate anion. The yield of the reaction did not improve when the acid was changed to HCl. Only the addition of base had a positive outcome for the aluminum; the isolation of the flat $\mathbf{Al_{13}^{o}}$ cluster. We have not yet been able to isolate the isostructural flat In_{13}^{o} from any of these reactions. The large ionic radius of indium might prevent the formation of the cubic closed packed array of the Anderson core. In the following chapter I describe the current syntheses of the flat $\mathbf{Al_{13}^{o}}$ cluster using different bases.

Treatment of aluminum nitrate with an organic nitroso-containing compound yields the "flat", tridecameric nanocluster, $Al_{13}(\mu_3\text{-}OH)_6(\mu_2\text{-}OH)_{18}(H_2O)_{24}(NO_3)_{15}$ ($\mathbf{Al_{13}^{o}}$) in good yields on a preparative scale under ambient conditions. Synthetic procedures yielding two different single crystal forms of the $\mathbf{Al_{13}^{o}}$ cation with two varying counterion compositions are described.

Aluminum is the third most abundant element and the most abundant metal in the earth's crust, found in many minerals and ores. Aluminum complexes are widespread in our environment, occurring in natural waters and clays usually as hydrated salts or clusters containing multiple aluminum ions held together through various bridging

groups.[6, 7, 19-26] Despite the widespread prevalence of natural aqueous aluminum oligomers, relatively few have been synthesized on preparative scale and analyzed by single crystal X-ray diffraction.[6] Furthermore, existing syntheses of many of these inorganic aqueous clusters suffer from long reaction times and/or poor yields (in cases where yields have been reported), hampering efforts to study the applications and bulk properties of these materials. [6, 23-27] Herein we report facile syntheses that yield bulk-scale single crystals of inorganic $Al_{13}(\mu_3\text{-}OH)_6(\mu_2\text{-}OH)_{18}(H_2O)_{24}^{15+}$ clusters with various counter-anions (**Scheme 3.5**).

Oligomeric aluminum clusters are found in two general structure types: 1) structures similar to the ε-Keggin tridecameric clusters composed of a central tetrahedral metal ion surrounded by edge-shared octahedral AlO_6 units;[21, 28-30] and 2) clusters comprised entirely of octahedrally coordinated Al cations (such as "flat"-$\mathbf{Al_{13}^0}$, **Figure 3.6**). Only a few reports of the latter class of clusters exist. [6, 23-27] We report the synthesis of the purely inorganic salt $Al_{13}(\mu_3\text{-}OH)_6(\mu_2\text{-}OH)_{18}(H_2O)_{24}(NO_3)_{15}$ ($\mathbf{Al_{13}^0}$), a member of the latter class. The synthesis of purely inorganic aluminum salts has been reported as difficult and often elusive:[6] the synthesis reported herein proceeds in reasonable isolated yields under ambient conditions and in preparative scales in a manner similar to the route we reported recently for the $\mathbf{Ga_{13}^0}$ congener.

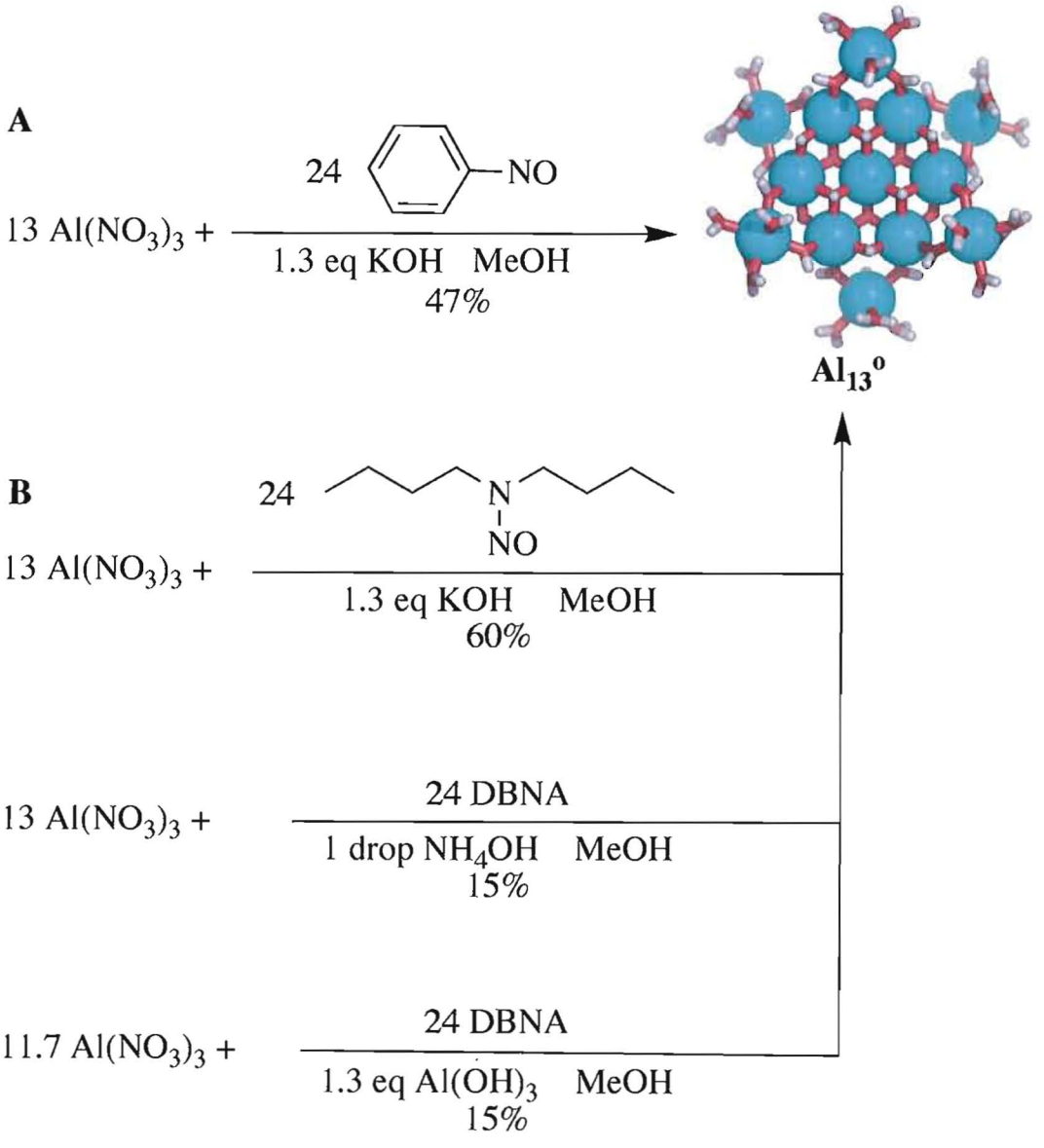

Scheme 3.5 Synthesis of "flat" $\mathbf{Al_{13}^{o}}$ nanocluster using the organic reductants nitrosobenzene (**A**) or *N*-nitroso-di-*n*-butylamine (**B**). The average Al-(μ_3-O), Al-(μ_2-O) and Al-O(H_2O) distances (Å) are 1.879(7), 1.850(9), 1.917(15) and 1.877(6), 1.848(5), 1.92(2), respectively, in **1** and **2**. Base = KOH, NH_4OH, or $Al(OH)_3$ (Note: in the case of $Al(OH)_3$, the use of 1.3 eq of base necessitates only an additional 11.7 eq of $Al(NO_3)_3$.)*

* Synthesis of $[Al_{13}(\mu_3\text{-}OH)_6(\mu\text{-}OH)_{18}(H_2O)_{24}](NO_3)_{15}$ **(1, route B).** Aluminum nitrate nonahydrate (0.25 g, 0.667 mmol, 13 eq) was dissolved in 2.5 mL of MeOH and N-nitroso-di-*n*-butylamine (0.34 g, 2.17 mmol, 42 eq) was added via a syringe. 2.5 mL of a 0.18M KOH solution in MeOH was then added to make a 0.09 M solution. This solution was thoroughly mixed and left

Two recent syntheses of the "flat" $\mathbf{Ga_{13}^{o}}$ Keggin-like structure $Ga_{13}(\mu_3\text{-}OH)_6(\mu_2\text{-}OH)_{18}(H_2O)_{24}(NO_3)_{15}$ were independently reported using gallium nitrate and an organic additive such as nitrosobenzene[1] or cucurbit[6]uril (CB[6]).[31] A related $\mathbf{Al_{13}^{o}}$ core structure has been reported previously: both a structure supported by exogenous aminocarboxylate ligands and the inorganic chloride salt are known.[25,26] However, the synthesis of the chloride salt suffers from a four and a half month preparation and only data on a single crystal were reported. Therefore, we sought to apply our synthetic strategy using nitroso organic compounds to prepare the analogous $\mathbf{Al_{13}^{o}}$ structures.

We have previously shown the simple conversion of $Ga(NO_3)_3$ into the flat-$\mathbf{Ga_{13}^{o}}$ nanocluster proceeds in the presence of nitrosobenzene. In this reaction, nitrosobenzene is believed to act as a scavenger for the nitrate counter-ions, in effect forcing the Ga^{3+} cations to form a higher nuclearity species. The stoichiometry for the process involves reaction of 13 eq $Ga(NO_3)_3$ with 24 eq of nitrosobenzene to prepare one eq of $\mathbf{Ga_{13}^{o}}$ in gram quantities and up to 65% yield.[1] Modification of this method to form the related tridecameric aluminum cluster involves a key modification (Scheme 3.4): The reaction to form $\mathbf{Al_{13}^{o}}$ requires the addition of 1.3 eq of base, presumably a result of the increased pKa of hydrated aluminum complexes over gallium.[32,†] Single crystals of $\mathbf{Al_{13}^{o}}$ were isolated in un-optimized yields of up to 47% in under two weeks from a methanolic

---

uncapped in a scintillation vial to evaporate over the course of 6-10 days. The remaining N-nitroso-di-*n*-butylamine was then removed via a syringe and the solution was washed with EtOAc (3 x 4mL), yielding a mixture of KNO_3 powder and single crystals of $\mathbf{Al_{13}^{o}}$. Crystals of **1** form in 60% yield with respect to aluminum nitrate. Alternate bases also effect the same transformation: NH_4OH (0.1 eq per eq of $Al(NO_3)_3$) provides a slightly different crystal form of the cluster (**2**) in 15% yield; while 1.3 eq $Al(OH)_3$ combined with 11.7 eq of $Al(NO_3)_3$ provide $\mathbf{Al_{13}}$ in 15% yield.

† Synthesis of $\mathbf{[Al_{13}(\mu_3\text{-}OH)_6(\mu\text{-}OH)_{18}(H_2O)_{24}](NO_3)_{15}}$ **(1, route A).** Methanolic solutions of aluminum nitrate nonahydrate (0.50 g, 1.33 mmol, 13 eq in 5 mL MeOH) and nitrosobenzene (0.303 g, 2.82 mmol, 24 eq in 5 mL MeOH) were mixed together and 1.3 eq KOH was added. The mixture evaporated slowly at room temperature over 4-8 days in a scintillation vial covered with tissue paper, yielding a dark thick oil embedded with large single crystals of **1**, which were isolated in 47% yield (with respect to aluminum nitrate).

solution of aluminum(III) nitrate nonahydrate, KOH and nitrosobenzene. A similar procedure using N-di-*n*-butylnitrosamine also affords $\mathbf{Al_{13}^{o}}$ in reasonable yields (15-60%, depending on the base), and provides for a far easier workup, as crystals are isolated from the remaining liquid nitrosoamine rather than the tarry sludge left over from the nitrosobenzene procedure. We have also found that this nitrosoamine provides higher yields of the related $\mathbf{Ga_{13}^{o}}$ complex as well as a series of related mixed-metal clusters, all of which can be isolated in gram quantities.[33]

A drawback to the use of KOH as the base in this procedure is isolation of pure $\mathbf{Al_{13}^{o}}$ from the powdery KNO_3 that presumably forms in the reaction as well. To avoid this time-consuming workup, we have successfully employed $Al(OH)_3$, NH_4OH, and NBu_4OH as alternate bases; all the salts that form as byproducts are soluble in the final oily mixture from which the $\mathbf{Al_{13}^{o}}$ crystals are collected (Route B, **Scheme 3.5**).

The single crystal X-ray structure of the "flat"-$\mathbf{Al_{13}^{o}}$ cluster reveals a planar centrosymmetrical Anderson-type[34,35] $Al(\mu_3\text{-}OH)_6Al_6(\mu_2\text{-}OH)_6$ core fragment surrounded by six aluminum ions.[‡] The outer six aluminum cations alternate above and

---

[‡] xray X-ray diffraction experiments were carried out on a Bruker Smart Apex diffractometer at 153 K (**1**) and 173 K (**2**) K using MoKα radiation (l=0.71070 Å). Absorption corrections were applied by SADABS. The structures were solved by direct methods, completed by subsequent difference Fourier syntheses, and refined by full matrix least squares procedures on F^2. Highly disordered NO_3 anions and solvent water molecules in the crystal structure of **1** were treated by SQUEEZE.[36]. . Correction of the X-ray data by SQUEEZE is 353 electron/cell; the calculated value for these nine NO_3 anions and seven water molecules in **1** is 349 electron/cell. All non-hydrogen atoms were refined with anisotropic thermal parameters. H atoms in **1** were found on the difference F-map and refined with isotropic thermal parameters. Some of the H atoms in the coordinated water molecules in **1** are disordered over three positions due to their involvement in three different H-bonds, and they were refined with occupation factor μ=0.66. H atoms in **2** were not found and have not been taken into consideration. There is also a partial occupancy NH_4^+ cation in **2** on a special position (μ=0.5). All calculations were performed by the Bruker SHELXTL package.

Crystal data for **1**: $H_{90}Al_{13}N_{15}O_{102}$, M_r=2283.61, colorless block, 0.31 x 0.18 x 0.09 mm, Triclinic, space group *P*-1 (no.2), a = 12.8256(8), b = 13.1667(8), c = 13.4201(8) Å, α = 77.6010(10), β = 74.0590(10), γ = 87.6480(10)°, V = 2127.9(2) Å^3, Z = 1, r_{calcd} = 1.785 g·cm^{-3}, μ = 0.312 mm^{-1}, F(000) = 1180, $2\theta_{max}$ = 56.58°, 22455 reflections collected, 9682 unique [R_{int} = 0.0203], R indices [I>2σ(I)]: R1 = 0.0479, wR2 = 0.1267, GOF = 1.069.

Crystal data for **2**: $H_{96}Al_{13}N_{17}O_{106}$, M_r=2381.68, colorless block, 0.08 x 0.08 x 0.05 mm, Triclinic, space group *P*-1 (no.2), a = 12.623(3), b = 13.251(3), c = 13.597(3) Å, α = 74.877(4), β = 72.419(4), γ = 86.790(4)°, V = 2092.4(2) Å^3, Z = 1, r_{calcd} = 1.890 g/cm^{-3}, μ = 0.326 mm^{-1}, F(000) = 1232, $2\theta_{max}$ = 50.0°, 15065 reflections collected, 7308 unique [R_{int} = 0.0700], R indices [I>2σ(I)]: R1 = 0.0836, wR2 = 0.1961, GOF = 1.051.

below the planar core defined by the central 7 metal ions, and they are coordinated by four terminal aquo ligands. Two μ_3-bridging hydroxide ligands connect each of these $Al(H_2O)_4$ fragments to each other and to the central core.[1, 19, 25, 26] Two different single crystal forms were obtained from the syntheses; however, the cluster cations are nearly identical (see bond lengths in Scheme 3.4 and Supporting Information). Synthetic routes **A** and **B** (base = KOH or $Al(OH)_3$) both provide structure **1** ($\mathbf{Al_{13}}$•$9(H_2O)$), whereas route **B** (base = NH_4OH) provides structure **2** ($\mathbf{Al_{13}}$•$(NO_3)(NH_4)(H_2O)_{10}$), which has an extra nitrate and ammonium counter-ion.

The $\mathbf{Al_{13}}^{o}$ polycations determined in this work have a similar structure to the $\mathbf{Ga_{13}}^{o}$ cluster cation in which all the metal centers are octahedral (Figure 1A).[1, 31] In the crystal structures, both the $\mathbf{Al_{13}}^{o}$ clusters are centrosymmetric in contrast to the $\bar{3}$ crystallographic symmetry of the Ga_{13} cluster cation, although the idealized symmetry of the $\mathbf{Al_{13}}^{o}$ clusters cations is close to $\bar{3}$. In **1** the $\mathbf{Al_{13}}^{o}$ clusters are surrounded by NO_3^- anions and solvent water molecules forming O-H···O hydrogen bonds. In the case of the crystals grown from the reaction using NH_4OH as base, one molecule of NH_4^+ also co-crystallizes, necessitating the presence of an extra NO_3^- counter-ion (16 total) for charge balance. The hydrogen atoms of both the coordinating water molecules and those of the bridging μ-OH ligands are involved in numerous intermolecular H-bonds. Similar hydrogen bonding is observed between clusters in $\mathbf{Ga_{13}}^{o}$ as well.

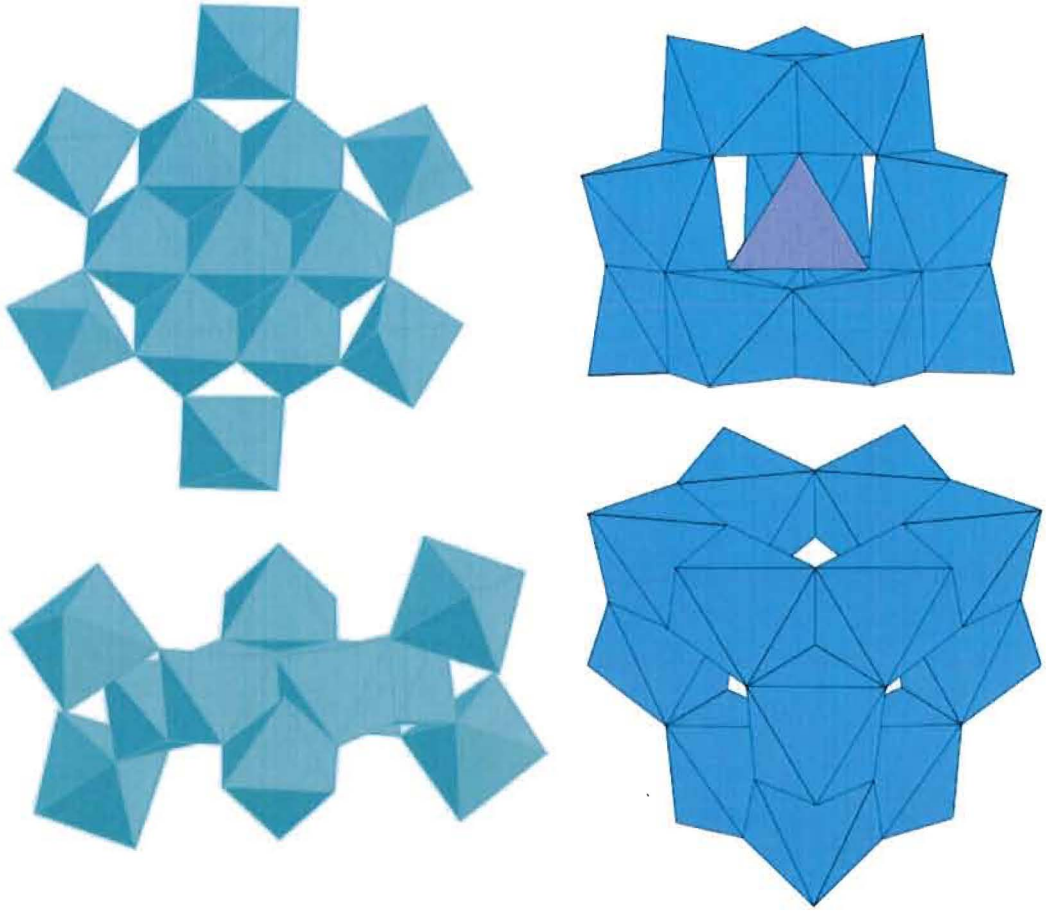

A B

Figure 3.6 A) Polyhedral representation of "flat" M_{13} Keggin-like nanoclusters; B) Polyhedral representation of ε-Keggin $M_{13}{}^{t}$ structure-type comprising 12 octahedral metal centers (blue) that share vertices with a central tetrahedral (purple) metal center.

Our method has allowed for the facile synthesis of $\mathbf{Al_{13}}^{o}$ clusters showing the generality of our strategy for preparing inorganic nanoclusters. A procedure for synthesizing preparative amounts of clusters of this type may have utility to researchers in the field trying to use these clusters as discrete molecular mimics of minerals or as single source precursors for thin film oxide materials.[6, 21]

Supporting Information Available. X-ray data and details of X-ray diffraction studies in CIF format, powder XRD and TGA data on $\mathbf{Al_{13}}$. This material is available free of charge via the Internet at http://pubs.acs.org.

CHAPTER IV

NOVEL HETEROMETALLIC TRIDECAMERIC INORGANIC NANOCLUSTER

The synthetic procedure in this chapter was developed by a number of lab members including Jason T. Gatlin and Zachary L. Mensinger. Zachary L. Mensinger contributed substantially to this chapter by participating in the development of a standard synthetic procedure. I was the primary contributor to the optimization of the synthetic conditions and developed the purification procedure. Dr. Lev N. Zakharov was helpful in solving the crystal structures. Stephen T. Meyers and Dr. Prof. Douglas A. Keszler were helpful in the VT PXRD characterization of the clusters. Stephen T. Meyers and Dr. Prof. Douglas A. Keszler also used the tridecameric clusters as synthons for the synthesis of the think film oxides. This work has not yet been published but will be submitted to the journal *Angewandte Chemie International Edition*. Zachary L. Mensinger initially identified the alternate nitroso reductant for cluster synthesis, which yields the identical cluster to the Nitrosobenzene synthesis. Dr. Prof. Darren W. Johnson was the principle investigator for this work.

The following chapter discusses the inorganic side of the tridecameric cluster formation. This bridge and the following chapter detail new research into heterometallic tridecameric nanoclusters. Modifications of the $\mathbf{Ga_{13}}^{o}$ synthesis via a slight change in the reaction pH allowed for the synthesis of the previously known analogous flat $\mathbf{Al_{13}}^{o}$ inorganic nanocluster. An alternate reductant was discovered that delivers both the $\mathbf{Ga_{13}}^{o}$ and the $\mathbf{Al_{13}}^{o}$ clusters in higher yields; this is presumably because of the ease of isolation.

There are numerous examples of mixed metal Keggin clusters of the ratio $MO_4(M'O_6)_{12}$, where M is the central tetrahedral metal and all the peripheral metal centers are octahedral. The previously know flat M_{13}^{o} clusters, $\mathbf{Al_{13}}^{o}$ and $\mathbf{Ga_{13}}^{o}$, have all been homometallic and the question raised is whether other flat M_{13}, both homo- and heterometallic clusters besides the previously known $\mathbf{Al_{13}}^{o}$[1, 2] and $\mathbf{Ga_{13}}^{o}$[3, 4] clusters be synthesized in the same manner. Searches of the literature have yielded no reported synthesis of heterometallic flat M_{13}^{o} clusters.

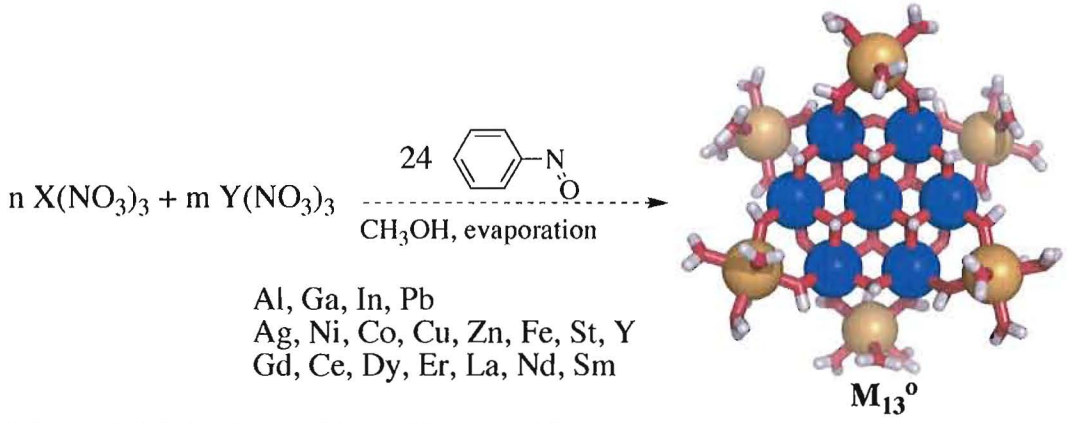

Scheme 4.1. Mixed group binary Metal combinations.

Multiple combinations and ratios of metals were used in an attempt to synthesize new heterometallic M_{13}^{o} clusters. In an attempt to determine the generality of this new

found reaction, over one hundred binary combinations of commercially available metal nitrate salts were combined with stoichiometric amounts of the original reductant nitrosobenzene in methanol and allowed to evaporate in the same manner as the original cluster formation. A major problem with the reaction set is that the organic additive of nitrosobenzene yields a very viscus dark oil. When these experiments were run, the new alternate reductant of DBNA had not yet been discovered. The vast majority of crystals screened using nitrosobenzene yielded only starting materials. In addition to mixing metals from groups a series of experiments was to set up that only contained group 13 metals with a 1:12 ratio of metal salts (Table 3.2.1), in the hope that the substitution would occur only at the central location.

Table 4.1. Ratios of the mixed group 13 cluster synthesis

Al	Ga	In
1	1	
1		1
	1	1
1	12	
12	1	
	12	1
	1	12
1		12
12		1

A series of new tridecameric heterometallic Ga/In clusters were synthesized by varying the starting ratio of $Ga(NO_3)_3$ and $In(NO_3)_3$ salts (**Scheme 4.1**). An n:m ratio of 1:12, $Ga(NO_3)_3$:$In(NO_3)_3$ resulted in a $\mathbf{Ga_7In_6^0}$ nanocluster. A $\mathbf{Ga_8In_5^0}$ cluster is obtained when the n:m ratio was 1:6, and a n:m ratio of 7:6 afforded $\mathbf{Ga_{10}In_3^0}$. Symmetry of the $\mathbf{Ga_7In_6^0}$ cluster cation is $\bar{3}$ which is analogous flat $\mathbf{Ga_{13}^0}$ and flat $\mathbf{Al_{13}^0}$ nanoclusters.[4, 5] All of the heterometallic clusters are isostructural with $\mathbf{Ga_{13}^0}$. They

posess the same $Ga_1(\mu_3\text{-}OH)_6Ga_6(\mu_2\text{-}OH)_6$ core, but vary in the gallium or indium atoms forming the third M-shell of the cluster (**Figure 4.1**). Unfortunately, there is no quick way to screen the crystal composition aside from collecting full XRD data sets. Bond distances and electron count allow for identification of the clusters (all clusters are similar, but possess different disorder in Ga/In – See Supplemental). This could be used as a predictive strategy for the formation of other heterometallic clusters.

Table 4.2. Starting material ratios compared to XRD and EPMA data of crystals.

	Starting Material		Characterization					
			XRD		EA		EPMA	
	Gallium	Indium	Gallium	Indium	Gallium	Indium	Gallium	Indium
Ga_{13}	13	0	13	0	13	0	-	-
$Ga_{12}In$	5	1	12	1	12	1	12	1
$Ga_{11}In_2$	2	1	11	2	11	2	11	2
$Ga_{10}In_3$	7	6	10	3	9	4	10	3
Ga_9In_4	1	2	9	4	-	-	-	-
Ga_8In_5	2	11	8	5	-	-	-	-
Ga_7In_6	1	12	7	6	6	7	6	7

The addition of acid did not yield new clusters, as the NO_3^- anion was used up and the starting metal salts were able to recrystalize back. The crystal structures and starting material ratios were successfully used to form a predictive method for future heterometallic clusters.

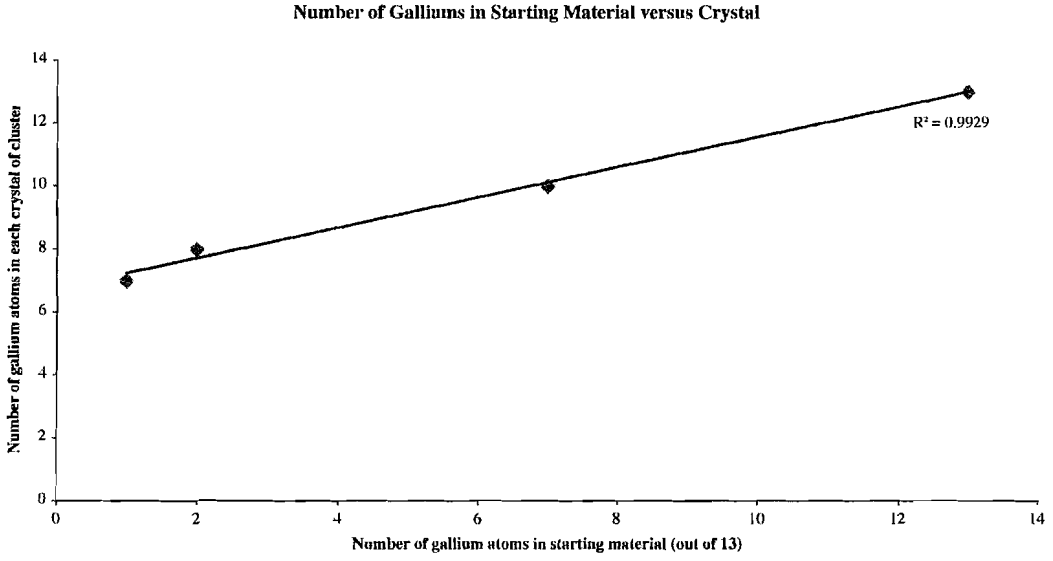

Graph 4.1. Plot of gallium numbers in crystal product versus starting material

Unfortunately, heterometallic and homometallic clusters of metals other than those from group 13 have not been obtained. Currently success with these experiments has centered on heterometallic group 13 metals of just Al, Ga and In metal centers. A few data points have been successful in predictively making all seven in the series from $\mathbf{Ga_{13}^{o}}$ to $\mathbf{Ga_7In_6^{o}}$, **Figure 4.2**. However there has been no observable indium substitution in the inner core. We theorize that it is related to the large ionic radius of the indium cation. Future work will need to explore the potential to incorporate other metals from other groups into the nanoclusters, as well as finishing out the mixed metal Group 13 series in both the gallium:indium and the aluminum:indium series. In addition to the mixed gallium and indium clusters, an analogous $\mathbf{Al_8In_5^{o}}$ tridecameric nanocluster was also successfully synthesized.

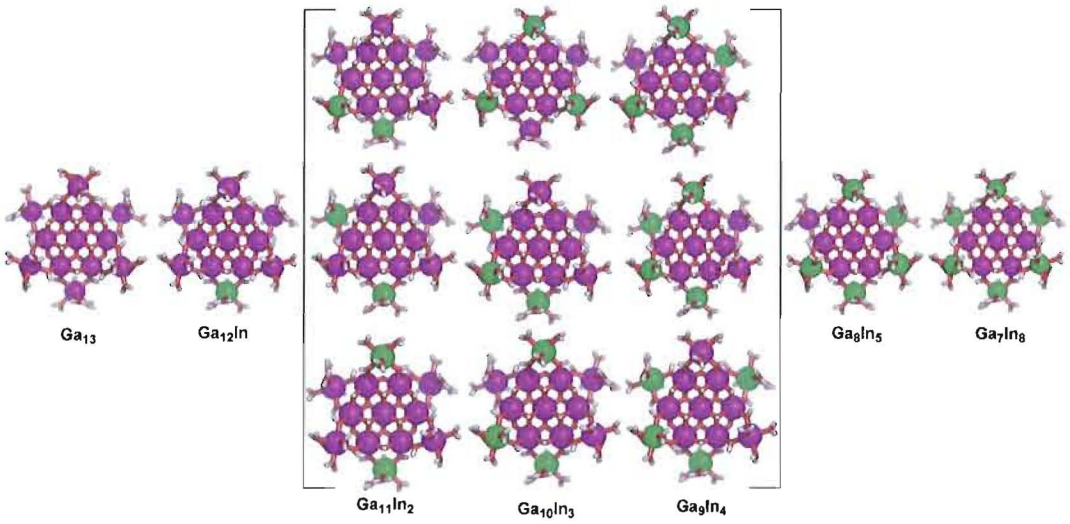

Figure 4.1. Gallium and Indium Heterometallic nanocluster series, with distribution.

After isolation of $\mathbf{Ga_{13}}^{o}$ and $\mathbf{Al_{13}}^{o}$ using DBNA, further experiments were carried out using the alternative reductant. This made screening for new crystals much easier, since the presence of crystals could easily be seen without magnification. Since decanting the oil formed as a byproduct made isolating the remaining crystalline product easy. There was less hunting in the organic residue for crystals.

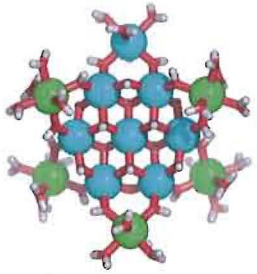

Figure 4.2. The heterometallic $\mathbf{Al_8In_5}^{o}$ cluster, synthesized by Z.L.M.

Surface chemistry of our nanoclusters by SEM and EPMA is being explored and will be discussed in Chapter V. In the following chapter the first synthesis of the heterometallic $\mathbf{Ga_7In_6}^{o}$ nanocluster is discussed. A potential use for these clusters is in

thin film oxides. This will be explored as part of a collaboration with the Keszler group at Oregon State University.

Our research has focused on inorganic metal-hydroxo nanoclusters of group 13 metals, such as our recently reported $Ga_{13}(\mu_3\text{-}OH)_6(\mu_2\text{-}OH)_{18}(H_2O)_{24}(NO_3)_{15}$ (flat-Ga_{13}^{o}) cluster (this structure was independently isolated and reported by Fedin, et al.).[6] The $M(\mu_3\text{-}OH)_6M_6(\mu_2\text{-}OH)_6$ central fragment of this cluster forms a planar core with six additional $M(H_2O)_4$ groups bound to the core via two μ_2-OH bridges each. The outer metal ions occupy alternate positions above and below the plane formed by the central seven metal ions. Metal complexes of this class are fairly rare, and typically consist of aluminum[1, 7, 8], though several gallium complexes have recently been reported as well (ours, Fedin, Heath). Inorganic-only and ligand-supported clusters have been synthesized, with the latter generally being more common. One aspect that has been notably absent so far in this class is mixing of metal compositions within the same molecule, as well as clusters containing indium. Mixed-metal clusters are well known for other metal-oxo-hydroxo and metal-oxo clusters, such as Keggin-Al_{13}^{t} and Anderson-type clusters, two classes of molecules that are related to our flat-M_{13}^{o}. In the case of Keggin tridecamers, the central tetrahedral metal can be substituted, forming compositions of M_1Al_{12} (M = Al, Ga, or Ge have been conclusively demonstrated, with others suggested).[9-19] Extensive reports exist for substitution of the central metal in B-type Anderson clusters as well, affording clusters of general formula $M(OH)_6Mo_6O_{18}^{n-}$, (M = Mn^{2+}, Fe^{2+}, Fe^{3+}, Co^{2+}, Co^{3+}, Ni^{2+}, Cu^{2+}, Zn^{2+}, Al^{3+}, Ga^{3+}, Cr^{3+}, Rh^{2+}, and Pt^{2+} and n = 2 or 3) in addition to various tungstates. To the best of our knowledge however, no such larger

nuclearity mixed-metal metal-hydroxo clusters consisting of aluminum or gallium have been reported.

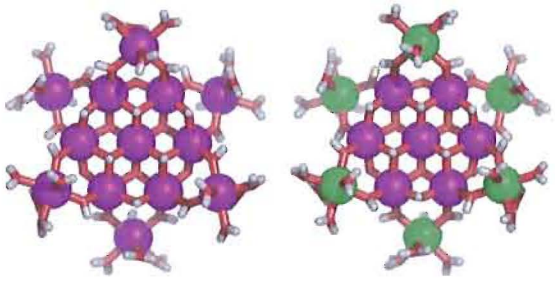

1 2

Figure 4.3. **1** is $Ga_{13}(\mu_3\text{-}OH)_6(\mu_2\text{-}OH)_{18}(H_2O)_{24}(NO_3)_{15}$ and **2** $Ga_7In_6(\mu_3\text{-}OH)_6(\mu_2\text{-}OH)_{18}(H_2O)_{24}(NO_3)_{15}$

Prior synthetic preparation of this class of compounds has at times also proven quite difficult. Their synthesis often requires caustic or acidic conditions and high temperatures. Crystallization periods of months or even years are not uncommon.[1, 7, 20] Due to these difficulties, relatively few metal-hydroxo clusters of aluminum and other group 13 metals have been synthesized, fewer still inorganic only clusters. An additional synthetic method for clusters of this class would be welcomed by researchers in the fields of environmental and geochemistry. Herein we report a previously unknown structure, $Ga_7In_6(\mu_3\text{-}OH)_6(\mu_2\text{-}OH)_{18}(H_2O)_{24}(NO_3)_{15}$ (flat-Ga_7In_6), consisting of a mixed-metal gallium-indium structure. This cluster can be synthesized reliably in moderate yields utilizing our previously reported synthetic method, and in excellent yields with the use of a different nitroso compound, presented herein.

As an example, we have already begun exploring one application for theses clusters, driven by a rising interest in printed macroelectronics and the high carrier mobilities recently reported in disordered Group-13 and other p-block oxides. [21-23] Most solution precursors for printed oxide films involve controlled hydrolysis of metal-organic compounds and the condensation of metal-hydoxo "sols" which are then pyrolyzed to form the oxide. Such films are beset by a variety of density, defect, and segregation issues relating to the inhomogeneous nature of the sol and retention of significant organic components. From this perspective, soluble all-inorganic, heterometallic hydroxo-clusters provide model oxide precursors driven by similar hydrolysis and condensation principles, but lacking detrimental organic moieties.

In this contribution we report a previously unknown structure, $Ga_7In_6(\mu_3\text{-}OH)_6(\mu_2\text{-}OH)_{18}(H_2O)_{24}(NO_3)_{15}$ (flat-Ga_7In_6), consisting of a mixed-metal gallium-indium structure. This cluster can be synthesized reliably in moderate yields utilizing previously reported synthetic methods, and in excellent yields with the use of a different nitroso compound, presented herein. Finally, we describe the adaptation of these structures as precursor solutions for oxide semiconductor thin-films by fabricating high-performance thin-film transistors (TFTs) with spin-coated $In_{0.92}Ga_{1.08}O_3$ channel layers.

Our previous report describes the mild preparation of the inorganic flat-$\mathbf{Ga_{13}}^{\circ}$ compound, prepared by dissolving $Ga(NO_3)_3$ and nitrosobenzene in MeOH followed by slow evaporation. Crystals are then manually separated from the resultant black tar-like product mixture. Using this method, yields up to 65% of flat-$\mathbf{Ga_{13}}^{\circ}$ could be obtained in small scale. This same procedure was applied to a mixture of $Ga(NO_3)_3$ and $In(NO_3)_3$ in a

1:12 ratio, which afforded a mixed-metal, flat-$\mathbf{Ga_7In_6^o}$ cluster in 25% yield. Again, crystals were manually separated from the black product mixture. The prospect of mixed-metal clusters of this class has not been addressed to our knowledge.

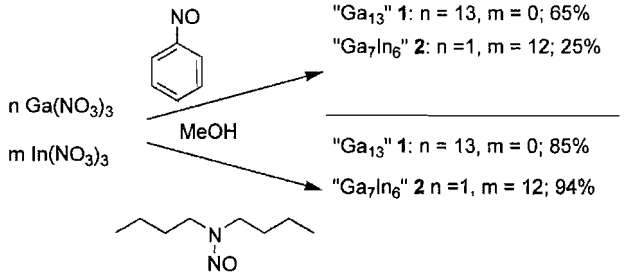

Scheme 4.2. Redox reaction forming $\mathbf{Ga_{13}^o}$ and heterometallic clusters.

Scheme 4.2 depicts the synthetic route to structures **1** and **2** using two different nitroso compounds. Symmetry of the flat-$\mathbf{Ga_7In_6^o}$ cluster cation is $\bar{3}$ as with the analogous flat-$\mathbf{Ga_{13}^o}$ cluster.[4] Compound **2** is isostructural with **1**, possessing the same $Ga(\mu_3\text{-}OH)_6Ga_6(\mu_2\text{-}OH)_6$ core, but varies with indium atoms forming the third M-shell in the cluster connected via μ_2-OH bridges (**Figure 4.2**). We have also conducted experiments aimed at controlling the ratio of Ga:In present in these mixed-metal clusters, and these results will be presented in a future publication. Unfortunately, there is currently no quick way to screen the crystal composition aside from collecting full XRD data sets, where bond distances and electron count allow for identification of the clusters. Surface chemistry by SEM and EPMA are being explored.

To address the problems of difficult isolation and limited reaction scale, we sought alternative nitroso compounds to nitrosobenzene. The most successful so far has been *N*-nitroso-di-*n*-butylamine. This compound is a slightly yellow viscous liquid with low vapor pressure. Use of this alternative nitroso compound affords clusters **1** and **2** in

superior yields, 85% and 95% respectively. The yields are likely increased in part because the reaction with *N*-nitroso-di-*n*-butylamine produces a mixture that is a transparent oil instead of the viscous black tar found in the reaction with nitrosobenzene. The solid crystalline product is thus easier to isolate from the reaction with *N*-nitroso-di-*n*-butylamine. *N*-nitroso-di-*n*-butylamine is removed via syringe, and the remaining crystals are washed with cold EtOAc (three times) and dried. *N*-nitroso-di-*n*-butylamine allows preparation of compounds **1** and **2** in gram scale quantities.

All-inorganic hydroxocation condensation routes to dense, high-quality oxide dielectric films have been lately demonstrated[24, 25] Based on these results, the discrete hydroxo clusters **1** and **2** were immediately recognized as potential oxide precursors operating on similar principles. Cluster **2** is of particular interest due to the large indium fraction and the excellent performance of In_2O_3-based semiconductors.

Thin Film Transistors with amorphous $In_{0.92}Ga_{1.08}O_3$ (IGO) channels derived from spin-coated aqueous solutions of **2** will be described more fully in a forthcoming publication, though preliminary device characteristics are presented in **Figure 4.4**. V_{on} for the device shown is, -6 V while on-to off current ratios are > 10^6 on thermally grown SiO_2 dielectrics. Field-effect mobilities for these bottom-gate devices are ~ 9 $cm^2 V^{-1} s^{-1}$ after annealing to 600 °C. The direct deposition of such high-performance semiconductors from aqueous solutions is unprecedented, and an important step towards printed macroelectronics.

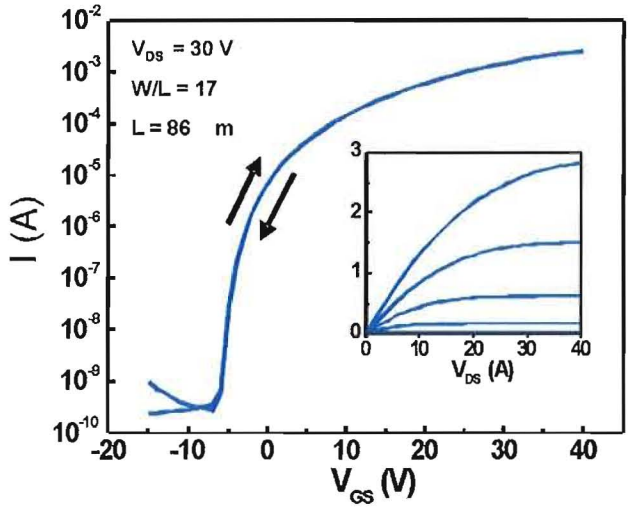

Figure 4.4. Preliminary TFT Characterisitic trace. Representative transfer and (inset) output characteristics for a bottom-gate IGO-channel TFT with a thermally grown SiO_2 dielectric. V_{GS} in the output curve is stepped from 0–40 V in 10 V steps

We have been able to devise a new green synthetic strategy for making clusters of gallium, which proceeds faster using fewer caustic chemicals and milder temperatures. We have expanded this strategy and shown general utility by synthesizing new heterometallic clusters of aluminum, gallium, and indium, doing so in a controlled fashion. The synthesis utilizes the organic oxidation of the easily oxidized compounds nitrosobenzene and *N*-nitroso-di-*n*-butylamine, coupled with the crystallization of a gallium cluster from solution.[4] Insofar as these molecules might hold promise as single source precursors for novel materials (e.g., thin films), developing a green synthetic method is highly relevant. We have also helped shed light on the mechanism of cluster growth. Previous work suggests that a M_2 fragment forms initially. We have yet to see any structure with different composition of the first seven metal atoms, suggesting the M_7

core might be particularly stable. The mixed-metal nature of this structure may also provide insight into the nature of mineral formation, as many minerals contain multiple metal ions.

We have been able to devise a new green synthetic strategy for making clusters of gallium, which proceeds faster using fewer caustic chemicals and milder temperatures. We have expanded this strategy and shown general utility by synthesizing new heterometallic clusters of aluminum, gallium, and indium, doing so in a controlled fashion. The synthesis utilizes the organic oxidation of the easily oxidized compounds nitrosobenzene and *N*-nitroso-di-*n*-butylamine, coupled with the crystallization of a gallium cluster from solution.[4] Insofar as these molecules might hold promise as single source precursors for novel materials (e.g., thin films), developing a green synthetic method is highly relevant. We have also helped shed light on the mechanism of cluster growth. Previous work suggests that a M_2 fragment forms initially. We have yet to see any structure with different composition of the first seven metal atoms, suggesting the M_7 core might be particularly stable. The mixed-metal nature of this structure may also provide insight into the nature of mineral formation, as many minerals contain multiple metal ions.

CHAPTER V

ToF-SIMS CHARACTERIZATION OF M_{13} INORGANIC NANOCLUSTERS

I was the primary contributor to the optimization of the synthetic conditions in this study and developed the purification and sample preparation procedure. Dr. Stephen L. Golledge was very helpful in the operation of the ToF-SIMS instrumentation, and in training and aiding me on data analysis. I was the primary contributor to the assignment and determination of peaks. This work has not yet been published but will be submitted to either *Surface and Interface Analysis* or the *Journal of the American Chemical Society*. Dr. Prof. Darren W. Johnson was the principal investigator for this work.

Characterization of the flat M_{13} nanoclusters has proven to be very difficult, especially in solution. The hydroxo protons of the nanocluster provide very little in the way of a spectroscopic handle in proton nuclear magnetic resonance (^{1}H-NMR) due to their rapid exchange in aqueous solution. No signal was seen for either ^{69}Ga or ^{71}Ga in solution NMR. This could be because of a low functional concentration for the instrument or it could be due to the difficultly in tuning a to new nucleus, although acquisition of aqueous Ga-NMR spectra has been reported in the literature. Solution high performance liquid chromatography-mass spectrometry (HPLC-MS) has aided in the isolation of the nitrobenzene product from the oxidation of nitrosobenzene (Chapter II). However, the HPLC-MS did not yield definitive results for the methanol dissolved tridecameric clusters. Current conditions tested for the cluster and other for organic by-products from the reaction have not yet yielded results. The stability of the intact cluster in aqueous solvents is not known, but it can be recrystalized after dissolving in MeOH.

As a result we have moved toward characterizing the crystalline products as solids. Solid state Ga-NMR has not yet been attempted but will most likely suffer from the same tuning problems as the solution studies; however, concentration should not be a factor here. All the tridecameric nanocluster products have been characterized by single crystal X-ray diffraction (SXRD) and then by thermogravometric analysis (TGA) of the crystals to determine the products. This information is very useful but only tells starting and ending points. In addition, the data collection process takes over half a day.

Elemental analysis has been attempted *via* normal induced coupled plasma (ICP) and with ionization from scanning electron microscopy (SEM) and electron probe micro analysis (EPMA) instruments. For EA, SEM and EPMA data collection itself is very fast, but there is much more time devoted to sample preparation. Characterization of the tridecameric nanoclusters or the organic product by various mass spectroscopic techniques has been attempted in the solid state on single crystals by Time of Flight Secondary Ionization Mass Spectrometry (ToF-SIMS). The following work describes in detail the solid-state characterization we have completed with SEM, EPMA and ToF-SIMS. This is a summary explaining characterization of current clusters; data analysis continues on previously collected samples.

The research strategy for producing tridecameric clusters yielded all seven variations of the outer ring substitution in the heterometallic M_{13} cluster, as detailed in chapters II and IV (**Figure 5.01**). The same samples were used for EA, SXRD, SEM, EPMA and ToF-SIMS. Not all instruments were used to collect data on all samples. ToF-SIMS instrumentation data were collected on samples **1-5** and **7**. Due to difficulty in data analysis, ToF-SIMS results from sample **1** are presented here with explanations of relevant future data analysis on the other collected data.

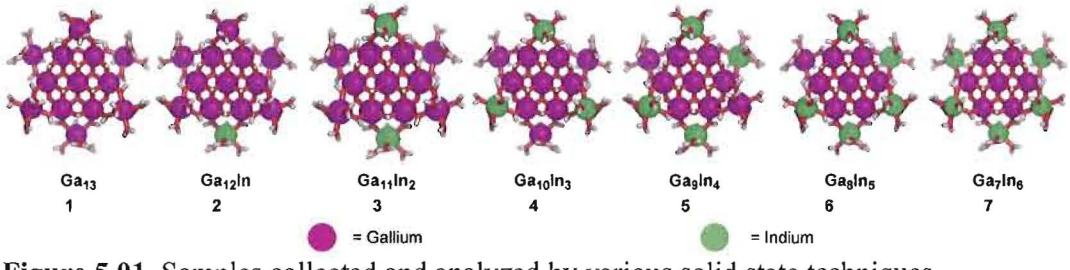

Figure 5.01. Samples collected and analyzed by various solid state techniques

All samples were first screened by single crystal XRD, and an electron count was performed in order to determine the occupancy of indium atoms in the outer ring. The same samples were then prepared for other analytical methods. All samples were used as solid single crystals. SEM samples were prepared with single crystals that were glued onto wafers of polished silica. SEM spectra of compounds **1** and **7** are shown in **Figure 5.02** and **Figure 5.03**, respectively. For sample **7** the areas under the gallium and indium peaks are integrated and yield a 7.5 to 5.5 ratio of gallium to indium. EPMA required the samples to be very flat; single crystals were embedded in resin, polished on an oil-lubricated grinder, then tested. The EPMA data did not agree with the data collected by other methods because of a poor instrument calibration. The results from SXRD, EA and EPMA data are shown in **Table 5.3**. The results are in reasonable agreement with the elemental analysis that was sent out for collection by ICP.

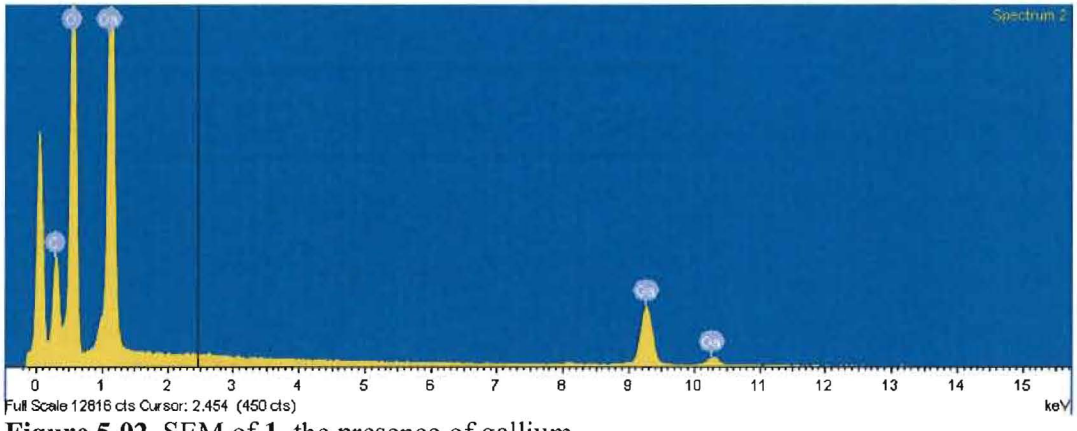

Figure 5.02. SEM of **1**, the presence of gallium

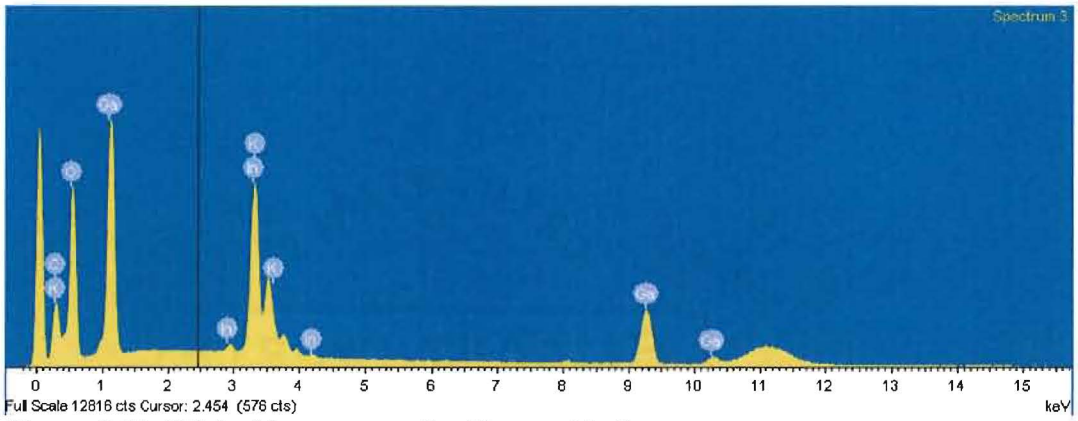

Figure 5.03. SEM of **2**, presence of gallium and indium

Table 5.1- Summary of XRD, EA and EPMA data: Starting Material, XRD, Elemental Analysis, and EPMA ratios

	Starting Material		Characterization					
			XRD		EA		EPMA	
	Gallium	Indium	Gallium	Indium	Gallium	Indium	Gallium	Indium
Ga_{13}	13	0	13	0	13	0	-	-
$Ga_{12}In$	5	1	12	1	12	1	12	1
$Ga_{11}In_2$	2	1	11	2	11	2	11	2
$Ga_{10}In_3$	7	6	10	3	9	4	10	3
Ga_9In_4	1	2	9	4	-	-	-	-
Ga_8In_5	2	11	8	5	-	-	-	-
Ga_7In_6	1	12	7	6	6	7	6	7

Surface chemistry from crystal ionization to catalyst screening has used ToF-SIMS for the characterization of metal complexes.[1] ToF-SIMS has proven to be useful in the quantitative analysis of surface complexes and depth profiling of thin films.[2-4] The literature thus far has focused on the first row transition metals.[5] The high resolution of the ToF-SIMS will aid in peak identification, although cluster fragmentation and isotope distributions will present challenges in data analysis.[5,6]

For compounds containing an element with an isotope distribution, MS can be both difficult because of the complex data generated and helpful in providing isotope

patterns. For the mixed metal clusters **2-7** the isotope distribution problem is compounded due to the addition of a second metal species with its own isotopic distribution. The distribution of multiple metals would be even more complicated. For that reason cluster **1** was analyzed first, to work out the issues in data analysis on a simpler compound.

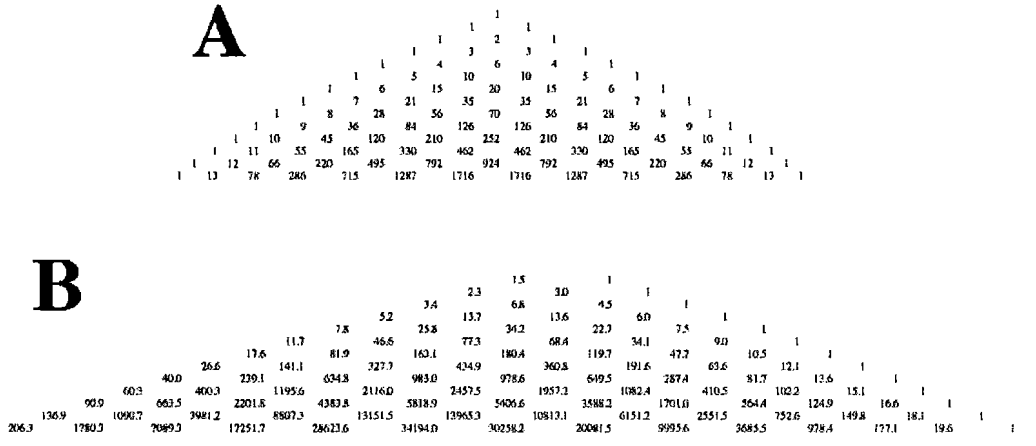

Figure 5.04. A.Standard Pascal's triangle distribution of a 1:1 isotope pattern of metals, B. Statistical distribution of isotopes of gallium species. The triangles show the relative abundance of isotope peaks for mulliple metal species of a simple 1:1 ratio and then the more complicated 1.5:1 gallium ratio.

A 1:1 ratio of isotopes would follow the standard Pascal Triangle, **Figure 5.04A**. The distribution pattern gets much more difficult when the isotopes are not in a 1:1 ratio.[7] The gallium isotope ratio is 60:40 of the ^{69}Ga and ^{71}Ga isotopes, which yields the distribution seen in **Figure 5.04B**. There is an "N +1 rule" for the dual isotopes of gallium. The analysis of that data is made more complex by the introduction of indium with ^{113}In and ^{115}In in a ratio of 4:96.

When two elements each with its own isotopes are present, the distribution patterns become much more complex. **Figure 5.05** shows a Ga_4 isotope pattern, an In_4 pattern, and a Ga_2In_2 pattern. Spectra C & E had to be enlarged in order to see all the peaks. The N+1 rule still applies for the number of metals present.

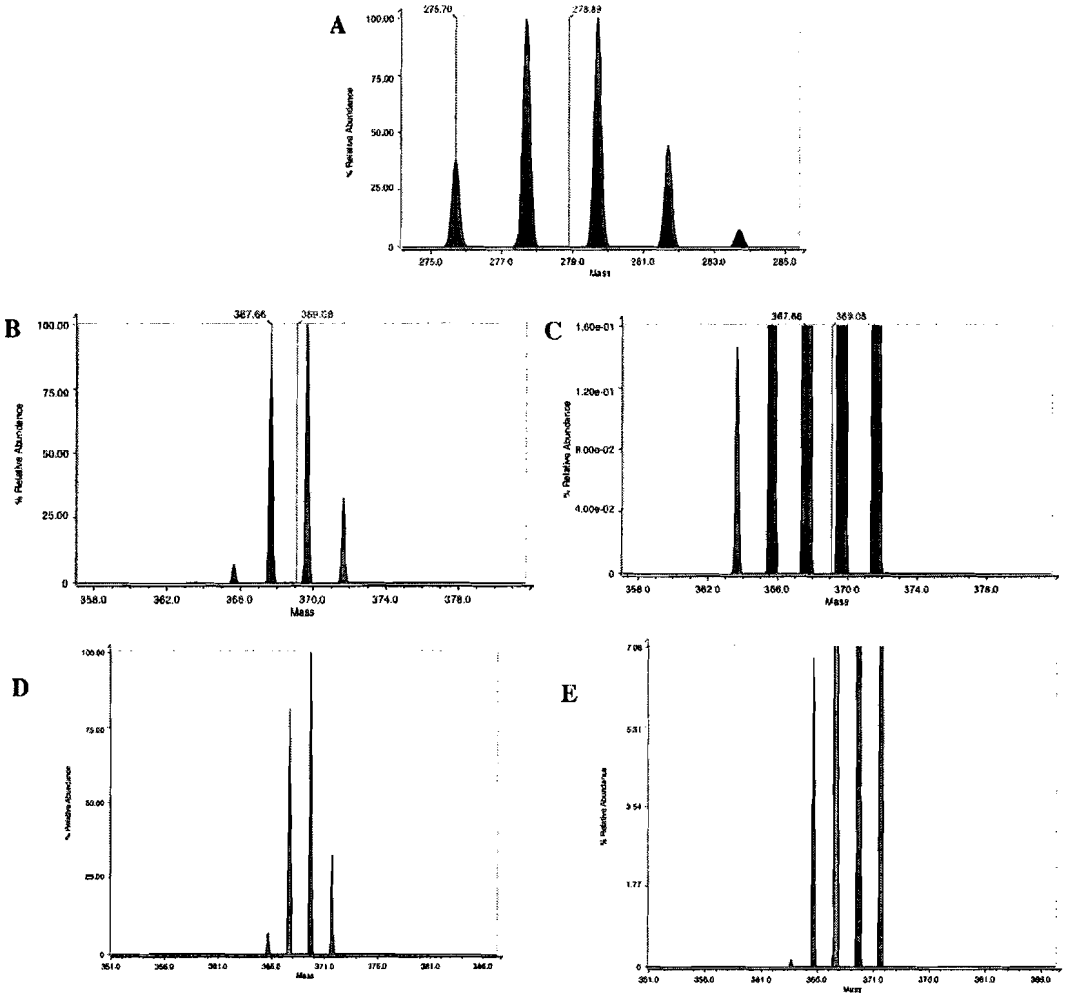

Figure 5.05. Isotope distributions of Ga_4, In_4, and Ga_2In_2.

The isotope distribution of the metals which originally concerned us actually proved to be quite useful, as the isotope patterns greatly aided in the determination of the number of metal centers that are in isolated clusters. They are much more complex with different isotopes. This has helped in the analysis of different spectra.

Different ionization energies in ToF-SIMS should allow for observation of different fragments, much as changing the cone voltage does on LC-MS. The Anderson-Evans cluster is held together with six (μ_3-OH) bonds aided with six (μ_2-OH) bonds, while the peripheral six metals in the tridecameric cluster are only held to the core by two (μ_2-OH) bonds each. The central core of seven metals of the tridecameric cluster should be a stable fragment, because it is the Anderson-Evans cluster, **Figure 1.01**. Thus, stable fragments should be ejected, although in these high-energy experiments small fragments could recombine into a larger stable clusters. A milder technique or other complementary analytical methods like MALDI or LC-MS would augment collected data and provide useful data.

In data analysis there are potentially two types of errors in the difference between actual fragments and the calculated components. Absolute error is the difference between the two, measured in m/z values Daltons/charge, while relative error is that difference divided by the target fragment then multiplied by one million, in units of ppm. As with NMR, the relative ppm error allows the signals to be related. Relative error shows the error progression along the spectra, which demonstrates how the error decreases as new points are added to the calibration curve, making each subsequent prediction more accurate.

There are very common fragments seen for metal oxo species depending on the oxidation state of the metals.[8, 9] There are also fewer options at such a low mass and almost no multiple metal species. All this allows for the entering of element counts into a spreadsheet to act as a mass calculator. This proved to be very useful, providing the beginning of the calibration curve for a more accurate peak fragment analysis and identification. The beginning of the calibration table is shown in **Table 5.2**. Patterns have already started to emerge of adding protons and isotope mixtures with multi metal clusters.

Table 5.2. Low nuclearity species peak assignments

Formula	Calculated	Observed	Error (Dalton)	Error (ppm)
$^{69}Ga_1O_3$	116.9238	116.9096	-0.0142	121
$^{69}Ga_1O_2(OH)_1$	117.9271	117.9191	-0.0080	68
$^{69}Ga_1O_1(OH)_2$	118.9305	118.9228	-0.0077	64
$^{69}Ga_1(OH)_3$	119.9338	119.9169	-0.0169	141
$^{69}Ga_2(OH)_2(H_2O)_1$	189.8672	189.8955	0.0283	149
$^{69}Ga_2(OH)_1(H_2O)_2$	190.8750	190.8611	-0.0139	73
$^{69}Ga_2(H_2O)_3$	191.8828	191.8849	0.0021	11
$^{69}Ga_2O_4$	201.8488	201.8332	-0.0156	77
$^{69}Ga_2O_3(OH)_1$	202.8521	202.8391	-0.0130	64
$^{69}Ga_2O_2(OH)_2$	203.8554	203.8230	-0.0324	159
$^{69}Ga_2O_1(OH)_3$	204.8588	204.8383	-0.0205	100
$^{69}Ga_2(OH)_4$	205.8621	205.8359	-0.0262	127
$^{69}Ga_2(OH)_3(H_2O)_1$	206.8699	206.8367	-0.0332	161
$^{69}Ga_2(OH)_2(H_2O)_2$	207.8778	207.8753	-0.0025	12
$^{69}Ga_2(OH)_1(H_2O)_3$	208.8856	208.8991	0.0135	65
$^{69}Ga_2(H_2O)_4$	209.8934	209.8755	-0.0179	85

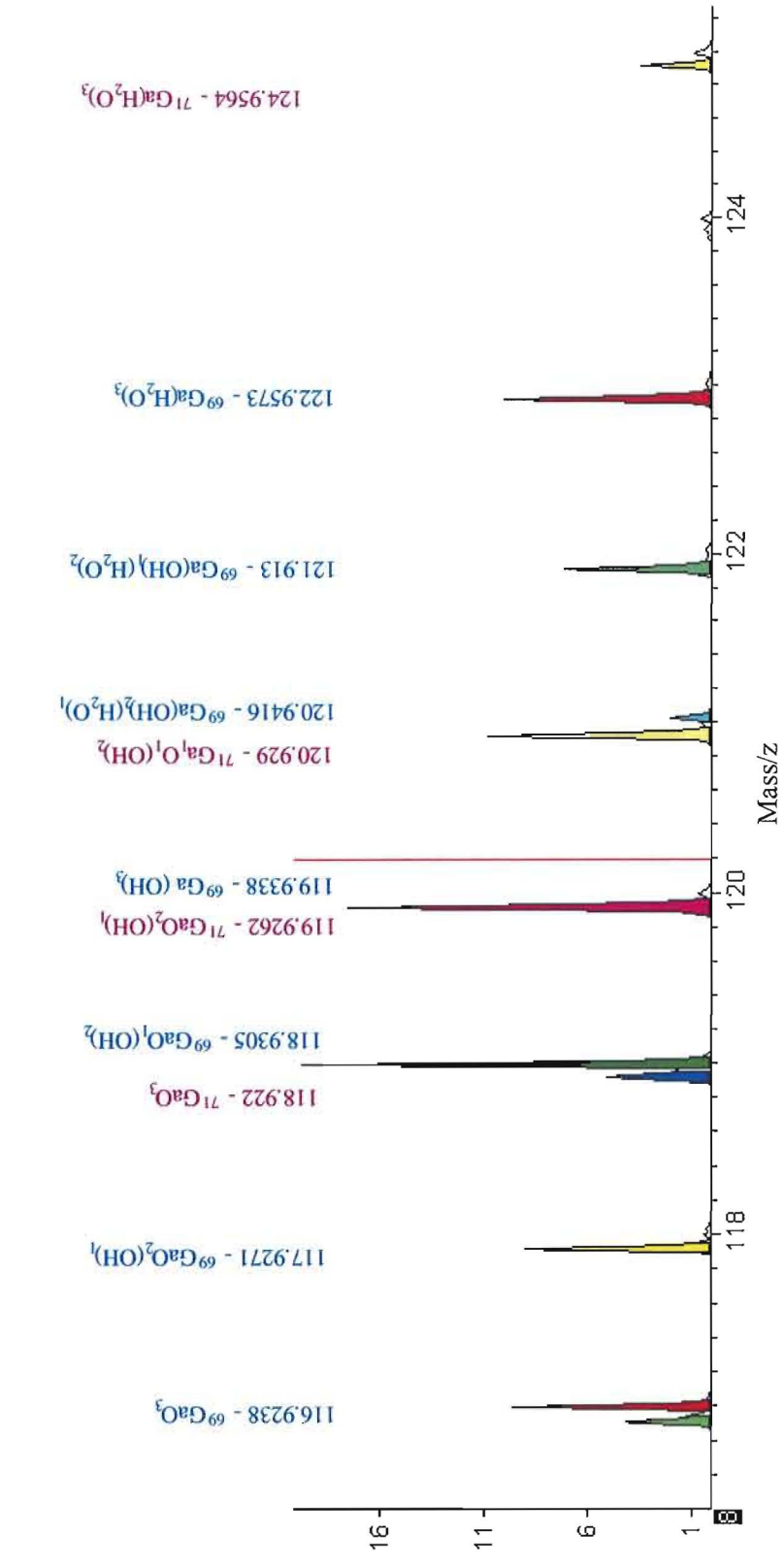

Figure 5.06. Low Mass range peak assignments..

When the mass and element are entered, a mass spectrum fragment calculator finds potential fragments that fit that stoichiometry. This calculator as well as most simple general chemistry calculators (that is, not part of a MS instrumentation package) do not take into account the isotopes of elements as seen, **Figure 5.06**. They only use the average mass, which means that no single peak can be entered in for its isotope clustering; only the middle or most intense peak is the target. This is where the real data is much more complicated than the simulated data without isotopes included. However, the same iMass program is able to show isotope distribution for a given molecular formula, **Figure 5.08b**. There appears to be a long range "AB: pattern, which could correlate to GaO and GaO_2 additions to the previous cluster. **Figure 5.07** shows a section of the ToF-SIMS spectra of compound **1** with an enlargement of the peaks clustered around 495 Daltons. This shows the interdigitated patterns as well as other small peaks that may be multiply-charged species.

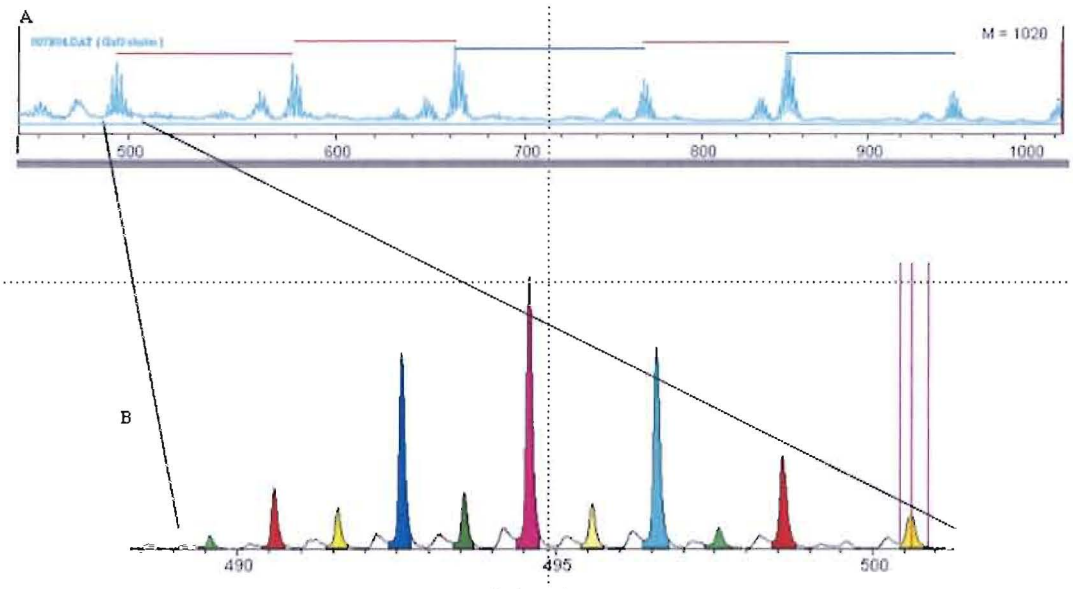

Figure 5.07. Mass spectrum of **1** from 550 to 1000 Daltons

With the aid of computer programs, data analysis has become much easier. There are programs used for protein characterization that use the spacing between the peaks to determine the charge of the fragments and, therefore, the mass of the parent ion. There are two ways of manually analyzing the data, either the plug and chug method of entering the mass and finding corresponding compounds *via* the commercially available mass spec fragment calculator, or plugging in chemically reasonable formulae and determining their mass. Both of these involve trial and error, but they do provide a good starting point. Alternately, the isotope distribution can be used to help determine a starting point with the ratios of the peaks revealing the number of gallium centers contained in each fragment. The difference is building up from the bottom or taking a top-down approach to peak assignment. The expanded section of **Figure 5.07B** is shown again in **Figure**

5.08A and the two interdigitated patterns that are offset by a single proton are color-coded. The red spectrum in A is very similar to the predicted pattern seen in B.

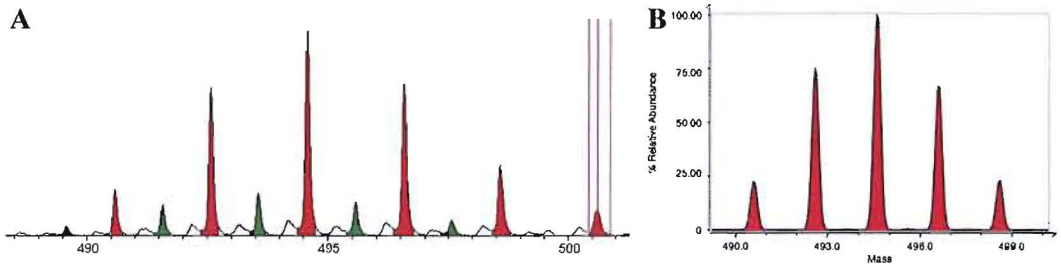

Figure 5.08. Expansion of Spectra 1 at 495 Daltons corresponding to a $Ga_5O_7(OH)_2$ fragment

A series of stable fragments were expected to be present, one of which was the Anderson-Evans core of M_7. The Anderson-Evans fragment was not observed. However, it was observed that there are other existing multiple metal clusters that could be potential fragments of a tridecameric cluster. There are two known M_8 clusters that are similar to the core of the M_{13} cluster.[10, 11] The physical difference between the two clusters involves the removal of one of the inner ring metal centers. This allows the two adjacent metals to bend out of the plane, relieving torsional strain. The remaining four metals are still planar as seen in Figure 5.09. If one outer metal is removed, and the structure is minimized and compared to the corresponding formula for the Anderson-Evans M_7 cluster, there is a large difference in minimized energies, with approximately 30 kcal/mol stabilizing energy for the Anderson-Evans cluster as determined by CAChe using the MM3 force field.[12]

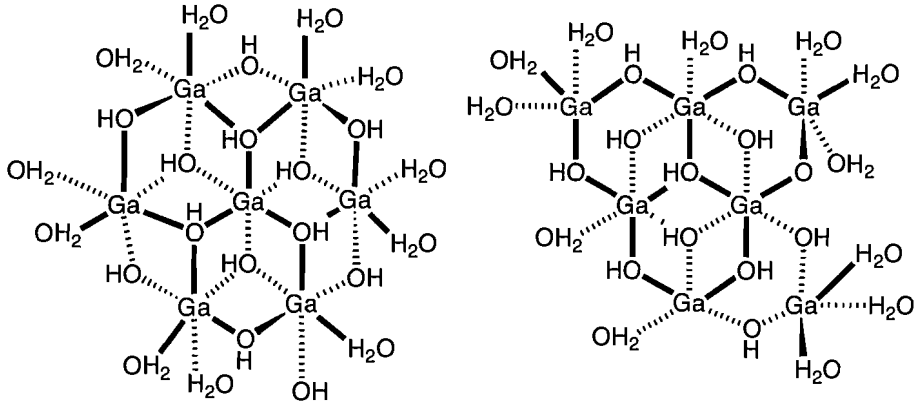

Figure 5.09. Stable M_7 POM fragments

Data that appears to be missing from the table is actually the result of peaks that are too small to resolve out the noise. This is where the isotope pattern has now provided diminishing returns, and where the smaller cluster that is made up exclusively of the lower isotope is very difficult to identify. ToF-SIMS is a highly energetic environment where electrons are easily transferred to the matrix and other fragments during flight, where actual fragments may not match expected ones.[13-19] Based on this data we can start to assign structures to the peaks that we see. **Figure 5.10** represents what we believe the fragments to be. This data assignment will help identify more peaks in the set and should be applicable to the heterometallic clusters **2-7**.

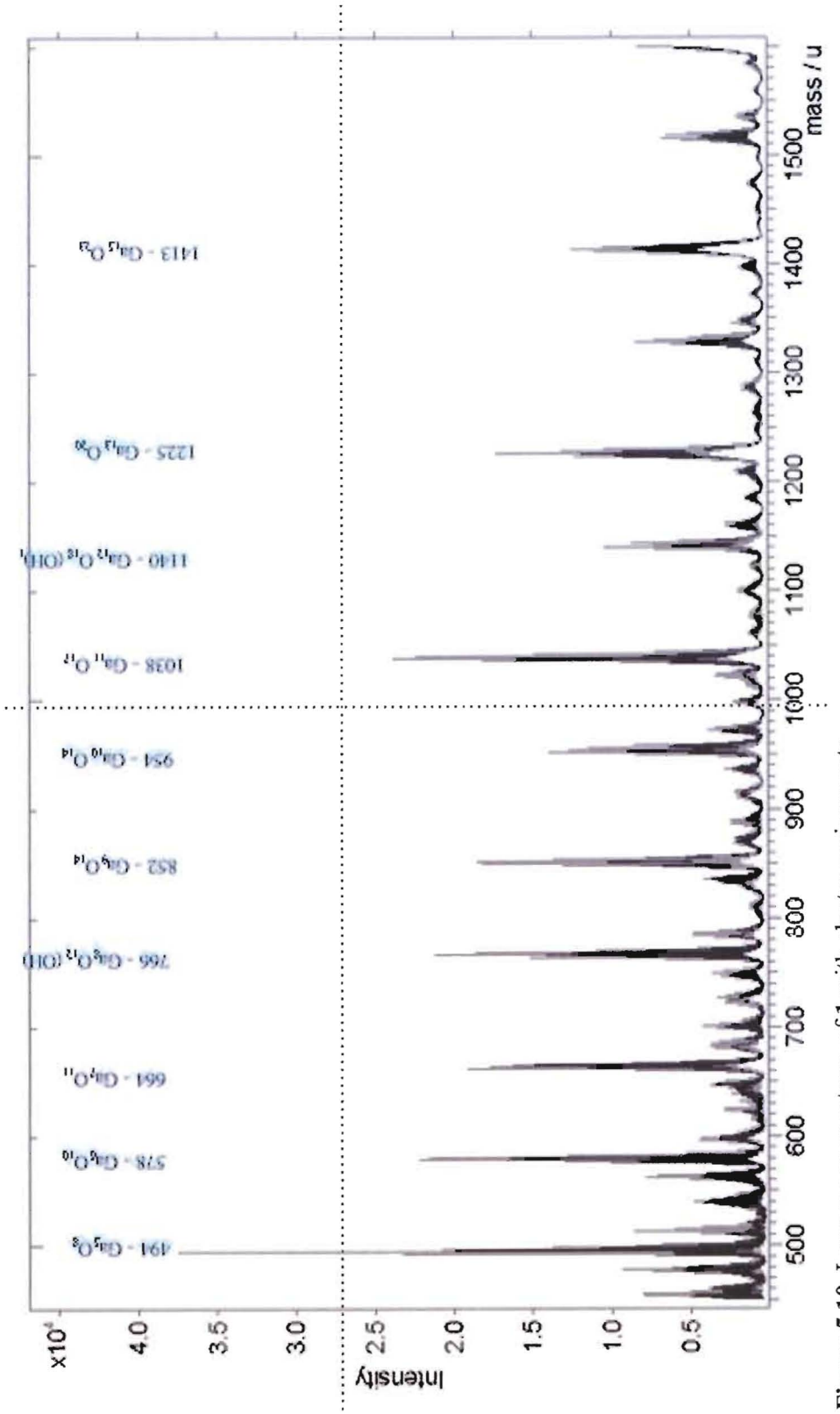

Figure 5.10. Long range spectrum of **1** with cluster assignments.

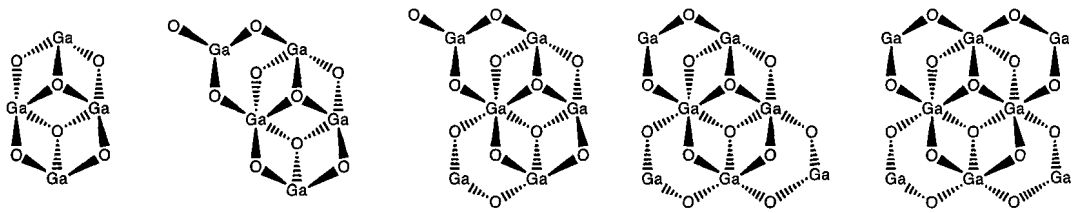

Figure 5.11. Clusters that fit peak identification for spectrum of **1**

Table 5.3. High Nuclearity species Peak assignments

Formula	Calculated	Observed	Error (Dalton)	Error (ppm)
$^{69}Ga_5O_8(OH)_1$	489.6258	489.5665	-0.0593	121
$^{69}Ga_4{}^{71}Ga_1O_8(OH)_1$	491.6250	491.5682	-0.0568	115
$^{69}Ga_3{}^{71}Ga_2O_8(OH)_1$	493.6241	493.5659	-0.0582	118
$^{69}Ga_2{}^{71}Ga_3O_8(OH)_1$	495.6232	495.5643	-0.0589	119
$^{69}Ga_1{}^{71}Ga_4O_8(OH)_1$	497.6223	497.5663	-0.0560	113
$^{69}Ga_6O_9(OH)_1$	574.5508	574.4926	-0.0582	101
$^{69}Ga_5{}^{71}Ga_1O_9(OH)_1$	576.5499	576.4900	-0.0599	104
$^{69}Ga_4{}^{71}Ga_2O_9(OH)_1$	578.5491	578.4900	-0.0591	102
$^{69}Ga_3{}^{71}Ga_3O_9(OH)_1$	580.5482	580.4900	-0.0582	100
$^{69}Ga_2{}^{71}Ga_4O_9(OH)_1$	582.5473	582.4900	-0.0573	98
$^{69}Ga_1{}^{71}Ga_5O_9(OH)_1$	584.5464	584.4900	-0.0564	97

Conclusions

We have shown that TOF-SIMS has the potential to be used for the characterization of polyoxometalates. While still not a fully developed method, it does show an increased potential for this technique in other characterizations of materials, and in some peak isolation and identification that can be adapted to other species. The first step is to try to apply these results to compound **7**, which has a complete substitution of the outer ring. This data shows that there are stable fragments in the gas phase. Previously this has been a concern. This new data could open the door for the use of

these clusters as synthons in a CVD or PVD method of film preparation, not just in the SILAR method that has been utilized thus far.[20, 21]

Future Works

Work continues on the calibration curve for additional peak assignments. The lessons learned here should next be applied to the compound 7. In the future we should also screen the analogous Al_{13} cluster using TOF-SIMS. The aluminum data will be useful for two reasons: the analogous cluster should yield very similar if not the same fragments, and the lack of isotopes should simplify the spectra with fewer peaks, helping improve the signal to noise ratio of the data. The slightly smaller ionic radii of aluminum may make the cluster more stable. Core fragments that are identified and predicted for the Ga samples should be able to be seen in heterometallic clusters. Organic ligands such as HEIDI may allow for large fragments to be seen because of stability imparted to the cluster by the ligand.

Working up the existing data with other programs would help with pattern identification.[22] Recent observations should allow for fragment predictions to be applied to some of the heterometallic clusters starting with **7**. The same clusters can be continued to be screened using other MS instruments, MALDI would be a prime starting point.

A parallel study should be to screen the ToF-SIMS of the known Ga_8 and Al_8 clusters, in order to test if they are indeed viable fragments of the Anderson-Evans core. Tof-SIMS has the potential to be used as much more than just an elemental analysis technique. The different heterometallic clusters in the series could help provide very useful data on the labiality of different metal bonds in analogous clusters under similar

conditions. Once we have finished with the gallium indium series we could use it as a base for the aluminum and indium series.

BRIDGE

The first five chapters of this thesis focused on inorganic oxo clusters. They include a small review, the synthesis, experiments, uses and characterization of tridecameric nanoclusters. Throughout these experiments there were numerous leads were not explored due to time constraints. The following chapter turns to a summary of the organic templated nanocages project that I researched for the first year and a half in Dr. Johnson's laboratory. I conducted the research on templated nanocages with assistance from three undergraduate (Michael N. Gonsalves, Pratistha Ranjitkar and Jean-Michel Moreau) and two rotation students (Eric L. Spitler and Charles A. Johnson, Jr.). Dr. Prof. Darren W. Johnson was the principle investigator for this work.

CHAPTER VI

SUMMARY OF INORGANIC TEMPLATED NANOCAGES

The goal of my original graduate research project was to create a rigid bis-bidentate organic ligand that would bridge multiple metal centers allowing for the creation of an enclosed cavity. Two different classes of rigid bis-bidentate ligands were explored: first the pyridine-imine binding motif based on a known self-assembled tetrahedron synthesized by Yan[1]; and second, a pyridine-pyrazole binding motif based on other self-assembled clusters by Ward.[2-5] A third binding motif based on the work of Saalfrank[6-9] was suggested and outlined but not yet tried. All of these ligands are modifications of previous ligands, with distal functionality built in to allow for the covalent coupling of the ligands into one nanocage templated by the four non-co-planar metals.

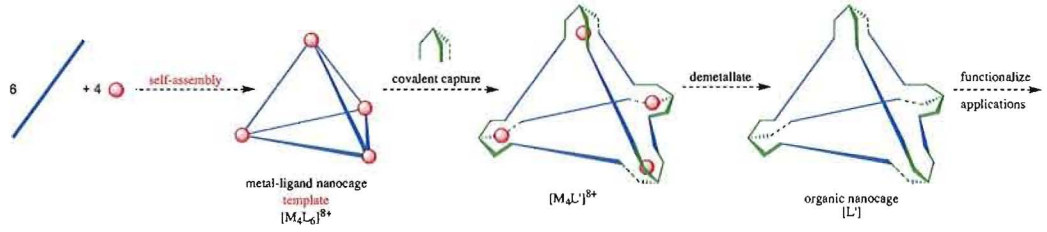

Scheme 6.1. The general scheme to use an M_4L_6 capsule as a template to form an organic nanocage, L'.

The general M_4L_6 tetrahedron template strategy is depicted above (**Scheme 6.1**). Six equivalents of an appropriately designed ligand (blue lines) are combined with four equivalents of metal (red spheres) to self-assemble a M_4L_6 tetrahedron (*metal-ligand*

nanocage template) related to the $Zn_4L_6^{8+}$ from the literature precedent. The next step is a covalent capture by a cap (green) that binds all six ligands together to yield the M_4L' complex. The final step of demetallation yields the *organic nanocage*, L'. This complex has a volume that is defined by its covalently linked shell.

The known appropriate crystal structures were imported into CAChe[10] with geometries locked. Then to the distal ends of the ligands carboxylic acids were added as handles for condensation with a three-fold symmetric compound. The overall structures were then minimized with a MM3 force field. In each case the propyl spacer of tris-(3-aminopropyl)amine (TRPN) provided a better fit than the ethyl spacer of the tris-(2-aminoethyl)amine (TREN).

Pyridine-Imine Type Ligands

The carboxylic acid derivative of the desired ligand was synthesized. The Yan procedure for crystallization of the tetrahedron was followed for the two different ester-protected ligands (ethyl and benzyl) as well as the deprotected carboxylic acid. Synthesis of the ester-protected ligands was carried out despite some serious solubility issues regarding the benzyl ester once it was condensed with benzidine. The condensation product of the terphenyl spacer of the 4.4"-terphenyl-diamine suffered from extremely poor solubility in various organic solvents. The deprotection of those ligands proved to be very difficult. The same condensation conditions did not work for other esters and spacer combinations, **Scheme 6.2**. In addition, there was a remarkable difference in the reactivity of the two different ester-protecting groups.

A second plan of attack was to try a capping-first strategy where the three-fold symmetric cap was first coupled to the 2-acyl-pyridine, then the pyridine was condensed to the rigid backbone spacer to form the imine. A series of two-fold symmetric backbones was explored, **Scheme 6.3**. This strategy allowed for the insertion of different rigid backbone scaffolds in a modular synthesis, **Figure 6.1**. Benzidine was the only diamine that was condensed with the acyl nicotinate and was still soluble for use as a ligand. The octofluoro version of benzidine did not condense with the 2-acyl pyridine. The *p*-terphenyl diamine did condense but was so insoluble that characterization of the deprotected product was almost impossible. Because of these difficulties, these two rigid spacers were not used, and work continued with the benzidine spacer.

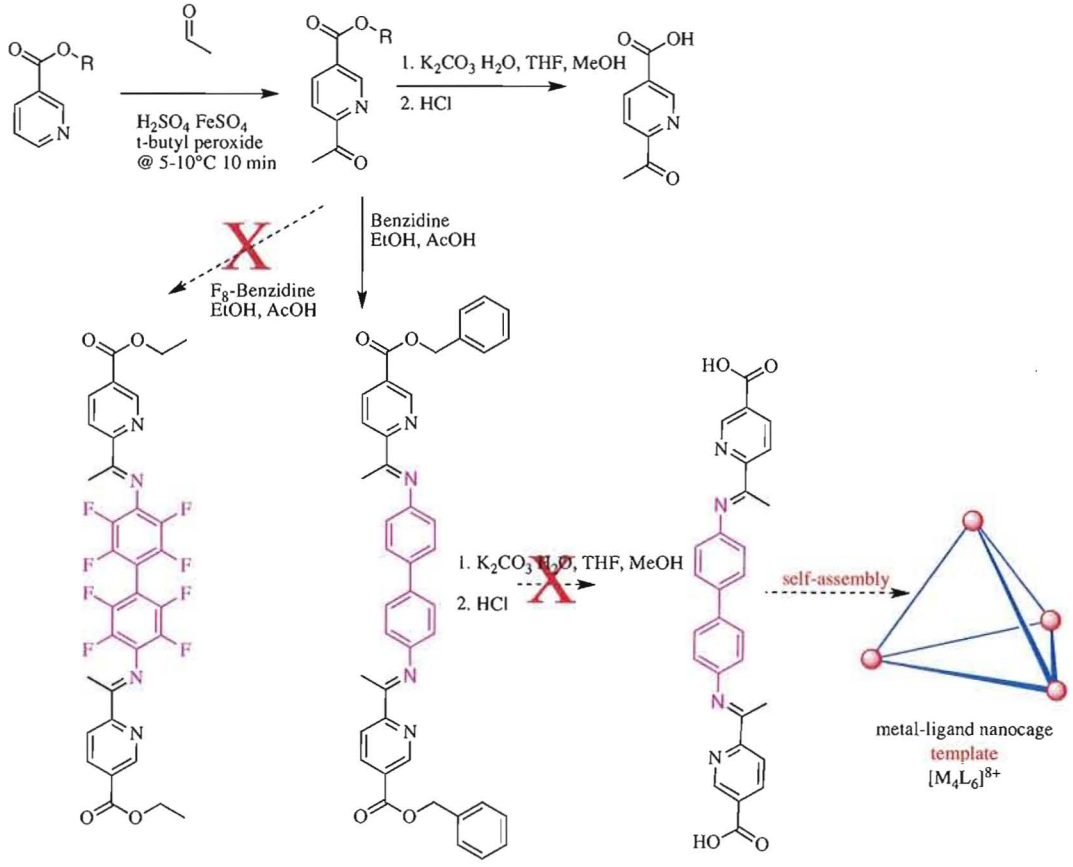

Scheme 6.2. Deprotection of benzyl ester ligand and metal-ligand self-assembly.

The benefit of a modular route allows for the order of reaction to be rearragned while reaching the same target. The capping-first strategy uses the same starting materials and even the same first reaction. But the deprotection happens second, as opposed to the condensation with the di-amine, in order to set up for the covalent capping. The 2-acylnicotinic acid as either the carboxylic acid or the activated ester could be coupled to the three-fold symmetric cap to yield the vertex **11**. The product was formed in very low over-all yields. An alternate scheme (**Scheme 6.3**) was not completed which had the potential for an even lower yield where the low yielding acylation reaction would need to be run on the three pyridines, yielding the same multiple

products. The acylation reactions of the nicotinic esters proceed in low yield; the redeeming quality is the low cost of the reagents and the easy reaction conditions. If the same acylation were tried on **12,** there would be a large mixture of products, and the increased bulk of the whole cap might help with the yield of the reaction, by favoring more acylation on the *para* position, making the difference between the two routes negligible.

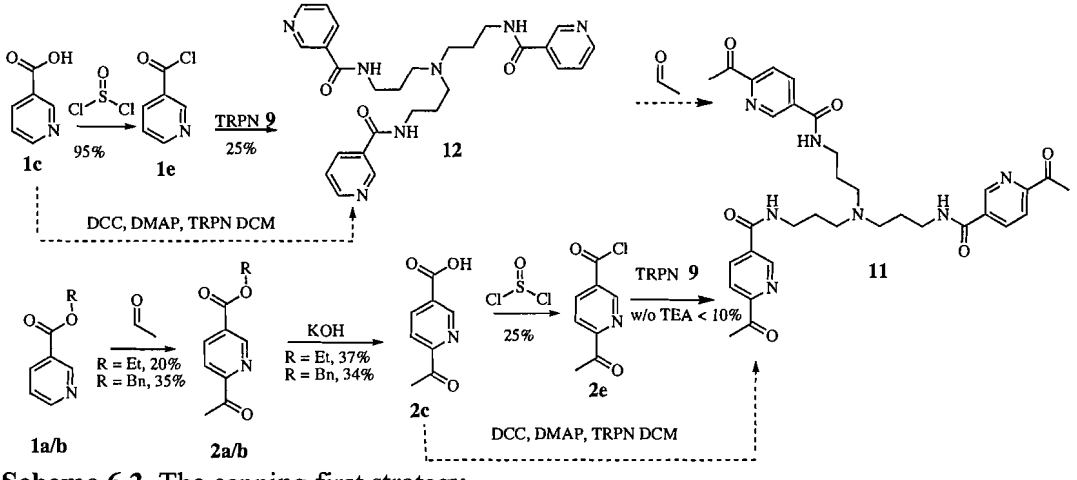

Scheme 6.3. The capping first strategy.

Use of other rigid spacers would allow for variations in the size of the cavity. Altering the symmetry of the scaffold would allow for different types of tetrahedra. The only tests so far have been on the first three linear *para*-substituted diamines that should have yielded the M_4L_6 tetrahedron. Using a three-fold symmetric backbone should yield a M_4L_4 tetrahedron, where the ligands are the faces of the tetrahedron instead of the edges. Changing the backbone phenyl spacers to acetylene spacers will change the edge length as well as the electronics of the system and the cavity size of the final product.

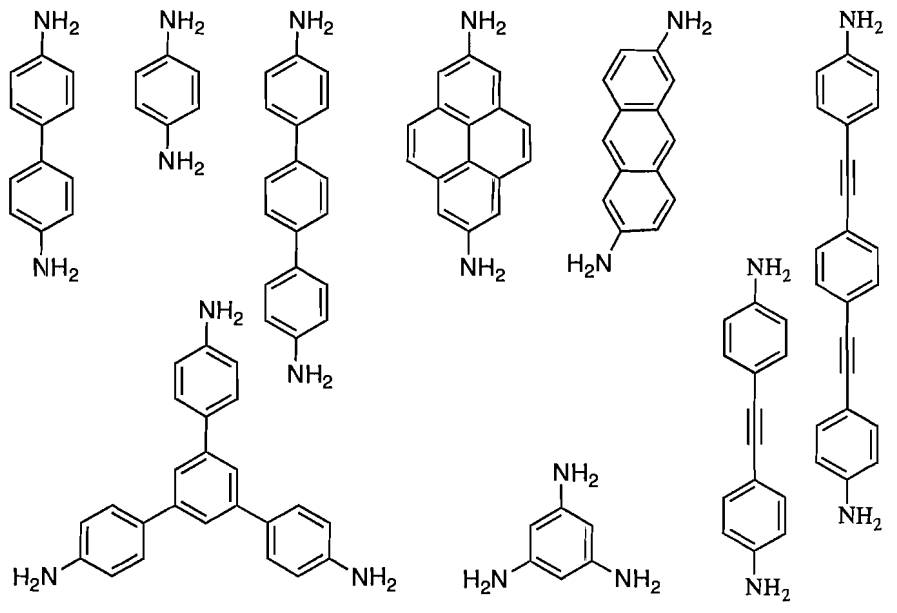

Figure 6.1. Rigid amine functional spacers, both two-fold and three-fold symmetric.

Before this project continues, Yan's ligand synthesis and tetrahedron assembly should be repeated. This will ensure that they can be synthesized in the lab. There are questions and issues about the self-assembly of the ligands into a discrete species. After those conditions have been successfully worked out, they can be applied to the tetrahedron self-assembly with any of the ligands available. Follow-up work needs to be done on a clean and reliable deprotection scheme for the ester-protected ligands. Then self-assembly attempts on the free carboxylic acid can be explored. Synthesizing the activated esters may make them too reactive under self-assembly conditions.

Pyridine-Pyrazole Type Ligands

An idea similar to the Yan synthesis is to prepare a known core ligand that self-assembles as a tetrahedron with distal functionality. The benefit of this scheme is that it allows for the use of the same nicotinic esters, **2a/b** from the previous schemes, as the starting material for the same acylation, and the M_4L_6 tetrahedron has literature precedent.[4, 11, 12]

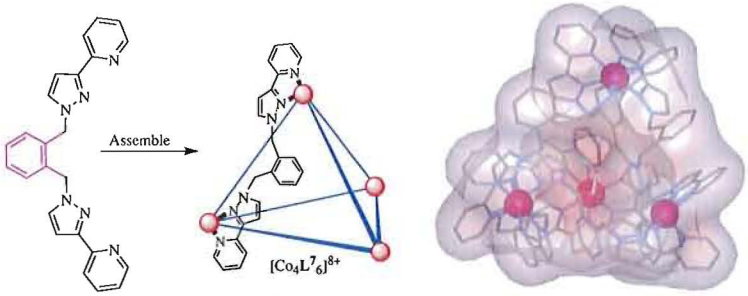

Scheme 6.4. The Ward based Pyridine-Pyrazole ligand self assembled and space filling surface with a BF_4^- counter ion encapsulated.

The conditions for the acylation reaction have already been worked out as a synthetic step for the pyridine-imine analog. In the pyridine-pyrazole ligand synthesis the second step was the condensation of the 2-acyl pyridine with DMF-DMA to make a vinylic amide. This step led to the unexpected product **15g** (methyl ester, not the desired benzyl) so continuing the synthesis proved to be problematic.

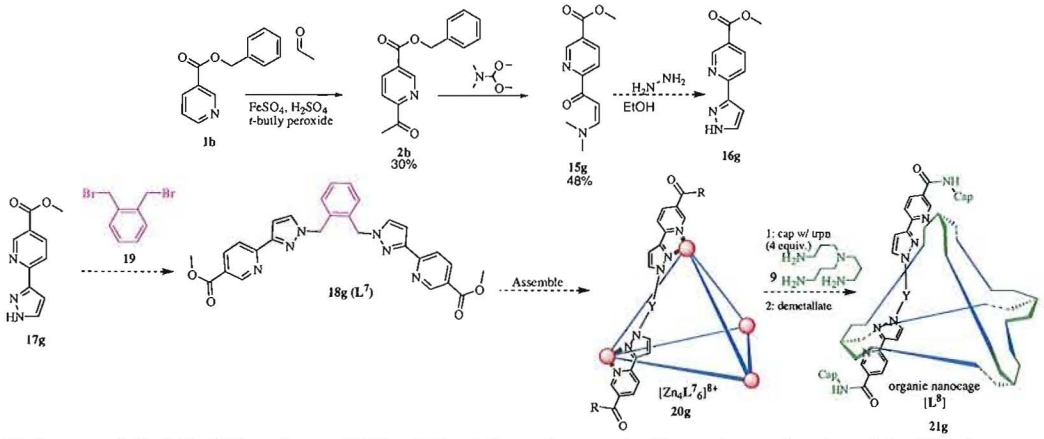

Scheme 6.5. Modification of Ward Pyridine-Pyrazole ligand synthesis with distal functionality.

The deprotection of the methyl ester ligand is a future goal. In the original work by Ward there is no distal functionality, just the vinylagous amide that can react with the hydrazine. In this case, the methyl ester reacted with hydrazine to yield no isolable product. The plan was to couple a dibromo compound to the pyrazole to form the bis-bidentate ligand. Ward synthesized and published this binding motif with several different spacers. Each spacer would allow access to different cluster types, including some three-fold symmetric spacers as well as others with alternate built-in functionality, **Figure 6.1**. Using a backbone spacer based on 2,6-lutidine would allow for the nitrogen in the ring to face into the cavity, changing the cavity properties by point the pyridine nitrogen into the cavity. A spacer built off of an α,α-dibromo-*o*-xylene with functionality on the 4 and 5 positions would have the opposite effect: to place some functionality facing the outside of the cluster.

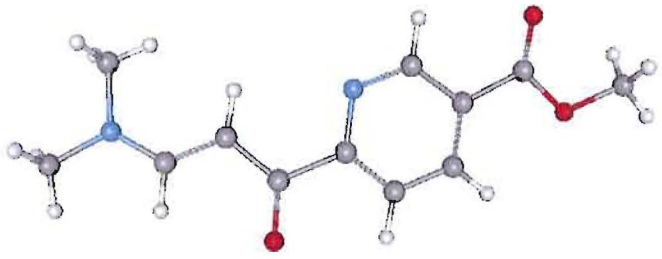

Figure 6.2. Crystal of Ligand **15g** post deprotection

The same reactivity and side product issues have arisen with the pyridine-pyrazole class of ligands as well. Because of this, Ward's ligand synthesis and tetrahedron self-assembly should be repeated in order to prove that the same products can be isolated and that the cage self-assembles. The major difference now is the new distal reactive functionality: the ester is not stable under the conditions of the DMA-DMF reation. The distal functionality should not interfere with the self-assembly of the ligands because according to modeling prformed on the target ligands .

The order of the reactions appears to be problematic, since the benzyl ester is too reactive as a protecting group for the acid. The same rearrangement of reaction sequence for this ligand should be explored, where the ligand is covalently capped before forming the pyrazole via the hydrazine closure reaction to form the pyrazole. Once there, many options for spacers are commercially available, and others with additional functionality are easily accessible.[4, 13]

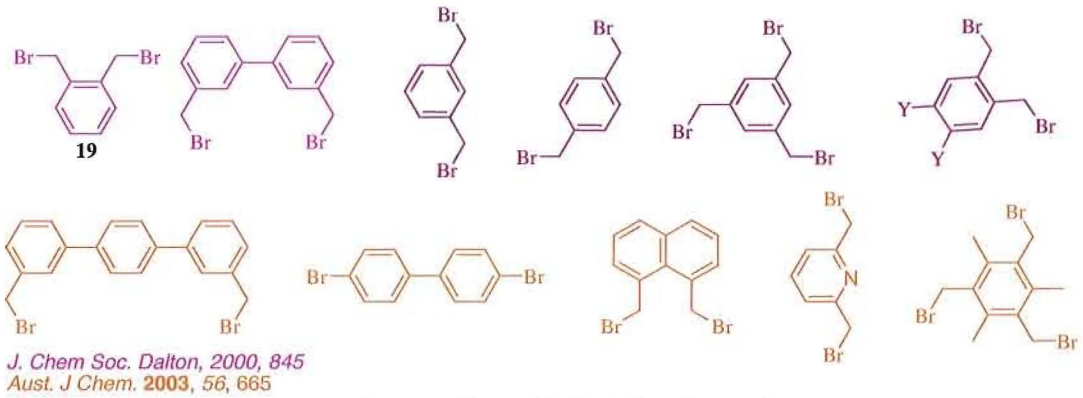

Figure 6.3. Dibromo spacers for coupling with Pyridine-Pyrazole

The reaction sequence with the pyridine-pyrazole based ligands needs to be changed, and proof-of-concept work needs to be done to prove that known ligands self-assemble in this laboratory. The functional group incompatibilities for the DMF-DMA reaction with the ester group will be difficult to over come. Once this is accomplished, the question of how to solve the reactivity issues can be addressed.

Diketone Type Ligands

Another type of ligand class that can be explored are the diketones. This class of ligands has been synthesized by the Saalfrank group.[14, 15] These ligands chelate to metals through two ketone oxygens, **Figure 6.4A**. Two binding units can be coupled together to yield a two-fold symmetric ligand, **Figure 6.4B**. The level of difficulty for differentiation of the two ends of the binding motif will depend on the synthetic scheme chosen. Designing a scheme that allows for the orthogonal synthesis of both the bind motif and a distal capping functionality will be difficult. If a linear method is chosen, where the core spacer is added first, then the active distal functionality can easily be added for the three-fold linked covalent capture into the complete inorganic nanocage.

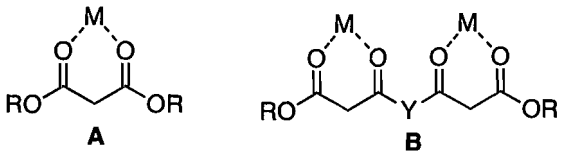

Figure 6.4. Saalfrank based ligands and diketo binding motif.

Spacers from the previous ligand classes could still be used with different reactions to yield complexes of similar size. This would allow a synthesis of the corresponding two-fold and three-fold ligands, varying only in the binding motifs, for the corresponding M_4L_6 and M_4L_4 type of templated nanocages. This modular synthesis allows for the same variation in electronics and functionality, as well as for the use for different ligand spacers.

The specific metals used for the self-assembly could be changed for other metals that bind more specifically, because they are there for the templating of the organic ligands. A bigger problem than the metal for all the self-assemblies might prove to be the counter-ions. A weakly coordinated counter ion is preferred in order to avoid competition with the ligand. A self-assembly with metal triflate or toslyate salts should be tried, to promote dissociation.

Mixed Atom Binding Sites

Currently all the ligands outlined here involve the same coordination atoms. There is also a variation on these that could be explored. The Yan-based pyridine-imine ligand motif uses two nitrogen atoms. The Ward-based pyridine-pyrazoles also uses two nitrogen atoms. While the Saalfrank type diketos still use lone pairs obtained from two oxygen atoms. Mixed ligand types could be added involving one nitrogen atom and one

oxygen atom. The ligands that currently contain oxygen could be substituted with sulfur, in order to change the HSAB properties of the ligands. This could allow for selectivity and tuning of the ligands for different metals.

APPENDIX A

SUPPLEMENTAL INFORMATION OF ANDERSON-EVANS CLUSTER REVIEW

Table A.1. All hits from the $M_6(\mu_2\text{-}O)_6$ ring (Search 1)

ABEREE	ECIZAS	HEFLUZ	LAQRAX	OLUQIV	SEDJAN	WASVAO
ABICOD	ECIZEW	HEFXUL	LAQREB	OMIQUW	SEDJER	WASVES
ABIXOZ	ECIZIA	HEGBEB	LATGAP	OXCFOR	SEDJIV	WATCEA
ABOCEA	ECOBII	HEGBUQ	LATGET	OXERHD10	SEDJOB	WATCIE
ABOCIE	ECOBOO	HEHNIR	LATGOD	PACFAB	SEDJUH	WATGUU
ABOHEE	ECOKUC	HEJMAK	LATGUJ	PADPOA	SEFSAY	WAVVIY
ABOHII	ECOSIY	HEJMAK01	LATHAQ	PADPUG	SEGVOP	WAVWOG
ABOHOO	EDABAN	HEJMEO	LATHEU	PAFHAG	SEGVOP01	WEBMAR
ABOKUX	EDACIW	HEJMEO01	LATHIY	PAFJUC	SEGVOP02	WEBMAR01
ABULUF	EDADAP	HEKFEI	LATHOE	PAFKAJ	SEGVOP11	WEBTOM
ABUMAM	EDAKOJ	HEMQUL	LATTIK	PAFMOY	SEHWOR	WECWEG
ABUMEQ	EDORIY	HEMRIA	LAWYIS	PAFWOI	SEHXAE	WECYEJ
ABUWIE	EDOYUR	HENRUN	LAXXOY	PAFWOI01	SEHXUY	WEDMUO
ACEGOF	EFANII	HENRUN10	LAYCAQ	PAGMUF	SEJYAH	WEDNAV
ACIXOZ	EFENOS	HEXWEM	LAYCIY	PAGNAM	SEMGOG	WEFQON
ACIZUH	EFEZEU01	HEXWOW	LAYCOE	PAGSOF	SERNEI	WEGWEL
ACOBAV	EFEZIY01	HEXYEO	LAZBUK	PAGSUL	SETBAU	WEHFUL
ACOHEG	EFUQUR	HEYLUS	LEBREQ	PAGTAS	SETBEY	WEHGEV
ACOLIN	EFUQUR01	HIDLEL	LEBSOB	PAGXIE	SEVRUG	WEHMEB
ACOTER	EGIQUG	HIGLOY	LEBYIA	PAHRIA	SEVSAN	WEHMIF
ADALOG	EGIQUG01	HIKSID	LECSAO	PAJFOW	SEYQES	WEJLIH
ADATOP	EGIQUG02	HIKSOJ	LECSES	PAKPAT	SIBCOV	WENWER
AEAMCU	EGUHAP	HIMSUR	LEFQOD	PAKPEX	SIBPAU	WEPNIO
AFIVUG	EHADEW	HIQGOD	LEFTIA	PAKPIB	SIGZOX	WEQPUD
AGEBUJ	EHAFAU	HIRBIT	LEGJUD	PAKSIE	SIJLEC	WESTOD
AGICUO	EHAHEA	HIRMAW	LEHZUT	PALQOI	SILZES	WESWUM
AGIDAV	EHEWOD	HOCNES	LERMUQ	PAMPEZ	SIMBOF	WETCON
AGIDEZ	EHORUO	HOJDIT	LESTEI	PANHIV	SIRHEG	WETFOQ
AGOJUB	EHORUO01	HOQHEA	LETKIE10	PANHOB	SIRHIK	WIBLOI
AGOYEA	EHOSAV	HOXOKM	LEXQIO	PANTII	SIRNOW	WICJAT
AGUZIL	EHOSAV01	HUDPIF	LIDJUD	PANVUW	SISTAP	WIDMOL

AHAFIY	EHUCOZ	HUDQEC	LIFWEC	PAPHOE	SISVUL	WIDMOL01
AHECIZ	EHUCUF	HUDQIG	LIFWIG	PAQVUZ	SISWAS	WIFNUU
AHECOF	EHUDAM	HUDQUS	LIGSAV	PARGAQ	SISXAT	WIFNUU01
AHOZOM	EHUDEQ	HUDRIH	LIKQAX	PATZOA	SISYEY	WIFVIQ
AHOZUS	EHUDIU	HUHNED	LIPRIL	PAVKOM	SISYEY01	WIGQIM
AJETEO	EJIQOD	HUHNIH	LIPROR	PAWHEA	SIXJIS	WIGYEQ
AJIMAH	EKABAT	HUJPIL	LIPRUX	PAXLAB	SIZPIA	WIHBAQ
AJIMEL	EKAQIQ	HUJPOR	LIQNOO	PAXXES	SIZROI	WIHQOT
AJIRUG	EKIYEC	HUJPUX	LISRUA	PAYZIZ	SIZYAB	WILGUT
AJITIW	EKIYOM	HUJQAE	LOKRUY	PAZCIC	SIZYEF	WIMRIT
AJIZUO	EKIZAZ	HUJQEI	LOQKIL	PAZNOU	SMADNB10	WIMRIT10
AJOCEH	EKIZED	HUJQIM	LOQMEJ	PAZQUD	SOFTOW	WIMRIT11
AKIRAN	EKIZIH	HUJQOS	LOQMEJ01	PAZVER	SOFTOW01	WIPSET
AKOPEV	EKULEB	HUJQUY	LOSFAA	PAZVOB	SOFYER	WIPSIX
AKUFOB	ELELUC	HUJRAF	LOSFEE	PAZZUM	SUGDUT	WIPSOD
ALARAG	ELERES	HUNDOJ	LOSXAS	PEBKEM	SUHJOU	WIPXIC
AMEVOD	ELOZAG	HUQNUC	LOSXEW	PEBSEV	SUJMUF	WIRYAX
APOZIO	EMAHAB	HUQPEO	LOSXOG	PEBSIZ	SUJNAM	WISWAW01
APUZOA	EMAHEF	HUTKEM	LOTTIX	PECQEU	SUJNIU	WIWZIL
AQACMN	EMAQOY	HUVKEO	LOWXUQ	PECZIH	SUJNOA	WIWZOR
AQACMN02	EMAQUE	HUVKIS	LOWYAX	PEFCOT	SUKQEU	WIWZUX
AQACMN03	EMEBAZ	HUVKOY	LOXWAW	PEFDAG	SUKXOL	WIXSIF
AQACMN04	EMEXEZ	HUXGUC	LOZTOJ	PEFTUQ	SULZEE	WIXWUV
AQOGAO	EMEXEZ01	HUZNIZ	LUDZEP	PEHBEJ	SULZEE10	WIXXAC
AQOKAS	EMIVEB	HUZNIZ01	LUFQIM	PEHCUA	SUMDEJ	WIXXOQ
AQOKAS01	EMORAZ	HUZPEX	LUGRUA	PEHSAW	SUNCAF	WIXXUW
AQOKEW	EMOXUZ	HUZVED	LUGSAH	PEJGOO	SURYIN	WIYXEH
ARADOM	EMUGIC	IBAKAY	LUGSEL	PEJRIF	SUSZOV	WIZLOG
ARAFII	EMUGIC01	IBAVIR	LUGSIP	PELYIO	SUWZEP	WOGCOK
AREKAJ	EMUJOL	IBAXUF	LUHZUJ	PEQNII	SUWZEP01	WOGCOK01
ARICAF	ENAHEG	IBECOH	LUJDID	PEVMUY	SUXRAE	WOHREQ
ARIDOU	ENEJOW	IBEFEB	LULHOP	PEVNAF	SUZPUY	WOHRIU
ARIDUA	ENESOF	IBEMEI	LULHUV	PEXWEU	TABGUZ	WOHROA
ARIFAI	ENESUL	IBEMIM	LULHUV01	PEYPOY	TABHAG	WOHRUG
ARIGAJ	ENETAS	IBEMOR	LUNCOM	PEZYOI	TABHEK	WOMVUP
ASAMUC	EQIXAD	IBEMOR01	LUQQOD	PIDGIS	TACFOT	WONSOH
ASANAJ	ERIJIY	IBEXAP	LUSHEM	PIDGIS01	TADDIL	WOPWIH
ASANEN	ERIJOE	IBEYOE	LUVQAU	PIHQAY	TADDIL01	WOQTUR
ASANIR	ERUBAU	IBIHUX	LUVVON	PIJCEQ	TADDIL10	WOTQOL
ASANOX	ERUBEY	IBILEL	LUVVUT	PIMZIU	TAFHIS	WOWTEH
ASAYOI	ERUSIT	IBILIP	LUVWAA	PIPDOH	TAFPUM	WOWTIL
ASEMIU	ESAXUR	IBILOV	LUXDOX	PIPHIF	TAGXEF	WOWZAJ
ASEROF	ESIXAF	IBOJOZ	LUYSIH	PIPHWO	TAHHAM	WOYHOH
ASERUL	ESIXEJ	ICEKOR	LUYSON	PIQGEB	TAHHEQ	WOYYUE
ASESAS	ESOJEB	ICELUX	LUYSUT	PIQGIF	TAHHIU	WUCHOR
ASESEW	ESOXIT	ICEMAE	MABGAY	PIQGOL	TALLOH	WUCHOR01
ASESIA	ESUWOE	ICOZOQ	MABGAY01	PIQSUD	TALPAX	WUCROB
ASOCAM	ETCMOM	ICUDUF	MABGEC	PIRHUT	TAMBAK	WUDTUK
ASOCEQ	ETPYOM10	ICUSEE	MABHIH	PIRHUT10	TAMPEC	WUFTOG
ASUPIN	ETUCUR	IDUTAC	MABHON	POBDOZ	TANBOX10	WUGFEJ
ATOSOR	EVEPUQ	IDUTAC01	MABHON01	POFYAK	TARLIH	WUNNEY

ATOSUX	EVEQIF	IFIPIW	MACHUU	POFZOZ	TASWEQ	WUNNIC
AVAPAO	EVUTEU	IFIPOC	MADFIH	POHCEU	TASWIU	WUPWIN
AVAPES	EWECUE	IFOJUI	MAJKUE	POHPEH	TASWOA	WUPWIN01
AVUWIX	EWESOO	IGOGOA	MAJTEW	POHPIL	TASWUG	WUPWOT
AWEMUK	EWOPEL	IGUKOK	MAJTEW01	POKYUJ	TAVQUC	WUPWUZ
AWEWEE	EWOSOY	IGULAX	MAJTEW02	POLTEP	TAVRAJ	WUQNUR
AWIQUS	EWUVAT	IHARUE	MAJTIA	POMGUT	TAWJIK	WUXTUE
AWIRON	EWUVEX	IHEWOH	MAKDIM	POPTET	TAWJOQ	XACZAD
AWIRON01	EWUVOH	IHUREI	MAKDOS	POQPEQ	TAWJOQ01	XADMEU
AWIRUT	EXELOI	IHURIM	MAMHAK	POQTIY	TAWNAH	XADMEU01
AWIRUT01	EXEPEC	IJAWEV	MAMMOC	POSPUI	TAWWUK	XADMEU02
AWOPEH	EXOGIH	IJAYUN	MAMMUI	POTSUM	TAWWUK01	XADRAW
AWUBOJ	EYERAB	IKAMEM	MAMNEU	POWGIR	TAWWUK02	XAFPEA
AXACAD	EYUHOV	IKAMIQ	MANMET	POYPOI	TAXKOT	XAFPEA01
AXACEH	EZAXEI	IKETIB	MAPMAR	POZQUQ	TAXKUZ	XAFPIE
AXAFEK	EZEYUD	IKETOH	MAPVAA	POZRAX	TAYNUD	XAFTUT
AXIKOH	EZEYUD01	IKETUN	MAQKIZ	PPHOMO10	TAYPAL	XAFVAB
AYOJIH	EZIFOI	IKILOD	MARGIV	PTACCO	TAZJOT	XAFVEF
AZACOT	EZUPOE	IKILUJ	MARGOB	PUBDAR	TBUAWO	XAFVIJ
AZOQOV	EZUPUK	ILEXIG	MASMOJ	PUBDEV	TBUAWO01	XAFXIM
AZOQUB	EZUQAR	ILOMEB	MATPDE10	PUJYAU	TBUAWO02	XAGCOY
AZUFOQ	EZUZAA	ILUFIE	MATTIK	PUKVIA	TBUAWO03	XAHKOG
AZUPUG	FABMIE	IMOGEW	MAVQIJ	PULHIN	TEBDOU	XAHQIH
BACLAT	FABMOK	INIKEV	MAVQOP	PUPXON	TEBSID	XAHQON
BACWEH	FACYUD	INIKIZ	MAWPOP	PUPYEE	TECJOA	XAHQUT
BACWEH10	FACYUD01	INIMOH	MAWPUV	PUQCIN	TECJUG	XAHRAA
BAFJUO	FACYUD02	INIRIG	MAWQAC	PUQCOT	TECPOH	XAJTAE
BAFVEK	FADXEO	INOPOQ	MAWQIK	PUQCUZ	TEDDUC	XAJVEK
BAGQOQ	FAFQOT	IPAMOX	MAWQOQ	PUTROL	TEDXIK	XALKOL
BAHYOZ	FAFQOT01	IPAMOX01	MAWQUW	PUYQAB	TEHKIB	XALXOY
BAHYOZ01	FAFQUZ	IPAMOY	MAWRAD	PUZCUI	TENSIO	XAMDAQ
BAJVIS	FAFQUZ01	IPUKEJ	MAWREH	QABYOI	TEPYAO	XAMKAY
BANBIB	FAFRAG	IPUKEJ01	MAWRIL	QACNEO	TEQTUE	XAMLED
BANBIB10	FAFRAG01	IPULOU	MAWROR	QADFOQ	TEQVAM	XARVUI
BANBOH	FAFREK	IPULUA	MAWRUX	QAFKOY	TERRIR	XARWET
BAOCMO	FAFREK01	IQEFOZ	MAYDEV	QAFXUR	TESPUC	XASKIL
BAOCMO01	FAFRIO	IQIREF	MAYNEG	QAFYAY	TETTIV	XASKOR
BAOCMO11	FAFRIO01	IQUBEB	MAYNIK	QAFYEC	TETVET	XASZOH
BAQBEB	FAFSAH	IRABIM	MAZDUN	QAGFOT	TEWHAE	XATYIA
BAQDED	FAGDOH	IRABOS	MECFUW	QAGVUQ	TEZLIT	XAVJIO
BAQDIH	FAGFAV	IREJAQ	MEDLIQ	QAGWAX	TIDGES	XAXROE
BAQFOO	FAGNEH	IREKOF	MEDLOW	QAJDEL	TIFMIE	XAXRUK
BAQWEV	FAHHEC	IRELAS	MEDXAU	QAJDIP	TIMQAH	XAXSAR
BAQWEV01	FAHVIU	IRUDII	MEDXEY	QAJDOV	TINMOS	XAXZAY
BARHOS	FAHVOA	ISADAH	MEDXIC	QAJKOC	TIPWOE	XAYJOX
BARHOS01	FAJJOQ	ISAGEO	MEDXUO	QAJKUI	TIQYOH	XAYZOM
BARXIB	FAJJUW	ISALOD	MEDYEZ	QAJLET	TIXHUD	XAZQOE
BAVLIU	FAJKAD	ISEDOZ	MEFLEO	QAKTOM	TIXJAL	XEDHIX
BAYBUY	FAJKEH	ISEXIN	MEGBAC	QANSII	TIXKUG	XEDVUY
BAYBUY01	FAJKEH01	ISOPIP	MEGBEG	QANSUU	TIXLAN	XEDWAF
BAZMAR	FAKPOX	ISOQUC	MEGCIL	QAPFUJ	TODLAZ	XEFGIZ

BAZMAR01	FALVOD	ITEFUI	MEJWON	QAPMAW	TOGHAY	XEFGOF
BEBYEN	FALVOD10	ITEGOD	MEJWUT	QAVDAT	TOGKOP	XEFGUL
BEDBES	FAMQOZ	ITUWOJ	MEJXAA	QAWDIC	TOGKUV	XEFNEC
BEDCAP	FAMQOZ01	IVOLUA	MEKMEU	QAWDOI	TOGYOD	XEFROP
BEDCIX	FAMQUF	IVUCIL	MEKQAU	QAWDUO	TOJRUF	XEHSOS
BEDYOZ	FANDII	IWIGEA	MEMJUJ	QAWPAF	TOKDOM	XEHSOS01
BEGDEX	FAPGUZ	IWULER	MEQHOF	QAWPIO	TOLTUJ	XEJTUB
BEHJUU	FAPHEK	IXABEO	MEQHUL	QAWZAQ	TOPLAL	XELLUV
BEJDAW	FAPHIO	IXIJEE	MEQHUL01	QAXLAD	TOQLEQ	XELLUV01
BEMPAL	FAPNEQ	IXODII	MEQJAT	QAXQEM	TOQLIU	XEMMIL
BEMQUG	FAPNIU	IXOPIU	MEQJEX	QAXTEO	TOTYIK	XEMMOR
BEMRAN	FAPVOI	IXUHUE	MEQZOX	QAYNEJ	TOTYIK01	XENDAV
BEMRER	FAQBUV	IYEDOF	MEWLEF	QAYPIP	TOTYOQ	XENDEZ
BENYOJ	FAQWEZ	IYEDOF01	MIBYIF	QAZJIK01	TOTYOQ01	XESQAN
BEPJAI	FAQXUR	IYEXOZ	MIBYOL	QEFJEQ	TOWXAE	XESQER
BEPJEM	FAQYAY	IYEXUF	MILHAQ	QEFJIU	TOWXAE01	XETVOH
BEPJIQ	FARLEQ	IYEYAM	MILHAQ01	QEGLIX	TOWXIM	XETVOH01
BEQQUK	FAVHUG	IYOCAA	MINTAE	QEHJIW	TOWXIM01	XEXBUX
BEQRAR	FAVYEH	IYOJEL	MITZEU	QEHJOC	TUFMUC	XEZFIR
BEQREV	FAWFIS	IYOJOV	MITZIY	QEHJUI	TUFXIB	XEZZAD
BEQXEB	FAWVAB	IYUSAW	MIZBEC	QEMCUG	TUHFAD	XEZZIL
BETCOT	FAXMIB	IZABUG	MIZBIG	QERBEU	TUMSUP	XIJGIG
BETFIQ	FAYVIL	IZEQUZ	MIZBOM	QERBIY	TUMVEC	XIKPAI
BETFOW	FAZZEM	JAGVET	MIZFEG	QERBOE	TUNYIK	XIKVOC
BETFOW01	FEGBUP	JAJYOJ	MIZFIK	QERBUK	TUQJAQ	XIMKAF
BETXAA	FEHQOZ	JAJYUP	MIZFOQ	QERCAR	TUSFOC	XINDAZ
BETYAB	FEHQOZ01	JAJZAW	MIZFUW	QERCIZ	TUVDAP	XIRJOX
BEVWUV	FEHQUF	JAMWEA	MOCLAR	QERTOW	TUVRAD	XIRNIV
BEVXAC	FEHQUF01	JAMWEA01	MODXAE	QERTOW01	TUWSOT	XISGUB
BEWXUX	FEJRER	JAPQOH	MODYIN	QERTUC	TUXZIV	XIWBAG
BEYBAJ	FEMDIL	JAPQUN	MODYOT	QERTUC01	TUYDEW	XOKHEK
BEYGER	FENDOS	JAPRAU	MOGWEK	QESJUT	TUYFAU	XOMFIO
BEYRON	FENDUY	JAPREY	MOGYIQ	QETZOE	TUYFAU01	XOSYEJ
BEYRON01	FEPDAG	JAQZOR	MOGYOW	QEVNIO	TUYGID	XOSYUZ
BIBDEV	FEPHOY	JAQZUX	MOGYUC	QEVZUM	TUYGOJ	XOSZIO
BIBXAL	FEPSOI	JARCOU	MOKMAA	QEYYAU	TUZDIB	XOTKAS
BIBXAL01	FEQFEN	JARDAH	MOMASA	QICSEA	UBEFIQ	XOXQOQ
BIBXAL02	FEQFEN01	JARDAH10	MONHOM	QIHVEI02	UBEGAJ	XOXQOQ01
BIBXAL03	FERLUK	JARLUJ	MOPROY	QIHVIM	UBEGEN	XOYSAF
BIBXAL04	FERNIA	JARWOP	MOTCED	QILKAX	UBUHII	XOYSEJ
BIBXAL05	FERREA	JATPEZ	MOTFIK	QILKEB	UCAXOM	XUBXOH
BICGID	FERTEC	JAVNEA	MOTFIK01	QIMNAB	UCAXUS	XUBXOH01
BICGOJ	FESLIY	JAVQON	MOTFIK02	QIMVEN	UCAYAZ	XUDROD
BICYNW	FESLOE	JAXBAM	MOYFIP	QIMWAK	UCESOK	XUDROD01
BIGLIN	FESLUK	JAXCEQ	MOYXIH	QIMYEQ	UCOTUB	XUGCEH
BIGLOT	FESQOJ	JAXCER	MOYXON	QIMYEQ01	UCUHUW	XUHTEZ
BIGLUZ	FESQUP	JAXDUH	MUFTIQ	QIMZER	UCUJAE	XUKWIJ
BIMCOQ	FESWUW	JAXFET	MUJSIT	QINQAF	UCUKAE	XUKWOP
BIMCUW	FESYUY	JAXGAQ	MUKYIA	QIRPOW	UCUKEI	XUQQIJ
BIMZUT	FESZAF	JAXLEA	MULTOC	QIYLAL	UDAPOE	XUQQIJ01
BINBAC	FETBAI	JAYBOA	MULTOC01	QIYLEP	UDAPUK	XURZIT

BIYPEE	FETLEV	JAZYIS	MULTOC02	QIYLIT	UDAQAR	XUTSIO
BOCSER	FEWMUQ	JEBCAV	MUNQER	QIYLOZ	UDAVUQ	XUTSIO01
BOKVAY	FEWROP	JEBCEZ	MURMUH	QOHYER	UDAZUU	XUVYES
BOQNIE	FEXVIO	JEBCID	MURNAO	QOKBUN	UDEBAG	XUVYIW
BOXHEB	FEXVOU	JEBJAC	MURNES	QOKCAU	UDEBEK	XUVYIW01
BUAMDW10	FEXVUA	JEBJEG	MUSYUU	QOLHOO	UDIQED	XUWLOQ
BUTKOQ	FEYBIV	JEBJIK	MUXLUM	QOLPIQ	UDOPUY	XUWQIP
BUVZUN	FEYBIV01	JEBJOQ	MUXTAA	QOPJAG	UDUXIA	XUXTEP
BUVZUN01	FEYBOB	JEBJUW	MUXTAA01	QOSYIG	UDUXOG	XUXVER
CACJEW	FEYBOB01	JEBKAD	MUXTAA02	QOSYOM	UDUXOG01	XUXVIV
CAKLIK	FEYBOB02	JECCIE	MUXTEE	QOSYUS	UFETOO	XUXWUI
CAKLIK01	FEZSAF	JECCOK	MUXTII	QOSZAZ	UFIGEV	XUYQAJ
CAKROV	FICSIU	JEDMIP	MUXTOO	QOSZED	UFIHAS	XUYRAK
CALLAC	FIDMEL	JEDMOV	MUXTUU	QOVVOM	UFIPII	XUZWEU
CALTUF	FIDMEL01	JEDMUB	MUXVAC	QOWHUF	UFIPUU	YABHUF
CALVAN	FIDMIP	JEDNAI	MUXVEG	QOWJAN	UFUTIY	YADFIS
CAPBUR	FIFRUI	JEGNAL	MUXVIK	QOWJER	UFUTOE	YAGHOD
CAPCAY	FIGXUP	JEJKOZ	MUXVOQ	QOWJIV	UFUTUK	YAGHOD01
CAPKUA	FIHJEL	JEJKUF	MUXVUW	QOXQUP	UGAXEF	YAGNOJ
CAPRUH	FIKPOF	JEKWEC	MUYSAA	QOXQUP01	UGUPER	YAHMUQ
CAQQUG	FIKPOF01	JEKWIG	MXSNOX	QOZBEM	UGUTAR	YAHNAX
CAQQUG01	FILVEC	JEMLUI	NABUOX11	QOZPAW	UHAGAL	YAKSEI
CARKUC	FINBOU	JETVEJ	NACNEL	QOZPEA	UHEBOY	YALGAU
CASNIU	FINSEB	JEWPUW	NACNIP	QUDBEW	UHIYEP	YALGEY
CASWUP	FINYEG	JEXCUK	NACWAQ	QUDTUE	UHIYIT	YALGIC
CASXAW	FINYIK	JIBXEX	NACWEU	QUDVAM	UHUTEW	YALGOI
CASXEA	FIQDOY	JICZAW	NADCUQ	QUDVEQ	UHUTEW01	YALKAX
CATFEI	FIQDOY01	JIDNIT	NADHIK	QUGNAH	UJADEO	YALKAX10
CATQEU	FITGEV	JIFNAN	NAHHIN	QUHLEK	UJADIS	YALXOY
CAVSIB	FITGIZ	JINJUL	NAJPAQ	QUHXAS	UJADOY	YAMHAW
CAWJEP	FIVKOK	JINKAS	NAJPIY	QUMBEF	UJASED	YAMHEA
CAWJIT	FIVTUA	JIQYIR	NAMAWP	QUMDOR	UJASED01	YAMLEE
CAXTIF	FIYGOK	JIRSOS	NAMOAS	QUQWEE	UJIGOJ	YANQOT
CAXTOL	FIYKII	JIRSOS10	NAMYEG	QUTNOI	UJIGUP	YANVOY
CAXTOL01	FIZLAC	JITGIC	NARROO	RABTIT	UJIHAW	YANVUE
CAZGOZ	FOBXEZ	JIYJEG	NARSAA	RADHEJ	UJINAC	YAPLEH
CECBUI	FOCLIT	JIYMIN	NARSIJ	RAGCIM	UJOTOC	YAPLIL
CECCAP	FOCLOZ	JODDIP	NATNAX	RAGCUY	UJUFOU	YAPVAN
CECCET	FOCLUF	JODLET	NATREF	RAGDAF	UJUFUA	YAPZEV
CECVUC	FOCXEB	JOFVIJ	NAVCAP	RAGXUS	UKETOT	YASLEK
CECWAJ	FODYON	JOHHAP	NAVFOG	RAGYAZ	UKOFIJ	YAVNOY
CECWEN	FOHSUQ	JOJZAJ	NAVPAC	RAGYOO	UKOTUJ	YAVYEZ
CECWIR	FOHSUQ10	JOJZAJ10	NAVQIL	RAHBOS	UKOVAR	YAVYID
CEDCUK	FONZIR	JOJZEN	NAVQOR	RAHFIP	UKOVEV	YAVYOJ
CEDHID	FONZOX	JOJZEN10	NAVYIT	RAHFOV	UKUCOS	YAWKUC
CEDYUG	FOROMO	JOMCUJ	NAVYOZ	RAKTEC	UKUDEJ	YAXJIQ
CEDZAN	FOTCAS	JONWUE	NAWDIY	RAKTOM	UKUDIN	YAXNEQ
CEFNEG	FOTCAS01	JOTLUZ	NAWSAF	RALWUW	UKUMIW	YAXRAQ
CEFNEG01	FOTCAS02	JOTQIS	NAWSIN	RAPDES	UKUNOD	YAYBOQ
CEJBID	FUFPIF	JOTROZ	NAXMUU	RAPDIW	UKUPOF	YAZDOS
CEJKEH	FUJCAO	JOTWOE	NAXNAB	RAQGIA	UKUPUL	YAZDUY

CEJLEI	FUSFAA	JOTWOE10	NAYPEJ	RAQGOG	ULEFOG	YAZYEE
CEJLEI01	FUSFEE	JOVDED	NAZBAS	RARQUX	ULOLUC	YAZYII
CEJWEU	GABFEV	JOWRAO	NAZKII	RASMEE	ULOPEQ	YEBLEX
CEJWIY	GAFXIU	JOXCII	NAZSAI	RASMII	ULOZEA	YEBLIB
CEKZIC	GAGMOR	JOXCII10	NBOETO	RASMOO	ULOZOK	YEDZOX
CEKZUO	GAJCUP	JOXCOO	NBOETO01	RASNOP	UMAJOH	YEFMEC
CEMLIP	GALRAN	JOXCOO10	NDIPRX10	RASNUV	UMAKEY	YEGVOV
CEMWIA	GAMCIH	JOZCAC	NECDUU	RASPAD	UMETOV	YEGVOW
CEQZIH	GAMQIV	JOZKAK	NECHIM	RASZER	UMETUB	YEKMUW
CEQZON	GANLEN	JUCCIT	NECKAI	RAVJEE	UMIHED	YELQIP
CIQRAV	GAQNAO	JUDHAR	NECKEM	RAWKAC	UMUJAN	YETYIF
CIQREZ	GAQTOH	JUDMAW	NECVEX	RAWKEG	UMUJER	YEVWIF
CIQYEG	GAQVEZ	JUMSAL	NECVIB	RAWKIK	VACJAL	YEWGOW
CIQYIK	GAQWEA	JUMZIA	NECVOH	RAXCAV	VACJAL01	YEWHUD
CIVPIG	GAQXUS	JUMZOG	NEJKIW	RAZJOS	VAFJER	YEWSIC
CIVPIG10	GAQYAZ	JUMZOG01	NELJAP	RAZNAI	VAGLAQ	YEYNOF
CIVPIG11	GARDEJ	JUQXEY	NELJAP01	RAZNAI01	VAHVUW	YIJJIK
CIYJAV	GARJEP	JURWEY	NELLOF	RAZNIP	VAJNIE	YIKDOL
COCNAJ	GARJIT	JURWIC	NEMBUC	RAZNOV	VAKDIU	YIKQIS
COPQAZ	GARJOZ	JURWOI	NENMIC	RAZQIT	VAKKAT	YIMFUV
COZNUA	GASPOG	JURWUO	NENMOI	RAZQOZ	VAKKIC	YIMGAC
CPTIOO	GASPUM	JUTYAY	NENNAV	RAZQUF	VAKLAU	YIMGAD
CUBPEU	GASROH	JUVTUP	NEPZAJ	RAZRAM	VAKYEM	YIMGAF
CUCQOG	GASXOO	JUXVIH	NEPZEN	RAZREQ	VAKYIQ	YIPXIE
CUCQOG01	GAXXAE	JUXVON	NERHUN	RAZRIU	VAKYOW	YIVJIW
CUDGEN	GAYNUP	KABTIQ	NETKIG	RAZROA	VAKYUC	YIYRED
CUGQEA	GEBYUH	KABTOW	NETLIH	RAZRUG	VAKZAJ	YIYRIH
CUGQEA01	GECNUX	KABZAP	NETLON	RAZSAN	VALPUT	YIZFES
CUGQIE	GECPAF	KABZET	NETMUU	RAZSIV	VALPUT01	YOBRIQ
CULKAV	GEFDOL	KAGBIE	NEWRAI	RAZVIY	VALPUT11	YODCUP
CULKAV01	GEFKEI	KAGBOK	NEWREM	REBNUH	VALXOW	YOFGAB
CUMSEI	GEFWIY	KAGBUQ	NEWRIQ	REBRAR	VAMNEC	YOFNAI
CUMSEI01	GEFWOE	KAGLEJ	NEWROW	REBSOG	VANLEC	YOHJEK
CUPNUW10	GEFWUK	KAGLEJ10	NEXCIC	REGGOZ	VANLIG	YOKVID
CUPXAC	GEGMAH	KAGZOH	NEXCOI	REGHEQ	VANVIP	YOTYAH
CURJOO	GEQLAP	KAHVIZ	NIDTOJ	REGMUM	VAPZUI	YOVGOF
CURKAB	GEQLET	KALCEG	NIJWEI	REGNAT	VAQJAZ	YOVKOJ
CURLIK	GETWIL	KALCIK	NIJWIM	RELXAH	VAQPIM	YOVLAW
CUXXAU	GEWDUH	KAMLAM	NIJWOS	RELXEL	VAQQAG	YOYROT
CUYVOH	GEYWUC	KAMMUH	NIKBOY	REPSOU	VAQQEK	YOYSAG
DABTOQ	GEYXAJ	KAMNAO	NIKMAV	REVCEA	VAQQIO	YOZWUF
DAGJEB	GEYXEN	KAMNES	NIKMAV01	REVCIE	VAVFII	YUBLAI
DAGJEB01	GEZDIY	KAMRUM	NIKMEZ	REVKIM	VAVMEK	YUBNIS
DAHLOO	GEZDIY01	KAMXAX	NIKMID	REVWAQ	VAWKEJ	YUBSET
DAHLUU	GEZJEA	KAMXAX10	NIKMID01	REVWEU	VAWZUP	YUBSET10
DAHMAB	GIBPEM	KAMXEB	NIKSUV	REXDED	VAXBAY	YUCFOR
DAHNAC	GIBPIQ	KAMXEB10	NIKSUV01	REZFIL	VAXJEK	YUFFUA
DAHYUH	GIBPOW	KANBOQ	NITBEX	REZGIM	VAXJUA	YUFTAU
DAHZOC	GICDAX	KANWOM	NITKOQ	RICCOV	VAZFIM	YUKHUH
DAKHEC	GIHSAR	KAPHIS	NIXJIN	RIGQED	VAZYEB	YUKJIX
DAKKEG	GIHSEV	KAPTUR	NIXLEL	RIGQUT	VAZYIF	YUNGOD

DAKNOT	GIHSEV01	KAQNAS	NIXLIP	RIGSAB	VECCEM	YUNTUW
DAKVUH	GIHSEV02	KARDAJ	NOCJEU	RILNUV	VEDFUG	YUPKAV
DAMMEK	GIHSIZ	KARDEN	NOCKUL	RILWUE	VEDGAN	YUTGOJ
DAMXEV	GIHSIZ01	KARDIR	NOCLAS	RIQDEA	VEDGOB	YUTGUP
DANRUF	GILXAA	KARDOX	NOCLEW	RIRNOV	VEDNEX	YUTJAY
DANTAO	GIRKOH	KASCIR	NOFSIK	RIRNOV01	VEFPIG	YUVLAC
DANTES	GISPON	KASFEQ	NOHSEI	RIYYAZ	VEFPOM	YUVVIU
DAQGAE	GISYAI	KATGUH	NOKGEZ	ROFYOA	VEFPUS	YUVVOA
DAQLIR	GOCXAX	KATHAO	NOKGEZ01	ROFYUG	VEFQAZ	YUVVUG
DAQNUE	GOCXEB	KATHES	NONKUW	ROFZAN	VEFQIH	YUVVUG01
DATJIS	GOCXIF	KATNEZ	NOQFUU	ROJGOM	VEFQON	YUXYEV
DATTEY	GODREW	KAVRIJ	NORXUN	ROJGUS	VEFTIK	YUXYIZ
DATTIC	GOFWIH	KAWWIO	NORXUN01	ROLKEI	VEFTOQ	YUXYIZ01
DATTOI	GOGCEK	KAWWIO10	NOXWAY	RONSUI	VEGPON	YUZCUR
DATVEA	GOGCIO	KAXNIH	NOXWEC	RONTAP	VEMLOO	ZAFYEK
DAVYOO	GOKLUN	KAXVUB	NOYLOC	ROPYAW	VENLIJ	ZAFYIO
DAWBAE	GOKLUN01	KAYDAP	NUBTOT	ROQFIM	VERDAX	ZAGJOG
DAWBOS	GOKLUN02	KAYFEW	NUFJUT	ROQRIY	VERDAX10	ZAGPOM
DEBGUM	GOLGUJ	KAYFOF	NUFKAA	RUFMOU	VERDEB	ZAGPUS
DEBSOT	GOMTOR	KAYFUL	NUGPIO	RUGSUH	VERDEB10	ZAKMON
DEBSUZ	GOMVOT	KAYHEX	NUKLOU	RUGTOC	VERDIF	ZAKMON01
DECXIT	GONRUW	KAYJIE	NUNQIW	RUHNIR	VERDIF10	ZATPOZ
DECXOZ	GONSAD	KAYYUE	NUQWEB	RUHNOX	VEZRAT	ZAVMEO
DECXUF	GOPDOE	KAZWIS	NURKOA	RUHNUD	VIJDOH	ZAVMIS
DEFPIO	GOQGIC	KAZXIS	NUSYUV	RUHSES	VIJDOH10	ZAVNEP
DEFPUA	GOQRUZ	KEBHEF	NUWHIW	RUHSES01	VINJUX	ZAVNIT
DEKWUL	GOQSAG	KEDZID	NUYMEZ	RUHSES02	VIRPIV	ZAVNOY
DEKWUL01	GOTKOP	KEDZOJ	NUYMID	RUHSIW	VIVSAU	ZAWREU
DERPEV	GOTTAK	KEDZUP	OBEGAE	RUHSIW01	VIVSEY	ZAXHAJ
DETSAW	GOVNAG	KEGRAP	OBEGEI	RUHSIW02	VIVTUP	ZAXHAJ01
DETSEA	GOXSOB	KEQMEY	OBEVIA	RUJLUD	VIWVEC	ZAXHEL
DEVVIJ	GOXSUH	KEQXEJ	OBEVOG	RUJMAK	VIZCAI	ZAXHIP
DEVVIJ01	GPASMO10	KEQYUA	OBIGAI	RULNIV	VIZCEM	ZAXHIS
DIDXAP	GUBFEO	KEQYUA01	OBIGAI01	RUMJOY	VIZCOW	ZAXHIT
DIDXAP10	GUBGAL	KEQZIP	OBIXOM	RUMJUE	VIZCOW01	ZAXHOV
DIDXET	GUBGAL01	KEQZIP01	OBUNEF	RUNTID	VIZFAL	ZEFJUP
DIDXET10	GUCWAC	KEVYEP	OCEFOS	RUNXON	VIZFAL10	ZEJVEP
DIFVAP	GUJNAA	KIBZUQ	OCEJAI	RUQMAR	VODJUT	ZENDIF
DIFYAS	GUJNAA01	KICSOE	OCEJOW	RUQTAY	VODKAA	ZEQWEX
DIHQOA	GUJNEE	KIJMUL	OCEPAO	RUTMAU	VODKEE	ZERGOS
DIHYUO	GUJNII	KIMRAZ	OCEZEB	RUWVIO	VOMVOI	ZESGIN
DIJQUI	GUMOAT	KIVQUB	OCEZUS	RUWVUA	VONNAN	ZESLAK
DIJRAP	GUMOSI	KIYGOO	OCIBAE	RUXYUE	VOPRIB	ZEVLUH
DILLAL	GUVLEO	KOGPAX	OCIBEI	RUXYUE01	VOPRIB10	ZEVMAO
DIQPAU	GUVLIS	KOGYAG	OCIJAM	RUYKAX	VOQGAJ	ZEVMES
DIQYUX	GUVLOY	KOGYEK	OCINAQ	SABNEP	VOQGEN	ZEYSIF
DIRFEP	GUVLUE	KOHVUY	OCINEU	SACYOL	VOQSOJ	ZEYXIL
DIZFOH	GUVTUN	KOKREH	OCIXIH	SACYUR	VOSGOZ	ZIGTUE
DIZFOH10	GUXQOF	KOKREH10	OCOCUF	SACYUR01	VUKSID	ZIGTUE01
DOLDAJ	GUXQUL	KOSMOU	OCUFEX	SACZAY	VUKSOJ	ZIGVAM
DOLDEN	GUXRAS	KOSMOU10	ODAWEV	SACZEC	VUKSUP	ZIGVAM01

DOLJUJ	GUYQUM	KOZXEC	ODEFIM	SACZIG	VUPSEE	ZIGVEQ
DOWWER	HABXUE	KUCNEB	ODEMUF	SACZOM	VUPSEE10	ZIHDID
DUGTOO	HABYAL	KUCNEB10	ODENAM	SACZUS	VUSBUG	ZIMMIR
DUKMOL	HABYEP	KULJIK	ODENEQ	SADBAB	VUTMIG	ZIPBUV
DUPJUT	HABYIT	KUNHIK	ODENIU	SADBEF	VUTMIG10	ZIRDOT
DUVVUL	HABYOZ	KUPDII	ODENUG	SADBIJ	VUTMOM	ZITXUV
DUVWAS	HABYUF	KURBEE	ODOLIC	SADBOP	VUZLIL	ZIZLAV
EBAHIZ	HACBAP	KURBII	OFIHOA	SADBUV	VUZNEJ	ZNHDNP
EBAHUL	HACSEJ	KURBOO	OFISEB	SADCAC	VUZVUH	ZOFKEK
EBAJAT	HADTOV	KURBUU	OFUPOU	SADCEG	WABKOA	ZOFKEK01
EBAKAU	HAFGIE	LABVOA	OFUPUA	SADCIK	WABNOC	ZOKFUA
EBAKEY	HAFGIE01	LABVUG	OFURAI	SADCOQ	WADJAM	ZOKHOW
EBAKIC	HAFKOP	LABWAN	OFUSEN	SADCUW	WADJIU	ZOPRUR
EBAKOI	HAGHUS	LADLIM	OGEJAL	SADDAD	WADKOC	ZORTUV
EBAKUO	HAHMEI	LADRUD	OGEJEP	SADDEH	WADXUU	ZORVAD
EBALAV	HAHMIM	LAHJUA	OGEMIW	SADDIL	WAFDEN	ZORVAF
EBEHAV	HAHMUY	LAHTUK	OGICIQ	SADDOR	WAFLAR	ZOWREI
EBEVIR	HAHNUA	LAHVAR	OGOLUR	SADDUX	WAHYAG	ZOZBEV
EBEZOB	HAJBUQ	LAHWIB	OHODEU	SADFAF	WAKMOK	ZOZBEV01
EBEZUH	HAJDIG	LAHWOH	OHOTUA	SADFEJ	WALBAN	ZOZBIZ
EBIHED	HAJDUS	LAHZOK	OHOVAI	SADFIN	WALDIX	ZUBJUB
EBOJOV	HAJFEE	LAHZUQ	OHOVEM	SADFOT	WALDOD	ZUBKEM
EBOVOH	HAJGIJ	LAKZIH	OHUHOO	SADFUZ	WALDUJ	ZUBKIQ
EBUFEM	HAJHEG	LAKZON	OHUHOO01	SAGDAF	WALFAR	ZUCTAS
EBUFEM01	HAKCUS	LAKZUT	OHUQUD	SAGKIV	WALHAS	ZUCTEW
EBUKIW	HAKYAT	LALBAC	OHUQUD01	SAGKOB	WALRUW	ZUCTEW01
EBUKOC	HAKZUO	LALCOR	OJEBOU	SAHMOE	WALSAD	ZUCTIA
EBUKUI	HAQFOU	LALCUX	OJEHEQ	SAHMUK	WALSEH	ZUCTIB
EBUQUO	HATREZ	LALJUE	OJEHIU	SAHNOF	WAMWUD	ZUFFUB
EBURAV	HATTIF	LALLEP	OJEHUG	SAHQAU	WANJUR	ZUFVOL
ECAHEW	HAVFIU	LALVUP	OJINOK	SAJTAY	WAPXIV	ZUFVUR
ECAJEY	HAVSAZ	LAMMUI	OKAYOO	SARFIB	WAPXOB	ZULGES
ECAJUO	HAVSED	LANDEK	OKAZAB	SARTAH	WAQBAS	ZULJOF
ECAQOP	HAYFES	LAPCUB	OKAZEF	SARXAL	WAQBEW	ZULJOF01
ECAVOU	HAYFES10	LAPJUH	OKETAZ	SATYOC	WAQBIA	ZUNYUC
ECAVUA	HAYFIW	LAPWII	OKUPIT	SAVBIB	WAQTOY	ZUVTOZ
ECEFIC	HAYFIW10	LAQKAQ	OLADEK	SAVBUN	WAQTUE	ZUZHEH
ECINAF	HAZCUG	LAQKEU	OLADIO	SAVJAA	WAQVAM	ZUZHIL
ECINEJ	HAZDOB	LAQPAU	OLAGOX	SAVJEE	WARBUN	ZZZGIE01
ECININ	HAZDOB10	LAQPAU01	OLAGOX01	SAVTEP	WARHIG	ZZZGIE11
ECIRUE	HAZHUL	LAQPEY	OLAGUD	SAWNAF	WARLOQ	ZZZJZU01
ECISAL	HAZSUX	LAQPEY01	OLAGUD01	SAXRIS	WARNEI	ZZZWQS
ECISEP	HAZTAE	LAQPUP	OLANIY	SAXTIU	WARQAH	ZZZWQS01
ECITAM	HAZTEI	LAQQEA	OLANIY01	SAZPEP	WASFUS	ZZZWQS02
ECITEQ	HECVIV	LAQQUQ	OLATIE	SEBWUR	WASTUG	

Table A.2. All hits from the $M_6(\mu_2\text{-}O)_{12}$ ring

ABIXOZ	ABOKUX	AGICUO	AGIDEZ	AJOCEH	AKUFOB	AQOKAS
AQOKAS01	AYOJIH	BAFVEK	BAOCMO	BAOCMO01	BAOCMO11	BEDBES
BEHJUU	BEQQUK	BEQRAR	BEQREV	BETCOT	BETFIQ	BOKVAY
CASXAW	CASXEA	CECWAJ	CECWEN	CECWIR	CEDYUG	CEKZIC
COPQAZ	CUDGEN	CUMSEI	CUMSEI01	DAHYUH	DAQNUE	DAVYOO
DAWBAE	DAWBOS	DIFVAP	DIFYAS	DIQYUX	ECOKUC	EKULEB
EMUJOL	ESAXUR	ESUWOE	EVUTEU	EZAXEI	FAFQOT	FAFQOT01
FAFQUZ	FAFQUZ01	FAFRAG	FAFRAG01	FAFREK	FAFREK01	FAFRIO
FAFRIO01	FAQYAY	FEXVIO	FEXVOU	FIDMIP	FIQDOY	FIQDOY01
GEGMAH	GEQLET	GEZDIY	GEZDIY01	GIRKOH	GOGCEK	GOGCIO
GOKLUN	GOKLUN01	GOKLUN02	GONRUW	GOTKOP	GOVNAG	GUVTUN
HAVSAZ	HAVSED	HEFXUL	HEGBUQ	HOQHEA	HUHNED	HUHNIH
HUQNUC	HUQPEO	HUZPEX	IBAXUF	IBEYOE	INIMOH	IPUKEJ
IPUKEJ01	IPULUA	IYEXOZ	JAPQOH	JAPQUN	JAPRAU	JAPREY
JAQZOR	JARCOU	JAVQON	JEJKOZ	JEJKUF	JIDNIT	JINKAS
JODDIP	JONWUE	JOZCAC	JUXVIH	JUXVON	KAQNAS	KATGUH
KATHAO	KATHES	KULJIK	KUPDII	LABVUG	LABWAN	LAHWIB
LAHWOH	LALCOR	LALCUX	LATTIK	LAWYIS	LEXQIO	LIPRIL
LIPROR	LIPRUX	LIQNOO	LUQQOD	MAMMOC	MARGOB	MAYNEG
MAYNIK	MEQHUL01	MEQJAT	MEQJEX	MEQZOX	MOGYOW	MOGYUC
MOMASA	MONHOM	NAMOAS	NAVYIT	NAWDIY	NECDUU	NERHUN
NEWRAI	NEWREM	NEWROW	NITBEX	NIXJIN	NOCJEU	NOCKUL
NOCLAS	NOCLEW	OCEZUS	OCIBAE	OCIBEI	OFISEB	OFURAI
OJEHEQ	OJEHIU	OJEHUG	OKETAZ	OKUPIT	PADPOA	PAFHAG
PAFKAJ	PAKPAT	PAKPEX	PAKPIB	PAVKOM	PAZVER	PAZVOB
PEFTUQ	PEJRIF	PIDGIS	PIDGIS01	POBDOZ	POFZOZ	POLTEP
POSPUI	POZRAX	PPHOMO10	PUBDAR	PUBDEV	QAFYAY	QAGVUQ
QAKTOM	QAVDAT	QAXLAD	QAYNEJ	QAYPIP	QIHVIM	QOZPAW
QOZPEA	QUDBEW	RAHBOS	RAPDES	RAPDIW	RAQGIA	RAQGOG
RASMEE	RASMII	RASMOO	RUGSUH	SACZAY	SACZEC	SACZIG
SACZOM	SACZUS	SADBAB	SADBEF	SADBIJ	SADBOP	SADBUV
SADCAC	SADCEG	SADCIK	SADCOQ	SADCUW	SADDAD	SADDEH
SADDIL	SADDOR	SADDUX	SADFAF	SADFEJ	SADFIN	SADFOT
SADFUZ	SAXRIS	SEFSAY	SIGZOX	SIRHEG	SIRHIK	SUKQEU
SULZEE	SULZEE10	SUZPUY	TAMPEC	TAWNAH	TAWWUK	TAWWUK01
TAWWUK02	TIXLAN	TOGYOD	TUFXIB	TUMSUP	TUNYIK	TUQJAQ
TUSFOC	UCOTUB	UDAZUU	UDEBAG	UDEBEK	UDIQED	UHAGAL
UKUMIW	UKUNOD	UMUJER	VACJAL	VACJAL01	VAKLAU	VEFPIG
VEFPOM	VEFPUS	VEFQAZ	VEFQIH	VEFQON	VONNAN	VOQSOJ
VUZLIL	WADKOC	WATGUU	WEFQON	WEQPUD	WESTOD	WESWUM
WETCON	WETFOQ	WIGQIM	WIGYEQ	WIHBAQ	XACZAD	XAFTUT
XAFVAB	XAFVEF	XAFVIJ	XALKOL	XALXOY	XAMKAY	XASKOR
XESQAN	XESQER	XEZFIR	XUTSIO	XUTSIO01	XUXTEP	XUYRAK
YAMHAW	YAMHEA	YAPLIL	YAVYEZ	YAVYID	YEBLIB	YEWGOW
YIKQIS	YIPXIE	YIYRED	YIYRIH	ZAVNOY	ZAWREU	ZIMMIR
ZIRDOT	ZUZHIL					

Table A.3. All hits from the $M_7(\mu_3\text{-}O)_6$ ring

CCDC Ref	Journal
AGICUO	Eur.J.Inorg.Chem. , 2002, , 1081
AGIDEZ	Eur.J.Inorg.Chem. , 2002, , 1081
AQOKAS	Inorg.Chem.Commun. , 2004, 7, 54
AQOKAS01	Inorg.Chem. , 2004, 43, 5850
BEDBES	Chem.Commun. , 2003, , 2664
BEHJUU	Chem.Lett. , 2003, 32, 1040
BEMPAL	Angew.Chem.,Int.Ed. , 2004, 43, 345
BETCOT	J.Am.Chem.Soc. , 2004, 126, 4766
BETFIQ	Inorg.Chem.Commun. , 2004, 7, 521
CASXEA	Inorg.Chem. , 2005, 44, 6062
CECWAJ	Eur.J.Inorg.Chem. , 2005, , 4891
CUDGEN	Inorg.Chim.Aeta , 1999, 295, 244
CUMSEI	Chem.Lett. , 1999, , 585
CUMSEI01	Inorg.Chem. , 2001, 40, 3725
DAHYUH	(Chinese J.Struct.Chem.) , 2004, 23, 1269
DAQNUE	Inorg.Chem.Commun. , 1999, 2, 399
DAWBAE	Inorg.Chim.Acta , 1999, 293, 129
DAWBOS	Inorg.Chim.Acta , 1999, 293, 129
EMUJOL	Inorg.Chem. , 2003, 42, 6604
ESAXUR	Phys.Rev.Lett. , 2002, 88, 167201
ESUWOE	Inorg.Chem.Commun. , 2004, 7, 356
FADXEO	J.Chem.Soc.,Dalton Trans. , 2002, , 829
GARJEP	Angew.Chem.,Int.Ed. , 2005, 44, 5044
HAVSAZ	J.Mol.Struct. , 2005, 753, 61
HEFXUL	Acta Chem.Scand. , 1998, 52, 1194
HEGBUQ	Acta Chem.Scand. , 1998, 52, 1194
HOQHEA	New J.Chem.(Nouv.J.Chim.) , 1999, 23, 185
HUHNED	Inorg.Chem. , 2002, 41, 5133
HUHNIH	Inorg.Chem. , 2002, 41, 5133
IBAXUF	Koord.Khim.(Russ.)(Coord.Chem.) , 2004, 30, 83
INIMOH	J.Cluster Sci. , 2003, 14, 193
IPUKEJ	Inorg.Chem. , 2003, 42, 6971
IPUKEJ01	Polyhedron , 2005, 24, 2443
IPULUA	Inorg.Chem. , 2003, 42, 7067
JAPQOH	New J.Chem.(Nouv.J.Chim.) , 2005, 29, 667
JAPQUN	New J.Chem.(Nouv.J.Chim.) , 2005, 29, 667
JAPRAU	New J.Chem.(Nouv.J.Chim.) , 2005, 29, 667
JAPREY	New J.Chem.(Nouv.J.Chim.) , 2005, 29, 667
JIDNIT	Acta Crystallogr.,Sect.B, 1977, 33, 303
JINKAS	J.Am.Chem.Soc. , 1991, 113, 1844
JONWUE	Angew.Chem.,Int.Ed. , 1992, 31, 191
JOZCAC	Polyhedron , 1992, 11, 1331
KUPDII	Angew.Chem.,Int.Ed. , 1992, 31, 1197
LAHWIB	Inorg.Chem. , 2004, 43, 5850
LAHWOH	Inorg.Chem. , 2004, 43, 5850
MAYNEG	Inorg.Chem. , 2005, 44, 8846
MAYNIK	Inorg.Chem. , 2005, 44, 8846
MEQZOX	Inorg.Chem. , 2001, 40, 5307
NECDUU	Inorg.Chem. , 1997, 36, 6443
NEWRAI	Angew.Chem.,Int.Ed. , 1997, 36, 2482
NEWROW	Angew.Chem.,Int.Ed. , 1997, 36, 2482
NITBEX	Chem.Commun. , 1997, , 1485
NOCJEU	Inorg.Chem. , 1998, 37, 1430
NOCKUL	Inorg.Chem. , 1998, 37, 1499
NOCLAS	Inorg.Chem. , 1998, 37, 1499
NOCLEW	Inorg.Chem. , 1998, 37, 1499
OCEZUS	Chem.-Eur.J. , 2006, 12, 2428
OCIBAE	Chem.-Eur.J. , 2006, 12, 2428
OCIBEI	Chem.-Eur.J. , 2006, 12, 2428
OFURAI	Angew.Chem.,Int.Ed. , 2002, 41, 2506
OJEHEQ	Eur.J.Inorg.Chem. , 2003, , 2406
OJEHIU	Eur.J.Inorg.Chem. , 2003, , 2406
OJEHUG	Eur.J.Inorg.Chem. , 2003, , 2406
PADPOA	Inorg.Chem. , 2004, 43, 5472
PAFKAJ	Angew.Chem.,Int.Ed. , 2004, 43, 4037
PAKPAT	Eur.J.Inorg.Chem. , 2005, , 1149
PAKPEX	Eur.J.Inorg.Chem. , 2005, , 1149
PAKPIB	Eur.J.Inorg.Chem. , 2005, , 1149
PAZVER	Inorg.Chem. , 1998, 37, 3759
PAZVOB	Inorg.Chem. , 1998, 37, 3759
POZRAX	J.Am.Chem.Soc. , 1998, 120, 7365
PUZCUI	Z.Anorg.Allg.Chem. , 2002, 628, 913
QAVDAT	J.Am.Chem.Soc. , 2005, 127, 12862
QAYNEJ	Chem.Lett. , 2000, , 770
QUDBEW	Chem.-Eur.J. , 2001, 7, 1796
RAPDES	J.Mol.Struct. , 2005, 743, 117
RAPDIW	J.Mol.Struct. , 2005, 743, 117
RAQGOG	Inorg.Chem. , 2005, 44, 1208
RASMEE	Cryst.Growth Des. , 2005, 5, 1531
RASMII	Cryst.Growth Des. , 2005, 5, 1531
RASMOO	Cryst.Growth Des. , 2005, 5, 1531
SUZPUY	J.Inorg.Biochem. , 1995, 59, 785
TAFHIS	Organometallics , 2003, 22, 2505
TAMPEC	Inorg.Chem. , 1991, 30, 3244
TAWWUK	Inorg.Chem. , 2005, 44, 5397
TAWWUK01	Inorg.Chem. , 2005, 44, 5397
TAWWUK02	Inorg.Chem. , 2005, 44, 5397
TUMSUP	Chem.-Eur.J. , 1996, 2, 1379
TUNYIK	Inorg.Chem. , 1996, 35, 6640
TUQJAQ	Chem.Commun. , 1997, , 721
TUSFOC	Angew.Chem.,Int.Ed. , 2003, 42, 223
UCOTUB	Chem.-Eur.J. , 2001, 7, 3438
UDAZUU	Angew.Chem.,Int.Ed. , 2001, 40, 3578
UDEBAG	Angew.Chem.,Int.Ed. , 2001, 40, 3578
UDEBEK	Angew.Chem.,Int.Ed. , 2001, 40, 3578
UKUMIW	Angew.Chem.,Int.Ed. , 2003, 42, 3763
VEFPIG	Chem.-Eur.J. , 2006, 12, 1767
VEFPOM	Chem.-Eur.J. , 2006, 12, 1767
VEFPUS	Chem.-Eur.J. , 2006, 12, 1767
VEFQIH	Chem.-Eur.J. , 2006, 12, 1767
VEFQON	Chem.-Eur.J. , 2006, 12, 1767
VINJUX	Koord.Khim.(Russ.)(Coord.Chem.) , 1990, 16, 354
WADKOC	Acta Crystallogr.,Sect.E, 2003, 59, m345
WATGUU	J.Mol.Struct. , 2005, 751, 184
WESTOD	J.Chem.Soc.,Dalton Trans. , 2000, , 1835
WESWUM	J.Chem.Soc.,Dalton Trans. , 2000, , 1835
WETCON	J.Chem.Soc.,Dalton Trans. , 2000, , 1835
WETFOQ	J.Chem.Soc.,Dalton Trans. , 2000, , 1835
XALKOL	Mendeleev Commun. , 2005, , 79
XALXOY	Acta Crystallogr.,Sect.E, 2005, 61, m611
XEFNEC	Appl.Organomet.Chem. , 2005, 19, 1263
XEZFIR	Angew.Chem.,Int.Ed. , 2001, 40, 1957
XUTSIO	Chem.Commun. , 2003, , 532
XUTSIO01	Inorg.Chem. , 2004, 43, 5850
XUYRAK	Acta Crystallogr.,Sect.E, 2003, 59, m116
YAMHAW	Eur.J.Inorg.Chem. , 2005, , 854
YAMHEA	Eur.J.Inorg.Chem. , 2005, , 854
YEBLIB	J.Solid State Chem. , 2006, 179, 122
ZUFFUB	Inorg.Chim.Acta , 1995, 231, 153

Table A.4. All hits from the $M_7(\mu_3\text{-}O)_6(\mu_2\text{-}O)_6$ ring

CCDC Ref	Journal
AGICUO	Eur. J. Inorg. Chem., 2002, , 1081
AGIDEZ	Eur. J. Inorg. Chem., 2002, , 1081
AQOKAS	Inorg.Chem.Commun. , 2004, 7, 54
AQOKAS01	Inorg. Chem., 2004, 43, 5850
BEDBES	Chem.Commun. , 2003, , 2664
BEHJUU	Chem.Lett. , 2003, 32, 1040
BETCOT	J.Am.Chem.Soc. , 2004, 126, 4766
BETFIQ	Inorg.Chem.Commun. , 2004, 7, 521
CASXEA	Inorg. Chem., 2005, 44, 6062
CUDGEN	Inorg.Chim.Acta , 1999, 295, 244
CUMSEI	Chem.Lett. , 1999, , 585
CUMSEI01	Inorg. Chem., 2001, 40, 3725
DAHYUH	Jiegou Huaxue(Chinese J.Struct.Chem.) , 2004, 23, 1269
DAQNUE	Inorg.Chem.Commun. , 1999, 2, 399
DAWBAE	Inorg.Chim.Acta , 1999, 293, 129
DAWBOS	Inorg.Chim.Acta , 1999, 293, 129
EMUJOL	Inorg. Chem., 2003, 42, 6604
ESAXUR	Phys.Rev.Lett. , 2002, 88, 167201
ESUWOE	Inorg.Chem.Commun. , 2004, 7, 356
HAVSAZ	J.Mol.Struct. , 2005, 753, 61
HEFXUL	Acta Chem.Scand. , 1998, 52, 1194
HEGBUQ	Acta Chem.Scand. , 1998, 52, 1194
HOQHEA	New J.Chem.(Nouv.J.Chim.) , 1999, 23, 185
HUHNED	Inorg. Chem., 2002, 41, 5133
HUHNIH	Inorg. Chem., 2002, 41, 5133
IBAXUF	Koord.Khim.(Russ.)(Coord.Chem.) , 2004, 30, 83
INIMOH	J.Cluster Sci. , 2003, 14, 193
IPUKEJ	Inorg. Chem., 2003, 42, 6971
IPUKEJ01	Polyhedron , 2005, 24, 2443
IPULUA	Inorg. Chem., 2003, 42, 7067
JAPQOH	New J.Chem.(Nouv.J.Chim.) , 2005, 29, 667
JAPQUN	New J.Chem.(Nouv.J.Chim.) , 2005, 29, 667
JAPRAU	New J.Chem.(Nouv.J.Chim.) , 2005, 29, 667
JAPREY	New J.Chem.(Nouv.J.Chim.) , 2005, 29, 667
JIDNIT	Acta Crystallogr.,Sect.B, 1977, 33, 303
JINKAS	J.Am.Chem.Soc. , 1991, 113, 1844
JONWUE	Angew.Chem.,Int.Ed. , 1992, 31, 191
JOZCAC	Polyhedron , 1992, 11, 1331
KUPDII	Angew.Chem.,Int.Ed. , 1992, 31, 1197
LAHWIB	Inorg. Chem., 2004, 43, 5850
LAHWOH	Inorg. Chem., 2004, 43, 5850
MAYNEG	Inorg. Chem., 2005, 44, 8846
MAYNIK	Inorg. Chem., 2005, 44, 8846
MEQZOX	Inorg. Chem., 2001, 40, 5307
NECDUU	Inorg. Chem., 1997, 36, 6443
NEWRAI	Angew.Chem.,Int.Ed. , 1997, 36, 2482
NEWROW	Angew.Chem.,Int.Ed. , 1997, 36, 2482
NITBEX	Chem.Commun. , 1997, , 1485
NOCJEU	Inorg. Chem., 1998, 37, 1430
NOCKUL	Inorg. Chem., 1998, 37, 1499
NOCLAS	Inorg. Chem., 1998, 37, 1499
NOCLEW	Inorg. Chem., 1998, 37, 1499
OCEZUS	Chem.-Eur.J. , 2006, 12, 2428
OCIBAE	Chem.-Eur.J. , 2006, 12, 2428
OCIBEI	Chem.-Eur.J. , 2006, 12, 2428
OFURAI	Angew.Chem.,Int.Ed. , 2002, 41, 2506
OJEHEQ	Eur. J. Inorg. Chem., 2003, , 2406
OJEHIU	Eur. J. Inorg. Chem., 2003, , 2406
OJEHUG	Eur. J. Inorg. Chem., 2003, , 2406
PADPOA	Inorg. Chem., 2004, 43, 5472
PAFKAJ	Angew.Chem.,Int.Ed. , 2004, 43, 4037
PAKPAT	Eur. J. Inorg. Chem., 2005, , 1149
PAKPEX	Eur. J. Inorg. Chem., 2005, , 1149
PAKPIB	Eur. J. Inorg. Chem., 2005, , 1149
PAZVER	Inorg. Chem., 1998, 37, 3759
PAZVOB	Inorg. Chem., 1998, 37, 3759
POZRAX	J.Am.Chem.Soc. , 1998, 120, 7365
QAVDAT	J.Am.Chem.Soc. , 2005, 127, 12862
QAYNEJ	Chem.Lett. , 2000, , 770
QUDBEW	Chem.-Eur.J. , 2001, 7, 1796
RAPDES	J.Mol.Struct. , 2005, 743, 117
RAPDIW	J.Mol.Struct. , 2005, 743, 117
RAQGOG	Inorg. Chem., 2005, 44, 1208
RASMEE	Cryst.Growth Des. , 2005, 5, 1531
RASMII	Cryst.Growth Des. , 2005, 5, 1531
RASMOO	Cryst.Growth Des. , 2005, 5, 1531
SUZPUY	J.Inorg.Biochem. , 1995, 59, 785
TAWWUK	Inorg. Chem., 2005, 44, 5397
TAWWUK01	Inorg. Chem., 2005, 44, 5397
TAWWUK02	Inorg. Chem., 2005, 44, 5397
TUMSUP	Chem.-Eur.J. , 1996, 2, 1379
TUNYIK	Inorg. Chem., 1996, 35, 6640
TUQJAQ	Chem.Commun. , 1997, , 721
TUSFOC	Angew.Chem.,Int.Ed. , 2003, 42, 223
UCOTUB	Chem.-Eur.J. , 2001, 7, 3438
UDAZUU	Angew.Chem.,Int.Ed. , 2001, 40, 3578
UDEBAG	Angew.Chem.,Int.Ed. , 2001, 40, 3578
UDEBEK	Angew.Chem.,Int.Ed. , 2001, 40, 3578
UKUMIW	Angew.Chem.,Int.Ed. , 2003, 42, 3763
VEFPIG	Chem.-Eur.J. , 2006, 12, 1767
VEFQIH	Chem.-Eur.J. , 2006, 12, 1767
VEFQON	Chem.-Eur.J. , 2006, 12, 1767
WADKOC	Acta Crystallogr.,Seet.E, 2003, 59, m345
WATGUU	J.Mol.Struct. , 2005, 751, 184
WESTOD	J.Chem.Soc.,Dalton Trans. , 2000, , 1835
WESWUM	J.Chem.Soc.,Dalton Trans. , 2000, , 1835
WETCON	J.Chem.Soc.,Dalton Trans. , 2000, , 1835
WETFOQ	J.Chem.Soc.,Dalton Trans. , 2000, , 1835
XALKOL	Mendeleev Commun. , 2005, , 79
XALXOY	Acta Crystallogr.,Sect.E, 2005, 61, m611
XEZFIR	Angew.Chem.,Int.Ed. , 2001, 40, 1957
XUTSIO	Chem.Commun. , 2003, , 532
XUTSIO01	Inorg. Chem., 2004, 43, 5850
XUYRAK	Acta Crystallogr.,Sect.E, 2003, 59, m116
YAMHAW	Eur. J. Inorg. Chem., 2005, , 854
YAMHEA	Eur. J. Inorg. Chem., 2005, , 854
YEBLIB	J.Solid State Chem. , 2006, 179, 122

Table A.5. All hits from the $M_{13}(\mu_3\text{-}O)_6(\mu_2\text{-}O)_{18}$ ring
Data table from Search 5, The M13 Fragment

BETCOT	*J. Am. Chem. Soc.*, **2004,** *126,* 4766
JIDNIT	*Acta Crystallogr., Sect. B*, **1977,** *33,* 303
JONWUE	*Angew. Chem., Int. Ed.*, **1992,** *31,* 191
MEQZOX	*Inorg. Chem.*, **2001,** *40,* 5307
OFURAI	*Angew. Chem., Int. Ed.*, **2002,** *41,* 2506
PAFKAJ	*Angew. Chem., Int. Ed.*, **2004,** *43,* 4037
QAVDAT	*J. Am. Chem. Soc.*, **2005,** *127,* 12862
SUZPUY	*J. Inorg. Biochem.*, **1995,** *59,* 785
TAWWUK	*Inorg. Chem.*, **2005,** *44,* 5397
TAWWUK01	*Inorg. Chem.*, **2005,** *44,* 5397
TAWWUK02	*Inorg. Chem.*, **2005,** *44,* 5397
UCOTUB	*Chem.-Eur. J.*, **2001**, *7,* 3438
UKUMIW	*Angew. Chem., Int. Ed.*, **2003,** *42,* 3763
VEFPIG	*Chem.-Eur. J.*, **2006**, *12,* 1767
VEFQIH	*Chem.-Eur. J.*, **2006**, *12,* 1767
WESTOD	*J. Chem. Soc., Dalton Trans.*, **2000,** 1835
WESWUM	*J. Chem. Soc., Dalton Trans.*, **2000,** 1835
WETCON	*J. Chem. Soc., Dalton Trans.*, **2000,** 1835
WETFOQ	*J. Chem. Soc., Dalton Trans.*, **2000,** 1835
YEBLIB	*J. Solid State Chem.*, **2006,** *179,* 122

APPENDIX B

SUPPLEMENTAL INFORMATION FOR Ga_{13} SYNTHESIS

Supporting Information

Experimental Section

1 forms *via* slow evaporation of a 5 mL methanolic solution of $Ga(NO_3)_3 \cdot 6H_2O$ (0.182 g, 0.500 mmol) in the presence of nitrosobenzene (0.0535 g, 0.500 mmol), yield of 0.905 g (0.326 mmol, 65%) was obtained. Crystals of **1** were shown to be representative of the bulk by comparison of the X-ray powder pattern collected on a fresh sample with the corresponding pattern calculated from the crystal structure (*Figures S1 and S2*). The initial light blue solution turns pale yellow after 1 day indicating the oxidation of nitrosobenzene to nitrobenzene. The pH of a solution of **1** dissolved in water (1.6 mM) was measured as 2.28. Dissolution of Ga_{13} cluster, **1**, in water followed by recrystallization *via* evaporation resulted in the sole formation of **1** as determined by single crystal unit cell determination and X-ray powder diffraction. In a preliminary effort to determine the effect of nitrozobenzene on the formation of **1**, the same reaction was conducted in presence of water, pyridine, 2,6-lutidine and nitrobenzene. These attempts were unsuccessful to generate **1** and resulted in the recrystallization of $Ga(NO_3)_3$

or in the formation of $GaL_2(NO_3)_3$ (where L = 2,6-lutidine). As an interesting caveat, crystals of the title compound were originally prepared by slow evaporation of a methanolic($-d_4$) solution of a confidential proprietary compound in the presence of an excess of gallium nitrate hydrate. This proprietary compound contained a nitroso functional group, and the crystallization of **1** has since been successfully repeated using only nitrosobenzene to mediate the crystallization.

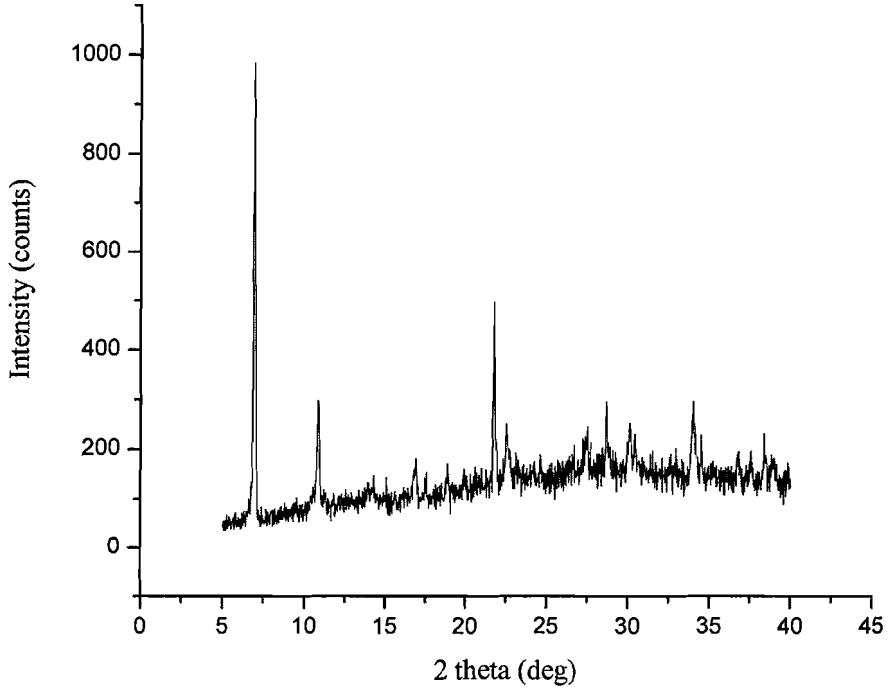

Figure B1. X-ray powder diffraction pattern of a fresh sample of **1**.

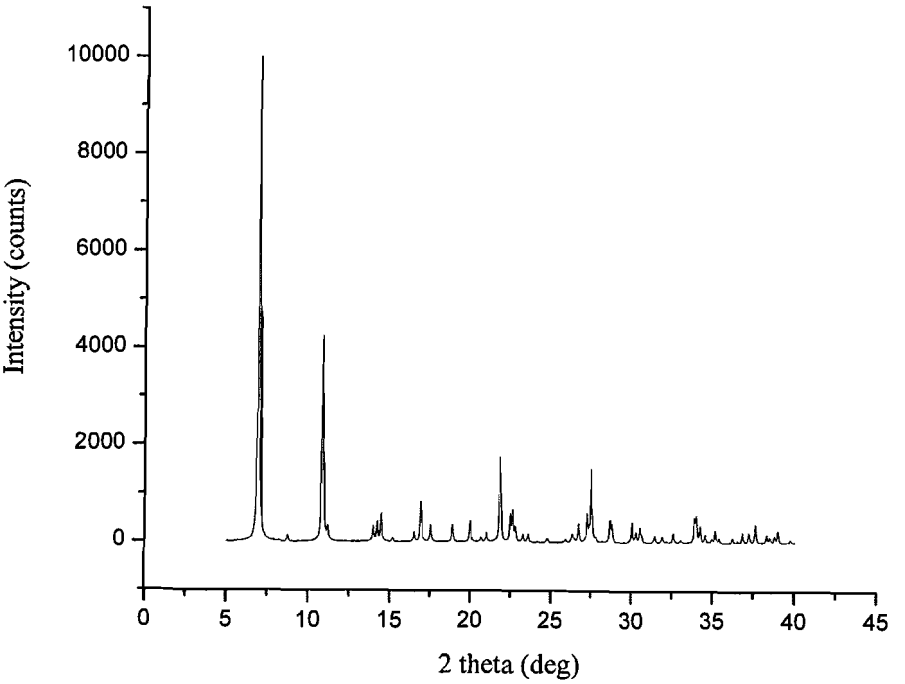

Figure B2. X-ray powder diffraction pattern calculated from the single crystal structure of **1**.

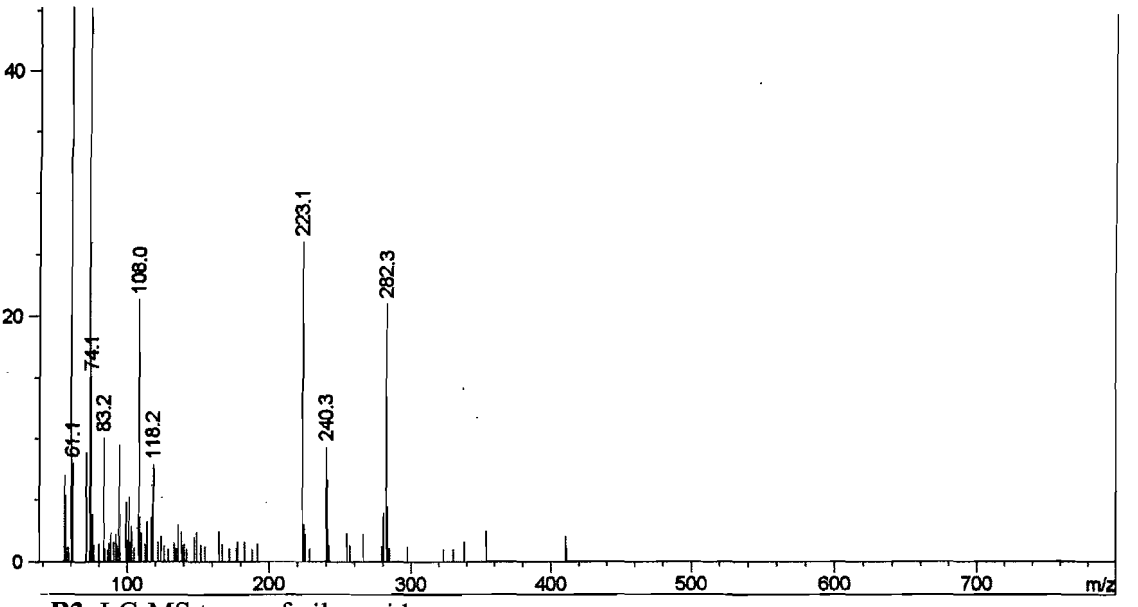

Figure B3. LC-MS trace of oily residue

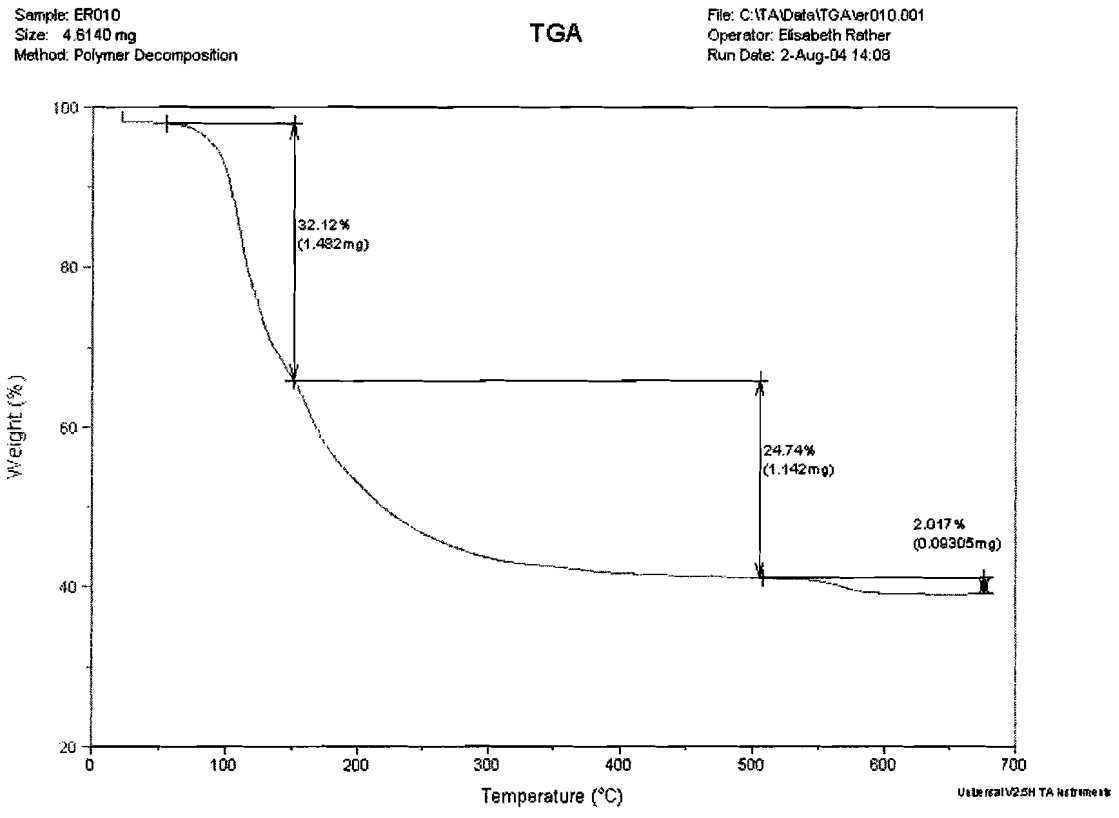

Figure B4. TGA of tridecameric inorganic nanocluster.

JTG6 XRD Data

The crystal was grown by evaporation from MeOH at 22 °C over 1 week. The crystal was mounted on a quartz fiber with paratone oil. Data in the frames corresponding to an arbitrary hemisphere of data (ω scans, 10 sec frames) were intergrated using SAINT.[1] Data were corrected for Lorentz and polarization effects. The data were further analyzed using XPREP.[2] An empirical absorption correction based on the measurement of redundant and equivalent reflections and an ellipsoidal model for the

absorption surface were applied using SADABS.[3] The structure solution and refinement were performed using SHELXTL (refined on F2).[2] All non-hydrogen atoms were refined anisotropically. Hydrogen atoms were included but not refined on all appropriate atoms. Special positions for the nitros.

Crystal size 0.45 x 0.25 x 0.15 mm; T = 21°C; Rhombohedral, R-3 (#148), a = 20.214 (3) Å, b = 20.214 (3) Å, c = 18.353 (4) Å, $\alpha = 90°$, $\beta = 90°$, $\gamma = 120°$; V = 6494.7 (19) $Å^3$, Z = 3, $\mu = 4.128\ mm^{-1}$, F(000) = 4116 $\rho_{calcd} = 2.127\ g\ mL^{-1}$, $2\Theta_{max} = 52.8°$. Of the 12652 reflections that were collected, 2832 were unique (Rint = 0.0318); equivalent reflections were merged. Empirical absorption correction: Tmax = 0.999, Tmin = 0.660. Final R1 = 0.0404 for 2832 data for $I>2\sigma(I)$ (189 Parameters, 6 restraints); for all 2832 data, *w*R2 = 0.1120, GOF = 1.153.

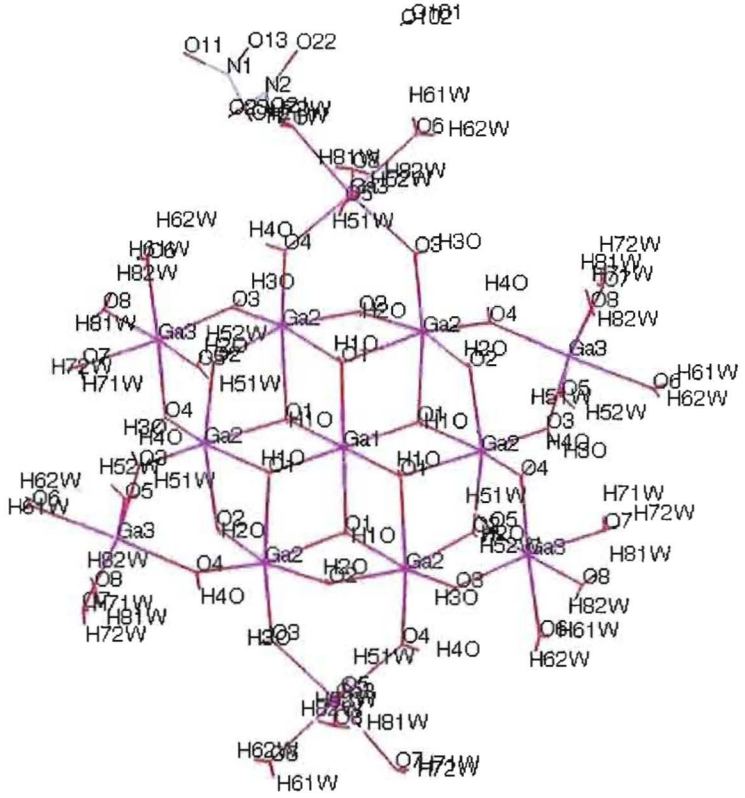

Figure B.5. Crystal Structure of Ga_{13}

Table B.1 Experimental Crystal data for Ga_{13}

$H_{72}Ga_{13}N_{15}O_{99}$
M_r = 2773.09
Trigonal
R-3
a = 20.214 (3) °A
b = 20.214 (3) °A
c = 18.353 (4) °A
α = 90.00
V = 6494.7 (19) °A3
Z = 3
D_x = 2.127 Mg m-3
D_m not measured

Data collection
Bruker P4 diffractometer
ω scans
Absorption correction:
SADABS
T_{min} = 0.702, T_{max} = 1.000
12648 measured reflections
2831 independent reflections
2500 reflections with
>2sigma(I)
R_{int} = 0.0320

Refinement
Refinement on F^2
$R[F^2 > 2 (F^2)]$ = 0.0310
$wR(F^2)$ = 0.0988
S = 1.035
2831 reflections

228 parameters
H atoms treated by a mixture of independent and constrained refinement

Mo Kα radiation
λ = 0.71073 Å
Cell parameters from ? reflections
Θ = ? –? °
v = 4.128 mm^{-1}
T = 293 (2) K
Polyhedron
Colorless
0.3 x 0.2 x 0.2 mm
Crystal source: ?

Θ max = 26.40°
h = -24 -> 25
k = -25 -> 25
l = -22 -> 22
? standard reflections every ? reflections
intensity decay: ?%

$w=1/[\ 2(F_o^2) + (0.0716P)^2 + 0.0000P]$
where $P = (F_o^2 + 2F_c^2)/3$
$(\Delta/\sigma)_{max}$ = 0.006
$\Delta\rho_{max}$ = 0.949 e $Å^3$
$\Delta\rho_{min}$ = -0.567 e $Å^3$
Extinction correction: none
Scattering factors from International Tables for Crystallography (Vol. C)

Table B.2. Fractional atomic coordinates and equivalent isotropic displacement parameters (Å2)
$U_{eq} = (1/3)\ \Sigma_i\ \Sigma_j U^{ij} a^i a^j \mathbf{a}_i.\mathbf{a}_j$.

	Occupancy	x	y	z	Ueq
Ga1	1	1.0000	1.0000	0.0000	0.0196 (2)
Ga2	1	0.837137 (19)	0.980265 (18)	-0.004021 (17)	0.01921 (13)
Ga3	1	0.697660 (19)	0.821112 (19)	0.09437 (2)	0.02311 (14)
O1	1	0.94201 (11)	1.03770 (11)	-0.05420 (13)	0.0206 (5)
O2	1	0.81260 (13)	0.88619 (12)	-0.05055 (12)	0.0220 (5)
O3	1	0.75336 (12)	0.92485 (12)	0.06121 (12)	0.0236 (5)
O4	1	0.79718 (13)	1.02078 (13)	-0.07527 (13)	0.0252 (5)
O5	1	0.73030 (15)	0.85021 (15)	0.19711 (14)	0.0366 (6)
O6	1	0.61213 (14)	0.84161 (15)	0.11670 (16)	0.0383 (6)
O7	1	0.62994 (14)	0.71683 (14)	0.13696 (15)	0.0361 (6)
O8	1	0.64377 (14)	0.77510 (15)	0.00175 (14)	0.0351 (6)
N1	1	0.72277 (17)	0.79552 (17)	0.80145 (17)	0.0350 (7)
O11	1	0.71311 (19)	0.74566 (17)	0.84609 (17)	0.0521 (8)
O12	1	0.7779 (2)	0.85971 (19)	0.80506 (18)	0.0694 (11)

O13	1	0.67501 (18)	0.77931 (17)	0.75176 (19)	0.0594 (9)
N2	1	0.6356 (2)	0.7175 (2)	0.3316 (2)	0.0496 (9)
O21	1	0.6723 (2)	0.7530 (2)	0.38610 (19)	0.0617 (9)
O22	1	0.5727 (3)	0.7093 (4)	0.3191 (3)	0.1118 (18)
O23	1	0.6625 (2)	0.6879 (2)	0.28942 (19)	0.0620 (9)
O1W	0.41	0.4695 (4)	0.7399 (5)	0.1144 (7)	0.076 (3)
O2W	0.36	0.4954 (6)	0.7571 (7)	0.2073 (7)	0.082 (4)
N3	0.40	0.8976 (12)	1.0014 (10)	-0.2688 (9)	0.192 (11)
O31	0.40	0.9191 (5)	1.0314 (5)	-0.2036 (3)	0.0442 (18)
O32	0.40	0.9065 (9)	0.9441 (10)	-0.3005 (8)	0.130 (6)
O33	0.40	0.8553 (12)	1.0232 (9)	-0.3095 (14)	0.45 (4)
N3B	0.10	0.9278 (16)	0.9982 (17)	-0.2055 (16)	0.098 (9)
O31B	0.10	0.961 (2)	1.0686 (18)	-0.200 (3)	0.098 (9)
O32B	0.10	0.9634 (18)	0.964 (2)	-0.206 (3)	0.098 (9)
O33B	0.10	0.8571 (16)	0.962 (2)	-0.211 (3)	0.098 (9)

Table B.3. Anisotropic displacement parameters (Å2)

	U_{11}	U_{22}	U_{33}	U_{12}	U_{13}	U_{23}
Ga1	0.0162 (3)	0.0162 (3)	0.0264 (4)	0.00809 (13)	0.000	0.000
Ga2	0.01709 (19)	0.01609 (19)	0.0241 (2)	0.00803 (13)	0.00043 (12)	0.00067 (12)
Ga3	0.0208 (2)	0.0206 (2)	0.0277 (2)	0.01018 (15)	0.00380 (13)	0.00216 (13)
O1	0.0203 (11)	0.0213 (11)	0.0225 (12)	0.0120 (9)	0.0009 (8)	0.0017 (8)
O2	0.0259 (11)	0.0209 (10)	0.0225 (11)	0.0142 (9)	-0.0053 (9)	-0.0030 (8)
O3	0.0240 (11)	0.0175 (10)	0.0283 (12)	0.0097 (9)	0.0062 (9)	0.0003 (9)
O4	0.0210 (11)	0.0209 (11)	0.0318 (12)	0.0089 (9)	-0.0063 (9)	0.0002 (9)
O5	0.0380 (14)	0.0430 (15)	0.0317 (14)	0.0225 (12)	-0.0004 (11)	-0.0036 (11)
O6	0.0324 (13)	0.0376 (15)	0.0508 (17)	0.0219 (12)	0.0112 (12)	0.0086 (12)
O7	0.0364 (14)	0.0264 (12)	0.0404 (14)	0.0119 (11)	0.0075 (11)	0.0085 (11)
O8	0.0359 (14)	0.0312 (13)	0.0349 (14)	0.0144 (11)	-0.0055 (11)	-0.0022 (11)
N1	0.0325 (16)	0.0331 (16)	0.0338 (17)	0.0121 (14)	-0.0071 (13)	-0.0049 (13)
O11	0.0584 (19)	0.0385 (16)	0.0523 (18)	0.0189 (14)	-0.0214 (15)	0.0058 (14)
O12	0.066 (2)	0.0501 (19)	0.0422 (19)	-0.0079 (17)	-0.0183 (16)	0.0020 (15)
O13	0.0482 (18)	0.0440 (17)	0.063 (2)	0.0058 (14)	-0.0312 (16)	0.0119 (15)
N2	0.059 (2)	0.062 (2)	0.040 (2)	0.040 (2)	-0.0015 (17)	-0.0036 (18)
O21	0.086 (3)	0.073 (2)	0.0492 (19)	0.057 (2)	-0.0072 (18)	-0.0143 (17)
O22	0.095 (3)	0.194 (6)	0.081 (3)	0.098 (4)	-0.012 (3)	-0.017 (4)
O23	0.084 (3)	0.066 (2)	0.049 (2)	0.046 (2)	-0.0035 (16)	-0.0127 (17)
O1W	0.023 (4)	0.052 (5)	0.144 (10)	0.013 (3)	-0.005 (5)	0.003 (5)
O2W	0.055 (6)	0.076 (7)	0.114 (10)	0.032 (6)	0.045 (6)	0.039 (7)
N3	0.18 (2)	0.133 (17)	0.24 (2)	0.060 (15)	0.122 (18)	0.075 (17)
O31	0.077 (5)	0.066 (5)	0.009 (3)	0.050 (4)	0.007 (3)	-0.007 (3)
O32	0.192 (17)	0.152 (14)	0.075 (9)	0.108 (13)	0.042 (9)	0.024 (8)
O33	0.19 (2)	0.048 (9)	1.12 (11)	0.064 (12)	0.19 (4)	-0.02 (3)

Table B.4. Selected geometric parameters (Å, °)

Ga1—O1^{i}	1.959 (2)	Ga2—O2	1.910 (2)
Ga1—O1^{ii}	1.959 (2)	Ga2—O3	1.913 (2)
Ga1—O1^{iii}	1.959 (2)	Ga2—O2^{iii}	1.917 (2)
Ga1—O1	1.959 (2)	Ga2—O4	1.922 (2)
Ga1—O1^{iv}	1.959 (2)	Ga2—O1	2.056 (2)
Ga1—O1^{v}	1.959 (2)	Ga2—O1^{v}	2.153 (2)

Ga3—O4^{v}	1.913 (2)
Ga3—O3	1.917 (2)
Ga3—O8	1.982 (3)
Ga3—O5	1.987 (3)
Ga3—O7	2.011 (2)
Ga3—O6	2.011 (2)
O1—Ga2^{iii}	2.153 (2)
O2—Ga2^{v}	1.917 (2)
O4—Ga3^{iii}	1.913 (2)
N1—O12	1.218 (4)
N1—O11	1.236 (4)
N1—O13	1.247 (4)
N2—O22	1.218 (5)
N2—O21	1.239 (5)
N2—O23	1.256 (5)
O1W—O2W	1.767 (18)
N3—O31	1.313 (15)
N3—O33	1.362 (16)
N3—O32	1.386 (14)
N3B—O32B	1.2215
N3B—O31B	1.2363
N3B—O33B	1.2420
N3B—O32B^{iv}	1.28 (6)
O31B—O32B^{iv}	1.26 (7)
O32B—O31B^{i}	1.26 (5)
O32B—O32B^{iv}	1.27 (5)
O32B—O32B^{i}	1.27 (8)
O32B—N3B^{i}	1.28 (5)

O1^{i}—Ga1—O1^{ii}	83.50 (9)
O1^{i}—Ga1—O1^{iii}	180.00 (12)
O1^{ii}—Ga1—O1^{iii}	96.50 (9)
O1^{i}—Ga1—O1	96.50 (9)
O1^{ii}—Ga1—O1	180.0
O1^{iii}—Ga1—O1	83.50 (9)
O1^{i}—Ga1—O1^{iv}	96.50 (9)
O1^{ii}—Ga1—O1^{iv}	83.50 (9)
O1^{iii}—Ga1—O1^{iv}	83.50 (9)
O1—Ga1—O1^{iv}	96.50 (9)
O1^{i}—Ga1—O1^{v}	83.50 (9)
O1^{ii}—Ga1—O1^{v}	96.50 (9)
O1^{iii}—Ga1—O1^{v}	96.50 (9)
O1—Ga1—O1^{v}	83.50 (9)
O1^{iv}—Ga1—O1^{v}	180.0
O2—Ga2—O3	89.06 (9)
O2—Ga2—O2^{iii}	164.25 (12)
O3—Ga2—O2^{iii}	96.90 (9)
O2—Ga2—O4	99.49 (10)
O3—Ga2—O4	103.75 (10)
O2^{iii}—Ga2—O4	93.26 (10)
O2—Ga2—O1	92.47 (10)
O3—Ga2—O1	166.37 (9)
O2^{iii}—Ga2—O1	78.37 (9)
O4—Ga2—O1	89.37 (9)
O2—Ga2—O1^{v}	76.16 (9)
O3—Ga2—O1^{v}	90.68 (9)
O2^{iii}—Ga2—O1^{v}	89.16 (9)
O4—Ga2—O1^{v}	164.96 (10)
O1—Ga2—O1^{v}	76.57 (12)
O4^{v}—Ga3—O3	96.35 (10)
O4^{v}—Ga3—O8	93.19 (11)
O3—Ga3—O8	97.20 (10)
O4^{v}—Ga3—O5	93.08 (11)
O3—Ga3—O5	92.92 (10)
O8—Ga3—O5	167.43 (11)
O4^{v}—Ga3—O7	91.29 (10)
O3—Ga3—O7	171.86 (10)
O8—Ga3—O7	85.13 (11)
O5—Ga3—O7	83.84 (11)
O4^{v}—Ga3—O6	177.38 (10)
O3—Ga3—O6	86.25 (10)
O8—Ga3—O6	86.79 (12)
O5—Ga3—O6	86.45 (11)
O7—Ga3—O6	86.10 (11)
Ga1—O1—Ga2	101.62 (10)
Ga1—O1—Ga2^{iii}	98.31 (10)
Ga2—O1—Ga2^{iii}	95.47 (9)
Ga2—O2—Ga2^{v}	108.99 (11)
Ga2—O3—Ga3	134.68 (12)
Ga3^{iii}—O4—Ga2	130.90 (12)
O12—N1—O11	121.3 (3)
O12—N1—O13	119.7 (3)
O11—N1—O13	119.0 (3)
O22—N2—O21	120.8 (4)
O22—N2—O23	119.4 (5)
O21—N2—O23	119.8 (4)
O31—N3—O33	117.9 (12)
O31—N3—O32	128.1 (13)

O33—N3—O32	113.8 (11)	N3B—O32B—O32B^{iv}	61 (3)
O32B—N3B—O31B	121.1	O31B^{i}—O32B—O32B^{iv}	174 (3)
O32B—N3B—O33B	119.7	N3B—O32B—O32B^{i}	121 (3)
O31B—N3B—O33B	119.2	O31B^{i}—O32B—O32B^{i}	116 (4)
O32B—N3B—O32B^{iv}	61 (3)	O32B^{iv}—O32B—O32B^{i}	60.0
O31B—N3B—O32B^{iv}	60 (3)	N3B—O32B—N3B^{i}	179 (4)
O33B—N3B—O32B^{iv}	175.2 (7)	O31B^{i}—O32B—N3B^{i}	58 (3)
N3B—O31B—O32B^{iv}	61 (2)	O32B^{iv}—O32B—N3B^{i}	117 (2)
N3B—O32B—O31B^{i}	123 (4)	O32B^{i}—O32B—N3B^{i}	57 (2)

Symmetry codes:
(i) 2−y, 1+x−y, z; (ii) 2−x, 2−y,−z; (iii) y, 1−x+y,−z; (iv) 1−x+y, 2−x, z; (v) 1 + x − y, x,−z.

We are exploring the generality of the nitroso oxidation reaction to see if other inorganic nanoclusters can be synthesized *via* the same method and if there are other possible oganic reductants that can be used to make the same type of clusters. Follow up work on making new clusters, trying other reductants and checking their functional group tolerance.

After publication in the Journal of the American Chemical Society our results were highlighted in the March 4th issue of Science as an Editor's choice.

EDITORS' CHOICE

edited by Gilbert Chin

CHEMISTRY

Reducing Nitrogen

The formation of stable and well-defined inorganic clusters often requires the presence of chelating organic ligands. Rather *et al.* report using an organic reaction to drive the formation of a hydroxyl-bridged Ga_{13} cluster. The oxidation of nitrosobenzene to nitrobenzene can be coupled to the reduction of nitrate, and using $Ga(NO_3)_3$ as the source of nitrate yields as a product the compound $[Ga_{13}(\mu_3\text{-}OH)_6(\mu_2\text{-}OH)_{18}(H_2O)_{24}](NO_3)_{15}$, in which the N:Ga stoichiometry has been reduced from 3:1 to 15:13. Unlike related Al_{13} clusters, which have a modified Keggin ion structure, x-ray crystallography reveals that the Ga_{13} cluster is similar to ligand-stabilized clusters in that it has an octahedral Ga core, which is bridged by hydroxyl groups to six Ga cations that are, in turn, surrounded by six hydrated Ga ions. All together, this cluster forms a disklike structure about 1 nm thick and about 2 nm in diameter. — PDS

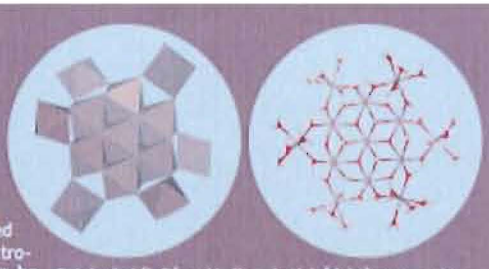

Polyhedral (left) and ball-and-stick (right) representations of the polycation (Ga atoms in pink, O atoms in red, and H atoms in white).

J. Am. Chem. Soc. 10.1021/ja043520t (2005).

VIROLOGY

Doubly Active Protease

Evasion of host immune responses is a common defensive strategy used by viruses and is clearly illustrated by the ability of hepatitis C virus (HCV) to cause chronic liver infection. HCV achieves evasion, in part, through expression of the NS3/4A protease, which interrupts the induction of α/β interferon (IFN) gene expression by interferon regulatory factor 3 (IRF3).

Two studies identify the targets of NS3/4A, and both pathways are shown to be pivotal in IRF3 induction. Li *et al.* observed that the Toll-like receptor 3 (TLR3) adapter protein TRIF was cleaved by NS3/4A in an in vitro assay system. This was sufficient to prevent the induction of IFN-β by an activating ligand of TLR3. Furthermore, compromising TLR3 signaling was found to be sufficient to permit the cellular replication of HCV RNA. Foy *et al.* determined that the retinoic acid–inducible gene I (RIG-I) signaling pathway was disrupted by NS3/4A, again leading to loss of IRF3 induction of IFN-β. The development of NS3/4A inhibitors may help guide improved therapeutic intervention in HCV infection. — SJS

Proc. Natl. Acad. Sci. U.S.A. 102, 2992; 2986 (2005).

MOLECULAR BIOLOGY

A Fourth Musketeer

In eukaryotic cells, the enzymatic activities of RNA polymerases I, II, and III produce ribosomal RNA (rRNA), messenger RNA, and transfer RNA (and 5S rRNA), respectively. However, the genome sequence of *Arabidopsis thaliana* revealed that another RNA polymerase might exist, and Onodera *et al.* provide evidence for a functional RNA polymerase IV (Pol IV). Mutant plants lacking *RPD1* and *RPD2*, genes encoding the two largest subunits of the putative Pol IV, were still viable, but higher order heterochromatin assembly into centromeres was disrupted. Generally, an increase in cytosine methylation favors the formation of condensed heterochromatin. In *rpd2* plants, cytosine methylation of the pericentromeric 5S rRNA gene clusters was low, and these clusters did not cycle from a decondensed transcriptionally active state into inactive heterochromatin. Because small interfering RNAs (siRNAs) complementary to 5S rRNA genes were also reduced, the authors suggest that Pol IV affects amplification of siRNAs that direct DNA methylation (of their corresponding genes) and hence promote the organization of condensed nuclear chromocenters. — LDC

Centromeres (green) and 5S rRNA genes (red) in wild-type (upper) and *rpd2* (lower) plants.

Cell 10.1016/S0092867405001510 (2005).

CHEMISTRY

Fast and Accurate

Methods for detecting explosives in a range of settings, such as airports, should be highly sensitive, highly specific, and applicable to nonvolatile and thermally unstable substances. Furthermore, they should be fast and not require much sample preparation. Current methods do not measure up; they involve manual sample transfer and are not ideal for detecting nonvolatile or thermally unstable substances.

Takáts *et al.* show that the recently developed desorption electrospray ionization (DESI) method meets these requirements. An electrospray is directed onto a surface bearing the analyte, and the resulting secondary ions are collected and analyzed by mass spectrometry. Sub-nanogram amounts of several explosives, including TNT, can be detected on a variety of surfaces such as paper, skin, and metal. Analysis takes just a few seconds, and no sample preparation is required. — JFU

Chem. Commun. 10.1039/b418699d (2005).

BIOCHEMISTRY

Freedom to Associate

The power-generating capacity of mitochondria is based on redox reactions (in complexes I, II, III, and IV) that establish an electrochemical gradient of protons, which is used to make ATP (in complex V). The redox reactions utilize the mobile electron carriers ubiquinone and cytochrome C, and considerations of

CONTINUED ON PAGE 1379

Published by AAAS

APPENDIX C

SUPPLEMENTAL INFORMATION FOR Al_{13} SYNTHESIS

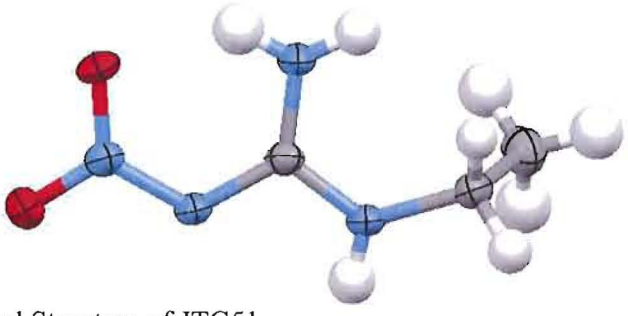

Figure C.01. Crystal Structure of JTG51

Table C.01. Crystal data and structure refinement for jtg51sx.

Identification code	jtg51sx	
Empirical formula	C3 H7 Ga N8 O12	
Formula weight	416.89	
Temperature	153(2) K	
Wavelength	0.71073 Å	
Crystal system	Monoclinic	
Space group	P2(1)/n	
Unit cell dimensions	a = 4.2248(11) Å	a= 90°.
	b = 16.046(4) Å	b= 96.281(4)°.
	c = 8.995(2) Å	g = 90°.
Volume	606.1(3) $Å^3$	
Z	1	
Density (calculated)	1.142 Mg/m^3	
Absorption coefficient	1.186 mm^{-1}	

F(000)	208
Crystal size	0.20 x 0.10 x 0.10 mm^3
Theta range for data collection	2.54 to 28.22°.
Index ranges	-5<=h<=5, -20<=k<=21, -11<=l<=11
Reflections collected	4938
Independent reflections	1404 [R(int) = 0.0313]
Completeness to theta = 28.22°	93.9 %
Absorption correction	Semi-empirical from equivalents
Max. and min. transmission	1.000 and 0.705
Refinement method	Full-matrix least-squares on F^2
Data / restraints / parameters	1404 / 0 / 114
Goodness-of-fit on F^2	1.033
Final R indices [I>2sigma(I)]	R1 = 0.0456, wR2 = 0.1028
R indices (all data)	R1 = 0.0632, wR2 = 0.1128
Largest diff. peak and hole	0.240 and -0.247 e.$Å^{-3}$

Table C.02. Atomic coordinates (x 10^4) and equivalent isotropic displacement parameters ($Å^2$x 10^3) for jtg51sx. U(eq) is defined as one third of the trace of the orthogonalized U^{ij} tensor.

	x	y	z	U(eq)
N(1)	7057(3)	640(1)	1266(2)	23(1)
N(2)	9442(3)	967(1)	-771(1)	23(1)
N(3)	10127(3)	1486(1)	-1848(2)	26(1)
N(4)	6728(4)	2020(1)	523(2)	30(1)
O(1)	9100(3)	2228(1)	-1976(1)	36(1)
O(2)	11837(3)	1203(1)	-2763(1)	35(1)
C(1)	7272(5)	975(1)	3981(2)	35(1)
C(2)	5246(4)	736(1)	2547(2)	26(1)
C(3)	7699(4)	1246(1)	334(2)	21(1)

Table C.03. Bond lengths [Å] and angles [°] for jtg51sx.

N(1)-C(3)	1.331(2)		
N(1)-C(2)	1.459(2)	C(3)-N(1)-C(2)	125.45(14)
N(1)-H(1)	0.83(2)	C(3)-N(1)-H(1)	114.9(13)
N(2)-N(3)	1.3332(18)	C(2)-N(1)-H(1)	119.6(13)
N(2)-C(3)	1.375(2)	N(3)-N(2)-C(3)	119.83(13)
N(3)-O(2)	1.2392(17)	O(2)-N(3)-O(1)	120.15(13)
N(3)-O(1)	1.2685(17)	O(2)-N(3)-N(2)	116.22(13)
N(4)-C(3)	1.325(2)	O(1)-N(3)-N(2)	123.62(13)
N(4)-H(4A)	0.86(2)	C(3)-N(4)-H(4A)	120.3(12)
N(4)-H(4B)	0.86(2)	C(3)-N(4)-H(4B)	111.1(14)
C(1)-C(2)	1.518(3)	H(4A)-N(4)-H(4B)	128.1(19)
C(1)-H(1A)	0.99(2)	C(2)-C(1)-H(1A)	109.6(12)
C(1)-H(1B)	0.99(2)	C(2)-C(1)-H(1B)	110.9(12)
C(1)-H(1C)	0.98(2)		
C(2)-H(2A)	0.975(19)		
C(2)-H(2B)	0.964(18)		

H(1A)-C(1)-H(1B)	109.8(16)	C(1)-C(2)-H(2B)	111.1(11)
C(2)-C(1)-H(1C)	110.0(12)	H(2A)-C(2)-H(2B)	108.0(15)
H(1A)-C(1)-H(1C)	109.6(18)	N(4)-C(3)-N(1)	121.12(15)
H(1B)-C(1)-H(1C)	106.8(16)	N(4)-C(3)-N(2)	126.59(14)
N(1)-C(2)-C(1)	113.71(15)	N(1)-C(3)-N(2)	112.29(13)
N(1)-C(2)-H(2A)	106.3(10)		
C(1)-C(2)-H(2A)	109.7(10)	Symmetry transformations used to	
N(1)-C(2)-H(2B)	107.8(11)	generate equivalent atoms:	

Table C.04. Anisotropic displacement parameters ($Å^2 x\ 10^3$) for jtg51sx. The anisotropic displacement factor exponent takes the form: $-2p^2[\ h^2\ a^{*2}U^{11} + ... + 2\ h\ k\ a^*\ b^*\ U^{12}\ ]$

	U^{11}	U^{22}	U^{33}	U^{23}	U^{13}	U^{12}
N(1)	32(1)	14(1)	25(1)	0(1)	8(1)	1(1)
N(2)	33(1)	14(1)	23(1)	1(1)	8(1)	2(1)
N(3)	36(1)	16(1)	25(1)	0(1)	7(1)	-1(1)
N(4)	49(1)	15(1)	29(1)	1(1)	17(1)	4(1)
O(1)	59(1)	15(1)	38(1)	7(1)	20(1)	7(1)
O(2)	51(1)	26(1)	31(1)	0(1)	20(1)	4(1)
C(1)	44(1)	37(1)	25(1)	0(1)	5(1)	5(1)
C(2)	32(1)	18(1)	29(1)	1(1)	10(1)	0(1)
C(3)	27(1)	16(1)	21(1)	-1(1)	1(1)	0(1)

Table C.05. Hydrogen coordinates ($x\ 10^4$) and isotropic displacement parameters ($Å^2 x\ 10^3$) for jtg51sx.

	x	y	z	U(eq)
H(1)	7850(40)	182(13)	1100(20)	34(5)
H(1A)	8360(50)	1512(14)	3840(20)	45(6)
H(1B)	5960(50)	1024(13)	4820(20)	44(6)

H(1C)	8860(50)	541(14)	4260(20)	48(6)
H(2A)	4220(40)	201(12)	2678(19)	30(5)
H(2B)	3600(40)	1144(11)	2290(20)	26(5)
H(4A)	5890(50)	2155(11)	1320(20)	32(5)
H(4B)	7270(50)	2344(13)	-170(20)	40(5)

Table C.06. Hydrogen bonds for jtg51sx [Å and °].

D-H...A	d(D-H)	d(H...A)	d(D...A)	<(DHA)
N(1)-H(1)...N(2)#1	0.83(2)	2.21(2)	3.0284(19)	172.4(18)
N(4)-H(4A)...O(1)#2	0.86(2)	2.04(2)	2.880(2)	165.5(17)
N(4)-H(4B)...O(1)	0.86(2)	1.88(2)	2.581(2)	137.1(19)

Symmetry transformations used to generate equivalent atoms:

#1 -x+2,-y,-z #2 x-1/2,-y+1/2,z+1/2

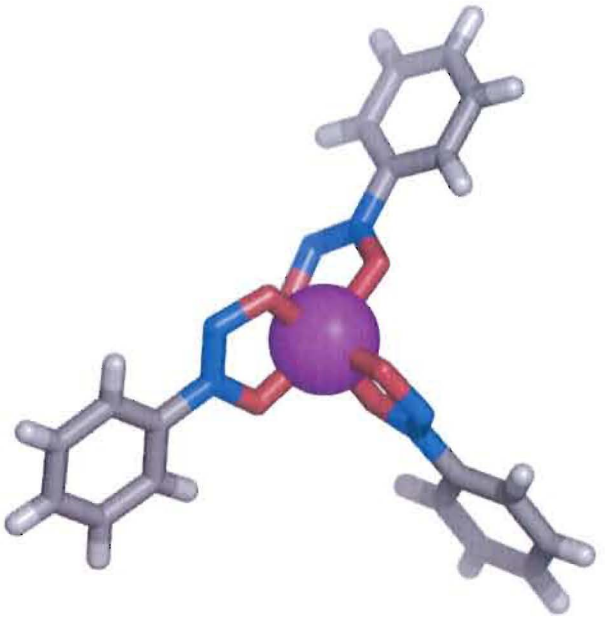

Figure C.02. Crystal structure of Jason1 – $Ga(cupferron)_3$

Table C.07. Crystal data and structure refinement for jason1.

Identification code	jason1	
Empirical formula	C18 H15 Ga1 N6 O6	
Formula weight	482.58	
Temperature	153(2) K	
Wavelength	0.71073 Å	
Crystal system	Monoclinic	
Space group	P2(1)/n	
Unit cell dimensions	a = 11.1379(7) Å	a= 90°.
	b = 17.0528(11) Å	b= 108.2530(10)°.
	c = 11.1715(7) Å	g = 90°.
Volume	2015.1(2) $Å^3$	
Z	4	
Density (calculated)	1.586 Mg/m^3	
Absorption coefficient	1.415 mm^{-1}	
F(000)	976	
Crystal size	0.25 x 0.18 x 0.10 mm^3	
Theta range for data collection	2.25 to 28.26°.	

Index ranges	-14<=h<=14, -21<=k<=22, -14<=l<=14
Reflections collected	17221
Independent reflections	4710 [R(int) = 0.0289]
Completeness to theta = 28.26°	94.4 %
Absorption correction	Semi-empirical from equivalents
Max. and min. transmission	1.000 and 0.835
Refinement method	Full-matrix least-squares on F^2
Data / restraints / parameters	4710 / 0 / 340
Goodness-of-fit on F^2	1.048
Final R indices [I>2sigma(I)]	R1 = 0.0333, wR2 = 0.0679
R indices (all data)	R1 = 0.0486, wR2 = 0.0741
Largest diff. peak and hole	0.316 and -0.291 e.Å^{-3}

Table C.08. Atomic coordinates (x 10^4) and equivalent isotropic displacement parameters (Å^{2}x 10^3) for jason1. U(eq) is defined as one third of the trace of the orthogonalized U^{ij} tensor.

	x	y	z	U(eq)
Ga(1)	4603(1)	7703(1)	10283(1)	24(1)
O(1)	4019(1)	7729(1)	8433(1)	28(1)
O(2)	5889(1)	8391(1)	9965(1)	28(1)
O(3)	5421(1)	6696(1)	10231(1)	28(1)
O(4)	5548(1)	7558(1)	12080(1)	29(1)
O(5)	3751(1)	8639(1)	10646(1)	28(1)
O(6)	2996(1)	7248(1)	10343(1)	32(1)
N(1)	4779(2)	8172(1)	8024(2)	25(1)
N(2)	5753(2)	8519(1)	8773(2)	28(1)
N(3)	6093(2)	6478(1)	11386(2)	22(1)
N(4)	6173(2)	6898(1)	12362(2)	26(1)
N(5)	2654(2)	8442(1)	10794(2)	24(1)
N(6)	2235(2)	7735(1)	10644(2)	30(1)
C(1)	4509(2)	8257(1)	6682(2)	27(1)

C(2)	3653(2)	7748(1)	5898(2)	32(1)
C(3)	3437(2)	7810(2)	4609(2)	40(1)
C(4)	4059(3)	8366(2)	4138(2)	48(1)
C(5)	4878(3)	8885(2)	4933(2)	46(1)
C(6)	5118(2)	8836(2)	6224(2)	38(1)
C(7)	6743(2)	5738(1)	11528(2)	23(1)
C(8)	6581(2)	5284(1)	10468(2)	31(1)
C(9)	7168(2)	4561(1)	10600(3)	38(1)
C(10)	7908(2)	4305(2)	11766(3)	40(1)
C(11)	8090(2)	4778(2)	12817(2)	38(1)
C(12)	7509(2)	5500(1)	12710(2)	29(1)
C(13)	1931(2)	9051(1)	11145(2)	25(1)
C(14)	887(2)	8850(2)	11505(2)	39(1)
C(15)	212(2)	9446(2)	11830(3)	45(1)
C(16)	570(2)	10216(2)	11805(3)	43(1)
C(17)	1621(2)	10401(2)	11463(3)	41(1)
C(18)	2316(2)	9816(1)	11133(2)	33(1)

Table C.09. Bond lengths [Å] and angles [°] for jason1.

Ga(1)-O(3)	1.9531(14)	O(6)-N(6)	1.305(2)
Ga(1)-O(1)	1.9633(14)	N(1)-N(2)	1.288(2)
Ga(1)-O(5)	1.9636(14)	N(1)-C(1)	1.441(3)
Ga(1)-O(4)	1.9687(15)	N(3)-N(4)	1.284(2)
Ga(1)-O(2)	1.9694(14)	N(3)-C(7)	1.439(2)
Ga(1)-O(6)	1.9710(15)	N(5)-N(6)	1.285(2)
O(1)-N(1)	1.318(2)	N(5)-C(13)	1.440(3)
O(2)-N(2)	1.309(2)	C(1)-C(2)	1.381(3)
O(3)-N(3)	1.325(2)	C(1)-C(6)	1.384(3)
O(4)-N(4)	1.309(2)	C(2)-C(3)	1.388(3)
O(5)-N(5)	1.327(2)	C(2)-H(2)	0.91(2)
		C(3)-C(4)	1.372(4)
		C(3)-H(3)	0.97(3)
		C(4)-C(5)	1.377(4)

C(4)-H(4)	0.94(3)	O(1)-Ga(1)-O(2)	79.39(6)
C(5)-C(6)	1.384(3)	O(5)-Ga(1)-O(2)	88.77(6)
C(5)-H(5)	0.91(3)	O(4)-Ga(1)-O(2)	94.14(6)
C(6)-H(6)	0.96(3)	O(3)-Ga(1)-O(6)	95.29(6)
C(7)-C(8)	1.378(3)	O(1)-Ga(1)-O(6)	92.27(6)
C(7)-C(12)	1.389(3)	O(5)-Ga(1)-O(6)	79.09(6)
C(8)-C(9)	1.382(3)	O(4)-Ga(1)-O(6)	96.74(6)
C(8)-H(8)	0.92(2)	O(2)-Ga(1)-O(6)	163.90(6)
C(9)-C(10)	1.376(4)	N(1)-O(1)-Ga(1)	109.96(11)
C(9)-H(9)	0.94(3)	N(2)-O(2)-Ga(1)	115.04(12)
C(10)-C(11)	1.387(4)	N(3)-O(3)-Ga(1)	110.15(11)
C(10)-H(10)	0.91(3)	N(4)-O(4)-Ga(1)	115.27(11)
C(11)-C(12)	1.379(3)	N(5)-O(5)-Ga(1)	110.07(11)
C(11)-H(11)	0.89(2)	N(6)-O(6)-Ga(1)	115.35(12)
C(12)-H(12)	0.92(2)	N(2)-N(1)-O(1)	122.61(16)
C(13)-C(18)	1.375(3)	N(2)-N(1)-C(1)	119.25(17)
C(13)-C(14)	1.387(3)	O(1)-N(1)-C(1)	118.14(16)
C(14)-C(15)	1.379(3)	N(1)-N(2)-O(2)	112.99(16)
C(14)-H(14)	0.94(3)	N(4)-N(3)-O(3)	122.51(16)
C(15)-C(16)	1.375(4)	N(4)-N(3)-C(7)	119.79(16)
C(15)-H(15)	0.90(3)	O(3)-N(3)-C(7)	117.71(15)
C(16)-C(17)	1.376(3)	N(3)-N(4)-O(4)	112.67(16)
C(16)-H(16)	0.92(3)	N(6)-N(5)-O(5)	122.19(16)
C(17)-C(18)	1.382(3)	N(6)-N(5)-C(13)	120.01(17)
C(17)-H(17)	0.95(3)	O(5)-N(5)-C(13)	117.80(16)
C(18)-H(18)	0.93(2)	N(5)-N(6)-O(6)	113.12(17)
		C(2)-C(1)-C(6)	122.4(2)
O(3)-Ga(1)-O(1)	89.59(6)	C(2)-C(1)-N(1)	118.26(19)
O(3)-Ga(1)-O(5)	168.87(6)	C(6)-C(1)-N(1)	119.3(2)
O(1)-Ga(1)-O(5)	100.16(6)	C(1)-C(2)-C(3)	118.0(2)
O(3)-Ga(1)-O(4)	79.32(6)	C(1)-C(2)-H(2)	119.4(15)
O(1)-Ga(1)-O(4)	166.28(6)	C(3)-C(2)-H(2)	122.5(15)
O(5)-Ga(1)-O(4)	91.72(6)	C(4)-C(3)-C(2)	120.5(2)
O(3)-Ga(1)-O(2)	98.38(6)	C(4)-C(3)-H(3)	118.6(15)

C(2)-C(3)-H(3)	120.9(16)	C(11)-C(12)-C(7)	118.4(2)
C(3)-C(4)-C(5)	120.5(2)	C(11)-C(12)-H(12)	122.2(14)
C(3)-C(4)-H(4)	120.5(18)	C(7)-C(12)-H(12)	119.4(14)
C(5)-C(4)-H(4)	119.0(18)	C(18)-C(13)-C(14)	121.9(2)
C(4)-C(5)-C(6)	120.5(3)	C(18)-C(13)-N(5)	118.59(18)
C(4)-C(5)-H(5)	123.2(17)	C(14)-C(13)-N(5)	119.5(2)
C(6)-C(5)-H(5)	116.3(17)	C(15)-C(14)-C(13)	118.1(2)
C(1)-C(6)-C(5)	118.0(2)	C(15)-C(14)-H(14)	123.5(17)
C(1)-C(6)-H(6)	119.9(15)	C(13)-C(14)-H(14)	118.4(17)
C(5)-C(6)-H(6)	122.1(15)	C(16)-C(15)-C(14)	120.8(2)
C(8)-C(7)-C(12)	121.9(2)	C(16)-C(15)-H(15)	120.8(16)
C(8)-C(7)-N(3)	118.14(18)	C(14)-C(15)-H(15)	118.4(17)
C(12)-C(7)-N(3)	119.92(18)	C(15)-C(16)-C(17)	120.1(2)
C(7)-C(8)-C(9)	118.6(2)	C(15)-C(16)-H(16)	120.1(16)
C(7)-C(8)-H(8)	118.8(14)	C(17)-C(16)-H(16)	119.8(16)
C(9)-C(8)-H(8)	122.6(14)	C(16)-C(17)-C(18)	120.4(2)
C(10)-C(9)-C(8)	120.5(2)	C(16)-C(17)-H(17)	121.5(15)
C(10)-C(9)-H(9)	120.8(16)	C(18)-C(17)-H(17)	118.1(15)
C(8)-C(9)-H(9)	118.7(16)	C(13)-C(18)-C(17)	118.7(2)
C(9)-C(10)-C(11)	120.2(2)	C(13)-C(18)-H(18)	120.8(16)
C(9)-C(10)-H(10)	120.3(16)	C(17)-C(18)-H(18)	120.5(16)
C(11)-C(10)-H(10)	119.5(16)		
C(12)-C(11)-C(10)	120.4(2)	Symmetry transformations used to	
C(12)-C(11)-H(11)	120.5(17)	generate equivalent atoms:	
C(10)-C(11)-H(11)	119.1(16)		

Table C.10. Anisotropic displacement parameters ($Å^2 x\ 10^3$) for jason1. The anisotropic displacement factor exponent takes the form: $-2p^2[\ h^2\ a^{*2}U^{11} + ... + 2\ h\ k\ a^*\ b^*\ U^{12}\ ]$

	U^{11}	U^{22}	U^{33}	U^{23}	U^{13}	U^{12}
Ga(1)	26(1)	20(1)	25(1)	-2(1)	7(1)	2(1)
O(1)	26(1)	28(1)	28(1)	0(1)	7(1)	-5(1)
O(2)	28(1)	31(1)	25(1)	-4(1)	6(1)	-3(1)

O(3)	33(1)	25(1)	21(1)	-1(1)	3(1)	8(1)
O(4)	36(1)	22(1)	27(1)	-3(1)	9(1)	5(1)
O(5)	24(1)	23(1)	37(1)	-1(1)	13(1)	-1(1)
O(6)	34(1)	20(1)	43(1)	-5(1)	16(1)	0(1)
N(1)	24(1)	24(1)	27(1)	-1(1)	7(1)	2(1)
N(2)	28(1)	29(1)	28(1)	-3(1)	9(1)	-1(1)
N(3)	24(1)	20(1)	23(1)	0(1)	6(1)	-1(1)
N(4)	30(1)	22(1)	26(1)	-2(1)	9(1)	1(1)
N(5)	24(1)	22(1)	26(1)	-1(1)	7(1)	0(1)
N(6)	32(1)	23(1)	37(1)	-3(1)	13(1)	-1(1)
C(1)	25(1)	31(1)	25(1)	0(1)	8(1)	10(1)
C(2)	29(1)	34(1)	31(1)	-4(1)	7(1)	5(1)
C(3)	36(1)	50(2)	32(1)	-8(1)	4(1)	6(1)
C(4)	44(2)	72(2)	25(1)	3(1)	9(1)	14(1)
C(5)	43(2)	63(2)	35(1)	12(1)	15(1)	-2(1)
C(6)	37(1)	44(2)	32(1)	2(1)	11(1)	-3(1)
C(7)	20(1)	18(1)	32(1)	2(1)	9(1)	-2(1)
C(8)	28(1)	27(1)	36(1)	-3(1)	6(1)	1(1)
C(9)	37(1)	26(1)	49(2)	-9(1)	11(1)	3(1)
C(10)	39(1)	24(1)	61(2)	7(1)	20(1)	8(1)
C(11)	38(1)	34(1)	41(1)	17(1)	11(1)	8(1)
C(12)	30(1)	27(1)	30(1)	3(1)	10(1)	0(1)
C(13)	23(1)	26(1)	25(1)	-3(1)	6(1)	4(1)
C(14)	31(1)	35(1)	54(2)	-3(1)	17(1)	-2(1)
C(15)	31(1)	49(2)	62(2)	-9(1)	24(1)	2(1)
C(16)	34(1)	42(2)	54(2)	-12(1)	17(1)	9(1)
C(17)	41(1)	31(1)	53(2)	-7(1)	19(1)	2(1)
C(18)	33(1)	27(1)	42(1)	-2(1)	17(1)	1(1)

Table C.11. Hydrogen coordinates (x 10^4) and isotropic displacement parameters ($Å^2$x 10 ^{3}) for jason1.

	x	y	z	U(eq)
H(2)	3280(20)	7371(14)	6240(20)	34(7)
H(3)	2870(30)	7452(15)	4030(30)	48(8)
H(4)	3930(30)	8400(16)	3270(30)	60(8)
H(5)	5300(20)	9266(17)	4660(20)	57(9)
H(6)	5670(20)	9199(15)	6800(20)	43(7)
H(8)	6080(20)	5471(13)	9710(20)	32(6)
H(9)	7070(20)	4254(15)	9870(20)	45(7)
H(10)	8260(20)	3819(15)	11860(20)	43(7)
H(11)	8580(20)	4607(15)	13560(20)	43(7)
H(12)	7600(20)	5823(13)	13400(20)	28(6)
H(14)	690(30)	8314(16)	11540(30)	55(8)
H(15)	-470(20)	9319(15)	12070(20)	46(7)
H(16)	110(20)	10608(15)	12010(20)	46(7)
H(17)	1890(20)	10927(15)	11460(20)	42(7)
H(18)	3000(20)	9942(14)	10870(20)	45(7)

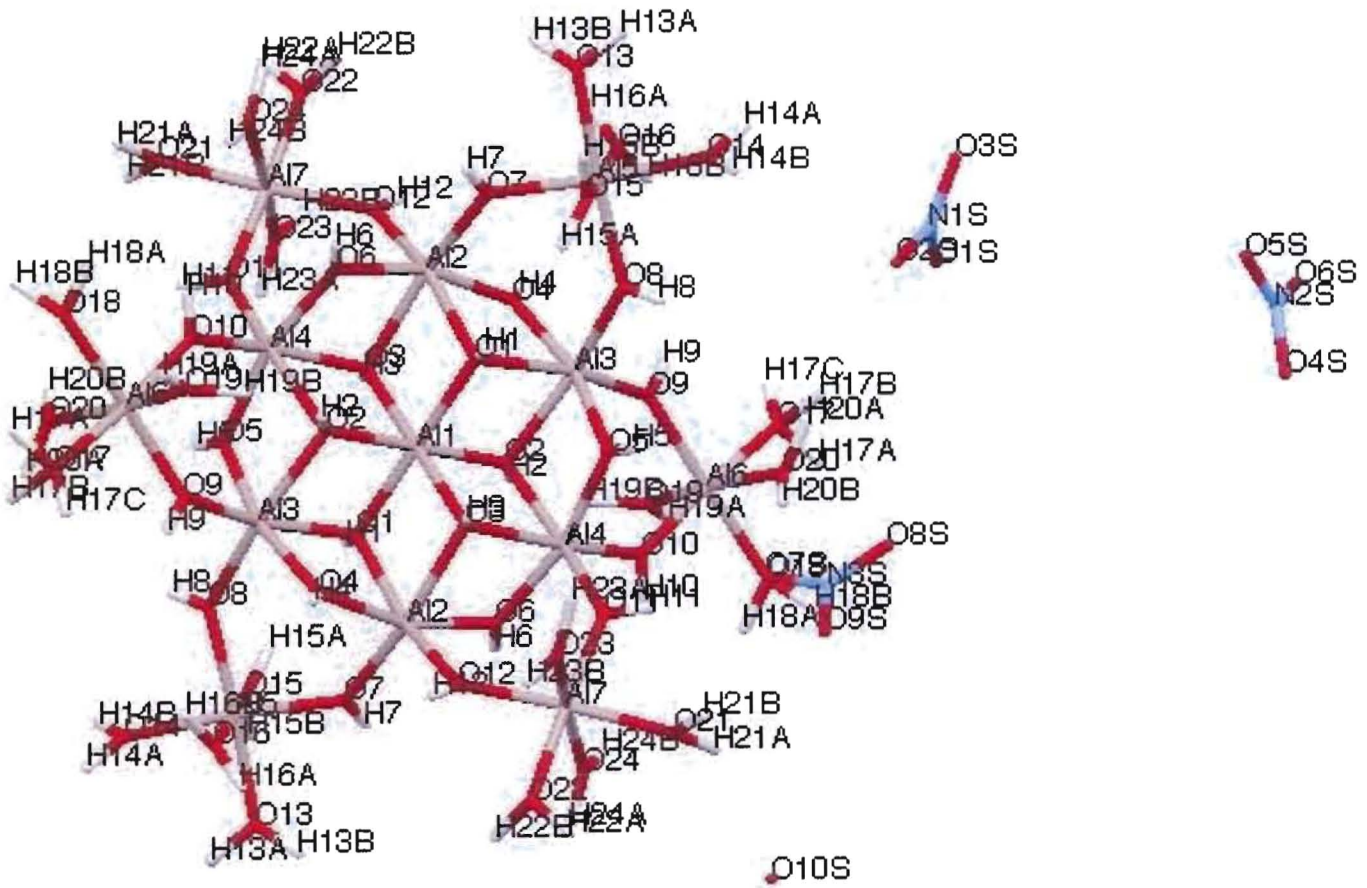

Figure C.03. Crystal structure of JTG27.

Table C.12. Crystal data and structure refinement for jtg27.

Identification code	jtg27	
Empirical formula	H88 Al13 N15 O101	
Formula weight	2265.59	
Temperature	153(2) K	
Wavelength	0.71073 ≈	
Crystal system	Triclinic	
Space group	P-1	
Unit cell dimensions	a = 12.8256(8) Å	a= 77.6010(10)°.
	b = 13.1667(8) Å	b= 74.0590(10)°.
	c = 13.4201(8) Å	g = 87.6480(10)°.
Volume	2127.9(2) $\approx^3$	
Z	1	
Density (calculated)	1.768 Mg/m^3	
Absorption coefficient	0.311 mm^{-1}	
F(000)	1170	
Crystal size	0.31 x 0.18 x 0.09 mm^3	
Theta range for data collection	1.58 to 28.29°.	
Index ranges	-15<=h<=16, -17<=k<=16, -17<=l<=17	
Reflections collected	22455	
Independent reflections	9682 [R(int) = 0.0203]	
Completeness to theta = 28.29∞	91.8 %	
Absorption correction	Semi-empirical from equivalents	
Max. and min. transmission	1.000 and 0.570	
Refinement method	Full-matrix least-squares on F^2	
Data / restraints / parameters	9682 / 26 / 542	
Goodness-of-fit on F^2	1.069	
Final R indices [I>2sigma(I)]	R1 = 0.0479, wR2 = 0.1264	
R indices (all data)	R1 = 0.0571, wR2 = 0.1322	
Largest diff. peak and hole	0.862 and -0.434 $e.\approx^{-3}$	

Table C.13. Bond lengths [Å] and angles [°] for jtg27.

Al(1)-O(2)	1.8710(14)	Al(5)-O(8)	1.8581(17)
Al(1)-O(2)#1	1.8710(14)	Al(5)-O(7)	1.8722(17)
Al(1)-O(1)	1.8823(14)	Al(5)-O(16)	1.8961(18)
Al(1)-O(1)#1	1.8823(14)	Al(5)-O(15)	1.9095(19)
Al(1)-O(3)#1	1.8850(15)	Al(5)-O(14)	1.9146(18)
Al(1)-O(3)	1.8850(15)	Al(5)-O(13)	1.9306(18)
Al(1)-Al(4)	2.9640(6)	Al(6)-O(9)	1.8492(18)
Al(1)-Al(4)#1	2.9640(6)	Al(6)-O(10)	1.8593(17)
Al(1)-Al(3)#1	2.9782(6)	Al(6)-O(19)	1.898(2)
Al(1)-Al(3)	2.9782(6)	Al(6)-O(20)	1.9051(19)
Al(2)-O(12)#1	1.8440(17)	Al(6)-O(17)	1.9346(19)
Al(2)-O(4)	1.8442(16)	Al(6)-O(18)	1.9390(18)
Al(2)-O(7)	1.8459(17)	Al(7)-O(11)	1.8548(17)
Al(2)-O(6)#1	1.8588(16)	Al(7)-O(12)	1.8676(18)
Al(2)-O(1)	2.0233(16)	Al(7)-O(24)	1.9079(18)
Al(2)-O(3)#1	2.0328(16)	Al(7)-O(23)	1.909(2)
Al(2)-Al(4)#1	2.9843(9)	Al(7)-O(22)	1.9165(18)
Al(2)-Al(3)	2.9923(9)	Al(7)-O(21)	1.9389(18)
Al(3)-O(5)	1.8456(17)	O(1)-H(1)	0.87(3)
Al(3)-O(8)	1.8459(17)	O(2)-H(2)	0.903(19)
Al(3)-O(4)	1.8461(16)	O(3)-Al(2)#1	2.0328(16)
Al(3)-O(9)	1.8472(17)	O(3)-H(3)	0.74(4)
Al(3)-O(2)	2.0022(16)	O(4)-H(4)	0.78(4)
Al(3)-O(1)	2.0166(16)	O(5)-H(5)	0.66(4)
Al(3)-Al(4)	2.9728(9)	O(6)-Al(2)#1	1.8588(16)
Al(4)-O(6)	1.8327(17)	O(6)-H(6)	0.74(4)
Al(4)-O(5)	1.8407(17)	O(7)-H(7)	0.71(3)
Al(4)-O(10)	1.8469(16)	O(8)-H(8)	0.73(3)
Al(4)-O(11)	1.8525(16)	O(9)-H(9)	0.66(3)
Al(4)-O(3)	1.9822(16)	O(10)-H(10)	0.73(4)
Al(4)-O(2)	2.0051(16)	O(11)-H(11)	0.78(3)
Al(4)-Al(2)#1	2.9843(9)	O(12)-Al(2)#1	1.8440(17)
		O(12)-H(12)	0.66(3)

O(13)-H(13A)	0.961(19)		
O(13)-H(13B)	0.989(19)	O(2)-Al(1)-O(2)#1	180.0
O(14)-H(14A)	1.003(19)	O(2)-Al(1)-O(1)	83.27(6)
O(14)-H(14B)	0.989(19)	O(2)#1-Al(1)-O(1)	96.73(6)
O(15)-H(15A)	0.992(19)	O(2)-Al(1)-O(1)#1	96.73(6)
O(15)-H(15B)	0.972(19)	O(2)#1-Al(1)-O(1)#1	83.27(6)
O(16)-H(16A)	0.954(19)	O(1)-Al(1)-O(1)#1	180.0
O(16)-H(16B)	0.961(19)	O(2)-Al(1)-O(3)#1	96.99(6)
O(17)-H(17A)	1.00(2)	O(2)#1-Al(1)-O(3)#1	83.01(6)
O(17)-H(17B)	0.99(2)	O(1)-Al(1)-O(3)#1	83.14(6)
O(17)-H(17C)	0.977(19)	O(1)#1-Al(1)-O(3)#1	96.86(6)
O(18)-H(18A)	0.951(19)	O(2)-Al(1)-O(3)	83.01(6)
O(18)-H(18B)	0.980(19)	O(2)#1-Al(1)-O(3)	96.99(6)
O(19)-H(19A)	0.98(2)	O(1)-Al(1)-O(3)	96.86(6)
O(19)-H(19B)	1.013(19)	O(1)#1-Al(1)-O(3)	83.14(6)
O(20)-H(20A)	0.98(2)	O(3)#1-Al(1)-O(3)	180.0
O(20)-H(20B)	0.926(18)	O(2)-Al(1)-Al(4)	41.82(5)
O(21)-H(21A)	0.965(19)	O(2)#1-Al(1)-Al(4)	138.18(5)
O(21)-H(21B)	0.952(19)	O(1)-Al(1)-Al(4)	89.80(5)
O(22)-H(22A)	0.977(19)	O(1)#1-Al(1)-Al(4)	90.21(5)
O(22)-H(22B)	0.983(19)	O(3)#1-Al(1)-Al(4)	138.81(5)
O(23)-H(23A)	0.98(2)	O(3)-Al(1)-Al(4)	41.19(5)
O(23)-H(23B)	0.983(19)	O(2)-Al(1)-Al(4)#1	138.18(5)
O(24)-H(24A)	0.957(19)	O(2)#1-Al(1)-Al(4)#1	41.82(5)
O(24)-H(24B)	0.964(18)	O(1)-Al(1)-Al(4)#1	90.20(5)
N(1S)-O(3S)	1.235(3)	O(1)#1-Al(1)-Al(4)#1	89.79(5)
N(1S)-O(1S)	1.252(3)	O(3)#1-Al(1)-Al(4)#1	41.19(5)
N(1S)-O(2S)	1.255(3)	O(3)-Al(1)-Al(4)#1	138.81(5)
N(2S)-O(4S)	1.197(3)	Al(4)-Al(1)-Al(4)#1	180.0
N(2S)-O(6S)	1.250(3)	O(2)-Al(1)-Al(3)#1	138.62(5)
N(2S)-O(5S)	1.256(3)	O(2)#1-Al(1)-Al(3)#1	41.38(5)
N(3S)-O(8S)	1.229(3)	O(1)-Al(1)-Al(3)#1	138.11(5)
N(3S)-O(9S)	1.236(3)	O(1)#1-Al(1)-Al(3)#1	41.89(5)
N(3S)-O(7S)	1.244(3)	O(3)#1-Al(1)-Al(3)#1	90.20(5)

O(3)-Al(1)-Al(3)#1	89.80(5)	O(4)-Al(2)-Al(3)	35.84(5)
Al(4)-Al(1)-Al(3)#1	119.963(17)	O(7)-Al(2)-Al(3)	86.55(6)
Al(4)#1-Al(1)-Al(3)#1	60.037(17)	O(6)#1-Al(2)-Al(3)	132.45(6)
O(2)-Al(1)-Al(3)	41.38(5)	O(1)-Al(2)-Al(3)	42.12(4)
O(2)#1-Al(1)-Al(3)	138.62(5)	O(3)#1-Al(2)-Al(3)	86.69(5)
O(1)-Al(1)-Al(3)	41.89(5)	Al(4)#1-Al(2)-Al(3)	118.83(3)
O(1)#1-Al(1)-Al(3)	138.11(5)	O(5)-Al(3)-O(8)	97.76(8)
O(3)#1-Al(1)-Al(3)	89.80(5)	O(5)-Al(3)-O(4)	164.18(8)
O(3)-Al(1)-Al(3)	90.20(5)	O(8)-Al(3)-O(4)	90.72(7)
Al(4)-Al(1)-Al(3)	60.037(17)	O(5)-Al(3)-O(9)	93.34(8)
Al(4)#1-Al(1)-Al(3)	119.964(17)	O(8)-Al(3)-O(9)	102.40(8)
Al(3)#1-Al(1)-Al(3)	180.00(2)	O(4)-Al(3)-O(9)	97.87(8)
O(12)#1-Al(2)-O(4)	98.17(8)	O(5)-Al(3)-O(2)	77.62(7)
O(12)#1-Al(2)-O(7)	103.20(8)	O(8)-Al(3)-O(2)	166.88(7)
O(4)-Al(2)-O(7)	91.80(8)	O(4)-Al(3)-O(2)	91.15(7)
O(12)#1-Al(2)-O(6)#1	90.84(8)	O(9)-Al(3)-O(2)	90.21(7)
O(4)-Al(2)-O(6)#1	163.36(8)	O(5)-Al(3)-O(1)	89.00(7)
O(7)-Al(2)-O(6)#1	99.76(8)	O(8)-Al(3)-O(1)	91.04(7)
O(12)#1-Al(2)-O(1)	165.14(8)	O(4)-Al(3)-O(1)	77.46(7)
O(4)-Al(2)-O(1)	77.33(7)	O(9)-Al(3)-O(1)	165.90(8)
O(7)-Al(2)-O(1)	91.17(7)	O(2)-Al(3)-O(1)	76.71(6)
O(6)#1-Al(2)-O(1)	90.41(7)	O(5)-Al(3)-Al(4)	36.19(5)
O(12)#1-Al(2)-O(3)#1	89.81(7)	O(8)-Al(3)-Al(4)	133.90(6)
O(4)-Al(2)-O(3)#1	89.47(7)	O(4)-Al(3)-Al(4)	133.24(6)
O(7)-Al(2)-O(3)#1	166.59(7)	O(9)-Al(3)-Al(4)	86.65(6)
O(6)#1-Al(2)-O(3)#1	76.53(7)	O(2)-Al(3)-Al(4)	42.15(4)
O(1)-Al(2)-O(3)#1	76.09(6)	O(1)-Al(3)-Al(4)	87.06(5)
O(12)#1-Al(2)-Al(4)#1	85.39(6)	O(5)-Al(3)-Al(1)	81.77(5)
O(4)-Al(2)-Al(4)#1	130.80(6)	O(8)-Al(3)-Al(1)	129.46(6)
O(7)-Al(2)-Al(4)#1	135.38(6)	O(4)-Al(3)-Al(1)	82.53(5)
O(6)#1-Al(2)-Al(4)#1	35.76(5)	O(9)-Al(3)-Al(1)	128.13(6)
O(1)-Al(2)-Al(4)#1	87.00(5)	O(2)-Al(3)-Al(1)	38.15(4)
O(3)#1-Al(2)-Al(4)#1	41.34(4)	O(1)-Al(3)-Al(1)	38.55(4)
O(12)#1-Al(2)-Al(3)	133.82(6)	Al(4)-Al(3)-Al(1)	59.743(17)

O(5)-Al(3)-Al(2)	131.29(6)	O(2)-Al(4)-Al(3)	42.07(4)
O(8)-Al(3)-Al(2)	85.72(6)	Al(1)-Al(4)-Al(3)	60.220(17)
O(4)-Al(3)-Al(2)	35.80(5)	O(6)-Al(4)-Al(2)#1	36.35(5)
O(9)-Al(3)-Al(2)	133.55(6)	O(5)-Al(4)-Al(2)#1	133.32(6)
O(2)-Al(3)-Al(2)	88.22(5)	O(10)-Al(4)-Al(2)#1	133.52(6)
O(1)-Al(3)-Al(2)	42.30(4)	O(11)-Al(4)-Al(2)#1	86.70(6)
Al(4)-Al(3)-Al(2)	120.20(3)	O(3)-Al(4)-Al(2)#1	42.64(5)
Al(1)-Al(3)-Al(2)	60.467(17)	O(2)-Al(4)-Al(2)#1	87.90(5)
O(6)-Al(4)-O(5)	165.52(8)	Al(1)-Al(4)-Al(2)#1	60.716(17)
O(6)-Al(4)-O(10)	97.29(8)	Al(3)-Al(4)-Al(2)#1	120.92(3)
O(5)-Al(4)-O(10)	91.13(7)	O(8)-Al(5)-O(7)	94.69(8)
O(6)-Al(4)-O(11)	91.31(7)	O(8)-Al(5)-O(16)	93.48(8)
O(5)-Al(4)-O(11)	98.60(8)	O(7)-Al(5)-O(16)	94.35(8)
O(10)-Al(4)-O(11)	101.25(8)	O(8)-Al(5)-O(15)	92.03(8)
O(6)-Al(4)-O(3)	78.40(7)	O(7)-Al(5)-O(15)	92.07(8)
O(5)-Al(4)-O(3)	90.70(7)	O(16)-Al(5)-O(15)	171.17(9)
O(10)-Al(4)-O(3)	166.47(8)	O(8)-Al(5)-O(14)	90.09(8)
O(11)-Al(4)-O(3)	91.73(7)	O(7)-Al(5)-O(14)	174.67(8)
O(6)-Al(4)-O(2)	90.53(7)	O(16)-Al(5)-O(14)	87.72(8)
O(5)-Al(4)-O(2)	77.66(7)	O(15)-Al(5)-O(14)	85.38(9)
O(10)-Al(4)-O(2)	90.05(7)	O(8)-Al(5)-O(13)	176.70(8)
O(11)-Al(4)-O(2)	168.22(7)	O(7)-Al(5)-O(13)	88.52(8)
O(3)-Al(4)-O(2)	77.25(6)	O(16)-Al(5)-O(13)	87.00(8)
O(6)-Al(4)-Al(1)	83.29(5)	O(15)-Al(5)-O(13)	87.11(9)
O(5)-Al(4)-Al(1)	82.25(5)	O(14)-Al(5)-O(13)	86.67(8)
O(10)-Al(4)-Al(1)	128.41(6)	O(9)-Al(6)-O(10)	93.71(8)
O(11)-Al(4)-Al(1)	130.34(6)	O(9)-Al(6)-O(19)	93.85(8)
O(3)-Al(4)-Al(1)	38.77(4)	O(10)-Al(6)-O(19)	92.68(8)
O(2)-Al(4)-Al(1)	38.48(4)	O(9)-Al(6)-O(20)	93.65(8)
O(6)-Al(4)-Al(3)	132.60(6)	O(10)-Al(6)-O(20)	95.49(8)
O(5)-Al(4)-Al(3)	36.31(5)	O(19)-Al(6)-O(20)	168.53(9)
O(10)-Al(4)-Al(3)	85.04(5)	O(9)-Al(6)-O(17)	91.53(8)
O(11)-Al(4)-Al(3)	134.89(6)	O(10)-Al(6)-O(17)	174.46(8)
O(3)-Al(4)-Al(3)	88.52(5)	O(19)-Al(6)-O(17)	85.17(9)

O(20)-Al(6)-O(17)	85.96(9)	Al(1)-O(3)-Al(2)#1	100.16(7)
O(9)-Al(6)-O(18)	177.69(8)	Al(4)-O(3)-Al(2)#1	96.02(7)
O(10)-Al(6)-O(18)	88.58(8)	Al(1)-O(3)-H(3)	119(3)
O(19)-Al(6)-O(18)	85.78(8)	Al(4)-O(3)-H(3)	121(3)
O(20)-Al(6)-O(18)	86.38(8)	Al(2)#1-O(3)-H(3)	116(3)
O(17)-Al(6)-O(18)	86.17(8)	Al(2)-O(4)-Al(3)	108.35(8)
O(11)-Al(7)-O(12)	94.33(8)	Al(2)-O(4)-H(4)	126(3)
O(11)-Al(7)-O(24)	92.91(7)	Al(3)-O(4)-H(4)	124(3)
O(12)-Al(7)-O(24)	94.74(8)	Al(4)-O(5)-Al(3)	107.50(9)
O(11)-Al(7)-O(23)	94.27(8)	Al(4)-O(5)-H(5)	126(3)
O(12)-Al(7)-O(23)	92.47(8)	Al(3)-O(5)-H(5)	126(3)
O(24)-Al(7)-O(23)	169.41(9)	Al(4)-O(6)-Al(2)#1	107.89(9)
O(11)-Al(7)-O(22)	177.52(8)	Al(4)-O(6)-H(6)	133(3)
O(12)-Al(7)-O(22)	88.10(8)	Al(2)#1-O(6)-H(6)	118(3)
O(24)-Al(7)-O(22)	86.43(8)	Al(2)-O(7)-Al(5)	133.89(10)
O(23)-Al(7)-O(22)	86.07(9)	Al(2)-O(7)-H(7)	116(2)
O(11)-Al(7)-O(21)	90.11(8)	Al(5)-O(7)-H(7)	108(2)
O(12)-Al(7)-O(21)	175.18(8)	Al(3)-O(8)-Al(5)	135.32(10)
O(24)-Al(7)-O(21)	86.89(8)	Al(3)-O(8)-H(8)	111(2)
O(23)-Al(7)-O(21)	85.32(8)	Al(5)-O(8)-H(8)	114(2)
O(22)-Al(7)-O(21)	87.48(8)	Al(3)-O(9)-Al(6)	135.40(10)
Al(1)-O(1)-Al(3)	99.56(7)	Al(3)-O(9)-H(9)	109(3)
Al(1)-O(1)-Al(2)	100.60(7)	Al(6)-O(9)-H(9)	114(3)
Al(3)-O(1)-Al(2)	95.58(7)	Al(4)-O(10)-Al(6)	137.19(10)
Al(1)-O(1)-H(1)	123.2(19)	Al(4)-O(10)-H(10)	107(3)
Al(3)-O(1)-H(1)	113.2(19)	Al(6)-O(10)-H(10)	116(3)
Al(2)-O(1)-H(1)	119.7(19)	Al(4)-O(11)-Al(7)	134.31(10)
Al(1)-O(2)-Al(3)	100.46(7)	Al(4)-O(11)-H(11)	113(2)
Al(1)-O(2)-Al(4)	99.70(7)	Al(7)-O(11)-H(11)	112(2)
Al(3)-O(2)-Al(4)	95.78(7)	Al(2)#1-O(12)-Al(7)	135.38(10)
Al(1)-O(2)-H(2)	130(3)	Al(2)#1-O(12)-H(12)	110(3)
Al(3)-O(2)-H(2)	116(3)	Al(7)-O(12)-H(12)	114(3)
Al(4)-O(2)-H(2)	109(3)	Al(5)-O(13)-H(13A)	119(3)
Al(1)-O(3)-Al(4)	100.04(7)	Al(5)-O(13)-H(13B)	118(3)

H(13A)-O(13)-H(13B)	111(4)	Al(7)-O(21)-H(21B)	130(3)
Al(5)-O(14)-H(14A)	127(3)	H(21A)-O(21)-H(21B)	105(4)
Al(5)-O(14)-H(14B)	123(3)	Al(7)-O(22)-H(22A)	120(3)
H(14A)-O(14)-H(14B)	109(4)	Al(7)-O(22)-H(22B)	119(2)
Al(5)-O(15)-H(15A)	124(3)	H(22A)-O(22)-H(22B)	110(4)
Al(5)-O(15)-H(15B)	127(3)	Al(7)-O(23)-H(23A)	131(4)
H(15A)-O(15)-H(15B)	104(4)	Al(7)-O(23)-H(23B)	119(3)
Al(5)-O(16)-H(16A)	126(3)	H(23A)-O(23)-H(23B)	109(5)
Al(5)-O(16)-H(16B)	127(2)	Al(7)-O(24)-H(24A)	122(3)
H(16A)-O(16)-H(16B)	106(4)	Al(7)-O(24)-H(24B)	125(2)
Al(6)-O(17)-H(17A)	107(7)	H(24A)-O(24)-H(24B)	113(3)
Al(6)-O(17)-H(17B)	117(4)	O(3S)-N(1S)-O(1S)	119.9(2)
H(17A)-O(17)-H(17B)	88(7)	O(3S)-N(1S)-O(2S)	121.1(2)
Al(6)-O(17)-H(17C)	130(3)	O(1S)-N(1S)-O(2S)	119.01(19)
H(17A)-O(17)-H(17C)	113(7)	O(4S)-N(2S)-O(6S)	119.7(3)
H(17B)-O(17)-H(17C)	93(5)	O(4S)-N(2S)-O(5S)	120.7(2)
Al(6)-O(18)-H(18A)	121(2)	O(6S)-N(2S)-O(5S)	119.6(2)
Al(6)-O(18)-H(18B)	137(3)	O(8S)-N(3S)-O(9S)	121.3(2)
H(18A)-O(18)-H(18B)	90(4)	O(8S)-N(3S)-O(7S)	118.4(2)
Al(6)-O(19)-H(19A)	128(3)	O(9S)-N(3S)-O(7S)	120.2(2)
Al(6)-O(19)-H(19B)	111(3)		
H(19A)-O(19)-H(19B)	121(4)		
Al(6)-O(20)-H(20A)	125(5)		
Al(6)-O(20)-H(20B)	121(2)		
H(20A)-O(20)-H(20B)	106(5)		
Al(7)-O(21)-H(21A)	121(3)		

Symmetry transformations used to generate equivalent atoms:
#1 -x+1,-y+1,-z

Table C.14. Hydrogen bonds for jtg27 [≈ and ∞].

D-H...A	d(D-H)	d(H...A)	d(D...A)	<(DHA)
O(4)-H(4)...O(4S)#2	0.78(4)	2.03(4)	2.800(3)	174(4)
O(5)-H(5)...O(8S)#3	0.66(4)	2.11(4)	2.767(3)	169(4)

O(6)-H(6)...O(3S)#4	0.74(4)	2.11(4)	2.838(2)	166(4)
O(7)-H(7)...O(2S)#5	0.71(3)	2.12(3)	2.828(2)	177(3)
O(8)-H(8)...O(9S)#3	0.73(3)	2.14(3)	2.864(3)	175(3)
O(9)-H(9)...O(6S)#6	0.66(3)	2.08(3)	2.733(3)	172(4)
O(10)-H(10)...O(1S)#3	0.73(4)	2.00(4)	2.728(2)	172(4)
O(11)-H(11)...O(7S)	0.78(3)	2.05(3)	2.794(3)	159(3)
O(12)-H(12)...O(5S)#3	0.66(3)	2.26(3)	2.915(3)	176(3)
O(14)-H(14A)...O(10S)#3	1.003(19)	1.64(2)	2.611(3)	163(4)
O(16)-H(16B)...O(6S)#6	0.961(19)	1.73(2)	2.670(3)	167(4)
O(17)-H(17C)...O(5S)#6	0.977(19)	1.85(3)	2.789(3)	160(5)
O(18)-H(18A)...O(2S)#3	0.951(19)	1.849(19)	2.795(3)	173(4)
O(20)-H(20B)...O(7S)	0.926(18)	1.74(2)	2.639(3)	165(4)
O(24)-H(24B)...O(1S)#3	0.964(18)	1.736(19)	2.691(2)	170(3)

Symmetry transformations used to generate equivalent atoms:

#1 -x+1,-y+1,-z #2 x,y,z-1 #3 -x+1,-y+1,-z+1

#4 x+1,y,z-1 #5 -x,-y+1,-z+1 #6 -x+1,-y+2,-z+1

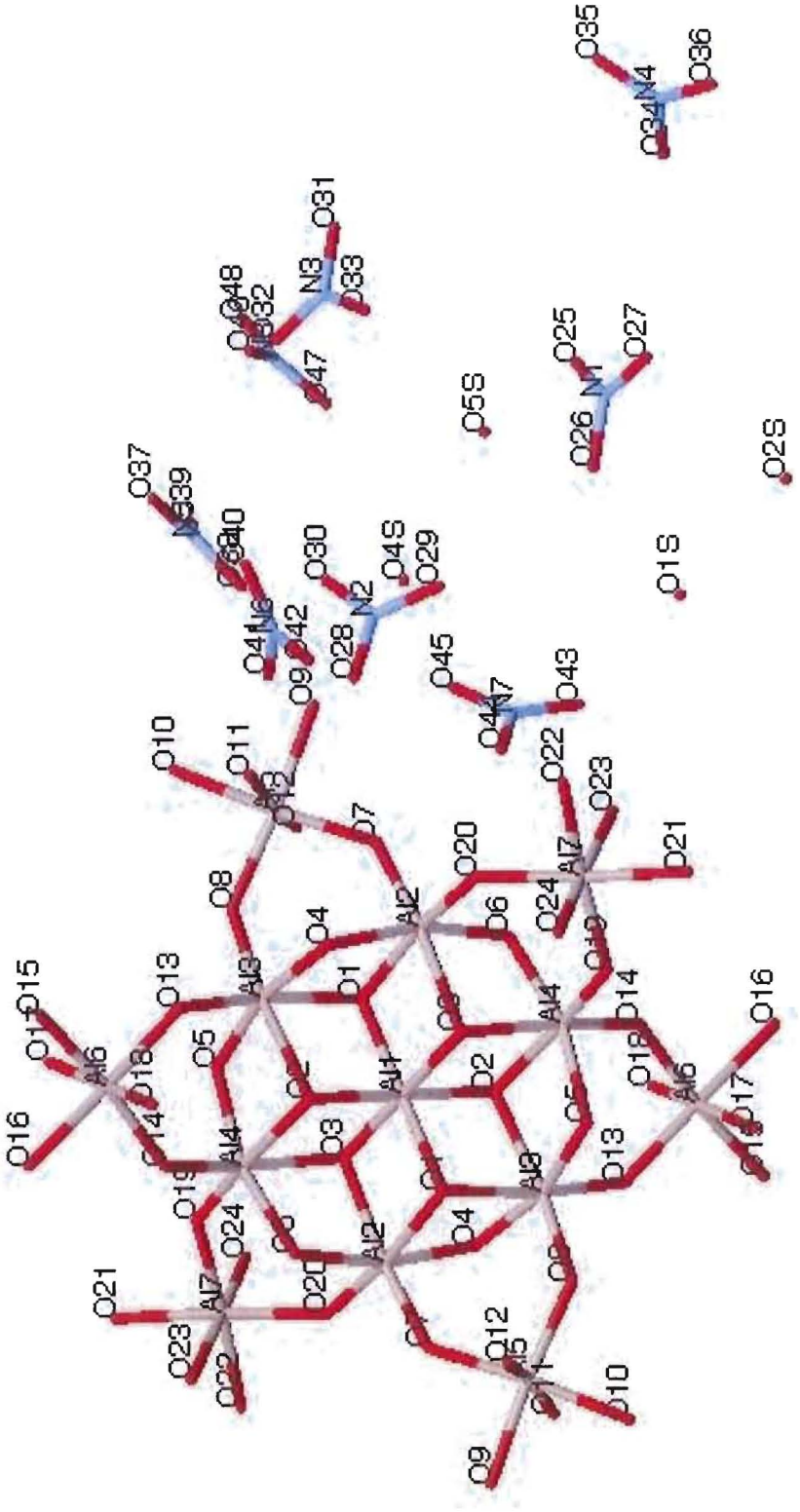

Figure C.04 Crystal structure of JTG81.

Table C.15. Crystal data and structure refinement for JTG81.

Identification code	jtg81	
Empirical formula	H96 Al13 N17 O106	
Formula weight	2381.68	
Temperature	173(2) K	
Wavelength	0.71073 Å	
Crystal system	Triclinic	
Space group	P-1	
Unit cell dimensions	a = 12.623(3) Å	a= 74.877(4)°.
	b = 13.251(3) Å	b= 72.419(4)°.
	c = 13.597(3) Å	g = 86.790(4)°.
Volume	2092.4(8) $Å^3$	
Z	1	
Density (calculated)	1.890 Mg/m^3	
Absorption coefficient	0.326 mm^{-1}	
F(000)	1232	
Crystal size	0.08 x 0.08 x 0.05 mm^3	
Theta range for data collection	1.59 to 25.00°.	
Index ranges	-14<=h<=15, -15<=k<=15, -16<=l<=16	
Reflections collected	15065	
Independent reflections	7308 [R(int) = 0.0700]	
Completeness to theta = 25.00°	99.1 %	
Absorption correction	Semi-empirical from equivalents	
Max. and min. transmission	0.9839 and 0.9744	
Refinement method	Full-matrix least-squares on F^2	
Data / restraints / parameters	7308 / 0 / 617	
Goodness-of-fit on F^2	1.051	
Final R indices [I>2sigma(I)]	R1 = 0.0836, wR2 = 0.1961	
R indices (all data)	R1 = 0.1399, wR2 = 0.2315	
Largest diff. peak and hole	0.811 and -0.588 $e.Å^{-3}$	

Table C.16. Atomic coordinates (x 10^4) and equivalent isotropic displacement parameters ($Å^2$x 10^3) for JTG81. U(eq) is defined as one third of the trace of the orthogonalized U^{ij} tensor.

	x	y	z	U(eq)
Al(1)	0	0	0	12(1)
Al(2)	1286(2)	-210(2)	1544(2)	13(1)
Al(3)	-340(2)	1484(2)	1362(2)	12(1)
Al(4)	-1666(2)	1698(2)	-155(2)	12(1)
Al(5)	2004(2)	2127(2)	1835(2)	15(1)
Al(6)	-2958(2)	2365(2)	2176(2)	14(1)
Al(7)	-1920(2)	2692(2)	-2655(2)	15(1)
O(1)	860(4)	842(3)	394(4)	14(1)
O(2)	-1188(4)	543(3)	910(4)	10(1)
O(3)	-344(4)	1065(3)	-1077(4)	12(1)
O(4)	13(4)	330(4)	2306(4)	14(1)
O(5)	-666(4)	2382(3)	207(4)	13(1)
O(6)	-2356(4)	724(3)	-530(4)	13(1)
O(7)	2180(4)	780(4)	1662(4)	14(1)
O(8)	706(4)	2345(4)	1448(4)	17(1)
O(9)	3370(4)	2043(4)	2216(4)	21(1)
O(10)	1936(4)	3529(4)	2026(4)	21(1)
O(11)	1246(4)	1694(4)	3318(4)	21(1)
O(12)	2955(4)	2707(4)	405(4)	22(1)
O(13)	-1596(4)	1838(3)	2306(4)	13(1)
O(14)	-2852(4)	1968(4)	925(4)	15(1)
O(15)	-3246(4)	2812(4)	3462(4)	20(1)
O(16)	-4396(4)	2921(4)	2099(4)	18(1)
O(17)	-2333(4)	3731(4)	1443(4)	19(1)
O(18)	-3687(4)	1081(4)	3085(4)	23(1)
O(19)	-1731(4)	2728(4)	-1352(4)	15(1)
O(20)	-1451(4)	1333(4)	-2624(4)	16(1)
O(21)	-2384(4)	4128(4)	-2830(4)	23(1)

O(22)	-2093(4)	2806(4)	-4060(4)	25(1)
O(23)	-3437(4)	2301(4)	-2083(4)	21(1)
O(24)	-444(4)	3242(4)	-3423(4)	20(1)
N(1)	12198(6)	2897(5)	-1806(5)	29(2)
O(25)	12806(5)	3686(5)	-2143(5)	44(2)
O(26)	11394(5)	2815(5)	-2135(5)	40(2)
O(27)	12418(5)	2124(4)	-1097(4)	25(1)
N(2)	9740(7)	5986(6)	-4097(6)	32(2)
O(28)	8770(5)	5858(5)	-4113(5)	45(2)
O(29)	10346(5)	5229(4)	-3936(5)	42(2)
O(30)	10121(5)	6897(4)	-4260(5)	42(2)
N(3)	9982(5)	5076(5)	1233(5)	21(2)
O(31)	10906(5)	5298(4)	1308(5)	37(2)
O(32)	9474(5)	5738(4)	732(4)	28(1)
O(33)	9601(4)	4163(4)	1686(4)	23(1)
N(4)	11390(6)	-518(5)	5114(5)	26(2)
O(34)	11350(7)	-319(5)	4180(5)	53(2)
O(35)	11337(7)	200(5)	5547(5)	52(2)
O(36)	11507(6)	-1429(4)	5588(5)	39(2)
N(5)	3597(7)	3213(7)	4292(6)	38(2)
O(37)	3249(6)	3395(6)	5196(5)	51(2)
O(38)	3249(5)	2420(5)	4135(5)	44(2)
O(39)	4332(6)	3813(5)	3573(5)	48(2)
N(6)	6193(6)	4692(5)	-391(6)	29(2)
O(40)	6591(5)	5110(5)	171(5)	39(2)
O(41)	6298(5)	5151(5)	-1347(5)	41(2)
O(42)	5673(5)	3840(5)	9(5)	37(2)
N(7)	4970(6)	115(5)	1242(5)	21(2)
O(43)	5728(5)	-406(4)	837(5)	32(1)
O(44)	4022(4)	-302(4)	1756(5)	27(1)
O(45)	5111(4)	1083(4)	1154(5)	29(1)
N(8)	5180(7)	2155(7)	6040(6)	40(2)
O(46)	4494(6)	1926(6)	6918(5)	53(2)
O(47)	5281(8)	1633(6)	5392(6)	75(3)

O(48)	5792(6)	2956(6)	5761(6)	61(2)
O(1S)	11338(5)	2069(4)	-3875(5)	35(2)
O(2S)	12613(5)	664(4)	-2714(4)	28(1)
O(3S)	14973(6)	-3726(6)	2028(7)	71(3)
O(4S)	4217(5)	488(5)	3997(6)	49(2)
O(5S)	12550(5)	5433(4)	-3695(5)	37(2)
N(1S)	15000	-5000	5000	71(4)

Table C.17. Bond lengths [Å] and angles [°] for JTG81.

Al(1)-O(1)	1.873(5)	Al(3)-O(1)	1.996(5)
Al(1)-O(1)#1	1.873(5)	Al(3)-O(2)	2.006(5)
Al(1)-O(2)	1.876(5)	Al(3)-Al(4)	2.977(3)
Al(1)-O(2)#1	1.876(5)	Al(4)-O(5)	1.842(5)
Al(1)-O(3)#1	1.887(5)	Al(4)-O(14)	1.848(5)
Al(1)-O(3)	1.887(5)	Al(4)-O(6)	1.850(5)
Al(1)-Al(3)	2.967(2)	Al(4)-O(19)	1.852(5)
Al(1)-Al(3)#1	2.967(2)	Al(4)-O(2)	2.018(5)
Al(1)-Al(2)	2.970(2)	Al(4)-O(3)	2.046(5)
Al(1)-Al(2)#1	2.970(2)	Al(4)-Al(2)#1	2.995(3)
Al(2)-O(7)	1.846(5)	Al(5)-O(8)	1.853(5)
Al(2)-O(4)	1.851(5)	Al(5)-O(7)	1.853(5)
Al(2)-O(20)#1	1.851(5)	Al(5)-O(11)	1.899(5)
Al(2)-O(6)#1	1.858(5)	Al(5)-O(12)	1.930(6)
Al(2)-O(1)	1.991(5)	Al(5)-O(9)	1.935(5)
Al(2)-O(3)#1	2.020(5)	Al(5)-O(10)	1.936(5)
Al(2)-Al(3)	2.969(3)	Al(6)-O(13)	1.859(5)
Al(2)-Al(4)#1	2.995(3)	Al(6)-O(14)	1.873(5)
Al(3)-O(13)	1.840(5)	Al(6)-O(17)	1.907(5)
Al(3)-O(8)	1.841(5)	Al(6)-O(18)	1.913(5)
Al(3)-O(5)	1.847(5)	Al(6)-O(15)	1.916(5)
Al(3)-O(4)	1.852(5)	Al(6)-O(16)	1.943(5)
		Al(7)-O(20)	1.857(5)
		Al(7)-O(19)	1.870(5)
		Al(7)-O(23)	1.881(5)

Al(7)-O(24)	1.917(5)	O(1)-Al(1)-O(2)#1	96.72(19)
Al(7)-O(21)	1.935(5)	O(1)#1-Al(1)-O(2)#1	83.28(19)
Al(7)-O(22)	1.955(6)	O(2)-Al(1)-O(2)#1	180.0(4)
O(3)-Al(2)#1	2.020(5)	O(1)-Al(1)-O(3)#1	83.47(19)
O(6)-Al(2)#1	1.858(5)	O(1)#1-Al(1)-O(3)#1	96.53(19)
O(20)-Al(2)#1	1.851(5)	O(2)-Al(1)-O(3)#1	96.49(19)
N(1)-O(25)	1.233(8)	O(2)#1-Al(1)-O(3)#1	83.51(19)
N(1)-O(26)	1.246(9)	O(1)-Al(1)-O(3)	96.53(19)
N(1)-O(27)	1.292(8)	O(1)#1-Al(1)-O(3)	83.47(19)
N(2)-O(29)	1.241(9)	O(2)-Al(1)-O(3)	83.51(19)
N(2)-O(28)	1.253(9)	O(2)#1-Al(1)-O(3)	96.49(19)
N(2)-O(30)	1.264(8)	O(3)#1-Al(1)-O(3)	180.0(4)
N(3)-O(32)	1.238(8)	O(1)-Al(1)-Al(3)	41.49(15)
N(3)-O(33)	1.254(7)	O(1)#1-Al(1)-Al(3)	138.51(15)
N(3)-O(31)	1.259(8)	O(2)-Al(1)-Al(3)	41.80(14)
N(4)-O(35)	1.232(8)	O(2)#1-Al(1)-Al(3)	138.20(14)
N(4)-O(36)	1.235(8)	O(3)#1-Al(1)-Al(3)	90.45(14)
N(4)-O(34)	1.244(8)	O(3)-Al(1)-Al(3)	89.55(14)
N(5)-O(38)	1.252(9)	O(1)-Al(1)-Al(3)#1	138.51(15)
N(5)-O(39)	1.256(10)	O(1)#1-Al(1)-Al(3)#1	41.49(15)
N(5)-O(37)	1.257(9)	O(2)-Al(1)-Al(3)#1	138.20(14)
N(6)-O(42)	1.244(8)	O(2)#1-Al(1)-Al(3)#1	41.80(14)
N(6)-O(41)	1.253(9)	O(3)#1-Al(1)-Al(3)#1	89.55(14)
N(6)-O(40)	1.275(9)	O(3)-Al(1)-Al(3)#1	90.45(14)
N(7)-O(43)	1.226(8)	Al(3)-Al(1)-Al(3)#1	180.00(6)
N(7)-O(44)	1.262(8)	O(1)-Al(1)-Al(2)	41.25(14)
N(7)-O(45)	1.274(8)	O(1)#1-Al(1)-Al(2)	138.75(14)
N(8)-O(46)	1.217(9)	O(2)-Al(1)-Al(2)	89.89(14)
N(8)-O(47)	1.229(10)	O(2)#1-Al(1)-Al(2)	90.11(14)
N(8)-O(48)	1.254(10)	O(3)#1-Al(1)-Al(2)	42.21(14)
		O(3)-Al(1)-Al(2)	137.79(14)
O(1)-Al(1)-O(1)#1	180.0(3)	Al(3)-Al(1)-Al(2)	60.00(6)
O(1)-Al(1)-O(2)	83.28(19)	Al(3)#1-Al(1)-Al(2)	120.00(6)
O(1)#1-Al(1)-O(2)	96.72(19)	O(1)-Al(1)-Al(2)#1	138.75(14)

O(1)#1-Al(1)-Al(2)#1	41.25(14)	O(3)#1-Al(2)-Al(1)	38.88(14)
O(2)-Al(1)-Al(2)#1	90.11(14)	Al(3)-Al(2)-Al(1)	59.94(6)
O(2)#1-Al(1)-Al(2)#1	89.89(14)	O(7)-Al(2)-Al(4)#1	133.26(18)
O(3)#1-Al(1)-Al(2)#1	137.79(14)	O(4)-Al(2)-Al(4)#1	132.76(18)
O(3)-Al(1)-Al(2)#1	42.21(14)	O(20)#1-Al(2)-Al(4)#1	87.22(17)
Al(3)-Al(1)-Al(2)#1	120.00(6)	O(6)#1-Al(2)-Al(4)#1	36.02(15)
Al(3)#1-Al(1)-Al(2)#1	60.00(6)	O(1)-Al(2)-Al(4)#1	87.69(15)
Al(2)-Al(1)-Al(2)#1	180.00(6)	O(3)#1-Al(2)-Al(4)#1	42.90(14)
O(7)-Al(2)-O(4)	92.0(2)	Al(3)-Al(2)-Al(4)#1	120.39(9)
O(7)-Al(2)-O(20)#1	100.3(2)	Al(1)-Al(2)-Al(4)#1	60.45(6)
O(4)-Al(2)-O(20)#1	98.6(2)	O(13)-Al(3)-O(8)	100.5(2)
O(7)-Al(2)-O(6)#1	97.4(2)	O(13)-Al(3)-O(5)	92.0(2)
O(4)-Al(2)-O(6)#1	165.1(2)	O(8)-Al(3)-O(5)	96.4(2)
O(20)#1-Al(2)-O(6)#1	91.1(2)	O(13)-Al(3)-O(4)	97.2(2)
O(7)-Al(2)-O(1)	90.3(2)	O(8)-Al(3)-O(4)	93.8(2)
O(4)-Al(2)-O(1)	77.9(2)	O(5)-Al(3)-O(4)	164.8(2)
O(20)#1-Al(2)-O(1)	169.1(2)	O(13)-Al(3)-O(1)	168.9(2)
O(6)#1-Al(2)-O(1)	90.5(2)	O(8)-Al(3)-O(1)	89.7(2)
O(7)-Al(2)-O(3)#1	166.7(2)	O(5)-Al(3)-O(1)	91.0(2)
O(4)-Al(2)-O(3)#1	89.9(2)	O(4)-Al(3)-O(1)	77.8(2)
O(20)#1-Al(2)-O(3)#1	92.5(2)	O(13)-Al(3)-O(2)	93.3(2)
O(6)#1-Al(2)-O(3)#1	78.4(2)	O(8)-Al(3)-O(2)	165.3(2)
O(1)-Al(2)-O(3)#1	77.2(2)	O(5)-Al(3)-O(2)	77.8(2)
O(7)-Al(2)-Al(3)	85.77(16)	O(4)-Al(3)-O(2)	89.6(2)
O(4)-Al(2)-Al(3)	36.70(15)	O(1)-Al(3)-O(2)	77.0(2)
O(20)#1-Al(2)-Al(3)	135.27(18)	O(13)-Al(3)-Al(1)	131.67(17)
O(6)#1-Al(2)-Al(3)	132.43(17)	O(8)-Al(3)-Al(1)	127.78(18)
O(1)-Al(2)-Al(3)	41.94(15)	O(5)-Al(3)-Al(1)	82.46(15)
O(3)#1-Al(2)-Al(3)	87.89(15)	O(4)-Al(3)-Al(1)	82.38(16)
O(7)-Al(2)-Al(1)	128.44(17)	O(1)-Al(3)-Al(1)	38.43(14)
O(4)-Al(2)-Al(1)	82.30(16)	O(2)-Al(3)-Al(1)	38.56(13)
O(20)#1-Al(2)-Al(1)	131.29(18)	O(13)-Al(3)-Al(2)	133.83(17)
O(6)#1-Al(2)-Al(1)	82.85(16)	O(8)-Al(3)-Al(2)	86.66(17)
O(1)-Al(2)-Al(1)	38.33(14)	O(5)-Al(3)-Al(2)	132.80(18)

O(4)-Al(3)-Al(2)	36.68(15)	O(14)-Al(4)-Al(2)#1	134.63(18)
O(1)-Al(3)-Al(2)	41.82(14)	O(6)-Al(4)-Al(2)#1	36.20(15)
O(2)-Al(3)-Al(2)	87.51(15)	O(19)-Al(4)-Al(2)#1	86.25(17)
Al(1)-Al(3)-Al(2)	60.05(6)	O(2)-Al(4)-Al(2)#1	86.77(15)
O(13)-Al(3)-Al(4)	87.38(17)	O(3)-Al(4)-Al(2)#1	42.22(14)
O(8)-Al(3)-Al(4)	132.45(18)	Al(3)-Al(4)-Al(2)#1	118.84(9)
O(5)-Al(3)-Al(4)	36.15(15)	O(8)-Al(5)-O(7)	94.7(2)
O(4)-Al(3)-Al(4)	131.99(18)	O(8)-Al(5)-O(11)	93.9(2)
O(1)-Al(3)-Al(4)	88.80(16)	O(7)-Al(5)-O(11)	94.4(2)
O(2)-Al(3)-Al(4)	42.44(14)	O(8)-Al(5)-O(12)	94.1(2)
Al(1)-Al(3)-Al(4)	60.70(6)	O(7)-Al(5)-O(12)	91.9(2)
Al(2)-Al(3)-Al(4)	120.75(9)	O(11)-Al(5)-O(12)	169.4(3)
O(5)-Al(4)-O(14)	92.7(2)	O(8)-Al(5)-O(9)	174.6(2)
O(5)-Al(4)-O(6)	163.5(2)	O(7)-Al(5)-O(9)	90.5(2)
O(14)-Al(4)-O(6)	98.6(2)	O(11)-Al(5)-O(9)	87.3(2)
O(5)-Al(4)-O(19)	97.0(2)	O(12)-Al(5)-O(9)	84.2(2)
O(14)-Al(4)-O(19)	103.9(2)	O(8)-Al(5)-O(10)	89.7(2)
O(6)-Al(4)-O(19)	91.9(2)	O(7)-Al(5)-O(10)	175.5(2)
O(5)-Al(4)-O(2)	77.6(2)	O(11)-Al(5)-O(10)	86.0(2)
O(14)-Al(4)-O(2)	90.3(2)	O(12)-Al(5)-O(10)	87.0(2)
O(6)-Al(4)-O(2)	90.2(2)	O(9)-Al(5)-O(10)	85.0(2)
O(19)-Al(4)-O(2)	165.0(2)	O(13)-Al(6)-O(14)	95.8(2)
O(5)-Al(4)-O(3)	88.2(2)	O(13)-Al(6)-O(17)	92.4(2)
O(14)-Al(4)-O(3)	165.9(2)	O(14)-Al(6)-O(17)	94.4(2)
O(6)-Al(4)-O(3)	77.9(2)	O(13)-Al(6)-O(18)	90.2(2)
O(19)-Al(4)-O(3)	89.9(2)	O(14)-Al(6)-O(18)	93.3(2)
O(2)-Al(4)-O(3)	76.13(19)	O(17)-Al(6)-O(18)	171.6(2)
O(5)-Al(4)-Al(3)	36.27(15)	O(13)-Al(6)-O(15)	91.0(2)
O(14)-Al(4)-Al(3)	86.10(17)	O(14)-Al(6)-O(15)	173.2(2)
O(6)-Al(4)-Al(3)	132.30(17)	O(17)-Al(6)-O(15)	86.4(2)
O(19)-Al(4)-Al(3)	133.17(18)	O(18)-Al(6)-O(15)	85.6(2)
O(2)-Al(4)-Al(3)	42.13(13)	O(13)-Al(6)-O(16)	177.7(2)
O(3)-Al(4)-Al(3)	86.36(15)	O(14)-Al(6)-O(16)	86.5(2)
O(5)-Al(4)-Al(2)#1	130.41(17)	O(17)-Al(6)-O(16)	87.9(2)

O(18)-Al(6)-O(16)	89.1(2)
O(15)-Al(6)-O(16)	86.8(2)
O(20)-Al(7)-O(19)	96.7(2)
O(20)-Al(7)-O(23)	94.1(2)
O(19)-Al(7)-O(23)	95.1(2)
O(20)-Al(7)-O(24)	91.3(2)
O(19)-Al(7)-O(24)	91.7(2)
O(23)-Al(7)-O(24)	170.7(2)
O(20)-Al(7)-O(21)	174.6(2)
O(19)-Al(7)-O(21)	88.4(2)
O(23)-Al(7)-O(21)	87.1(2)
O(24)-Al(7)-O(21)	86.8(2)
O(20)-Al(7)-O(22)	88.4(2)
O(19)-Al(7)-O(22)	174.2(2)
O(23)-Al(7)-O(22)	87.1(2)
O(24)-Al(7)-O(22)	85.5(2)
O(21)-Al(7)-O(22)	86.4(2)
Al(1)-O(1)-Al(2)	100.4(2)
Al(1)-O(1)-Al(3)	100.1(2)
Al(2)-O(1)-Al(3)	96.2(2)
Al(1)-O(2)-Al(3)	99.6(2)
Al(1)-O(2)-Al(4)	100.9(2)
Al(3)-O(2)-Al(4)	95.4(2)
Al(1)-O(3)-Al(2)#1	98.9(2)
Al(1)-O(3)-Al(4)	99.5(2)
Al(2)#1-O(3)-Al(4)	94.9(2)
Al(2)-O(4)-Al(3)	106.6(3)
Al(4)-O(5)-Al(3)	107.6(2)
Al(4)-O(6)-Al(2)#1	107.8(2)
Al(2)-O(7)-Al(5)	135.7(3)
Al(3)-O(8)-Al(5)	134.6(3)
Al(3)-O(13)-Al(6)	133.4(3)
Al(4)-O(14)-Al(6)	133.3(3)
Al(4)-O(19)-Al(7)	133.2(3)
Al(2)#1-O(20)-Al(7)	133.2(3)
O(25)-N(1)-O(26)	122.5(7)
O(25)-N(1)-O(27)	118.3(7)
O(26)-N(1)-O(27)	119.2(7)
O(29)-N(2)-O(28)	120.9(7)
O(29)-N(2)-O(30)	118.9(8)
O(28)-N(2)-O(30)	120.2(8)
O(32)-N(3)-O(33)	121.8(6)
O(32)-N(3)-O(31)	121.0(6)
O(33)-N(3)-O(31)	117.3(6)
O(35)-N(4)-O(36)	120.8(7)
O(35)-N(4)-O(34)	119.5(7)
O(36)-N(4)-O(34)	119.7(7)
O(38)-N(5)-O(39)	121.2(8)
O(38)-N(5)-O(37)	120.1(8)
O(39)-N(5)-O(37)	118.6(8)
O(42)-N(6)-O(41)	119.2(7)
O(42)-N(6)-O(40)	120.6(7)
O(41)-N(6)-O(40)	120.1(7)
O(43)-N(7)-O(44)	120.2(6)
O(43)-N(7)-O(45)	121.4(6)
O(44)-N(7)-O(45)	118.4(6)
O(46)-N(8)-O(47)	121.8(9)
O(46)-N(8)-O(48)	120.3(8)
O(47)-N(8)-O(48)	117.8(8)

Symmetry transformations used to generate equivalent atoms:

#1 -x,-y,-z

Table C.18. Anisotropic displacement parameters ($Å^2 x\ 10^3$)for JTG81. The anisotropic displacement factor exponent takes the form: $-2p^2[\ h^2a^{*2}U^{11} + ... + 2\ h\ k\ a^*\ b^*\ U^{12}\ ]$

	U^{11}	U^{22}	U^{33}	U^{23}	U^{13}	U^{12}
Al(1)	13(2)	8(2)	16(2)	-2(1)	-7(1)	2(1)
Al(2)	14(1)	9(1)	16(1)	-3(1)	-7(1)	3(1)
Al(3)	12(1)	7(1)	16(1)	-3(1)	-7(1)	4(1)
Al(4)	14(1)	7(1)	15(1)	-3(1)	-7(1)	5(1)
Al(5)	17(1)	9(1)	23(1)	-6(1)	-10(1)	6(1)
Al(6)	14(1)	10(1)	18(1)	-4(1)	-5(1)	3(1)
Al(7)	15(1)	11(1)	19(1)	-2(1)	-9(1)	5(1)
O(1)	15(3)	6(2)	23(3)	-4(2)	-10(2)	7(2)
O(2)	10(2)	5(2)	16(3)	-1(2)	-7(2)	1(2)
O(3)	11(3)	8(2)	19(3)	-5(2)	-5(2)	2(2)
O(4)	15(3)	12(3)	19(3)	-7(2)	-9(2)	9(2)
O(5)	18(3)	8(2)	14(3)	-1(2)	-8(2)	5(2)
O(6)	16(3)	10(2)	14(3)	-2(2)	-8(2)	1(2)
O(7)	16(3)	10(3)	19(3)	-7(2)	-8(2)	3(2)
O(8)	18(3)	11(3)	22(3)	-5(2)	-8(2)	3(2)
O(9)	16(3)	24(3)	28(3)	-10(2)	-11(2)	6(2)
O(10)	23(3)	16(3)	31(3)	-11(2)	-13(3)	5(2)
O(11)	23(3)	21(3)	21(3)	-7(2)	-9(2)	10(2)
O(12)	23(3)	16(3)	23(3)	0(2)	-8(2)	2(2)
O(13)	15(3)	7(2)	16(3)	-4(2)	-3(2)	2(2)
O(14)	15(3)	11(3)	19(3)	-3(2)	-5(2)	8(2)
O(15)	23(3)	16(3)	19(3)	-8(2)	-3(2)	4(2)
O(16)	14(3)	17(3)	23(3)	-6(2)	-5(2)	5(2)
O(17)	19(3)	12(3)	26(3)	-4(2)	-8(2)	3(2)
O(18)	27(3)	16(3)	23(3)	-2(2)	-7(2)	4(2)
O(19)	16(3)	12(3)	14(3)	1(2)	-6(2)	6(2)
O(20)	17(3)	12(3)	17(3)	1(2)	-7(2)	3(2)
O(21)	27(3)	16(3)	29(3)	-5(2)	-12(3)	8(2)
O(22)	31(3)	22(3)	26(3)	-4(2)	-17(3)	7(2)

O(23)	14(3)	23(3)	25(3)	-5(2)	-8(2)	4(2)
O(24)	20(3)	12(3)	26(3)	-4(2)	-4(2)	2(2)
N(1)	31(4)	23(4)	30(4)	-8(3)	-5(3)	1(3)
O(25)	31(4)	29(4)	64(5)	0(3)	-12(3)	-4(3)
O(26)	39(4)	39(4)	51(4)	-15(3)	-27(3)	7(3)
O(27)	34(3)	18(3)	17(3)	7(2)	-7(3)	-8(2)
N(2)	40(5)	24(4)	29(4)	-10(3)	-2(4)	1(4)
O(28)	37(4)	31(4)	61(5)	-11(3)	-9(3)	5(3)
O(29)	50(4)	18(3)	65(5)	-11(3)	-28(4)	10(3)
O(30)	54(4)	17(3)	42(4)	-15(3)	12(3)	-11(3)
N(3)	18(4)	15(4)	30(4)	-6(3)	-7(3)	-2(3)
O(31)	28(3)	22(3)	64(4)	-5(3)	-26(3)	2(3)
O(32)	32(3)	15(3)	35(3)	2(3)	-18(3)	7(2)
O(33)	24(3)	6(3)	34(3)	0(2)	-6(3)	-3(2)
N(4)	40(4)	16(4)	21(4)	-6(3)	-8(3)	6(3)
O(34)	120(7)	25(4)	24(4)	-9(3)	-36(4)	20(4)
O(35)	111(6)	17(3)	19(3)	-7(3)	-4(4)	-5(4)
O(36)	74(5)	20(3)	29(3)	-6(3)	-23(3)	14(3)
N(5)	38(5)	47(5)	37(5)	-25(4)	-12(4)	15(4)
O(37)	51(4)	58(5)	45(4)	-28(4)	-4(4)	-3(4)
O(38)	51(4)	42(4)	55(4)	-32(4)	-25(4)	12(3)
O(39)	48(4)	43(4)	39(4)	-10(3)	8(4)	2(3)
N(6)	24(4)	25(4)	34(4)	0(3)	-11(3)	7(3)
O(40)	44(4)	30(4)	52(4)	-5(3)	-34(3)	1(3)
O(41)	42(4)	45(4)	32(4)	-1(3)	-14(3)	4(3)
O(42)	47(4)	21(3)	46(4)	-5(3)	-22(3)	2(3)
N(7)	29(4)	12(3)	23(4)	-1(3)	-12(3)	3(3)
O(43)	23(3)	22(3)	44(4)	-7(3)	-1(3)	9(3)
O(44)	17(3)	18(3)	42(4)	-5(3)	-5(3)	-4(2)
O(45)	17(3)	24(3)	50(4)	-18(3)	-8(3)	3(2)
N(8)	48(5)	41(5)	28(5)	-1(4)	-13(4)	-5(4)
O(46)	39(4)	85(6)	28(4)	-4(4)	-5(3)	-18(4)
O(47)	126(8)	42(5)	50(5)	-20(4)	-12(5)	13(5)
O(48)	57(5)	66(5)	57(5)	8(4)	-31(4)	-14(4)

O(1S)	30(3)	24(3)	51(4)	-10(3)	-13(3)	11(3)
O(2S)	32(3)	16(3)	31(3)	-3(2)	-6(3)	5(2)
O(3S)	34(4)	45(5)	136(8)	-42(5)	-16(5)	19(3)
O(4S)	33(4)	48(4)	61(5)	-6(4)	-12(3)	-3(3)
O(5S)	54(4)	21(3)	41(4)	-10(3)	-19(3)	-2(3)
N(1S)	49(8)	58(9)	99(11)	-42(8)	7(8)	6(7)

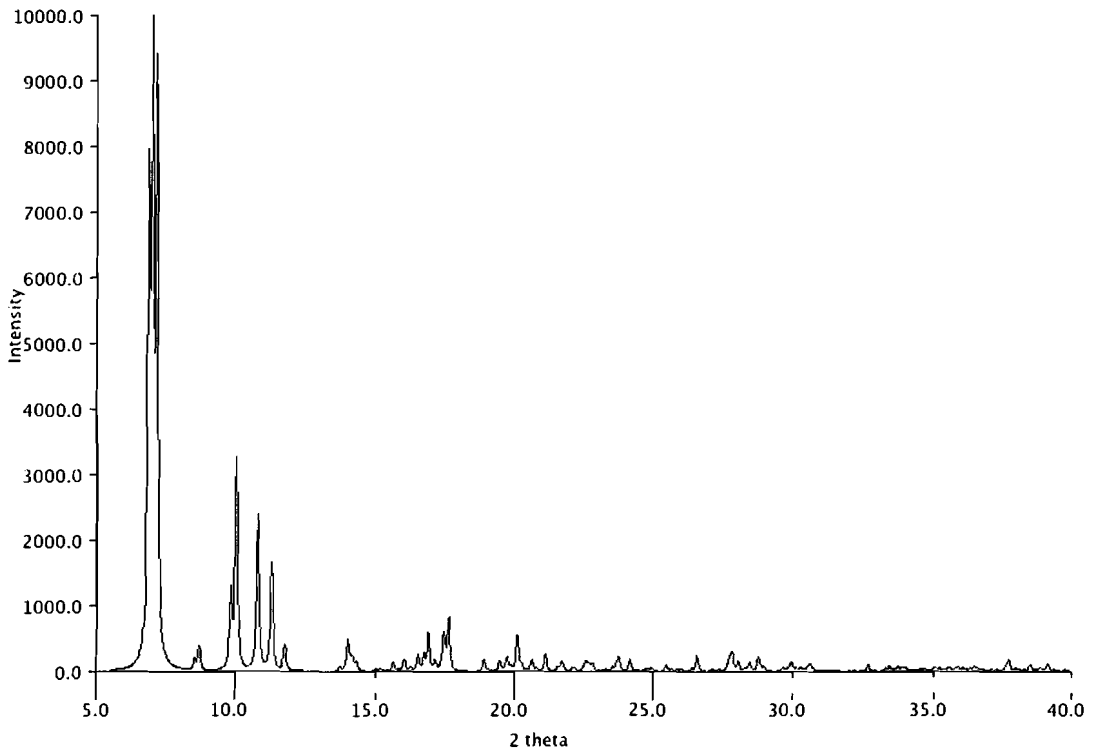

Figure C.05. X-ray powder diffraction pattern calculated from the single crystal structure of **1**.

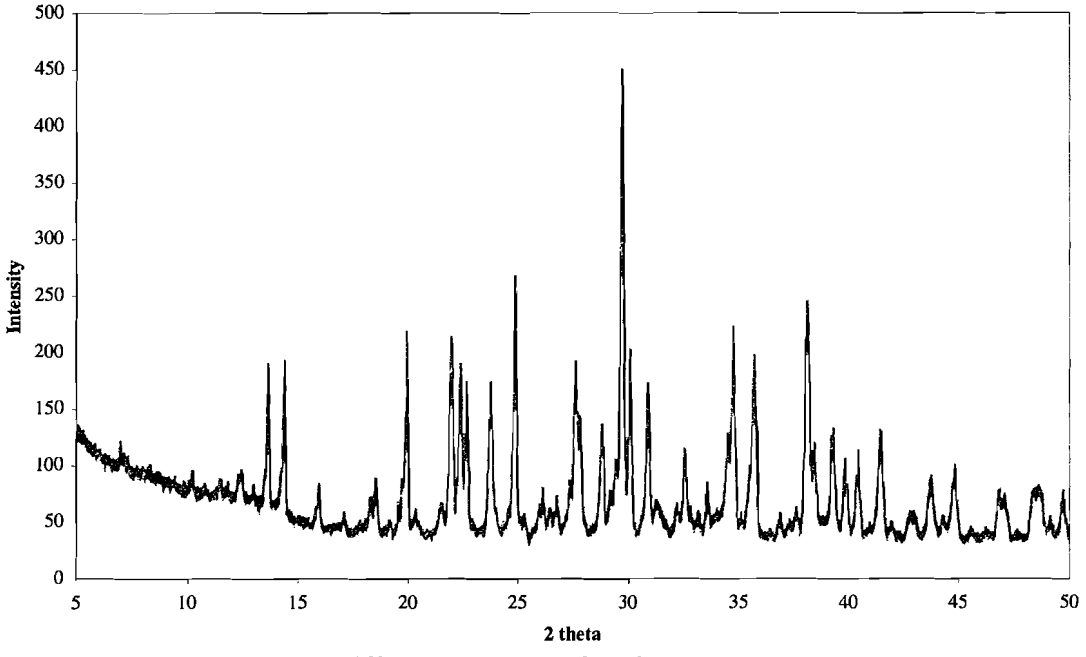

Figure C.06. X-ray powder diffraction pattern of **JTG27**.

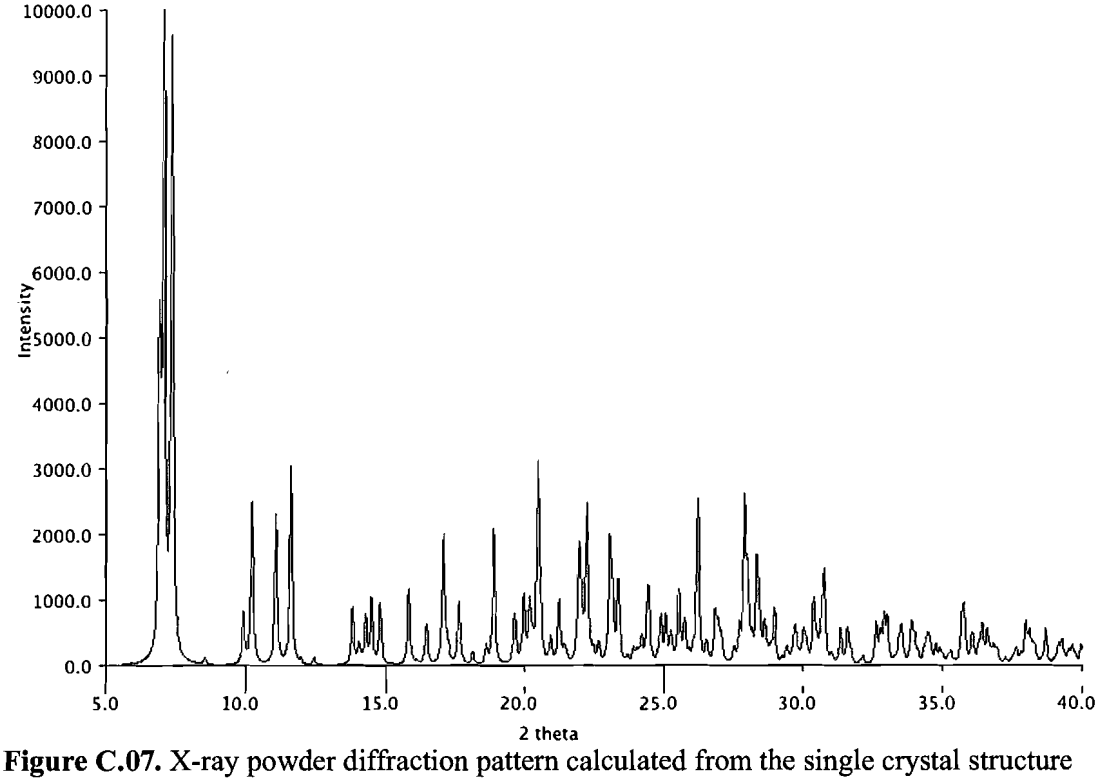

Figure C.07. X-ray powder diffraction pattern calculated from the single crystal structure of **JTG81**.

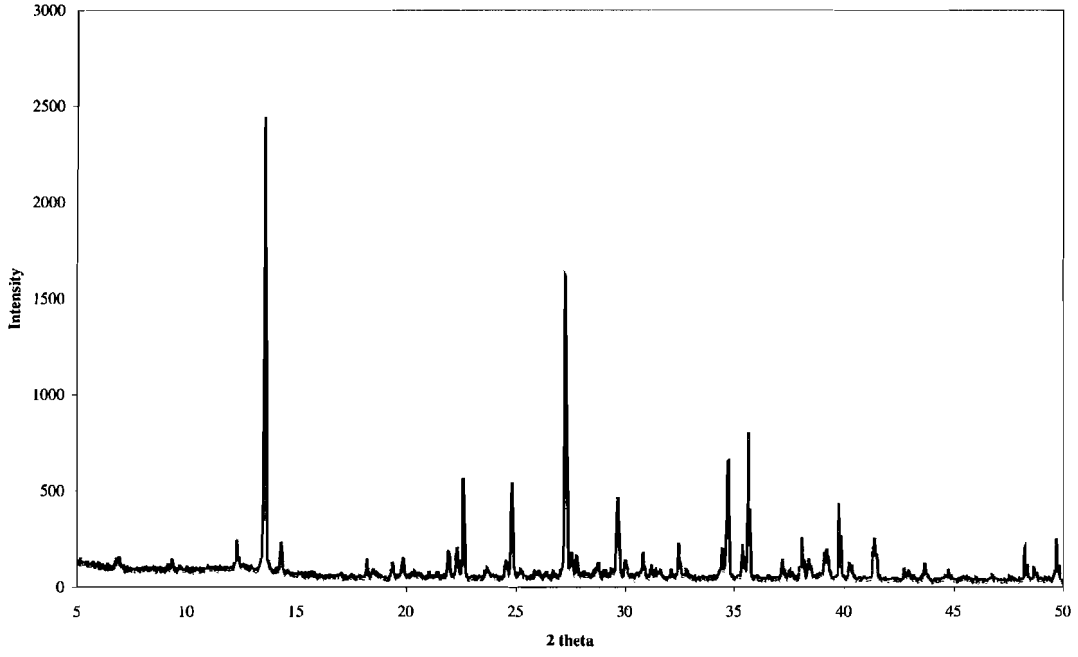

Figure C.08. X-ray powder diffraction pattern of **JTG81**.

TGA were run at 2°c/min from room temperature up to 600°C then held iosthermic for 5min.

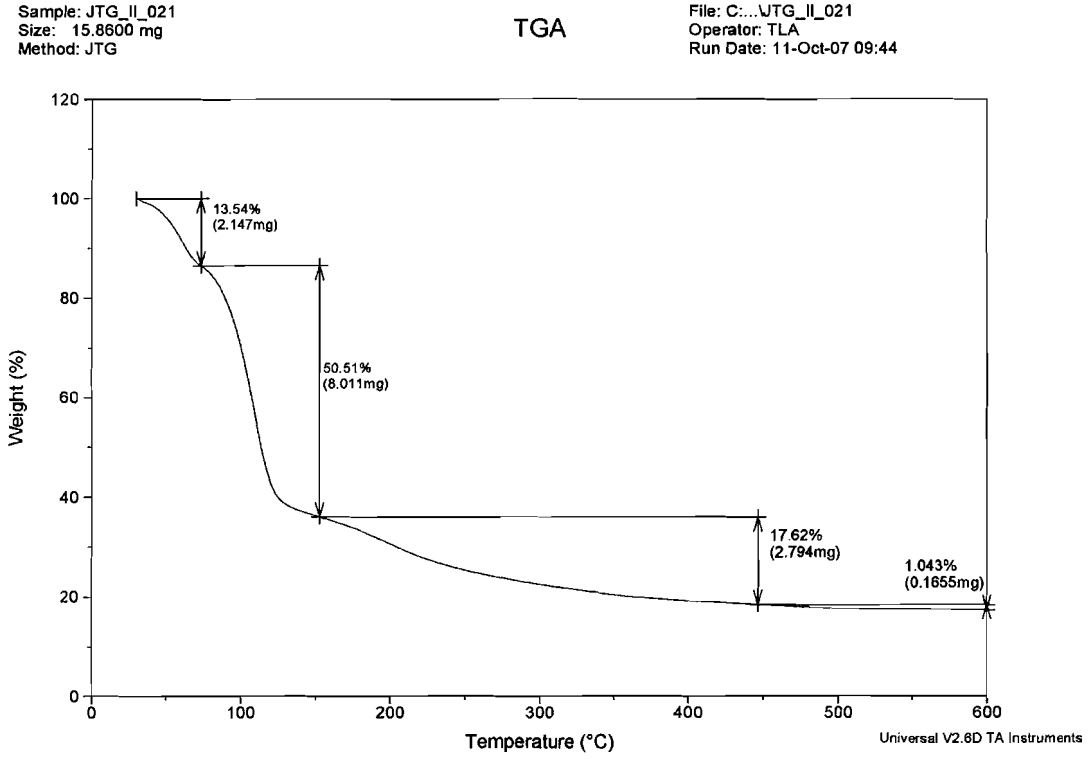

Figure C.09. TGA thermogram of **JTG27**.

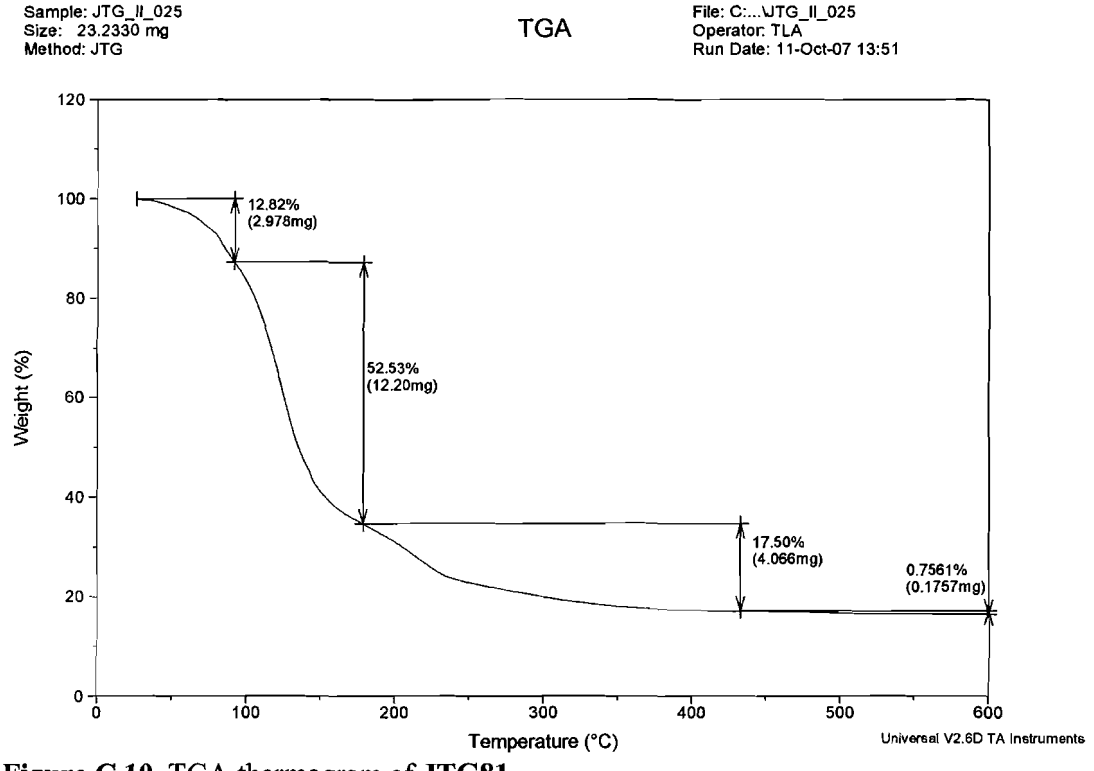

Figure C.10. TGA thermogram of **JTG81**.

APPENDIX D

SUPPLEMENTAL INFORMATION FOR HETEROMETALLIC NANOCLUSTERS

Other heterometallic clusters

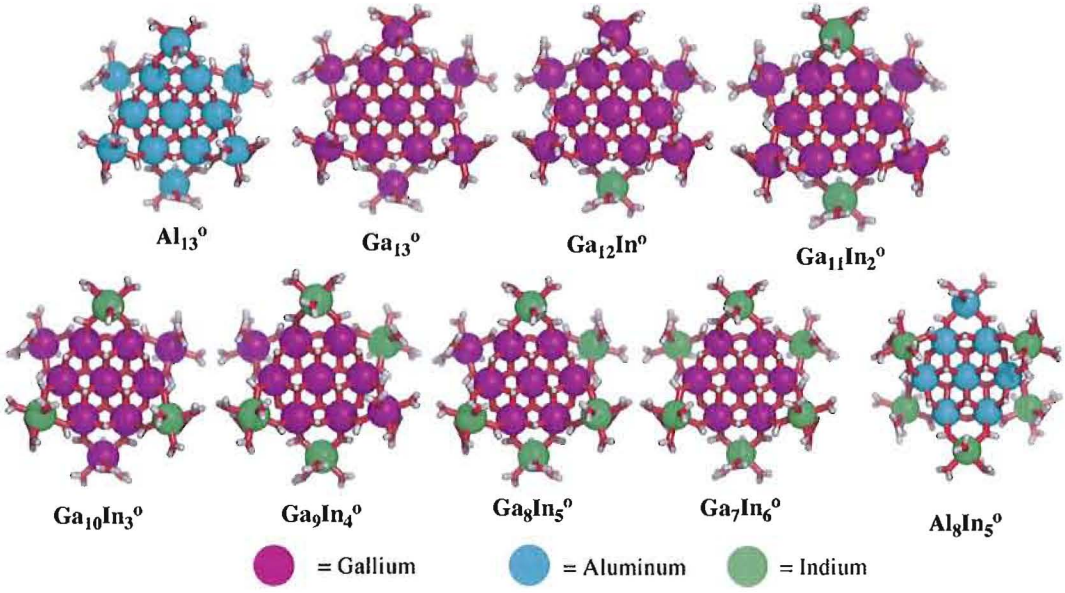

Figure D.01. Ball and stick representation of crystal structures.

EXPERIMETNAL

$[Al_7Al_1In_5(\mu_3\text{-}OH)_6(\mu\text{-}OH)_{18}(H_2O)_{24}](NO_3)_{15}$ (**Al_8In_5**)

N-nitroso-di-*n*-butylamine (0.64 g, 4.02 mmol, 24 eq.) is added to a solution of aluminum(III) nitrate (0.25 g, 1.2 mmol, 7 eq.) and indium(III) nitrate (0.30 g, 1.01 mmol, 6 eq.) in 5 mL of 0.26M NaOH/MeOH. The mixture is allowed to evaporate over 2-5 days at which point crystals begin to form in the same manner as before. This method

affords the Al_8In_5 cluster in 10% yield with respect to aluminum.

$[Ga_7Ga_3In_3(\mu_3\text{-}OH)_6(\mu\text{-}OH)_{18}(H_2O)_{24}](NO_3)_{15}$ **($Ga_{10}In_3$)**

Gallium (III) nitrate (0.5 g, 1.95 mmol, 7 equivalent) and indium (III) nitrate (0.5 g, 1.66 mmol, 6 equivalents) are dissolved in 5mL of methanol and nitrosobenzene (0.7 g, 6.53 mmol, 24 equivalents) is dissolved in 2mL of methanol, the solutions are mixed together. The mixture is allowed to slowly evaporate at room temperature over 4-8 days, yielding large single crystals in 35% yield with respect to gallium nitrate.

Alternative reductant. N-nitroso-di-*n*-butylamine (1.06 g, 6.69 mmol, 24 eq.) is added to $Ga(NO_3)_3$ (0.5 g, 1.95 mmol, 7 eq.) and $In(NO_3)_3$ (0.5 g, 1.66 mmol, 6 eq.) in methanol, as a homogenous solution. The mixture is allowed to evaporate over 2-5 days at which point crystals begin to form in the same manner as before. This alternative method produces the same Ga_7In_6 cluster in 47% yield with respect to gallium. More crystals can be isolated by ppt from the oil with EtOAc, this power can be re-crystallized from MeOH to yield an additional 35-40% of crystals over the evaporation. These crystals are crystallographically identical to the original batch. The total over all crystal yield is 85-90% in respect to Gallium.

The refinement of the crystal structure of **$Ga_{10}In_3$** without symmetry restrictions on occupation factors for the Ga and In atoms shows that the refined occupation factors of the Ga(1) and Ga(2) atoms are very close to those based on the crystal symmetry. The occupation factor of the In atom is less than the needed occupation factor of 1.0 based on symmetry. Refinement of the structure with the Ga and In atoms sharing the same In(1) position shows that the ratio of the occupation factors of Ga and In in this position is 1:1,

i.e. the investigated compound is $[Ga_7Ga_3In_3(\mu_3\text{-}OH)_6(\mu\text{-}OH)_{18}(H_2O)_{24}](NO_3)_{15}$. The average In(Ga)-O($H_2O$) distance in **$Ga_{10}In_3$**, 2.073(6) A, is between the average Ga-O(H_2O) and In-O(H_2O) distances in **Ga_{13}** and $[Ga_7In_6$ clusters, 1.997(16) and 2.162(4) Å, respectively.

Crystal data for Ga_7In_6 (Dave4): $C_6H_{96}Ga_7In_6N_{15}O_{99}$, Mr= 3139.94. Colorless block, 0.15x0.15x0.07 mm, rhombohedral, space group $R\bar{3}$ (no. 148), a=20.694(2), b=20.694(2), c=18.266(4) Å, V=6774(2) Å^3, Z=3, ρ_{calcd}=2.309 g·cm^{-3}, μ= 3.703 mm^{-1}, F(000)=4620, $2\theta_{max}$=56.50°, 16202 reflections collected, 3588 unique [R_{int}=0.0203], R indeces [$I>2\sigma(I)$]: $R1$=0.0211, $wR2$=0.0582, GOF=1.035.

Crystal data for 3a(jtg63): $C_6H_{96}Ga_{9.1}In_{3.9}N_{15}O_{99}$, Mr= 3045.23 Colorless block, 0.20x0.20x0.10 mm, rhombohedral, space group $R\bar{3}$ (no. 148), a=20.4329(10), b=20.4329(10), c=18.4080(18) Å, V=6655.8(8) Å^3, Z=3, ρ_{calcd}=2.279 g·cm^{-3}, μ= 3.86 mm^{-1}, F(000)=4507, $2\theta_{max}$=56.50°, 14035 reflections collected, 3500 unique [R_{int}=0.0176], R indeces [$I>2\sigma(I)$]: $R1$=0.0237, $wR2$=0.0698, GOF=1.034.

***Crystal data for* $Ga_{10}In_3$** (jtg65): $C_6H_{96}Ga_{10.3}In_{2.7}N_{15}O_{99}$, Mr= 2991.11. Colorless block, 0.10x0.10x0.05 mm, rhombohedral, space group $R\bar{3}$ (no. 148), a=20.2946(12), b=20.2946(12), c=18.456(2) Å, V=6583.1(9) Å^3, Z=3, ρ_{calcd}=2.239 g·cm^{-3}, μ= 3.96 mm^{-1}, F(000)=4442, $2\theta_{max}$=56.56°, 13757 reflections collected, 3460 unique [R_{int}=0.0217], R indeces [$I>2\sigma(I)$]: $R1$=0.0326, $wR2$=0.0951, GOF=1.067.

***Crystal data for* $Ga_{12}In_1$** (jtg66): $C_6H_{96}Ga_{11.9}In_{1.1}N_{15}O_{99}$, Mr= 2918.95. Colorless block, 0.10x0.10x0.05 mm, rhombohedral, space group $R\bar{3}$ (no. 148), a=20.1387(14), b=20.1387(14), c=18.490(3) Å, V=6494.3(11) (2) Å^3, Z=3, ρ_{calcd}=2.239 g·cm^{-3}, μ= 4.08

mm^{-1}, F(000)=4355, $2\theta_{max}$=56.48°, 13623 reflections collected, 3412 unique [R_{int}=0.0317], *R* indeces [$I>2\sigma(I)$]: *R*1=0.0328, *wR*2=0.0886, GOF=1.055.

Crystal data for **Al_8In_5** (dwjr21): $C_6H_{96}Al_{7.7}In_{5.3}N_{15}O_{99}$, Mr= 2779.27. Colorless block, 0.18x0.14x0.08 mm, rhombohedral, space group $R\bar{3}$ (no. 148), *a*=20.4094(13), *b*=20.4094(13), *c*=18.500(2) Å, *V*=6673.8(10) $Å^3$, Z=3, ρ_{calcd}=2.075 $g\cdot cm^{-3}$, μ= 1.58 mm^{-1}, F(000)=4166, $2\theta_{max}$=56.50°, 15029 reflections collected, 3481 unique [R_{int}=0.0247], *R* indeces [$I>2\sigma(I)$]: *R*1=0.0359, *wR*2=0.0960, GOF=1.134.

X-ray diffraction experiments were carried out on a Bruker Smart Apex diffractometer at 153 K (**Ga_7In_6**) and 173 K (**Ga_9In_4**, **$Ga_{10}In_3$**, **$Ga_{12}In_1$**, **Al_8In_5**) using MoKα radiation (λ=0.71070 Å). Absorption corrections were applied by SADABS (T_{min}/T_{max} = 0.762 (**Ga_7In_6**), 0.709 (**Ga_9In_4**), 0.769 (**$Ga_{10}In_3$**), 0.743 (**$Ga_{12}In_1$**) and 0.825 (**Al_8In_5**)). Crystals of **Ga_7In_6**, **Ga_9In_4**, **$Ga_{10}In_3$**, **$Ga_{12}In_1$** and **Al_8In_5** are hexagonal and have the same space group $R\bar{3}$ (no. 148). In all structures the M_{13} cations are on a $\bar{3}$ axes. Two NO_3 anions (in general positions) provide twelve NO_3 anions per the M_{13} cation. Three other NO_3 anions and solvent methanol molecules (in general positions as well) are highly disordered and randomly fill six other possible positions around the M_{13} cation. In all structures highly disordered NO_3 anions and solvent methanol molecules were treated by SQUEEZE. Corrections of the X-ray data by SQUEEZE (638 (**Ga_7In_6**), 642(**Ga_9In_4**), 596(**$Ga_{10}In_3$**), 620 (**$Ga_{12}In_1$**) and 637 (**Al_8In_5**) electron/cell) are close to the required value of 603 electron/cell for 9 NO_3 anions and 18 methanol molecules in the full unit cell. All non-H atoms were refined with anisotropic thermal parameters. H atoms in **Ga_7In_6** were found on the difference F-map and refined with isotropic thermal

parameters. In other structures H atoms have not been taken into consideration.

Refinements of the crystal structures of **Ga_7In_6** without symmetry restrictions on occupation factors for the Ga and In atoms show that the refined occupation factors of the Ga(1) and Ga(2) atoms are very close to those based on the crystal symmetry. The found Ga(1)-O and Ga(2)-O distances in structures **Ga_7In_6**, **Ga_9In_4**, **$Ga_{10}In_3$** and **$Ga_{12}In_1$**are close each other and the similar distances found in the Ga_{13} cation. It indicates that in all these structures the central M_7 part of the M_{13} cations are formed by the Ga atoms only. The same situation was found for the structure of **Al_8In_5** where the central Al_7 core of the M_{13} cations are formed by the Al atoms only. In contrast refinement of occupation factors for the In atom in "Ga(3)-position" show that only in structure of **Ga_7In_6** occupation factor for the In atom is close to required value of 1.0. In all other structure occupation factors for the In atoms in this position are less than the needed occupation factor of 1.0 based on symmetry. The final refinement of the structures of **Ga_9In_4**, **$Ga_{10}In_3$**, **$Ga_{12}In_1$**and **6** were done for a model with the Ga and In atoms sharing the same "Ga(3)-position" position. It was found that based on single crystal X-ray diffraction data the ratios Ga/In in the investigated compounds are Ga_7In_6 (**Ga_7In_6**), $Ga_{9.1}In_{3.9}$ (**Ga_9In_4**), $Ga_{10.3}In_{2.7}$ (**$Ga_{10}In_3$**), $Ga_{11.9}In_{1.1}$ (**$Ga_{12}In_1$**) and $Al_{7.7}In_{5.3}$ (**Al_8In_5**). The found ratio are close to those found for these compounds by other methods (Table *). The values of the Ga(In)-O(H) and Ga(In)-OH_2 distances found in these compounds are also indicate that in all compounds the Ga atoms in the "Ga(3)-position" positions only are replaced by the In atoms. The average In-O(H_2O) distance in **Ga_7In_6**, 2.162(4) Å, is close to the distances found before in complexes with the Bi-O(H_2O) bond, for example 2.156 and 1.158 Å in

catena-[(μ2-Oxalato-O,O',O',O''')-bis(μ2-O',O'',O''')-tetraaqua-diindium dihydrato][1]. Decreasing the In ratio in the row Ga_7In_6 (**Ga_7In_6**), $Ga_{9.1}In_{3.9}$ (**Ga_9In_4**), $Ga_{10.3}In_{2.7}$ (**$Ga_{10}In_3$**), $Ga_{11.9}In_{1.1}$ (**$Ga_{12}In_1$**), Ga13 is followed by decreasing the average In(Ga)-O(H_2O) distances in this row: 2.162(4) Å (**Ga_7In_6**), 2.105(6) Å (**Ga_9In_4**), 2.074(7) Å (**$Ga_{10}In_3$**), 2.033(6) Å (**$Ga_{12}In_1$**) and 2.00(2) Å (the Ga_{13} cation). The average In(Al)-O(H_2O) distance in **Al_8In_5** ($Al_{7.7}In_{5.3}$) is 2.156(7) Å.

The Al_{13}^{o} cluster cation has the similar structure as the Ga_{13}^{o} cluster cation where all the metal centers are octahedrally coordinated (Figure 1). The $M_1(\mu_3\text{-}OH)_6M_6(\mu_2\text{-}OH)_6$ core fragment (M = Ga, Al) forms a central core and six $M_1(H_2O)_4$ groups (M_1=In, Ga, Al) are connected to this core via two alkoxo (μ_2-OH) bridges each group alternating above and below the plane and forming the third M-shell in the cluster cation. In all these structures the Al_{13} cluster cations have $\bar{3}$ symmetry as for the Ga_{13} cluster cation.

In the all crystal structures the M_{13} clusters are surrounded by NO_3 anions and solvent water or methanol molecules forming O-H···O hydrogen bonds. Both H atoms of water molecules coordinated to the M (Al, Ga, In) atoms and the H atoms at the bridging μ-O atoms are involved in such H-bonds.

Ga10In3

Table D.01. Crystal data and structure refinement for jtgr36.

Identification code	jtgr36	
Empirical formula	H72 Ga10 In3 N15 O102	
Formula weight	2956.39	
Temperature	153(2) K	
Wavelength	0.71073 Å	
Crystal system	Rhombohedral	
Space group	R-3	
Unit cell dimensions	a = 20.3239(4) Å	a= 90°.
	b = 20.3239(4) Å	b= 90°.
	c = 18.3780(7) Å	g = 120°.
Volume	6574.2(3) $Å^3$	
Z	3	
Density (calculated)	2.240 Mg/m^3	
Absorption coefficient	3.949 mm^{-1}	
F(000)	4350	
Crystal size	0.14 x 0.12 x 0.06 mm^3	
Theta range for data collection	1.60 to 28.26°.	
Index ranges	-26<=h<=23, -25<=k<=27, -23<=l<=20	
Reflections collected	16312	
Independent reflections	3478 [R(int) = 0.0227]	
Completeness to theta = 28.26°	95.6 %	
Absorption correction	Semi-empirical from equivalents	
Max. and min. transmission	1.000 and 0.835	
Refinement method	Full-matrix least-squares on F^2	
Data / restraints / parameters	3478 / 16 / 242	
Goodness-of-fit on F^2	1.097	
Final R indices [I>2sigma(I)]	R1 = 0.0379, wR2 = 0.1117	
R indices (all data)	R1 = 0.0421, wR2 = 0.1154	
Largest diff. peak and hole	1.976 and -1.003 $e.Å^{-3}$	

Table D.02. Atomic coordinates (x 10^4) and equivalent isotropic displacement parameters ($Å^2$x 10^3) for jtgr36. U(eq) is defined as one third of the trace of the orthogonalized U^{ij} tensor.

	x	y	z	U(eq)
Ga(1)	0	0	0	14(1)
Ga(2)	1424(1)	1624(1)	-37(1)	15(1)
In(1)	3049(1)	1813(1)	-944(1)	19(1)
Ga(3)	3049(1)	1813(1)	-944(1)	19(1)
O(1)	735(2)	1878(2)	-493(2)	18(1)
O(2)	953(1)	580(1)	-539(2)	16(1)
O(3)	2213(2)	2047(2)	-754(2)	21(1)
O(4)	2714(2)	1517(2)	-2017(2)	31(1)
O(5)	3600(2)	2315(2)	15(2)	34(1)
O(6)	2450(2)	726(2)	-624(2)	21(1)
O(7)	3930(2)	1600(2)	-1149(2)	37(1)
O(8)	3739(2)	2886(2)	-1381(2)	29(1)
N(1S)	736(2)	2766(2)	-1991(2)	26(1)
O(1S)	1048(3)	3228(2)	-2496(2)	49(1)
O(2S)	846(3)	2220(3)	-1935(2)	54(1)
O(3S)	316(2)	2854(2)	-1566(2)	37(1)
N(2S)	3819(3)	4155(3)	42(2)	40(1)
O(4S)	3731(4)	4698(3)	147(3)	75(2)
O(5S)	3530(2)	3592(2)	460(2)	48(1)
O(6S)	4214(2)	4150(2)	-495(2)	46(1)
N(3S)	895(12)	950(20)	-2627(16)	250(18)
O(7S)	1567(8)	1318(10)	-2897(9)	120(5)
O(8S)	360(7)	944(7)	-2974(7)	86(4)
O(9S)	844(10)	624(11)	-2033(10)	132(7)
O(10S)	5345(5)	2624(5)	-1137(5)	55(2)
O(11S)	5056(7)	2430(7)	-2162(6)	75(3)
O(12S)	1183(5)	837(5)	-2012(5)	44(2)

Table D.03. Bond lengths [Å] and angles [°] for jtgr36.

Ga(1)-O(2)#1	1.959(3)
Ga(1)-O(2)#2	1.959(3)
Ga(1)-O(2)#3	1.959(3)
Ga(1)-O(2)#4	1.959(3)
Ga(1)-O(2)	1.959(3)
Ga(1)-O(2)#5	1.959(3)
Ga(2)-O(6)#1	1.908(3)
Ga(2)-O(1)	1.911(3)
Ga(2)-O(1)#4	1.913(3)
Ga(2)-O(3)	1.914(3)
Ga(2)-O(2)	2.059(2)
Ga(2)-O(2)#1	2.153(3)
In(1)-O(6)	2.006(3)
In(1)-O(3)	2.010(3)
In(1)-O(5)	2.064(4)
In(1)-O(7)	2.077(4)
In(1)-O(4)	2.075(3)
In(1)-O(8)	2.076(3)
O(1)-Ga(2)#1	1.913(3)
O(1)-H(1)	0.99(2)
O(2)-Ga(2)#4	2.153(3)
O(2)-H(2)	0.99(2)
O(3)-H(3)	0.99(2)
O(4)-H(4A)	0.99(2)
O(4)-H(4B)	0.99(2)
O(5)-H(5A)	0.99(2)
O(5)-H(5B)	0.99(2)
O(6)-Ga(2)#4	1.908(3)
O(6)-H(6)	0.97(2)
O(7)-H(7A)	1.00(2)
O(7)-H(7B)	0.98(2)
O(8)-H(8A)	0.92(8)
O(8)-H(8B)	0.70(7)
N(1S)-O(3S)	1.234(5)
N(1S)-O(2S)	1.241(5)
N(1S)-O(1S)	1.245(5)
N(2S)-O(4S)	1.219(7)
N(2S)-O(5S)	1.254(6)
N(2S)-O(6S)	1.275(6)
N(3S)-O(9S)	1.254(17)
N(3S)-O(8S)	1.255(16)
N(3S)-O(7S)	1.285(17)
N(3S)-O(12S)	1.34(2)
O(9S)-O(12S)	0.605(19)
O(2)#1-Ga(1)-O(2)#2	96.67(10)
O(2)#1-Ga(1)-O(2)#3	180.0(2)
O(2)#2-Ga(1)-O(2)#3	83.33(10)
O(2)#1-Ga(1)-O(2)#4	96.67(10)
O(2)#2-Ga(1)-O(2)#4	96.67(10)
O(2)#3-Ga(1)-O(2)#4	83.33(10)
O(2)#1-Ga(1)-O(2)	83.33(10)
O(2)#2-Ga(1)-O(2)	180.0(3)
O(2)#3-Ga(1)-O(2)	96.67(10)
O(2)#4-Ga(1)-O(2)	83.33(10)
O(2)#1-Ga(1)-O(2)#5	83.33(10)
O(2)#2-Ga(1)-O(2)#5	83.33(10)
O(2)#3-Ga(1)-O(2)#5	96.67(10)
O(2)#4-Ga(1)-O(2)#5	180.00(18)
O(2)-Ga(1)-O(2)#5	96.67(10)
O(6)#1-Ga(2)-O(1)	89.82(12)
O(6)#1-Ga(2)-O(1)#4	95.82(12)
O(1)-Ga(2)-O(1)#4	165.25(14)

O(6)#1-Ga(2)-O(3)	102.46(12)	Ga(2)-O(2)-H(2)	136(6)
O(1)-Ga(2)-O(3)	98.00(12)	Ga(2)#4-O(2)-H(2)	103(6)
O(1)#4-Ga(2)-O(3)	94.08(12)	Ga(2)-O(3)-In(1)	129.06(15)
O(6)#1-Ga(2)-O(2)	166.21(11)	Ga(2)-O(3)-H(3)	111(5)
O(1)-Ga(2)-O(2)	93.17(11)	In(1)-O(3)-H(3)	117(5)
O(1)#4-Ga(2)-O(2)	78.25(11)	In(1)-O(4)-H(4A)	120(3)
O(3)-Ga(2)-O(2)	90.46(11)	In(1)-O(4)-H(4B)	119(6)
O(6)#1-Ga(2)-O(2)#1	91.34(11)	H(4A)-O(4)-H(4B)	93(6)
O(1)-Ga(2)-O(2)#1	75.97(11)	In(1)-O(5)-H(5A)	124(6)
O(1)#4-Ga(2)-O(2)#1	90.25(11)	In(1)-O(5)-H(5B)	140(5)
O(3)-Ga(2)-O(2)#1	165.01(11)	H(5A)-O(5)-H(5B)	94(7)
O(2)-Ga(2)-O(2)#1	76.38(14)	Ga(2)#4-O(6)-In(1)	133.08(15)
O(6)-In(1)-O(3)	95.19(11)	Ga(2)#4-O(6)-H(6)	104(4)
O(6)-In(1)-O(5)	100.04(12)	In(1)-O(6)-H(6)	121(4)
O(3)-In(1)-O(5)	92.89(13)	In(1)-O(7)-H(7A)	97(8)
O(6)-In(1)-O(7)	86.27(13)	In(1)-O(7)-H(7B)	110(4)
O(3)-In(1)-O(7)	178.54(13)	H(7A)-O(7)-H(7B)	146(9)
O(5)-In(1)-O(7)	86.91(15)	In(1)-O(8)-H(8A)	109(5)
O(6)-In(1)-O(4)	91.62(12)	In(1)-O(8)-H(8B)	120(5)
O(3)-In(1)-O(4)	92.31(12)	H(8A)-O(8)-H(8B)	112(7)
O(5)-In(1)-O(4)	166.75(14)	O(3S)-N(1S)-O(2S)	121.6(4)
O(7)-In(1)-O(4)	87.59(14)	O(3S)-N(1S)-O(1S)	119.4(4)
O(6)-In(1)-O(8)	171.91(13)	O(2S)-N(1S)-O(1S)	119.0(4)
O(3)-In(1)-O(8)	91.50(12)	O(4S)-N(2S)-O(5S)	120.9(5)
O(5)-In(1)-O(8)	84.12(14)	O(4S)-N(2S)-O(6S)	120.6(5)
O(7)-In(1)-O(8)	87.04(14)	O(5S)-N(2S)-O(6S)	118.5(5)
O(4)-In(1)-O(8)	83.57(14)	O(9S)-N(3S)-O(8S)	126.6(19)
Ga(2)-O(1)-Ga(2)#1	109.38(13)	O(9S)-N(3S)-O(7S)	115.2(17)
Ga(2)-O(1)-H(1)	140(10)	O(8S)-N(3S)-O(7S)	118.2(17)
Ga(2)#1-O(1)-H(1)	72(10)	O(9S)-N(3S)-O(12S)	26.6(10)
Ga(1)-O(2)-Ga(2)	101.77(12)	O(8S)-N(3S)-O(12S)	151(2)
Ga(1)-O(2)-Ga(2)#4	98.52(11)	O(7S)-N(3S)-O(12S)	89.8(14)
Ga(2)-O(2)-Ga(2)#4	95.59(10)	O(12S)-O(9S)-N(3S)	85(2)
Ga(1)-O(2)-H(2)	114(6)	O(9S)-O(12S)-N(3S)	68.4(18)

Symmetry transformations used to generate equivalent atoms:	#1 x-y,x,-z #2 -x,-y,-z #3 -x+y,-x,z #4 y,-x+y,-z #5 -y,x-y,z

Table D.04. Anisotropic displacement parameters ($Å^2 x\ 10^3$) for jtgr36. The anisotropic displacement factor exponent takes the form: $-2p^2[\ h^2\ a^{*2}U^{11} + ... + 2\ h\ k\ a^*\ b^*\ U^{12}\ ]$

	U^{11}	U^{22}	U^{33}	U^{23}	U^{13}	U^{12}
Ga(1)	13(1)	13(1)	17(1)	0	0	7(1)
Ga(2)	14(1)	14(1)	17(1)	0(1)	0(1)	7(1)
In(1)	19(1)	17(1)	22(1)	2(1)	3(1)	10(1)
Ga(3)	19(1)	17(1)	22(1)	2(1)	3(1)	10(1)
O(1)	16(1)	17(1)	20(1)	3(1)	1(1)	8(1)
O(2)	15(1)	15(1)	16(1)	0(1)	0(1)	7(1)
O(3)	20(1)	19(1)	23(1)	5(1)	6(1)	9(1)
O(4)	32(2)	30(2)	33(2)	-4(1)	-8(1)	17(1)
O(5)	37(2)	39(2)	29(2)	9(1)	4(1)	21(2)
O(6)	20(1)	19(1)	21(1)	3(1)	5(1)	9(1)
O(7)	44(2)	32(2)	42(2)	3(2)	8(2)	24(2)
O(8)	33(2)	32(2)	25(2)	1(1)	0(1)	18(2)
N(1S)	31(2)	25(2)	24(2)	2(1)	0(1)	16(2)
O(1S)	72(3)	37(2)	48(2)	22(2)	39(2)	35(2)
O(2S)	100(4)	63(3)	31(2)	17(2)	16(2)	66(3)
O(3S)	40(2)	41(2)	39(2)	19(2)	17(2)	27(2)
N(2S)	42(2)	42(2)	30(2)	4(2)	1(2)	19(2)
O(4S)	113(5)	75(3)	64(3)	0(3)	7(3)	66(4)
O(5S)	50(2)	44(2)	37(2)	4(2)	14(2)	14(2)
O(6S)	51(2)	48(2)	31(2)	7(2)	10(2)	18(2)

Table D.05. Hydrogen coordinates (x 10^4) and isotropic displacement parameters ($Å^2$x 10^3) for jtgr36.

	x	y	z	U(eq)
H(1)	310(70)	1670(90)	-850(70)	240(70)
H(2)	930(60)	390(60)	-1040(20)	120(40)
H(3)	2280(50)	2530(30)	-940(50)	100(30)
H(4A)	2940(30)	1270(30)	-2310(30)	38(15)
H(4B)	2180(20)	1110(40)	-2120(50)	110(30)
H(5A)	3640(60)	2790(30)	210(50)	120(40)
H(5B)	3750(50)	2170(50)	480(30)	80(30)
H(6)	2440(40)	320(30)	-910(30)	60(20)
H(7A)	3660(70)	1060(30)	-990(80)	180(60)
H(7B)	4410(20)	2080(20)	-1170(40)	60(20)
H(8A)	3520(50)	2930(40)	-1800(40)	70(20)
H(8B)	3870(40)	3210(40)	-1160(40)	38(18)

Table D.06. Hydrogen bonds for jtgr36 [Å and °].

D-H...A	d(D-H)	d(H...A)	d(D...A)	<(DHA)
O(1)-H(1)...O(2S)	0.99(2)	2.27(17)	2.721(5)	106(11)
O(1)-H(1)...O(6)#5	0.99(2)	2.21(16)	2.835(4)	119(13)
O(2)-H(2)...O(9S)	0.99(2)	1.92(7)	2.759(17)	142(9)
O(2)-H(2)...O(12S)	0.99(2)	1.95(7)	2.752(9)	136(8)
O(3)-H(3)...O(1S)#6	0.99(2)	1.85(5)	2.762(4)	153(8)
O(4)-H(4A)...O(6S)#7	0.99(2)	1.78(2)	2.772(5)	176(5)
O(4)-H(4B)...O(12S)	0.99(2)	1.83(6)	2.700(10)	144(8)
O(4)-H(4B)...O(7S)	0.99(2)	2.07(9)	2.696(16)	119(7)
O(5)-H(5A)...O(5S)	0.99(2)	1.81(3)	2.793(6)	168(9)
O(5)-H(5B)...O(1S)#8	0.99(2)	1.96(7)	2.680(5)	128(6)

O(5)-H(5B)...O(2S)#8	0.99(2)	2.38(3)	3.343(5)	162(7)
O(6)-H(6)...O(3S)#3	0.97(2)	1.85(2)	2.809(4)	170(7)
O(7)-H(7A)...O(5S)#4	1.00(2)	2.19(7)	3.115(5)	154(12)
O(7)-H(7A)...O(4S)#4	1.00(2)	2.70(14)	3.082(7)	103(9)
O(7)-H(7B)...O(10S)	0.98(2)	1.65(4)	2.573(10)	156(7)
O(7)-H(7B)...O(11S)	0.98(2)	2.14(6)	2.773(12)	121(5)
O(8)-H(8A)...O(5S)#9	0.92(8)	2.05(8)	2.935(5)	160(7)
O(8)-H(8A)...O(3S)#6	0.92(8)	2.47(8)	2.993(5)	116(6)
O(8)-H(8B)...O(6S)	0.70(7)	2.08(7)	2.775(6)	177(7)

Symmetry transformations used to generate equivalent atoms:

#1 x-y,x,-z #2 -x,-y,-z #3 -x+y,-x,z #4 y,-x+y,-z

#5 -y,x-y,z #6 -x+1/3,-y+2/3,-z-1/3 #7 x-y+1/3,x-1/3,-z-1/3

#8 -y+2/3,x-y+1/3,z+1/3 #9 -x+y+1/3,-x+2/3,z-1/3

Supplimental information for Heterometallic paper

Experimental Section

All chemicals were used as received: metal salts from Strem, N-nitroso-di-*n*-butylamine from TCI, and nitrosobenzene from Aldrich. IR spectra were taken using a Nicolet Magna 550 spectrometer and UV-visible spectra were measured on a Hewlett Packard 8453 spectrometer. TGA was performed on a Thermal Analysis 2950.

$[Ga_{13}(\mu_3\text{-}OH)_6(\mu\text{-}OH)_{18}(H_2O)_{24}](NO_3)_{15}$ (**1**)

Synthesized as previously described.[2]

Alternative organic additive. N-nitroso-di-*n*-butylamine (1.15 g, 7.26 mmol, 24 equivalents.) is added to gallium(III) nitrate (1.0 g, 3.91 mmol, 13 equivalents) in 10mL of methanol, as a homogeneous solution. The mixture was evaporated over 5 days at which point the methanol and nitrosoamine are no longer miscible and crystals begin to form on the sides and bottom of reaction vessel. After 4 more days the methanol completely evaporates giving a single liquid layer. The remaining oil is decanted and single crystals of **1** are washed with cold ethyl acetate (3x) and dried under air. This alternative method produces the identical Ga_{13} cluster in 85% yield with respect to gallium. The yield can be increased to nearly quantitative by precipitation of poorer quality crystals from the residual oil with cold ethyl acetate and re-crystallizing from methanol.

$[Ga_7In_6(\mu_3\text{-}OH)_6(\mu\text{-}OH)_{18}(H_2O)_{24}](NO_3)_{15}$ (**2**)

Gallium(III) nitrate (1.73 mg, 0.006 mmol, 1 equivalent) and indium(III) nitrate (24.7 mg, 0.082 mmol, 12 equivalents) are dissolved in 5 mL of methanol. Nitrosobenzene

(17.6 mg, 0.165 mmol, 24 equivalents) was dissolved in 2 mL of methanol, and the solutions were mixed together. The mixture was evaporated at room temperature over 10-12 days, yielding large single crystals of **2** in 25% yield with respect to indium nitrate. Alternate method. N-nitroso-di-*n*-butylamine (0.93g, 5.9 mmol 24 eq.) was added to a solution of $Ga(NO_3)_3$ (0.068g, 0.267 mmol, 1 eq.) and $In(NO_3)_3$ (0.872g, 2.97 mmol, 12 eq.) in methanol, and formed a homogenous solution. The mixture was evaporated at room temperature over 10-12 days, affording **2** in 94% yield.

Crystal data for 2 (Dave4): $C_6H_{96}Ga_7In_6N_{15}O_{99}$, Mr= 3139.94. Colorless block, 0.15x0.15x0.07 mm, rhombohedral, space group *R*`3 (no. 148), *a*=20.694(2), *b*=20.694(2), *c*=18.266(4) Å, *V*=6774(2) $Å^3$, Z=3, r_{calcd}=2.309 g×cm^{-3}, m= 3.703 mm^{-1}, F(000)=4620, $2\theta_{max}$=56.50°, 16202 reflections collected, 3588 unique [R_{int}=0.0203], *R* indeces [$I>2\sigma(I)$]: *R*1=0.0211, *wR*2=0.0582, GOF=1.035.

X-ray diffraction experiments were carried out on a Bruker Smart Apex diffractometer at 153 K (**2**) using MoKa radiation (l=0.71070 Å). Absorption corrections were applied by SADABS (T_{min}/T_{max} = 0.570 (**1**) and 0.762 (**2**). Crystal of **2**, is hexagonal and have the same space group *R*`3 (no. 148). In all structures the $M_{13}$ cations are on a`3 axes. Two NO_3 anions (in general positions) provide twelve NO_3 anions per the M_{13} cation. Three other NO_3 anions and solvent molecules (methanol in **2**) are highly disordered and randomly fill six other possible positions around the M_{13} cation. In the crystal structure of **1** a disorder of NO_3 anions and solvent water molecules are more complex. In all structures highly disordered NO_3 anions and solvent methanol molecules

were treated by SQUEEZE.[3] Corrections of the X-ray data by SQUEEZE are 353 and 638 electron/cell, respectively for **1** and **2**; to the required values are 349 electron/cell for 9 NO_3 anions and 7 water molecules in **1** and 603 electron/cell for 9 NO_3 anions and 18 methanol molecules in **2.** All non-H atoms were refined with anisotropic thermal parameters except the atoms of the disordered NO_3 anion. In all structures H atoms were found on the difference F-map and refined with isotropic thermal parameters except those in disordered water molecules, which were not taken into consideration.

Refinements of the crystal structures of **2** without symmetry restrictions on occupation factors for the Ga and In atoms show that the refined occupation factors of the Ga(1) and Ga(2) atoms are very close to those based on the crystal symmetry. The found Ga(1)-O and Ga(2)-O distances in structure **2** is similar distances found in the Ga13 cation [*]. It indicates that in all these structures the central M_7 part of the M_{13} cations are formed by the Ga atoms only. In contrast refinement of occupation factors for the In atom in "Ga(3)-position" show that only in structure of **2** occupation factor for the In atom is close to required value of 1.0. In all other structure occupation factors for the In atoms in this position are less than the needed occupation factor of 1.0 based on symmetry. The values of the Ga(In)-O(H) and Ga(In)-OH_2 distances found in these compounds are also indicate that in all compounds the Ga atoms in the "Ga(3)-position" positions only are replaced by the In atoms. In the all crystal structures the M_{13} clusters are surrounded by NO_3 anions and solvent water or methanol molecules forming O-H···O hydrogen bonds Both H atoms of water molecules coordinated to the M (Ga, In) atoms and the H atoms at the bridging m-O atoms are involved in such H-bonds. The average

In(Ga)-O(H_2O) distance in Ga_{13} and [Ga_7In_6 clusters, 1.997(16) and 2.162(4) Å, respectively. These distances are close to the distances found before in complexes with the Bi-O(H_2O) bond, for example 2.156 and 1.158 Å in catena-[(μ2-Oxalato-O,O',O',O''')-bis(μ2-O',O'',O''')-tetraaqua-diindium dihydrato].[1]

Supporting information available

These data can be obtained free of charge via www.ccdc.cam.ac.uk/conts/retrieving.html (or from the Cambridge Crystallographic Data Centre, 12, Union Road, Cambridge CB21EZ, UK; fax: (+44)1223-336-033; or deposit@ccdc.cam.ac.uk).

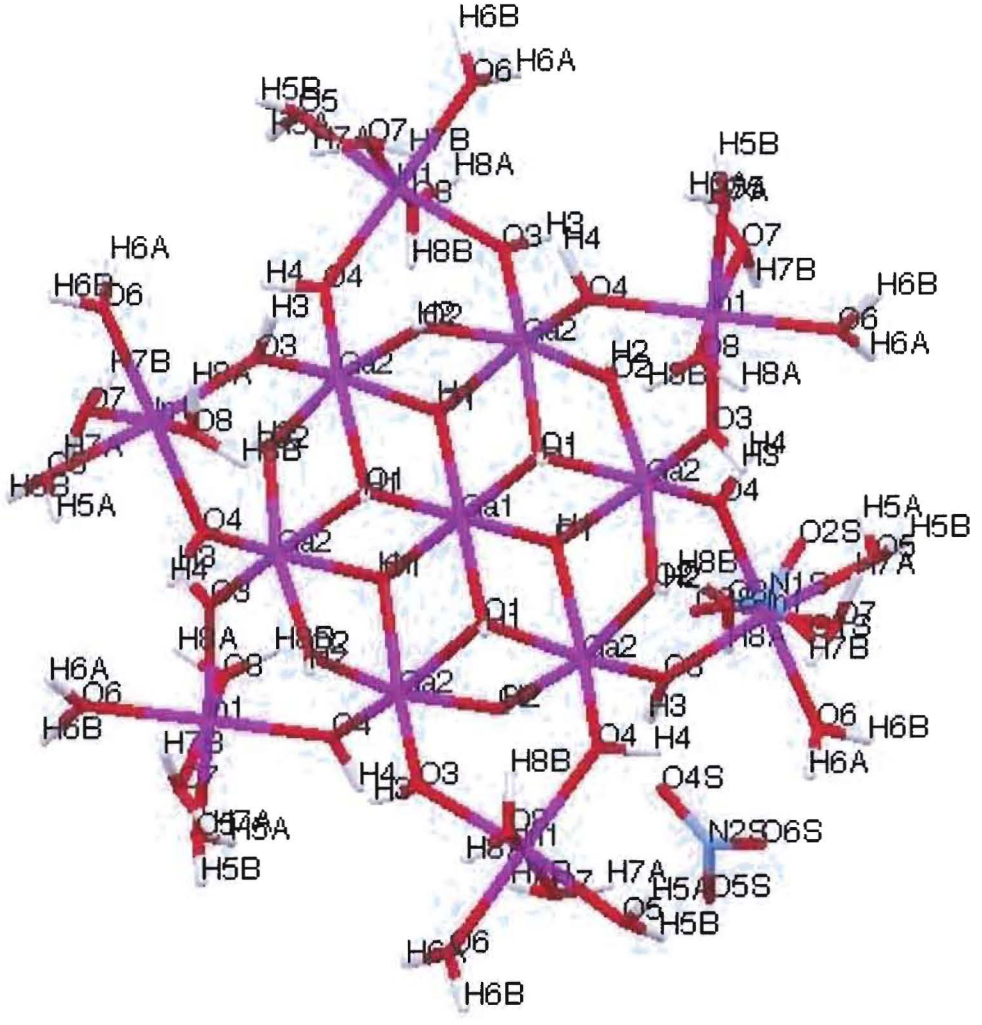

Figure D.02 Ga7In6

Crystal Data from Ga7In6 Heterometallic Anderson-like nanocluster.
Table D.07. Crystal data and structure refinement for dav4.

Identification code	dav4	
Empirical formula	C6 H96 Ga7 In6 N15 O99	
Formula weight	3139.94	
Temperature	153(2) K	
Wavelength	0.71073 Å	
Crystal system	Rhombohedral	
Space group	R-3	
Unit cell dimensions	a = 20.694(2) Å	a= 90°.
	b = 20.694(2) Å	b= 90°.
	c = 18.266(4) Å	g = 120°.
Volume	6774.2(16) $Å^3$	
Z	3	
Density (calculated)	2.309 Mg/m^3	
Absorption coefficient	3.703 mm^{-1}	
F(000)	4620	
Crystal size	0.15 x 0.15 x 0.07 mm^3	
Theta range for data collection	1.59 to 28.25°.	
Index ranges	-27<=h<=27, -26<=k<=20, -22<=l<=24	
Reflections collected	16202	
Independent reflections	3588 [R(int) = 0.0203]	
Completeness to theta = 28.25°	96.3 %	
Absorption correction	Semi-empirical from equivalents	
Max. and min. transmission	1.000 and 0.762	
Refinement method	Full-matrix least-squares on F^2	
Data / restraints / parameters	3588 / 12 / 213	
Goodness-of-fit on F^2	1.035	
Final R indices [I>2sigma(I)]	R1 = 0.0211, wR2 = 0.0582	
R indices (all data)	R1 = 0.0222, wR2 = 0.0588	
Largest diff. peak and hole	1.015 and -0.438 $e.Å^{-3}$	

Table D.08. Atomic coordinates (x 10^4) and equivalent isotropic displacement parameters ($Å^2$x 10^3) for dav4. U(eq) is defined as one third of the trace of the orthogonalized U^{ij} tensor.

	x	y	z	U(eq)
Ga(1)	6667	3333	8333	20(1)
Ga(2)	6462(1)	1728(1)	8370(1)	20(1)
In(1)	7880(1)	1517(1)	9290(1)	22(1)
O(1)	7031(1)	2758(1)	8875(1)	21(1)
O(2)	7392(1)	2196(1)	7849(1)	23(1)
O(3)	8375(1)	2630(1)	8970(1)	26(1)
O(4)	6792(1)	1295(1)	9101(1)	25(1)
O(5)	7484(1)	407(1)	9717(1)	27(1)
O(6)	8999(1)	1724(1)	9480(1)	39(1)
O(7)	7923(1)	1001(1)	8272(1)	33(1)
O(8)	7870(1)	1789(1)	10428(1)	41(1)
N(1S)	7414(1)	1304(1)	6346(1)	29(1)
O(1S)	7767(2)	1176(1)	5877(1)	57(1)
O(2S)	6986(1)	798(1)	6765(1)	39(1)
O(3S)	7496(1)	1943(1)	6383(1)	50(1)
N(2S)	9188(1)	2884(1)	1706(1)	40(1)
O(4S)	8656(2)	2973(2)	1819(2)	74(1)
O(5S)	9749(1)	3190(1)	2117(1)	55(1)
O(6S)	9180(1)	2473(1)	1195(1)	47(1)

Table D.09. Bond lengths [Å] and angles [°] for dav4.

Ga(1)-O(1)#1	1.9656(15)	Ga(1)-O(1)#4	1.9657(15)
Ga(1)-O(1)	1.9656(15)	Ga(1)-O(1)#5	1.9657(15)
Ga(1)-O(1)#2	1.9657(15)	Ga(2)-O(3)#4	1.9075(16)
Ga(1)-O(1)#3	1.9657(15)	Ga(2)-O(2)#4	1.9109(15)
		Ga(2)-O(4)	1.9117(16)
		Ga(2)-O(2)	1.9184(15)
		Ga(2)-O(1)	2.0673(15)

Ga(2)-O(1)#4	2.1589(15)	O(1)#2-Ga(1)-O(1)#3	96.89(6)
In(1)-O(3)	2.0823(15)	O(1)#1-Ga(1)-O(1)#4	96.89(6)
In(1)-O(4)	2.0903(15)	O(1)-Ga(1)-O(1)#4	83.11(6)
In(1)-O(8)	2.1565(19)	O(1)#2-Ga(1)-O(1)#4	179.998(1)
In(1)-O(5)	2.1620(16)	O(1)#3-Ga(1)-O(1)#4	83.11(6)
In(1)-O(6)	2.1627(18)	O(1)#1-Ga(1)-O(1)#5	96.89(6)
In(1)-O(7)	2.1668(17)	O(1)-Ga(1)-O(1)#5	83.11(6)
O(1)-Ga(2)#5	2.1590(15)	O(1)#2-Ga(1)-O(1)#5	83.11(6)
O(1)-H(1)	1.000(19)	O(1)#3-Ga(1)-O(1)#5	180.00(8)
O(2)-Ga(2)#5	1.9109(15)	O(1)#4-Ga(1)-O(1)#5	96.89(6)
O(2)-H(2)	0.986(18)	O(3)#4-Ga(2)-O(2)#4	90.16(7)
O(3)-Ga(2)#5	1.9074(16)	O(3)#4-Ga(2)-O(4)	101.79(7)
O(3)-H(3)	0.970(19)	O(2)#4-Ga(2)-O(4)	96.80(7)
O(4)-H(4)	0.976(19)	O(3)#4-Ga(2)-O(2)	95.14(7)
O(5)-H(5A)	0.949(19)	O(2)#4-Ga(2)-O(2)	166.14(8)
O(5)-H(5B)	0.949(19)	O(4)-Ga(2)-O(2)	94.64(7)
O(6)-H(6A)	0.97(2)	O(3)#4-Ga(2)-O(1)	165.87(7)
O(6)-H(6B)	1.00(2)	O(2)#4-Ga(2)-O(1)	94.09(6)
O(7)-H(7A)	0.945(19)	O(4)-Ga(2)-O(1)	91.09(6)
O(7)-H(7B)	0.940(18)	O(2)-Ga(2)-O(1)	77.87(6)
O(8)-H(8A)	0.957(19)	O(3)#4-Ga(2)-O(1)#4	91.88(6)
O(8)-H(8B)	0.99(2)	O(2)#4-Ga(2)-O(1)#4	75.79(6)
N(1S)-O(2S)	1.239(3)	O(4)-Ga(2)-O(1)#4	164.55(7)
N(1S)-O(1S)	1.238(3)	O(2)-Ga(2)-O(1)#4	91.21(6)
N(1S)-O(3S)	1.248(3)	O(1)-Ga(2)-O(1)#4	76.17(8)
N(2S)-O(4S)	1.221(3)	O(3)-In(1)-O(4)	94.40(6)
N(2S)-O(5S)	1.257(3)	O(3)-In(1)-O(8)	92.62(7)
N(2S)-O(6S)	1.257(3)	O(4)-In(1)-O(8)	93.83(7)
		O(3)-In(1)-O(5)	172.72(6)
O(1)#1-Ga(1)-O(1)	179.998(1)	O(4)-In(1)-O(5)	91.85(6)
O(1)#1-Ga(1)-O(1)#2	83.11(6)	O(8)-In(1)-O(5)	83.23(8)
O(1)-Ga(1)-O(1)#2	96.89(6)	O(3)-In(1)-O(6)	86.56(7)
O(1)#1-Ga(1)-O(1)#3	83.11(6)	O(4)-In(1)-O(6)	178.87(7)
O(1)-Ga(1)-O(1)#3	96.89(6)	O(8)-In(1)-O(6)	86.72(8)

O(5)-In(1)-O(6)	87.23(7)	H(5A)-O(5)-H(5B)	110(4)
O(3)-In(1)-O(7)	100.66(7)	In(1)-O(6)-H(6A)	119(4)
O(4)-In(1)-O(7)	93.14(7)	In(1)-O(6)-H(6B)	129(4)
O(8)-In(1)-O(7)	164.48(8)	H(6A)-O(6)-H(6B)	105(5)
O(5)-In(1)-O(7)	82.70(7)	In(1)-O(7)-H(7A)	116(3)
O(6)-In(1)-O(7)	86.09(7)	In(1)-O(7)-H(7B)	109(2)
Ga(1)-O(1)-Ga(2)	101.95(7)	H(7A)-O(7)-H(7B)	119(3)
Ga(1)-O(1)-Ga(2)#5	98.78(6)	In(1)-O(8)-H(8A)	121(3)
Ga(2)-O(1)-Ga(2)#5	95.78(6)	In(1)-O(8)-H(8B)	100(5)
Ga(1)-O(1)-H(1)	122(2)	H(8A)-O(8)-H(8B)	117(6)
Ga(2)-O(1)-H(1)	115(2)	O(2S)-N(1S)-O(1S)	119.7(2)
Ga(2)#5-O(1)-H(1)	118(2)	O(2S)-N(1S)-O(3S)	121.5(2)
Ga(2)#5-O(2)-Ga(2)	109.95(7)	O(1S)-N(1S)-O(3S)	118.8(2)
Ga(2)#5-O(2)-H(2)	122.7(19)	O(4S)-N(2S)-O(5S)	119.9(3)
Ga(2)-O(2)-H(2)	117.6(19)	O(4S)-N(2S)-O(6S)	121.3(3)
Ga(2)#5-O(3)-In(1)	131.83(8)	O(5S)-N(2S)-O(6S)	118.7(2)
Ga(2)#5-O(3)-H(3)	114(3)		
In(1)-O(3)-H(3)	112(3)	Symmetry transformations used to	
Ga(2)-O(4)-In(1)	127.57(8)	generate equivalent atoms:	
Ga(2)-O(4)-H(4)	106(3)	#1 -x+4/3,-y+2/3,-z+5/3 #2 -y+1,x-y,z	
In(1)-O(4)-H(4)	121(3)	#3 -x+y+1,-x+1,z	
In(1)-O(5)-H(5A)	113(3)	#4 y+1/3,-x+y+2/3,-z+5/3 #5 x-	
In(1)-O(5)-H(5B)	116(3)	y+1/3,x-1/3,-z+5/3	

Table D.10. Anisotropic displacement parameters ($Å^2 x\ 10^3$) for dav4. The anisotropic displacement factor exponent takes the form: $-2p^2[\ h^2\ a^{*2}U^{11} + ... + 2\ h\ k\ a^*\ b^*\ U^{12}\ ]$

	U^{11}	U^{22}	U^{33}	U^{23}	U^{13}	U^{12}
Ga(1)	17(1)	17(1)	25(1)	0	0	9(1)
Ga(2)	16(1)	18(1)	26(1)	0(1)	-1(1)	8(1)
In(1)	20(1)	18(1)	25(1)	-1(1)	-2(1)	8(1)
O(1)	21(1)	19(1)	24(1)	1(1)	-1(1)	10(1)
O(2)	20(1)	21(1)	26(1)	-2(1)	2(1)	9(1)

O(3)	24(1)	19(1)	32(1)	1(1)	-5(1)	9(1)
O(4)	20(1)	21(1)	33(1)	2(1)	-2(1)	8(1)
O(5)	27(1)	25(1)	28(1)	5(1)	2(1)	12(1)
O(6)	21(1)	37(1)	52(1)	-7(1)	1(1)	9(1)
O(7)	41(1)	29(1)	27(1)	1(1)	3(1)	17(1)
O(8)	30(1)	46(1)	32(1)	-13(1)	2(1)	9(1)
N(1S)	38(1)	29(1)	23(1)	-3(1)	-3(1)	20(1)
O(1S)	92(2)	44(1)	52(1)	19(1)	40(1)	48(1)
O(2S)	45(1)	29(1)	40(1)	-2(1)	12(1)	17(1)
O(3S)	83(2)	31(1)	39(1)	-4(1)	7(1)	31(1)
N(2S)	35(1)	47(1)	35(1)	-1(1)	-1(1)	17(1)
O(4S)	55(2)	118(2)	69(2)	0(2)	4(1)	59(2)
O(5S)	33(1)	69(2)	51(1)	-28(1)	-6(1)	15(1)
O(6S)	43(1)	58(1)	29(1)	-11(1)	-6(1)	16(1)

Table D.11. Hydrogen coordinates (x 10^4) and isotropic displacement parameters ($Å^2$x 10^3) for dav4.

	x	y	z	U(eq)
H(1)	7040(20)	2740(20)	9422(10)	60(11)
H(2)	7375(18)	2114(18)	7316(10)	46(9)
H(3)	8765(19)	2960(20)	9310(20)	82(14)
H(4)	6361(19)	807(16)	9210(30)	96(16)
H(5A)	7140(20)	290(20)	10111(17)	75(13)
H(5B)	7280(20)	15(19)	9370(20)	84(14)
H(6A)	9390(20)	2020(30)	9130(30)	120(20)
H(6B)	9160(40)	1400(30)	9720(30)	160(30)
H(7A)	7471(16)	585(18)	8110(20)	82(14)
H(7B)	8209(16)	1376(15)	7930(15)	41(8)
H(8A)	8324(17)	2050(20)	10700(20)	81(14)
H(8B)	7550(40)	2020(50)	10410(50)	230(50)

Table D.12. Hydrogen bonds for dav4 [Å and °].

D-H...A	d(D-H)	d(H...A)	d(D...A)	<(DHA)
O(2)-H(2)...O(3S)	0.986(18)	1.784(19)	2.758(3)	169(3)
O(3)-H(3)...O(2S)#5	0.970(19)	1.86(2)	2.825(2)	175(4)
O(4)-H(4)...O(1S)#6	0.976(19)	1.81(2)	2.774(3)	167(5)
O(5)-H(5A)...O(5S)#7	0.949(19)	2.06(3)	2.921(3)	150(4)
O(5)-H(5A)...O(2S)#6	0.949(19)	2.30(4)	2.983(2)	128(3)
O(5)-H(5B)...O(6S)#8	0.949(19)	1.84(2)	2.778(3)	168(4)
O(6)-H(6A)...O(4S)#9	0.97(2)	2.12(3)	3.044(4)	157(5)
O(6)-H(6A)...O(5S)#9	0.97(2)	2.27(4)	3.085(3)	141(4)
O(7)-H(7A)...O(5S)#8	0.945(19)	1.86(2)	2.807(3)	175(4)
O(7)-H(7B)...O(1S)#7	0.940(18)	1.759(19)	2.683(3)	167(3)
O(8)-H(8A)...O(6S)#10	0.957(19)	1.78(2)	2.736(3)	175(4)

Symmetry transformations used to generate equivalent atoms:

#1 -x+4/3,-y+2/3,-z+5/3 #2 -y+1,x-y,z #3 -x+y+1,-x+1,z

#4 y+1/3,-x+y+2/3,-z+5/3 #5 x-y+1/3,x-1/3,-z+5/3

#6 -y+2/3,x-y-2/3,z+1/3 #7 -x+5/3,-y+1/3,-z+4/3

#8 x-y,x-1,-z+1 #9 -y+4/3,x-y-1/3,z+2/3 #10 x,y,z+1

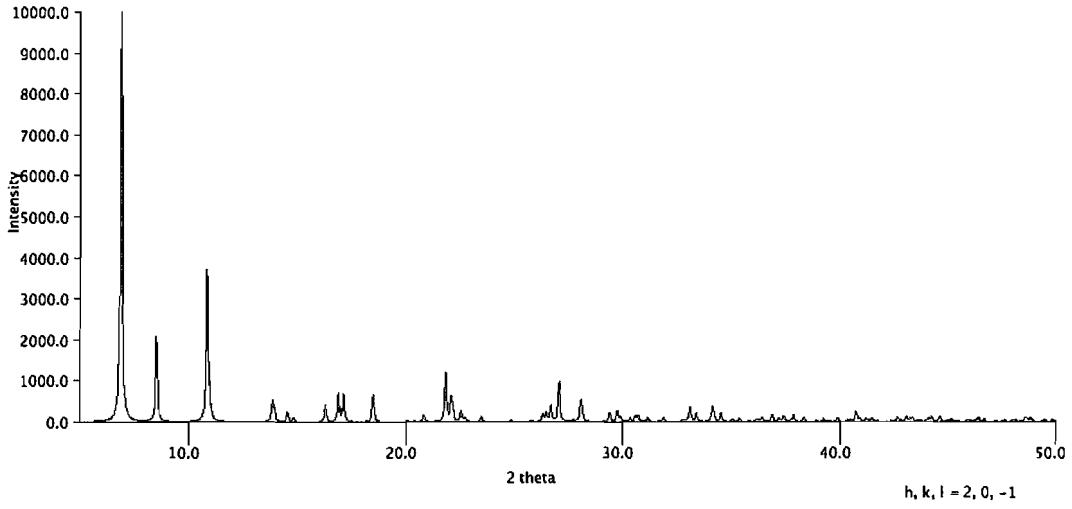

Figure D.03. Predicted powder spectra of Ga_7In_6.

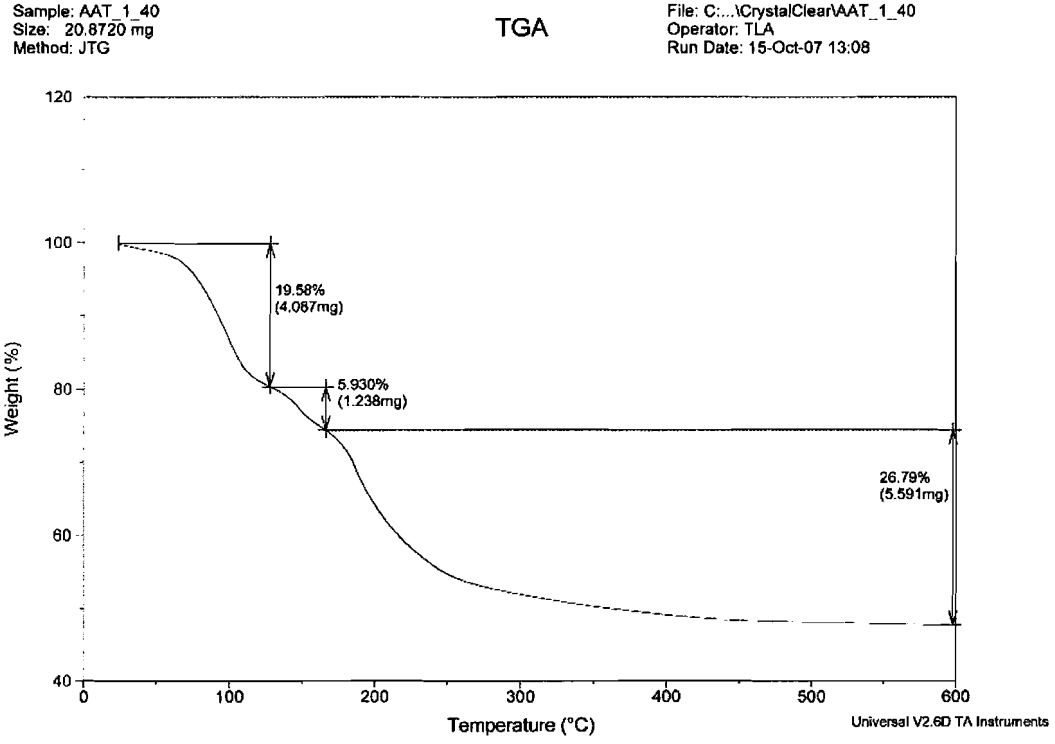

Figure D.04. TGA thermogram of Ga_7In_6.

APPENDIX E

SUPPLEMENTAL INFORMATION FOR ToF-SIMS ANALYSIS

Isotope distribution of Ga clusters.

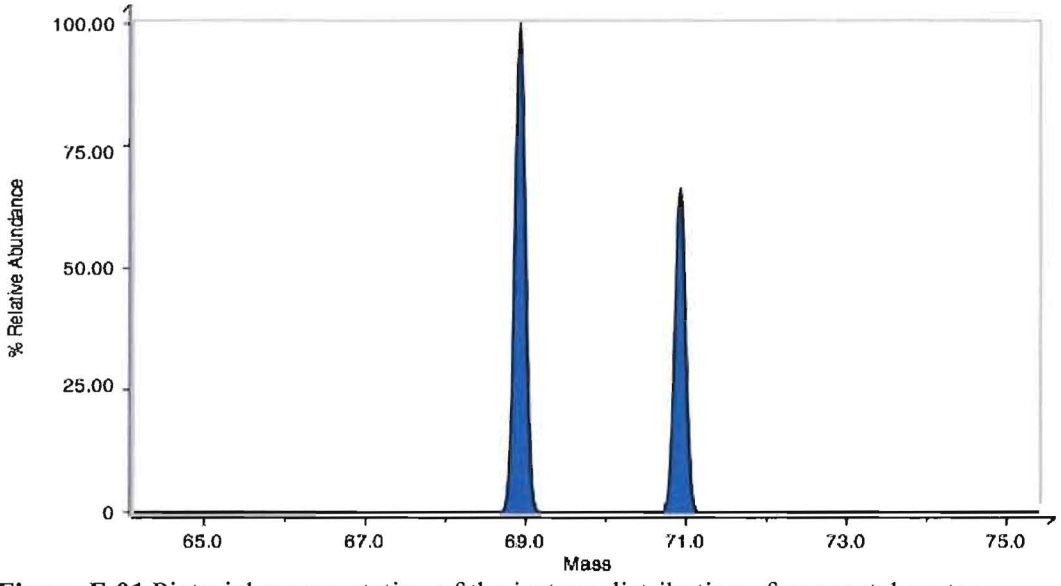

Figure E.01 Pictorial representation of the isotope distribution of one metal center.

Table E.01 Statistical distribution of one metal center.

# of Metals	1	
^{69}Ga	1	
^{71}Ga		1
ratio	1	1
% of each	60.108	39.892
mass	68.926	70.925

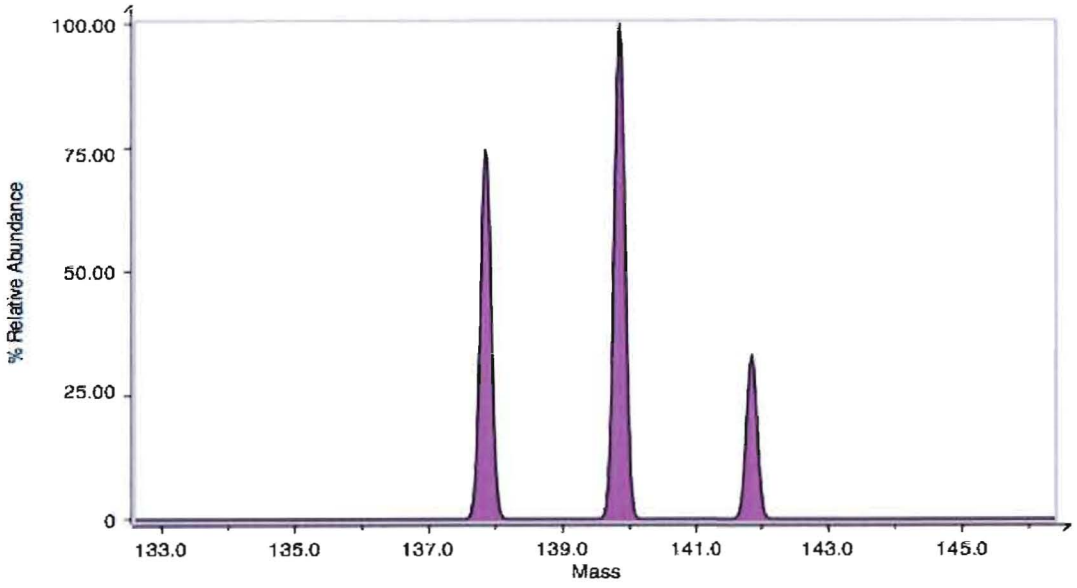

Figure E.02. Pictorial representation of the isotope distribution of two metal centers.

Table E.02. Statistical distribution of two metal centers.

# of Metals	2		
^{69}Ga	2	1	
^{71}Ga		1	2
ratio	1	2	1
% of each	36.130	47.957	15.914
mass	137.85	139.85	141.85

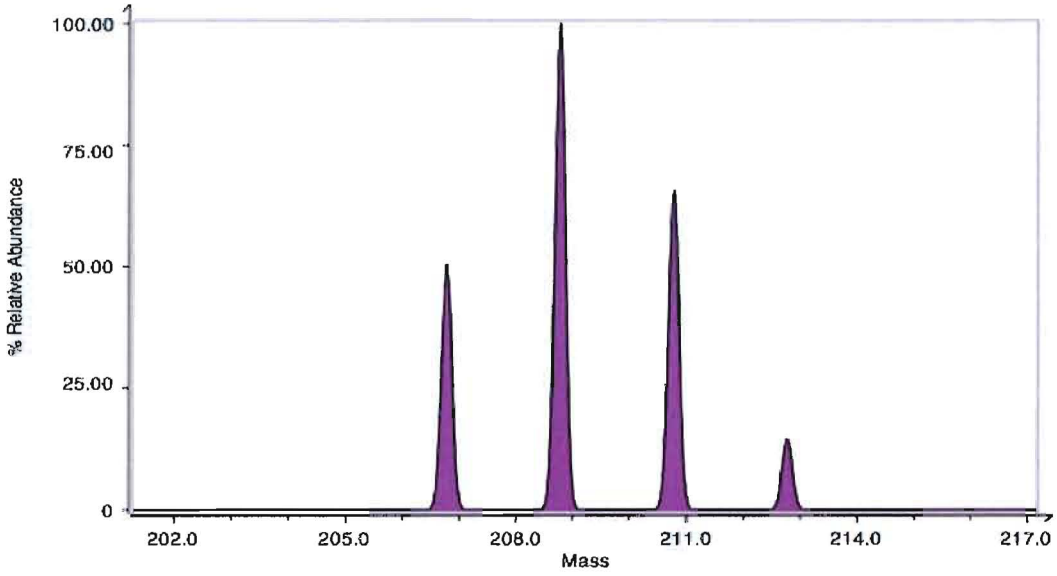

Figure E.03. Pictorial representation of the isotope distribution of three metal centers.

Table E.03. Statistical distribution of three metal centers.

# of Metals	3			
^{69}Ga	3	2	1	
^{71}Ga		1	2	3
ratio	1	3	3	1
% of each	21.717	43.239	28.696	6.348
mass	206.78	208.78	210.77	212.77

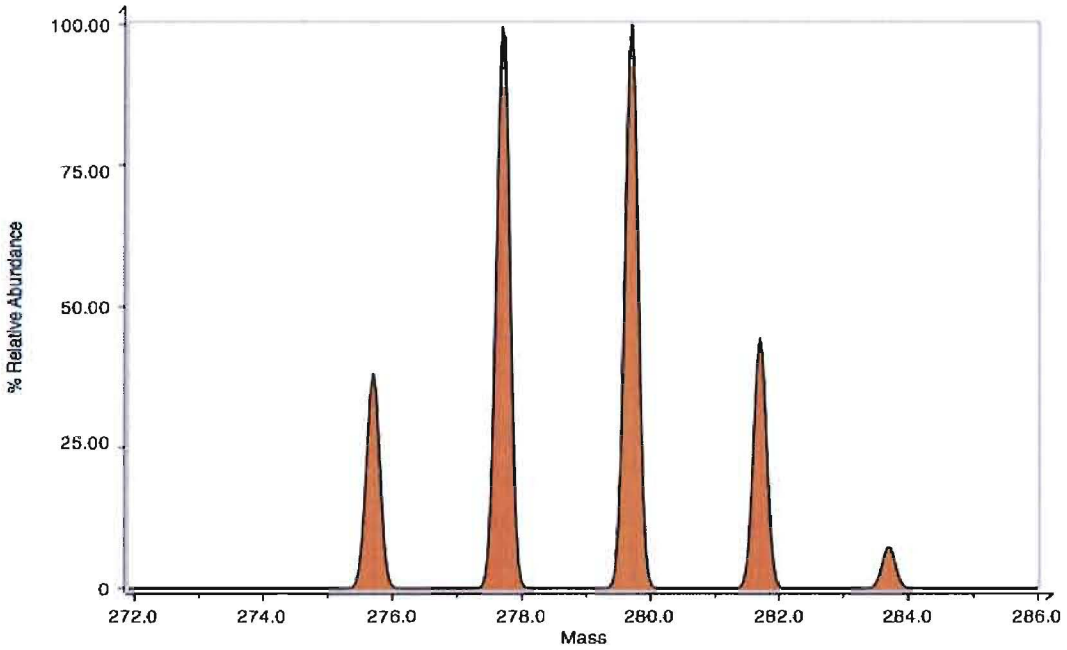

Figure E.04. Pictorial representation of the isotope distribution of four metal centers.

Table E.04 Statistical distribution of four metal centers.

# of Metals	4				
^{69}Ga	4	3	2	1	
^{71}Ga		1	2	3	4
ratio	1	4	6	4	1
% of each	13.054	34.653	34.497	15.263	2.532
mass	275.70	277.70	279.70	281.70	283.70

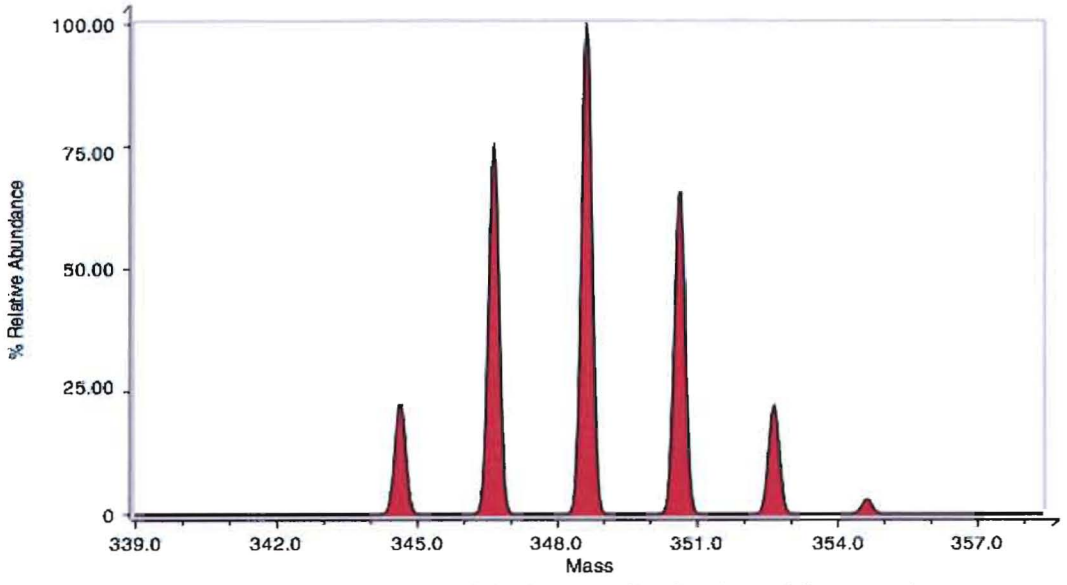

Figure E.05. Pictorial representation of the isotope distribution of five metal centers.

Table E.05. Statistical distribution of five metal centers.

# of Metals	5					
^{69}Ga	5	4	3	2	1	
^{71}Ga		1	2	3	4	5
ratio	1	5	10	10	5	1
% of each	7.846	26.037	34.560	22.936	7.611	1.010
mass	344.63	346.63	348.63	350.63	352.62	354.62

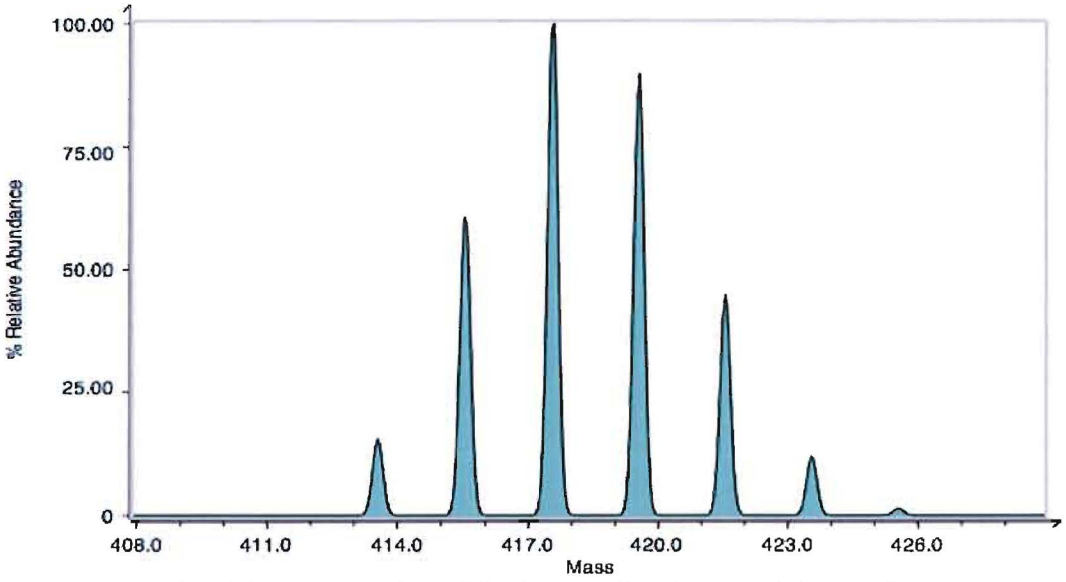

Figure E.06 Pictorial representation of the isotope distribution of six metal centers.

Table E.06 Statistical distribution of six metal centers.

# of Metals	6						
^{69}Ga	6	5	4	3	2	1	
^{71}Ga		1	2	3	4	5	6
ratio	1	6	15	20	15	6	1
% of each	4.7162	18.78	31.16	27.573	13.725	3.6434	0.403
mass	413.55	415.55	417.55	419.55	421.55	423.55	425.55

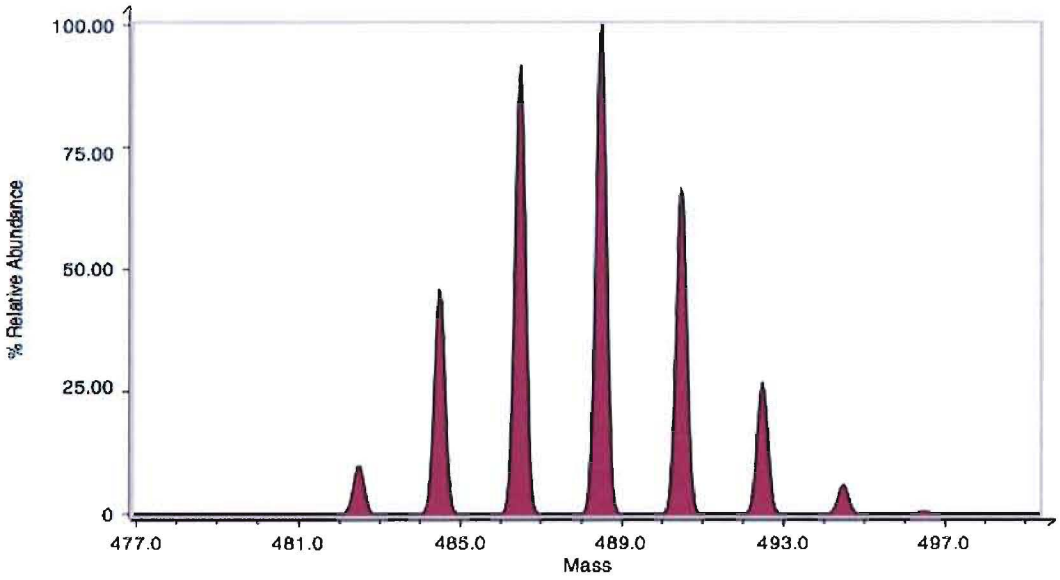

Figure E.07 Pictorial representation of the isotope distribution of seven metal centers.

Table E.07 Statistical distribution of seven metal centers.

# of Metals	7							
^{69}Ga	7	6	5	4	3	2	1	
^{71}Ga		1	2	3	4	5	6	7
ratio	1	7	21	35	35	21	7	1
% of each	2.8348	13.17	26.221	29.004	19.249	7.665	1.6957	0.1608
mass	482.48	484.48	486.48	488.48	490.48	492.47	494.47	496.47

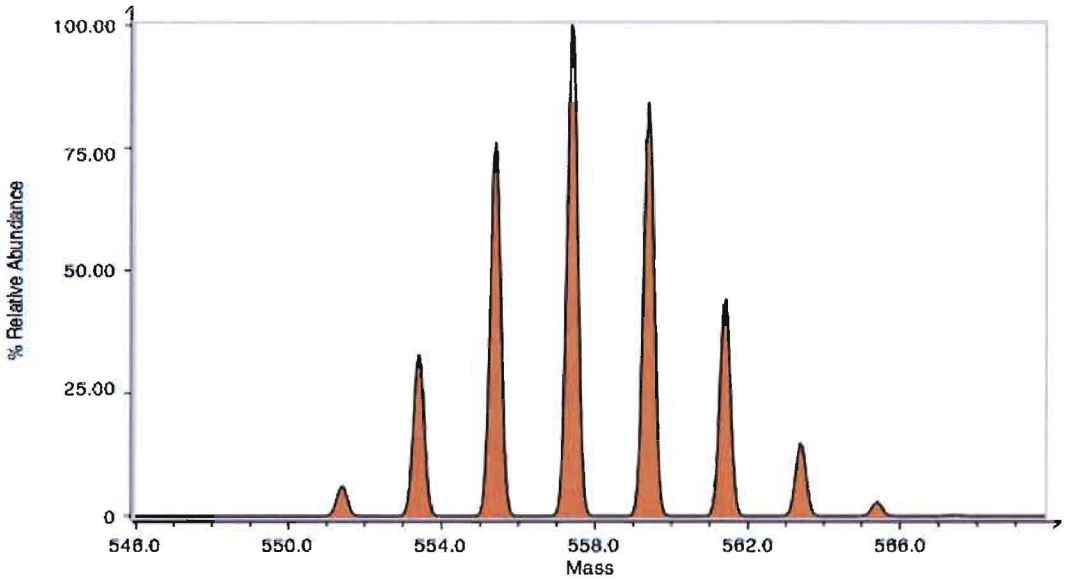

Figure E.08. Pictorial representation of the isotope distribution of eight metal centers.

Table E.08. Statistical distribution of eight metal centers.

# of Metals	8								
^{69}Ga	8	7	6	5	4	3	2	1	
^{71}Ga		1	2	3	4	5	6	7	8
ratio	1	8	28	56	70	56	28	8	1
% of each	1.704	9.0469	21.015	27.894	23.14	12.286	4.077	0.7731	0.0641
mass	551.4	553.4	555.4	557.4	559.4	561.4	563.4	565.4	567.4

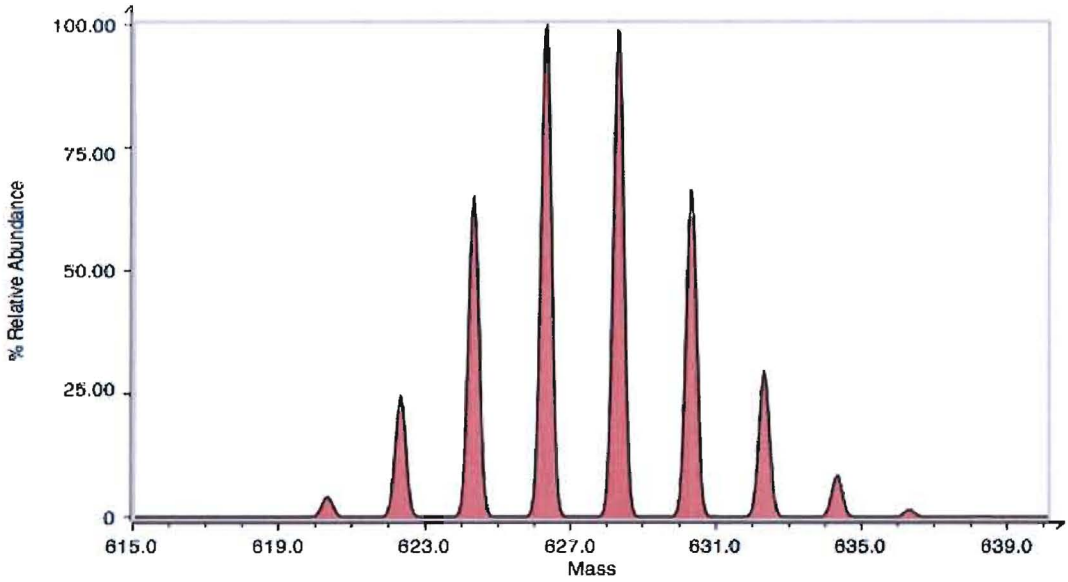

Figure E.09 Pictorial representation of the isotope distribution of nine metal centers.

Table E.09. Statistical distribution of nine metal centers.

# of Metals	9									
^{69}Ga	9	8	7	6	5	4	3	2	1	
^{71}Ga		1	2	3	4	5	6	7	8	9
ratio	1	9	36	84	126	126	84	36	9	1
% of each	1.0242	6.1177	16.241	25.15	25.037	16.616	7.3518	2.0911	0.3469	0.0256
mass	620.33	622.33	624.33	626.33	628.33	630.33	632.32	634.32	636.32	638.32

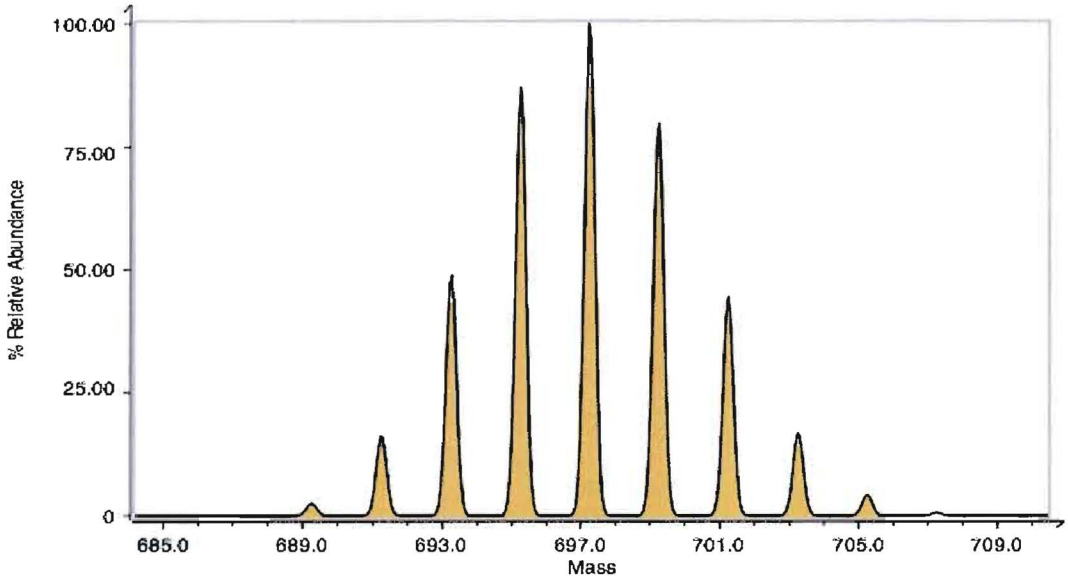

Figure E.10 Pictorial representation of the isotope distribution of ten metal centers.

Table E.10. Statistical distribution of ten metal centers.

# of Metals	10										
^{69}Ga	10	9	8	7	6	5	4	3	2	1	
^{71}Ga		1	2	3	4	5	6	7	8	9	10
ratio	1	10	45	120	210	252	210	120	45	10	1
% of each	0.6156	4.0858	12.202	21.596	25.082	19.975	11.047	4.1897	1.0427	0.1538	0.0102
mass	689.26	691.25	693.25	695.25	697.25	699.25	701.25	703.25	705.25	707.25	709.25

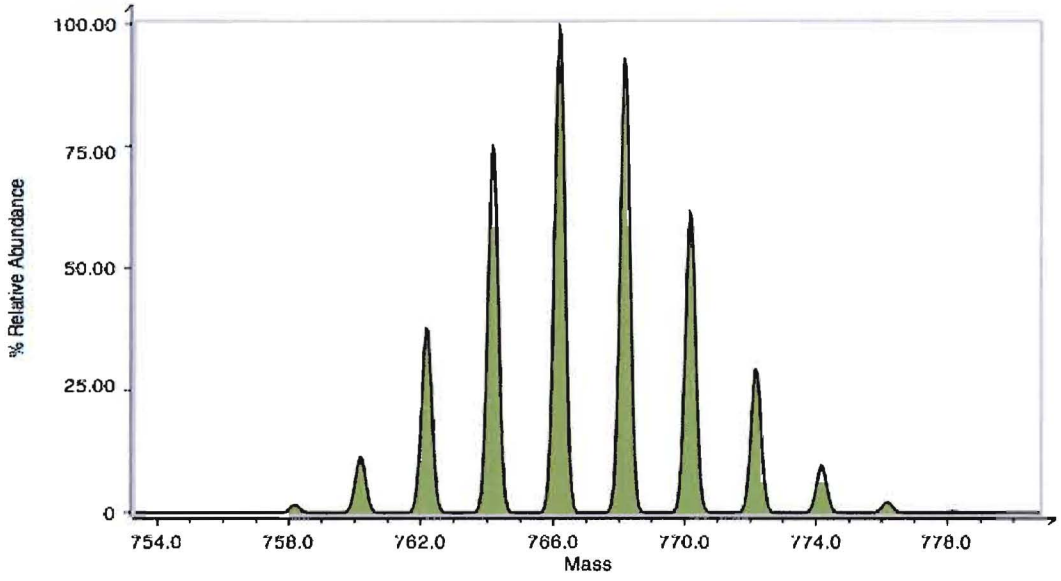

Figure E.11 Pictorial representation of the isotope distribution of eleven metal centers.

Table E.11. Statistical distribution of eleven metal centers.

# of Metals	11											
^{69}Ga	11	10	9	8	7	6	5	4	3	2	1	
^{71}Ga		1	2	3	4	5	6	7	8	9	10	11
ratio	1	11	55	165	330	462	462	330	165	55	11	1
% of each	0.37	2.7015	8.9645	17.848	23.691	22.012	14.609	6.9254	2.2981	0.5084	0.0675	0.0041
mass	758.18	760.18	762.18	764.18	766.18	768.18	770.18	772.18	774.17	776.17	778.17	780.17

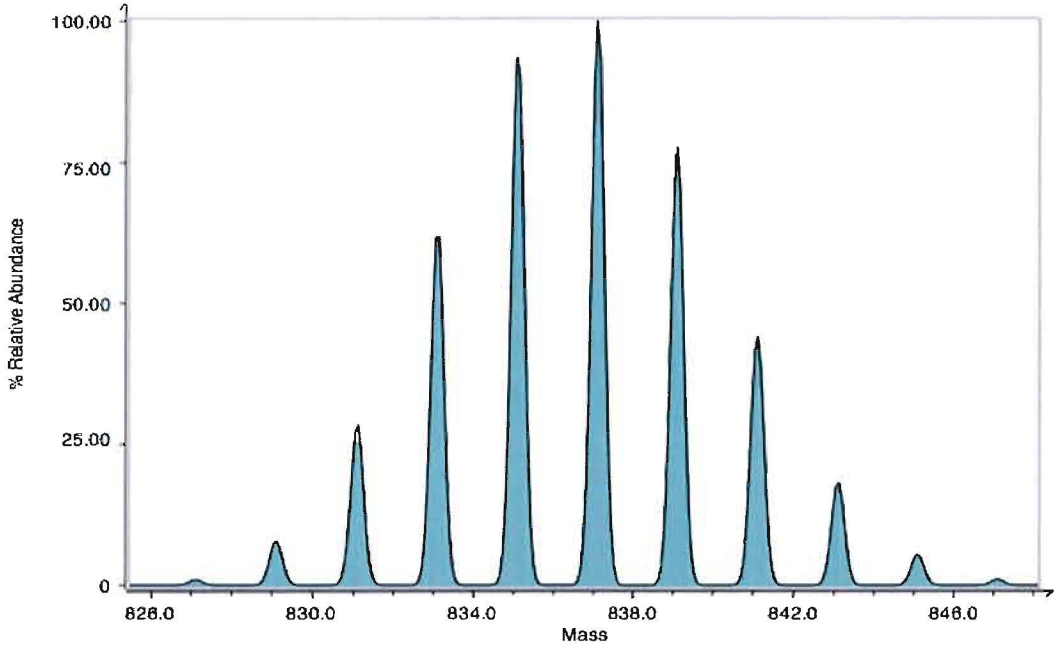

Figure E.12. Pictorial representation of the isotope distribution of twelve metal centers.

Table E.12. Statistical distribution of twelve metal centers.

# of Metals	12												
^{69}Ga	12	11	10	9	8	7	6	5	4	3	2	1	
^{71}Ga		1	2	3	4	5	6	7	8	9	10	11	12
ratio	1	12	66	220	495	792	924	792	495	220	66	12	1
% of each	0.2224	1.7714	6.466	14.304	21.36	22.682	17.562	9.9905	4.144	1.2223	0.2434	0.0294	0.0016
mass	827.11	829.11	831.11	833.1	835.1	837.1	839.1	841.1	843.1	845.1	847.1	849.1	851.1

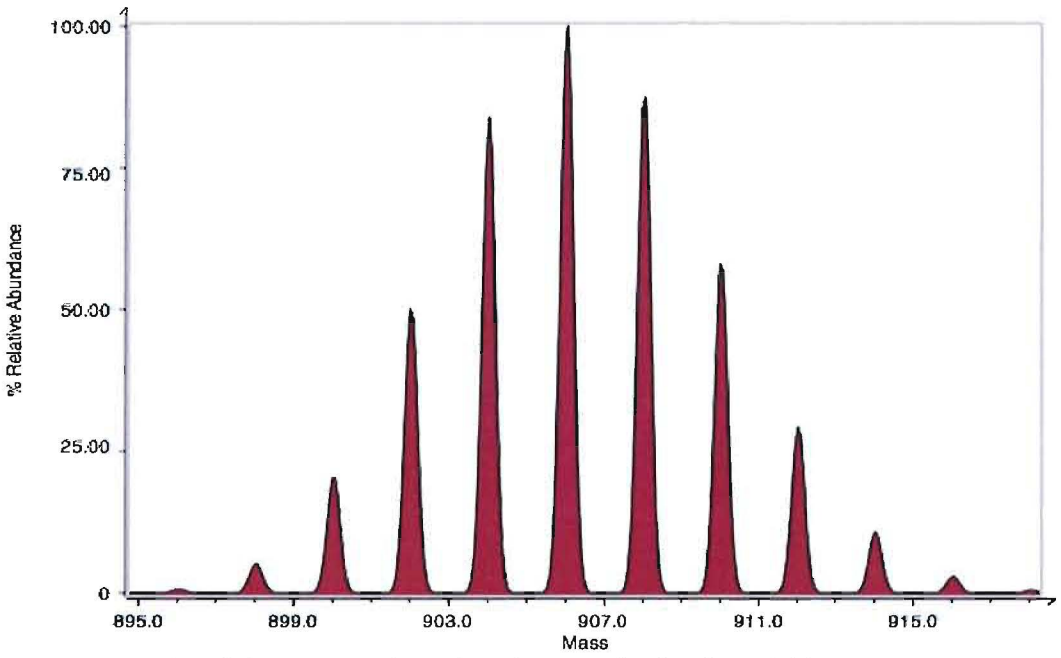

Figure E.13 Pictorial representation of the isotope distribution of thirteen metal centers.

Table E.13. Statistical distribution of thirteen metal centers.

# of Metals	13													
^{69}Ga	13	12	11	10	9	8	7	6	5	4	3	2	1	
^{71}Ga		1	2	3	4	5	6	7	8	9	10	11	12	13
ratio	1	13	78	286	715	1287	1716	1716	1287	715	286	78	13	1
% of each	0.1337	1.1535	4.5933	11.178	18.546	22.155	19.605	13.011	6.4763	2.3879	0.6339	0.1147	0.0127	0.0006
mass	896.03	898.03	900.03	902.03	904.03	906.03	908.03	910.03	912.03	914.02	916.02	918.02	920.02	922.02

APPENDIX F

SUPPORTING INFORMATION FOR ORGANIC NANOCAGE SUMMARY

NMR of compound:

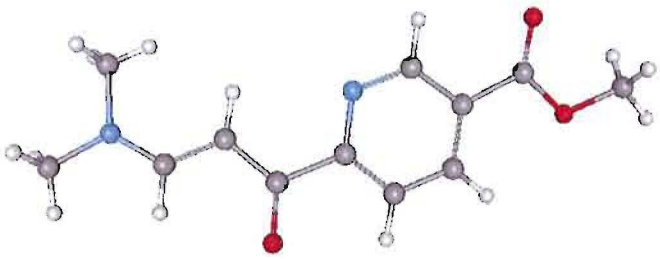

Figure F.1. Crystal of Ligand **15g** post deprotection

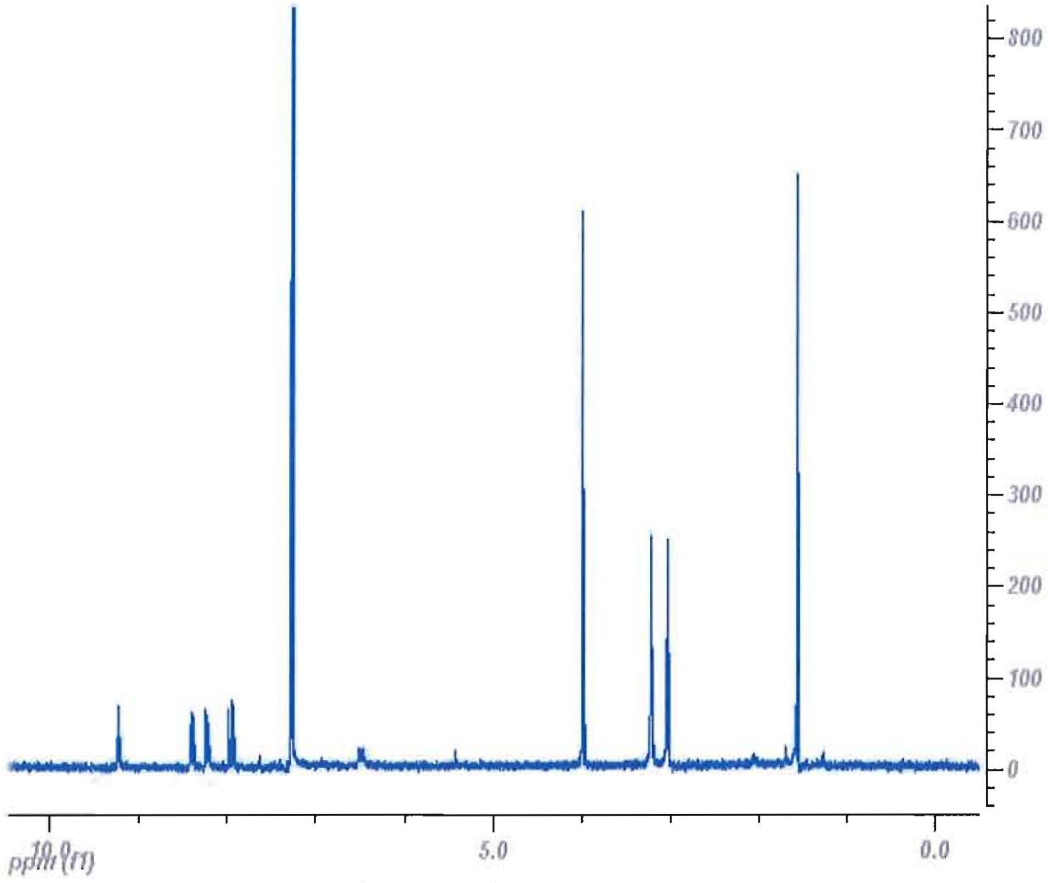

Figure F.2. Proton Spectrum of compound **15g**

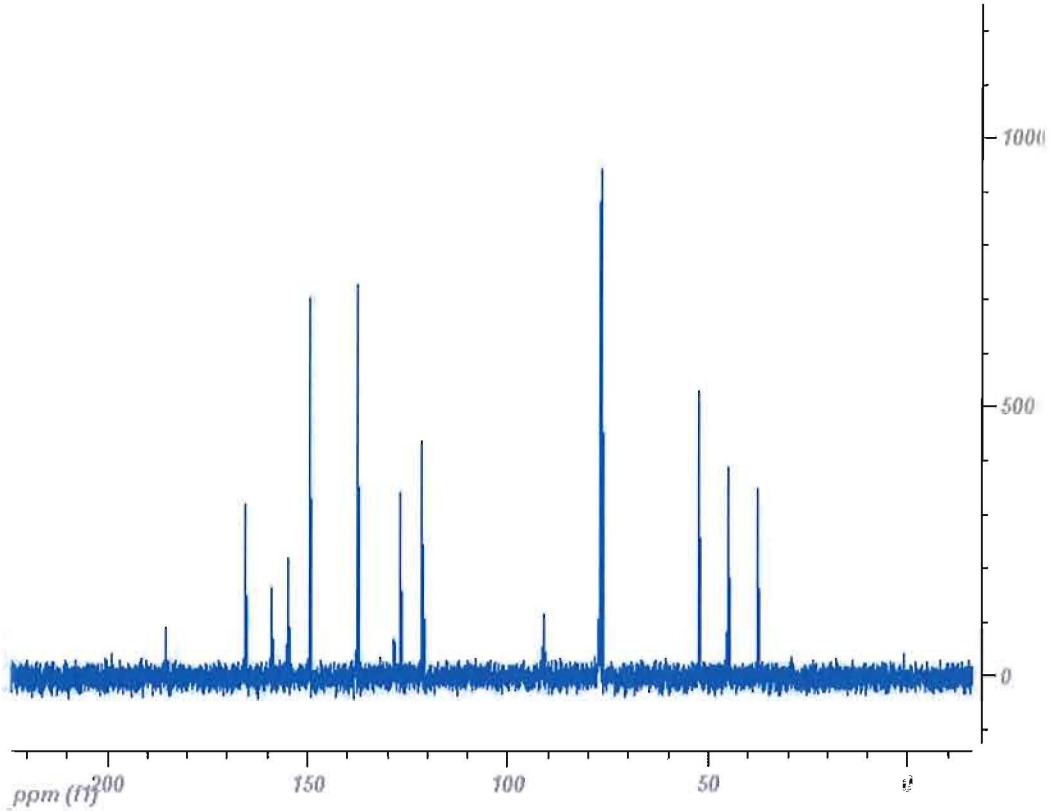

Figure F.3. Carbon Spectrum of compound **15g**

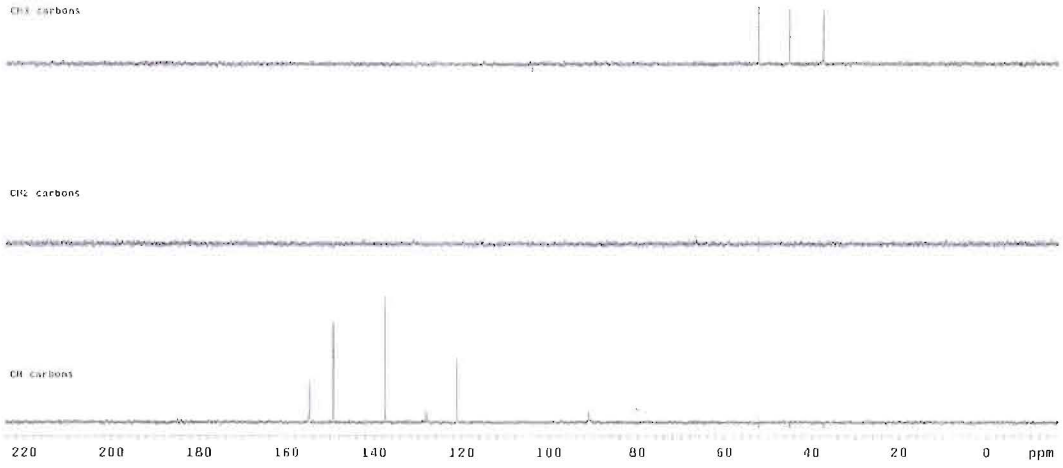

Figure F.4. DEPT Spectrum of ligand **15g**

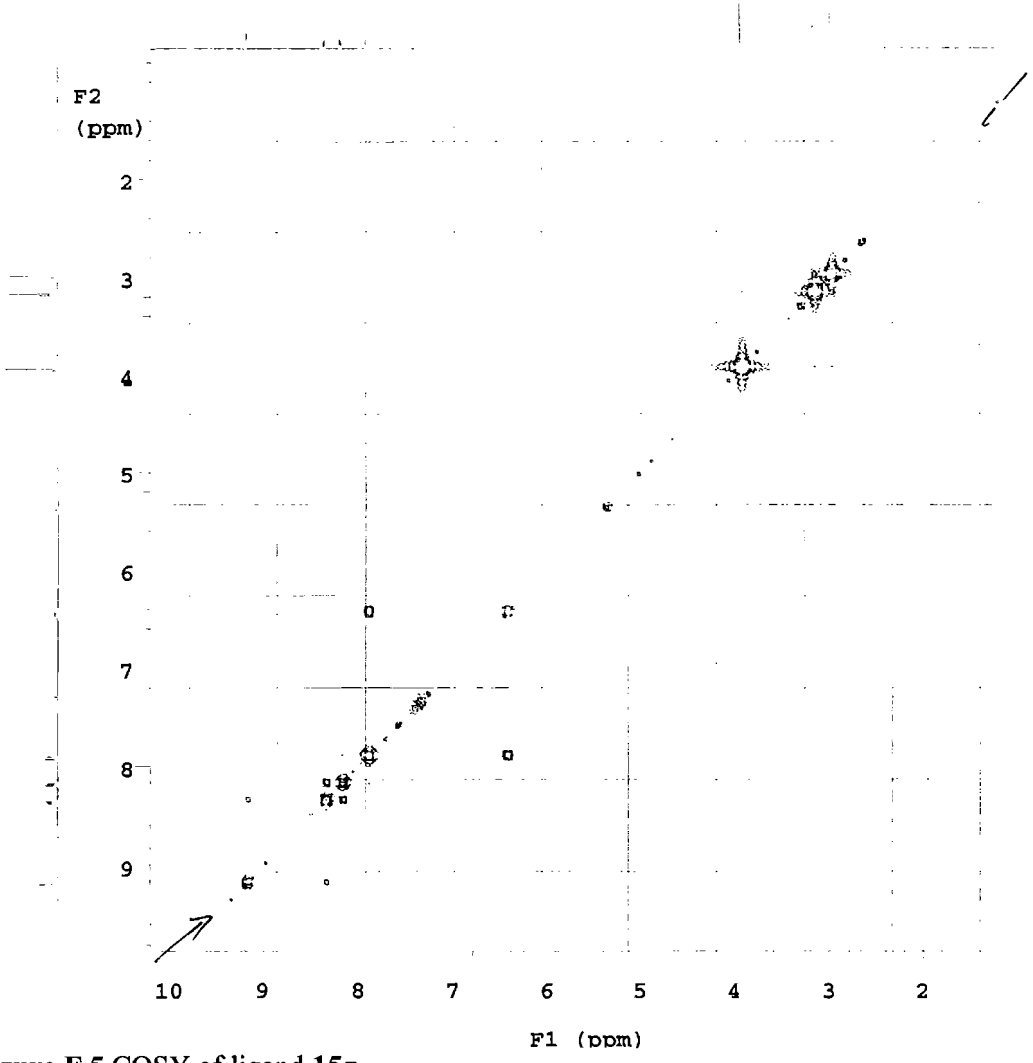

Figure F.5 COSY of ligand **15g**

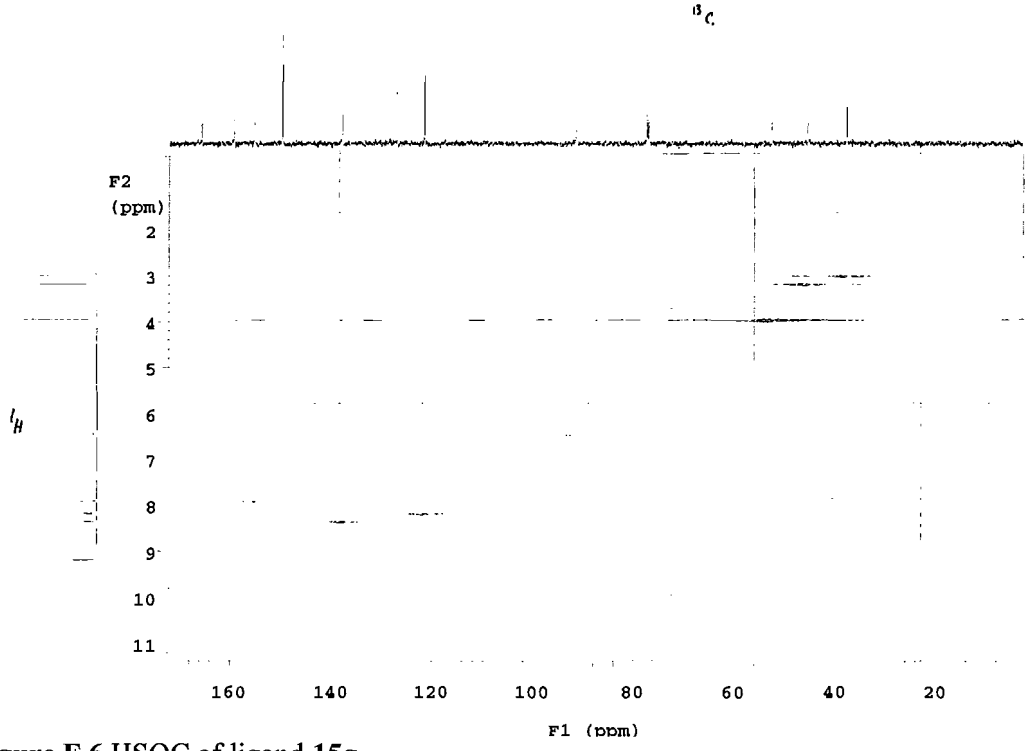

Figure F.6 HSQC of ligand **15g**

Cyrstal Structure of Ethyl projected ligand

APPENDIX G

TEMPLATED ORGANIC NANOCAGES

Abstract

Synthetic schemes and characterization of new bis-bidentate Schiff base ligands for making of three dimensional nanoscale organic cages. The organic nanocages will be achieved by a templated approach to the formation of covalently capped M_4L_6 tetrahedron. These tetrahedron are beginning characterization and will later be internally and/or externally functionalized for application.

Introduction

Supramolecular chemistry governs many process vital to life from DNA replication to inter cellular communication.[1,2] It is not surprising that nature used the principles of supramolecular chemistry in forming the blueprint of life itself - DNA. A double stranded DNA helix is held together by hydrogen bonding between the strands allowing it to be unwound and copied during replication without breakage. A single strand of DNA is a template for its complementary strand resulting in spontaneous self-assembly.[2,3]

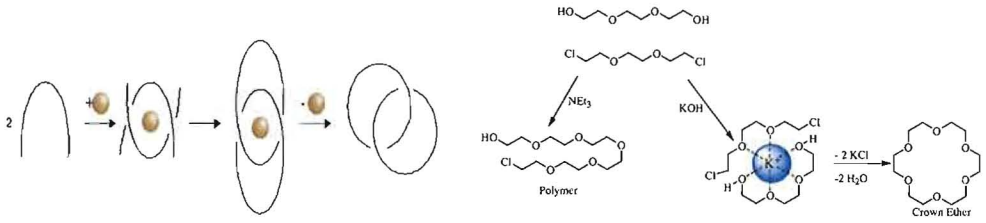

Figure G.1 DNA, Crown ether, general cartoon figures on the reaction of a template. [1,4]

Single metal ions can be used as a template for the synthesis of corands, cryptands or catenanes. [1] Single metals can also be used as templates, similar to DNA, in which they act as a guide to bring two different compounds together, allowing the organic pieces to react to form cryptands or catenanes.[5-7]

Another useful strategy in organic synthesis is the use of multiple metal centers as template to form large macrocyclces. In this case, the metal ions exist in a plane[8-12] however a variety of supramolecular compounds (e.g. tetrahedron or octahedron) possess multiple metal ions lying in three dimensions in order to enclose a volume.[13-15] These metal centers are not part of a template scheme; they represent core components of the supramolecular assembly. Without the metals these complexes would simply fall apart. It is surprising then that no one has tried to use multiple metals (in three dimensions) as a template, trapping the complex and removing the metal to provide a classical organic cage compound.[16,17]

The proposed research will utilize metal centers as templates for the supramolecular self-assembly of nanoscale organic cages. Multiple metals can obviously be used to make larger or more complex structures than a single metal template would provide.[18] The key difference in the strategy outlined below versus previous strategies is

that four metals centers are in a non-planar arrangement. This will lead to a three dimensional complex, with additional functionality to allow for covalent capture. Careful ligand design coupled with selection of appropriate metals will force the ligand to bridge multiple metals forming the three dimensional complexes to be used as templates (**Schemes G.1** and **G.2**).[5,19-25]

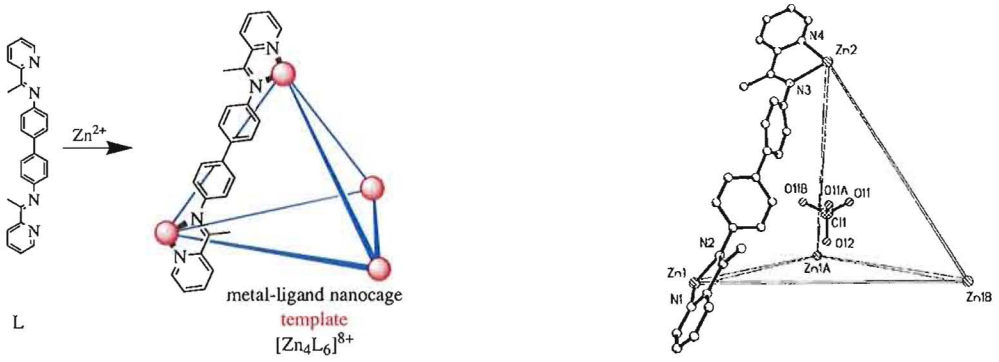

Scheme G.1. Yan's self-assembled tetrahedron with perchlorate counter ion with Zn^{2+} vertices[19]. Literature precedent with crystals structure of metal-ligand nanocage synthesis & Crystal structure of Yan's tetrahedron with an encapsulated perchlorate anion.

Our preliminary work is based on a related tetrahedron synthesized by Yan and co-workers.[19] The Yan complex is not templated, they have no way of removing the metal without destroying the complex, but it does self-assemble. The fundamental change from the Yan group to this project is to add functionality to the distal ends of the ligand, allowing for the covalent capping to occur (**Scheme G.2**).

The general M_4L_6 tetrahedron template strategy is depicted below (**Scheme G.2**). Six equivalents of an appropriately designed ligand (blue lines) are combined with four equivalents of metal (red spheres) to self-assemble a M_4L_6 tetrahedron (*metal-ligand*

nanocage template) related to the $Zn_4L_6^{8+}$ from **Scheme G.1**. The next step is covalent capture by a cap (green) that binds all six ligands together to yield the M_4L' complex. The final step of demetallation yields the *organic nanocage*, L'. This complex has a volume that is defined by its covalently linked shell, which we hope to exploit for guest-host and metal binding studies.

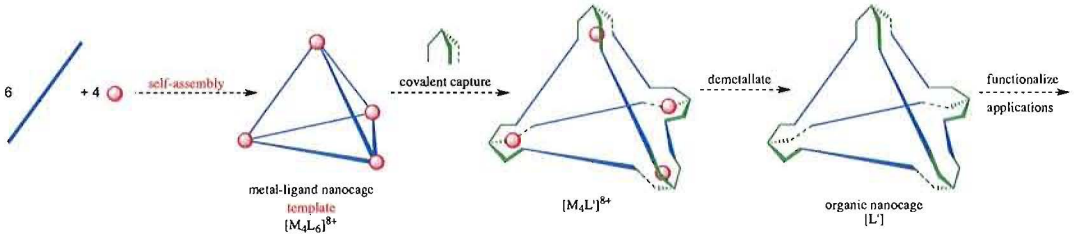

Scheme G.2. The general scheme to use an M_4L_6 capsule as a template to form an organic nanocage, L'

There are numerous possibilities for the uses of the organic nanocages once they are made. Once the organic nanocage is created, it is pre-organized to be a specific chelator for metals. This is both its strength and weakness. This attribute will make it difficult to remove the template metal from the cage, because as the organic nanocage is a wrap-around-ligand, it will have stronger binding.[1,26-29] The cages can be modified on the interior or the exterior for a variety of applications after demetallation, such as sensing, extracting or catalysis.[30]

Results

The proposed synthetic route of **5d** (**Scheme G.3**) is a modification with increased yields.[31] The products are then coordinated with Zn^{2+} followed by capping and

demetallation to yield the desired L' organic nanocage is shown below (**Scheme G.4**). Functionalization at the five position on the pyridine ring, from the Yan tetrahedron will allow for a capping amide reaction to covalently bind adjacent ligands together. After the covalent capture of the template the nanocage can be demetallated.

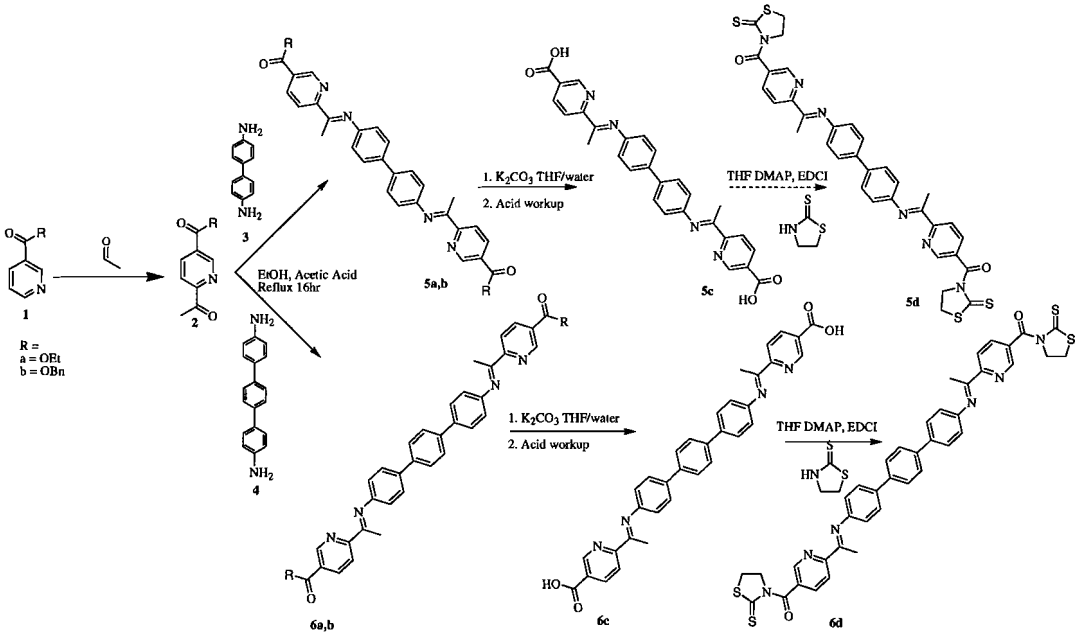

Scheme G.3. Synthetic scheme to make the L' nanocages. [19,31]

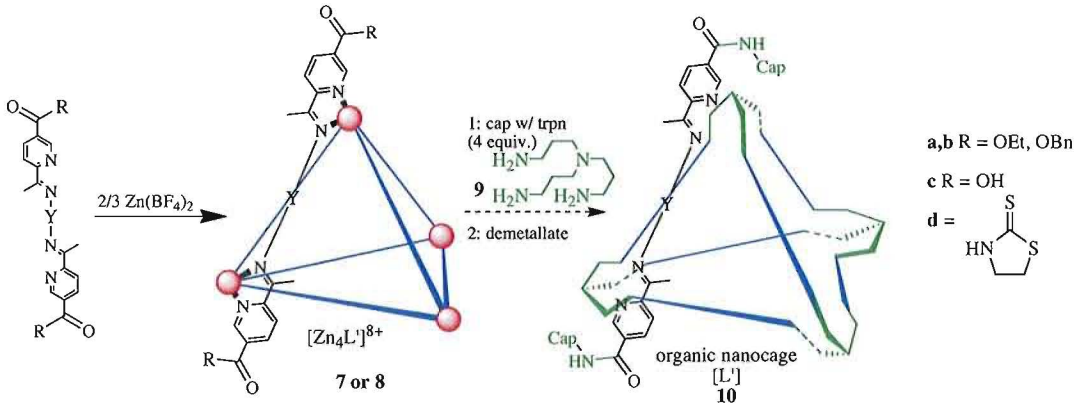

Scheme G.4. Self-assembly of ligands **5** or **6** to form the template organic nanocage **7** and **8**.

The starting pyridine ring for this synthesis can be substituted with either a carboxylic acid or an ester (ethyl or benzyl) in the 3 position. These different groups affect the yields of the first step. The rigid diamine spacer has also been varied, using benzidine, **3** (4-4'-diaminobiphenyl) and **4** (4-4"-diaminoterphenyl) modification of the ligand at the distal end and the 3 position of the pyridine ring (**Scheme G.3**). **Figure G.2** shows the models of complexes that we wish to make as the carboxylic acid, the capped ester and the dovetailed organic nanocage. Computer modeling shows that the ester is far enough away from the Schiff base binding motif not to interfere in the complexation with the metal (**Figure G.2A**).[32] **Figure G.2B** addresses the sterics of the cap and **Figure G.2C** is the goal of phase one: the demetallated organic nanocage.

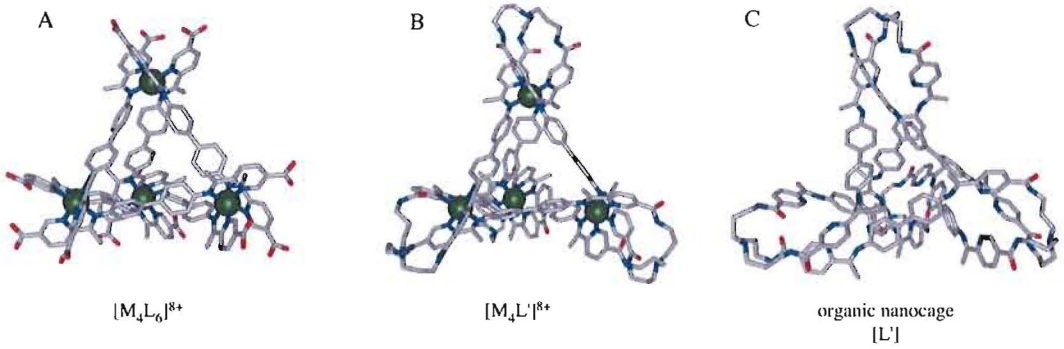

Figure G.2. Computer model with MM3 of target M_4L_6 tetrahedron, capped M_4L' and then de-metallated L' complexes.[32]

Ligand Synthesis

The target ligands of **5d** and **6d**, substituted with activated ester groups, pose a better likelihood of yielding the tetrahedron template. This would avoid having to remove all 12 ester groups on complex **7a,b** and **8a,b** simultaneously and provides tetrahedron complex **7d** ready to be capped with the amine without changing a functional group.

The first target ligand, **5a,** has an ethyl protected carboxylic acid at its distal ends. The first step of the synthesis (**Scheme G.3**) proceeds with an acceptable yield of 11 to 23% .[31] The acylation reaction works on a variety of ester R groups (R= OH, OEt or OBn). The different R groups affect the yield and solubility of the ligands after the condensation reaction to yield ligands **5a, 5b, 6a** and **6b**. Although TLC of the acylation reaction shows that only one species is isolated from column chromatography, NMR reveals 6:1 ratio of compounds **2a** and **11,** respectively is obtained (**Figure G.3A**). Overall crude yields can be increased by shortening the reaction time to limit the

formation of side product **11**. Repeated attempts to separate the desired product from the side product gave the same result so the mixture was carried onto the following step, condensation with **3**.

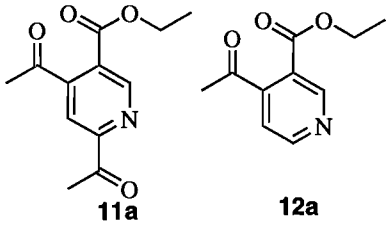

Figure G.3. Acylation side products **11a** & **12a** from the formation of ketone **2a**.

The condensation reaction of **2a** with **3** (**Scheme G.5**) is done in absolute ethanol by adding two equivalents of ketone, **2a**, to one equivalent of benzidine, **3**, at reflux with catalytic acetic acid for four hours to provide **5a** in 86% yield. Ligand **5a** precipitates out of the reaction mixture, helping with yield and purification. Washing with cold methanol removes unreacted starting materials. Analytically pure ketone, **2a**, is not needed for the condensation reaction because the disubsituted ketone (**11a**) can easily be removed after the condensation reaction to yield pure **5a** (**Figure G.3A** and **C**) by precipitation.

Many different reaction conditions have been tried to optimize the yield of **4a** (see experimental).[33,34] Increasing the ratio of ketone to benzidine to five to one should drive the reaction to completion in benzidine and thus make the column chromatographic separation easier (**3** and **5a** have very similar R_f values). Unreacted **2a** can then be recovered and reused. Current yields in absolute ethanol with the acetic acid catalyst are

in excess of 85% analytically pure ligand **5a**. Single crystal x-ray structure confirms the structure of **5a** as the free base ligand (**Figure G.4**).

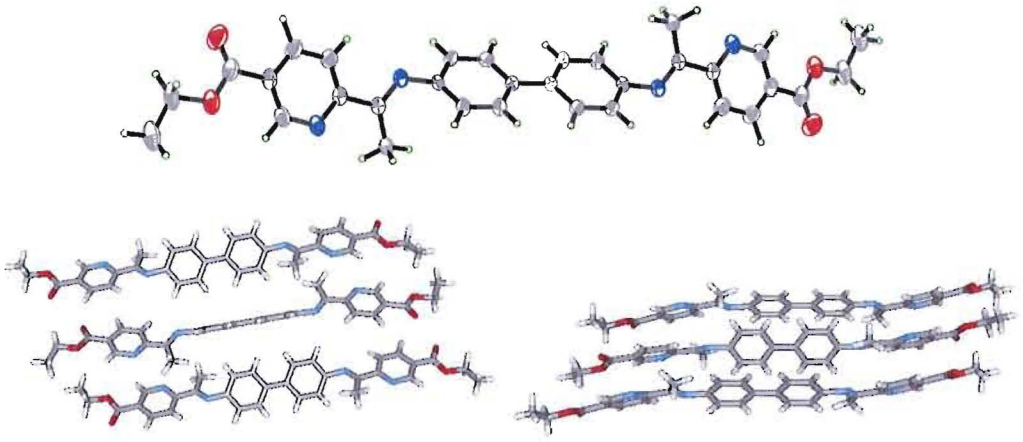

Figure G.4. Ortep of **5a** single crystal structure, and packing pictures.

Benzidine, **3**, and 4-4"-terphenyldiamine, **4**, both crystallize with the rings completely planar; this is not the lowest energy confirmation that we would expect, but it does allow for greater edge to face interaction between adjacent molecules in the cell. The angle of the plane of one biphenyl to the adjacent is about 70°. [35] The biphenyl portion of **5a** crystallizes in a planar fashion as well, but it places the adjacent ligands in a complete 90° edge to face arrangement. This increases the strength of the edge to face interactions and it stacks the pyridine rings face to face with an offset angle. This packing in the solid state may help to explain the unusual behavior of **5a** in DMSO solution. (**Figure G.5**)

Ligand **5a** has an expected spectrum in $CDCl_3$, but when dissolved in DMSO it behaves quite differently (**Figure G.5**), suggesting it forms a not-well-understood,

concentration-dependent oligomer in DMSO. This issue is not only concentration dependent, but also solvent dependent.

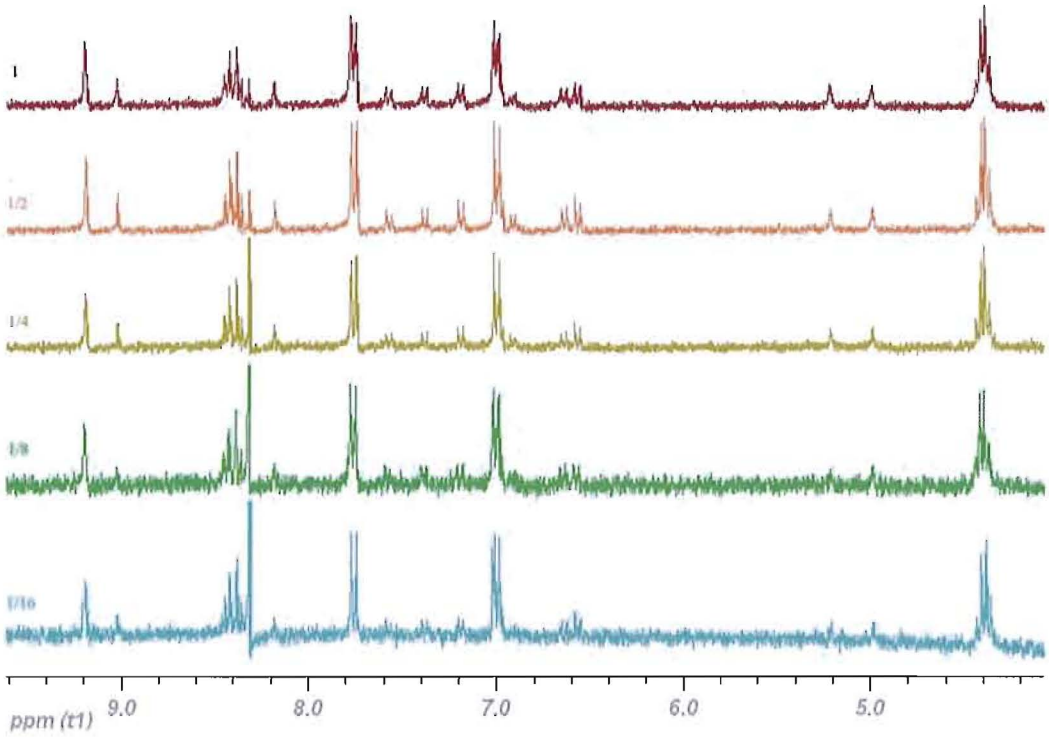

Figure G.5. ^{1}H NMR spectra of ligand **5a** in DMSO at various concentrations, showing the concentration dependent behavior. At 1/16 concentration mostly monomer appears to be present.

The same batch of pure ligand is sequentially dissolved in one solvent, analyzed, dried down and resuspended in a different NMR solvent. The ligand, in going from chloroform to DMSO, shows first the simple then the complex spectra, then back to a clean spectrum, again in chloroform (**Figure G.6**).

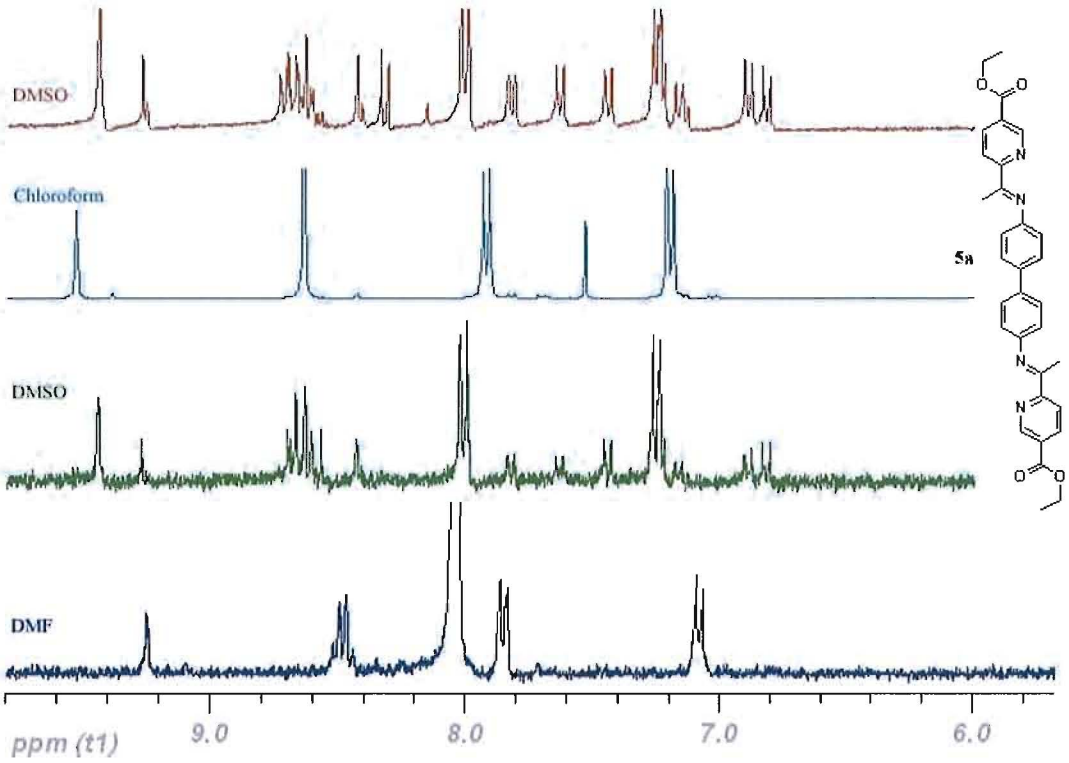

Figure G.6 ^{1}H NMR of ligand **5a** showing the solvent and concentration effects are reversible.

Concurrently ligand **6b** was synthesized by the same procedure.[36] Ligand **6b** has very poor solubility in all solvents. The same route from intermediate ketones **2a** and **2b** also synthesized the two crossover ligands **5b** and **6a**. All four ligands are concurrently being carried on for self-assembly and de-protection reactions.

Deprotection

Two different routes for deprotection have been explored. The first route was to deprotect ketone **2b** with potassium carbonate into the carboxylic acid **2c** then activate with 2-mercaptothiazoline to yield the activate ester **2d** for capping and condensation

reactions.[37] This same route is being explored to convert ligands **5d** and **6a** into **5d** and **6d**. The second route under investigation involves heating of **5a** in DMSO/water solution at 95°C with potassium hydroxide. By NMR spectroscopy both reactions appear to have removed the ethyl groups, although the ligand has not yet been purified.

Self-assembly of Ligands

Because of the unusual behavior of **5a** in DMSO, metallation and further studies will be attempted in DMF. Ligand **5a** has been heated with two-thirds equivalents of $Zn(BF_4)_2$ or $Zn(OTf)_2$ to yield a new compound that is currently being characterized in d7-DMF. By ^1H NMR spectroscopy there are new peaks that do not correspond to any of the starting materials. It seems that both the tetrafluoroborate and the triflate counter ions yield similar results, although it appears to take longer for the reaction to occur with the triflate salt.[38,39]

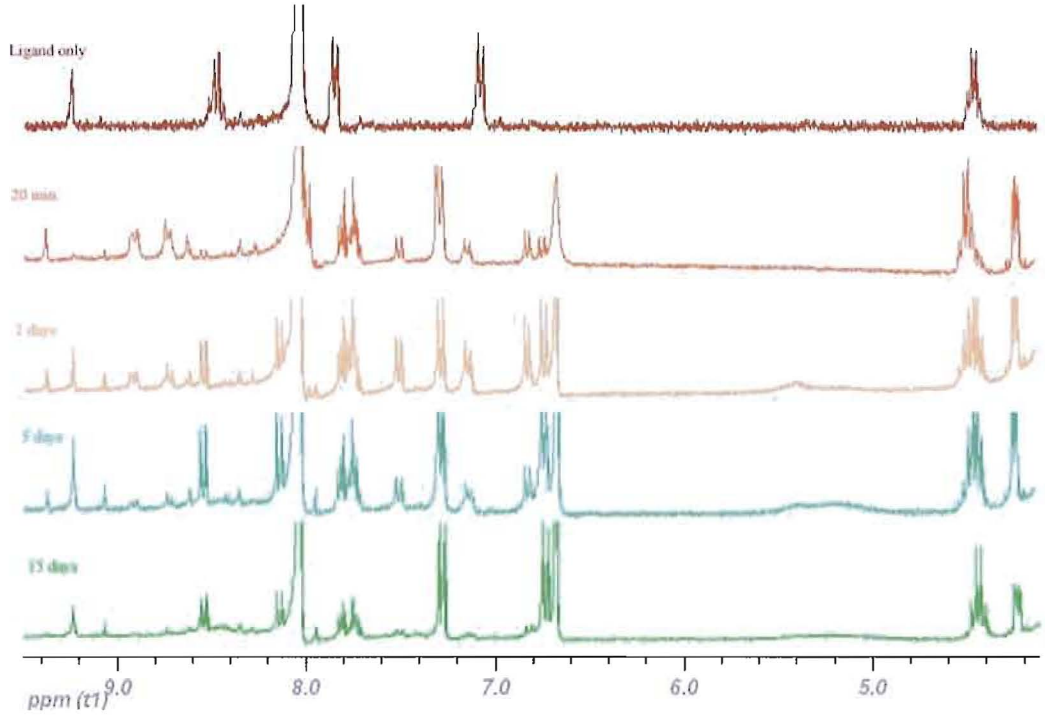

Figure G.7. Time points of **5a** in DMF with 2/3rds equivalents of $Zn(BF_4)_2$.

A different ^1H NMR spectrum can be obtained on multi milligram scale by running the reaction in a Schlenk tube. A pasty solid is obtained by heating 2 equivalents of ligand **5a** with 1 equivalent of $Zn(BF_4)_2$ in DMF at 60°C for 16 hours, reducing the volume, and precipitating with ethyl acetate. Unreacted ligand was extracted by washing with ethyl acetate. The paste was dried in vacuo. Other metallation reactions with ligand **5a** and other metals are currently being tried.

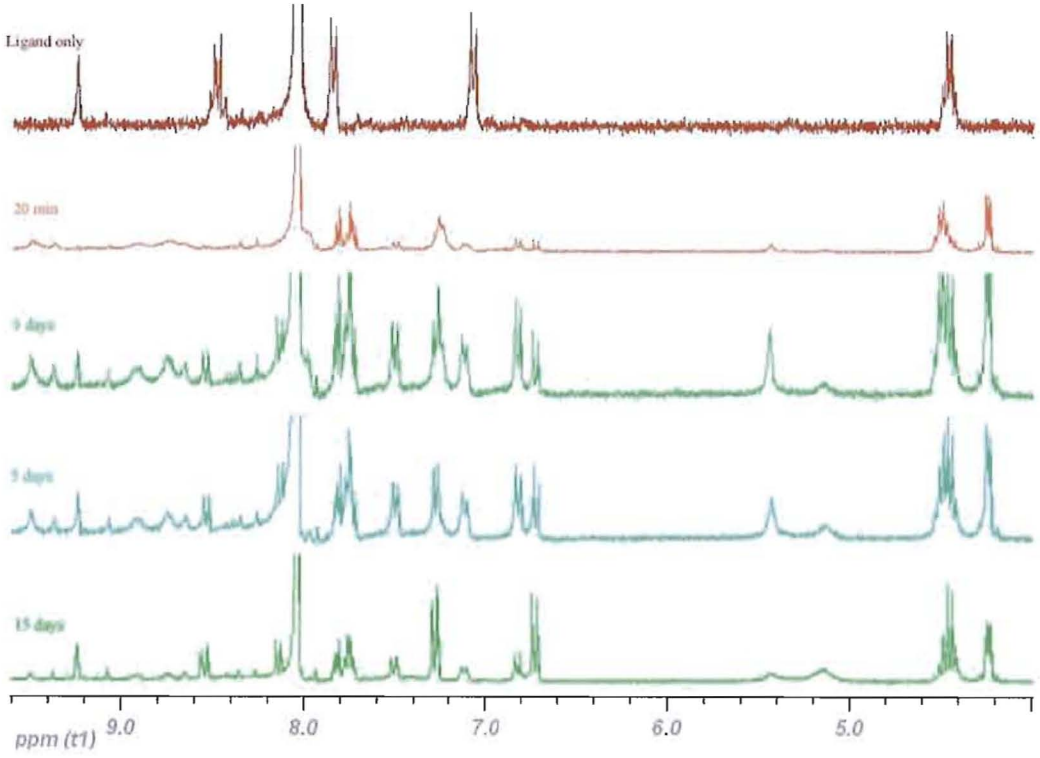

Figure G.8. Time points of **5a** in DMF with 2/3rds equivalents of $Zn(OTf)_2$.

Metallation reactions are being tried with the other isolated and characterized ligands (**5b**, **6a** and **6b**). Metallation will also be attempted on deprotected acid ligands (**5c** and **6c**) as well as the target thiazoline activated esters (**5d** and **6d** when they are prepared). Ligands **6a** and **6b** exhibit very poor solubility. Heating and cooling to room temperature causes the ligand crash out very quickly. The addition of $Zn(BF_4)_2$ to the solution helps keep the ligands in solution. Many other attempts at crystalization and characterization of the complex are in progress.

Concurrent Work on Alternate schemes

Activated Esters

Anticipating that the capping of the templated cage will be very difficult in high yields; possible solutions to this problem are to increase the yield or to change the order of the reactions to do the more difficult reaction earlier. The first method we are trying is to activate the ester to facilitate the formation of 12 amide bonds simultaneously. The main goal is to get to ligand **5d** or **6d** from Scheme 3. This is a modification of the project as it was unfolding

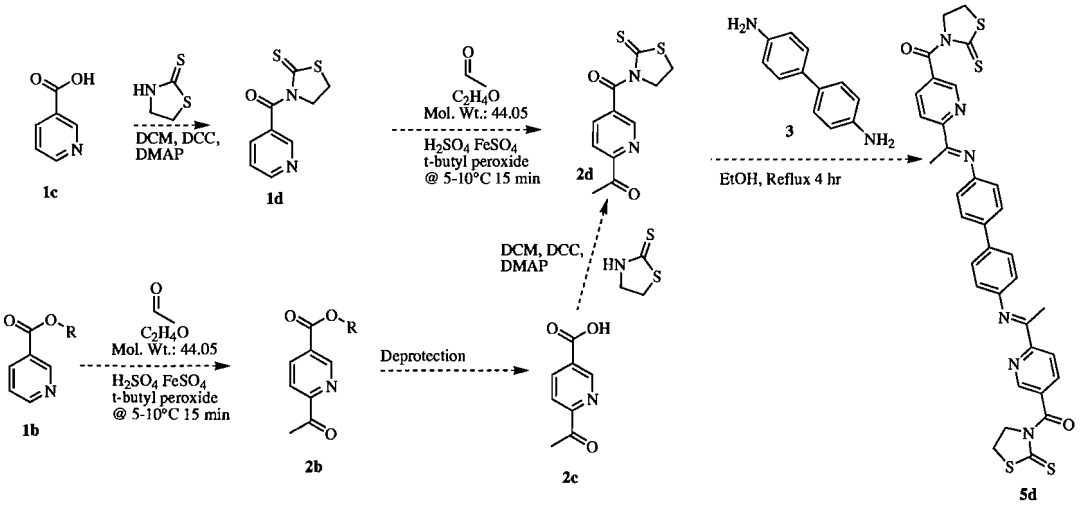

Scheme G.5 projected route to get to intermediate eight and nine, as alternative to scheme 3

The modified **Scheme G.5** to get to ligand **5d** by an alternate route proved to be just as difficult. The thiazoline-activated ester is characteristically yellow because of the conjugation of the atoms. The activated thiazoline ester works so well that the diamine

that is the backbone for the condensation instead makes an amide bond.[37] This characteristic color disappears during the condensation reaction attempts as the diamine reacts with the thiazoline to form an amide. This has proved that the condensation needs to be done before the activation or the capping needs to be done before the condensation.

Capping First

The second possibility to solve the capping problem is to cap the ligands before they are fully assembled. This alternate scheme will run the same reactions but in a different order. The burgundy line is the spacer, the benzidine (**3**) or the 4,4"-diaminotertphenyl (**4**) that is used in the condensation with the ketone to make the Schiff base. An orange-burgundy-orange line is the same as a blue line from Scheme 3. The orange end is the ketone for the condensation. The R group could be ethyl ester, benzyl ester, acid or the activated thiazoline esters, but here instead the ketone is capped to yield a new intermediate. This new intermediate will undergo self-assembly (using the metals) and condensation (with the diamine core) at the same time. By CAChe modeling, a L_3 helicate should be able to form without metal, but because of ligand design the M_2L_3 complex should not be stable.

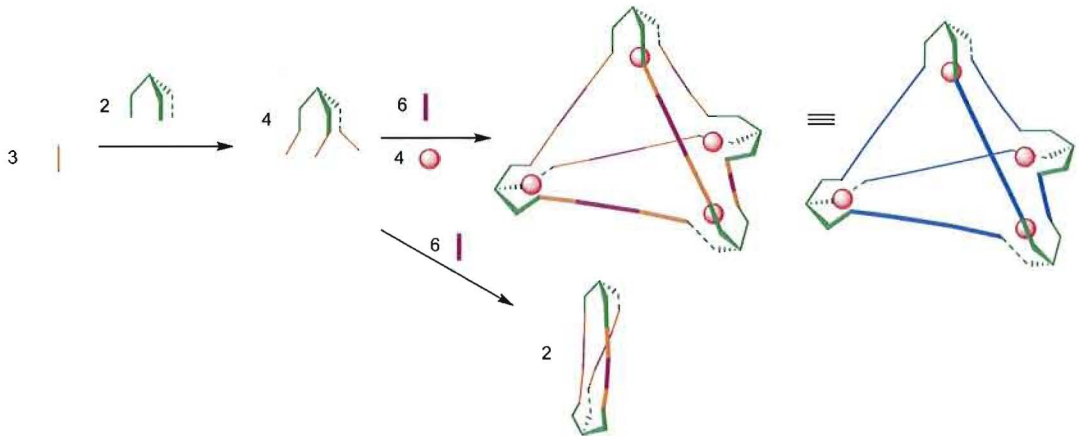

Scheme G.6 Alternate scheme for the capping of the ligands before self-assembly

A major concern about condensing the backbone and self-assembling the complex at the same time is that the new intermediate (**13**) would be a good metal chelator, because it would have the ability to wrap around the metal, much like EDTA.[40,41] But CAChe modeling suggests that the Zn center would be strained. Starting with benzyl nicotinate, **1b**, and acylation to **2b** affords a higher yield than using nicotinic acid, **1c**, or ethyl nicotinate, **1a**. Then ketone **2b** is modified into ketone **2d**; as seen before, **2d** cannot be condensed with **3** or **4** to yield ligand **5d** or **6d** respectively. Therefore **2d** will be reacted with TRPN, **9**, to yield the capped ketone. This new intermediate will be condensed with a diamine (**3** or **4**) either in the presence or absence of Zn^{2+}, which should afford the capped metal templated organic nanocage (**14**) or the non-metal helicate (**15**).

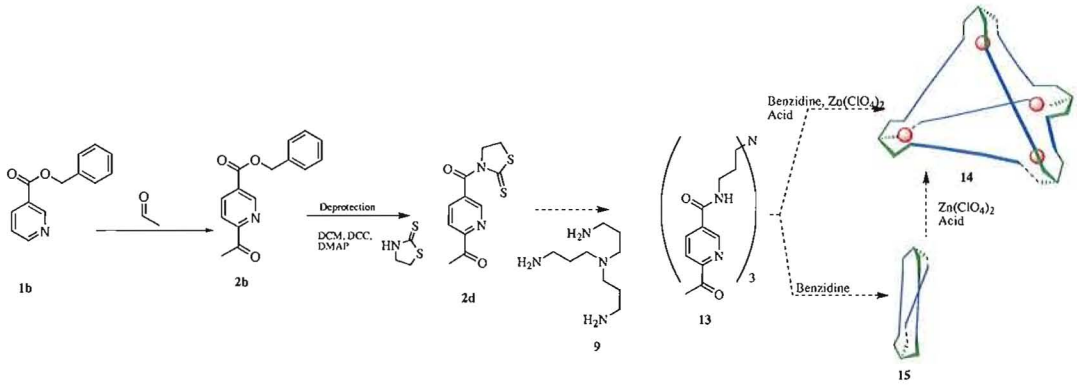

Scheme G.7 acylation, activation, capping condensation coupled with SA.

Future Work

Currently we stand two steps from the completion of the first main goal the templated organic nanocage. Those two steps are the capping and then demetallation of the cage. The first objective is to complete the ligand synthesis route and the characterization of the intermediates. Ligands **5a** and **5b** need to be converted into the acid of **5c**, which then must be fully characterized. The same functional group interconversion needs to be finished on the larger ligand **6**. Both ligands **5c** and **6c** will be metallated and the resulting complexes will be characterized. Then free ligands **5c** and **6c** will be activated into ligands **5d** and **6d**, which will also be metallated.

Each of the ligands (**a, b, c** or **d**) should self-assemble into the supramolecular complex. The biggest problem will be the formation of all 12 amide bonds to yield **7** or **8** from **Scheme G.4**. The current progress is showing that we may need to use activated esters to prepare for capping (ligands **5d** and **6d**). The complexes made with R functional groups **a, b** or **c** will still need to be capped after assembly.

The final step to yield the organic nanocage is the demetallation of the capped template. The basic plan is to make the metal less stable in the cage and then extract it. Possible demetallation solutions are to reduce the Schiff base to the amine then remove the metal with EDTA[7,42,43] or couple a chromatographic separation[44] for the easy release of the metal by precipitation of an insoluble metal salt.

We will continue working with the existing ligand **5a,b** and **6a,b** to assemble cages and characterize them. One plan is to use these ligands with other metals centers. Other metals have different coordination geometries. We could exploit this in an attempt to make coordination polymers.[45-47] If coordination polymers are made then they could still be covalently capped and demetallated. They would be very interesting and possibly very useful structures for metal remediation or possibly drug delivery.[48] If coordination polymers are not made, instead a discreet species like a square or a grid can be made.[49,50]

The self-assembly was not accurate because of the DMSO concentration effects (Figure 5). There are a series of experiments to try in DMF, since it appears to allow for the formation of a new discreet species. We will try the same self-assembly reactions with adamantane present, looking for the encapsulation of it as guest during complex formation. Ward noticed that an anionic guest helps with self-assembly their complexes [ref]; we will work more on the self-assembly of tetrahedron **5a** using $Zn(OTf)_2$ as the metal source, but determine if the addition of KBF_4 as a possible guest will accelerate the formation of the complex. The larger cages (**8**) made from the longer ligand **6**, will need a larger anionic guest like IO_4^-, MnO_4^- or ReO_4^-. We will try to self-assemble ligand and

complex in one step, using a one-pot synthesis of **2b** or **2d**, with **3** and $Zn(BF_4)_2$ in DMF, or chloroform to see if complex **7b** or **7d** will form.[51,52]

New Ligands

A major branch point is to synthesize different ligands. We plan to build off this existing strategy by using new diamine spacers. [47,53] Increased size and bulk as well as added flexibility should allow for the synthesis of M_2L_3 helicates.[54-58] New topologies can also be explored by changing to three- or four-fold symmetric linkers. The new spacers would allow for the formation of M_4L_4 cube complexes.[59,60]

Another aspect of the project would be to work on a new design of ligands that still have a similar binding motif of the Schiff base but are assembled differently and with higher yields. Using a bipyridyl functionality for the binding motif would require alternate functionality on the ends to allow for a linker to make a bis ligand and the covalent cap at the other end.[10,61] Another prime alternative is to use a pyrazolylpyridine binding motif as the bidentate ligand.[18,62] The pyrazolylpyridine rings would be able to be differentially functionalized. Using a catechol adjacent Schiff base would create a new binding motif for the metal.[15] This new binding group could be coupled with any of the current or future diamine cores. These new ligands would be able to achieve different complexes and should also be able to make the coordination polymers.[63]

This project has many directions that it can go. The existing ligand strategy will yield multiple organic nanocages soon. These cages can then be tested for guest-host chemistry and functionalized for testing with external applications.

Experimental

General Experimental. All NMR spectra were taken on a 300MHz or a 500MHz Varian INOVA Spectrometer instrument in $CDCl_3$, unless otherwise noted. All reactions were performed under an inert N_2 atmosphere. Compounds were purchased from a commercial supplier and used without further purification unless otherwise noted. ESI-MS was performed on an Agilent 1100 LC-ESIMS by means of direct injection, using THF as the mobile phase. Desert Analytic of Tucson, AZ performed elemental analysis. Single crystal X-ray data were collected using a Bruker SMART APEX diffractometer equipped with a CCD area detector using Mo-K_α ($\lambda = 0.71073$ Å) radiation.

6-Acetyl-ethyl nicotinic (2a Scheme 3) A chilled solution of H_2SO_4 (5.2 mL, 92 mmol), ethyl nicotinate **1a** (4.6 mL, 33 mmol) and acetaldehyde (5.5 mL, 96 mmol, added via a pre-chilled syringe) in water (15 mL) was prepared. A suspension of iron sulfate (26.9 gm, 97 mmol) in water (65 mL) was added drop wise by one syringe while t-butyl peroxide (9.8 mL, 67 mmol, 70% solution in water) was added by a second syringe. Both reagents were added dropwise over three minutes. The reaction was stirred for a total of 15 minutes from the beginning of addition until the removal of the ice bath.

The reaction was extracted twice with chloroform (2 x 20 mL). The organic layers were combined and washed once with brine (1 x 20 mL), then dried over $MgSO_4$, filtered and reduced by rotary evaporation. Crude yield a mixture of **1a, 2a, 12a** and **11a** was 3.29 gm, ca. 51.6 %. The product was purified by column chromatography (silica

gel, 9:1 hexanes: ethyl acetate). The desired product, **2a**, is the first to elute. The other products can be isolated by this method as well. Final yield of **2a** was 0.300 gm, 9% of crude. ^{1}H NMR δ = 9.26 (s, 1H), 8.41 (dd, J = 8.1, 2.7 Hz, 1H), 8.09 (dd, J = 8.1, 0.6 Hz, 1H), 4.44 (q, J = 7.0 Hz, 2H), 2.75 (s, 3H), 1.43 (t, J = 7.0 Hz, 3H)

Undesired products

1a ^{1}H NMR δ = 9.22 (s, 1H), 8.76 (dd, J = 4.5, 1.8 Hz, 1H), 8.27 (d of t, J = 6.0, 1.8 Hz, 1H), 7.38 (dd, J = 7.8, 2.7 Hz, 1H), 4.42 (q, J = 7.2 Hz, 2H), 1.30 (t, J = 7.2 Hz, 3H)

11a ^{1}H NMR δ = 9.19 (s, 1H), 8.22 (d, J = 4.8 Hz, 1H), 7.20 (d, ^{4}J = 0.6 Hz, 1H), 4.41 (q, J = 7.2 Hz, 2H), 2.55 (s, 3H), 1.38 (t, J = 7.2 Hz, 3H)

12a ^{1}H NMR δ = 9.16 (s, 1H), 7.95 (s, 1H), 4.42 (q, J = 6.9 Hz, 2H), 2.75 (s, 3H), 2.58 (s, 3H), 1.40 (t, J = 6.9 Hz, 3H)

6-Acetyl-benzyl nicotinate. (**2b Scheme G.3**) A chilled solution of H_2SO_4 (3.4 mL, 58 mmol), benzyl nicotinate, **1b**, (5.0 gm, 23 mmol) and acetaldehyde (3.3 mL, 58. mmol, added via a pre-chilled syringe) in water (10 mL) was prepared. A suspension of iron sulfate (16 gm, 58 mmol) in water (20 mL) was added dropwise by one syringe while t-butyl peroxide (8.0 mL, 58 mmol, 70% solution in water) was added by a second syringe. Both reagents were added dropwise over three minutes. The reaction was stirred for a total of 10 minutes from the beginning of addition until the removal of the ice bath.

The reaction was extracted ten times with chloroform (10 x 10 mL). The organic layers were combined and washed once with brine (1 x 20 mL), then dried over $MgSO_4$, filtered and reduced by rotary evaporation. The product was purified by column chromatography (silica gel, 9:1 hexanes: ethyl acetate). The desired product, **2b**, is the first to elute. The other products can be isolated by this method as well. Final yield of **2b** was 1.27 gm, 21.3% yield overall. ^{1}H NMR δ = 9.26 (s, 1H), 8.41 (dd, J = 8.1, 2.7 Hz, 1H), 8.09 (dd, J = 8.1, 0.6 Hz, 1H), 7.41 (m, 5H), 5.42 (s, 2H), 2.75 (s, 3H),; ^{13}C NMR δ = 164.9, 156.0, 151.2, 150.5, 138.2, 124.2, 121.3, 62.1, 26.2, 14.5.

Table G.1 Acylation results

Ester	Time (min)	crude %	product	Product Overall %	
1a	15	57.3	**2a**	7.5	JTG/MNG
1a	15	50.9	**2a**	6.1	JTG/MNG
1a	15	53.8	**2a**	7.5	JTG/MNG
1a	10	73.2	**2a**	10.1	JTG/MNG
1a	10	82.2	**2a**	10.9	JTG/MNG
1b	15	not determined	**2b**	16.0	CAJ
1b	10	not determined	**2b**	21.3	CAJ
1b	10	not determined	**2b**	17.0	CAJ
1b	10	not determined	**2b**	23.0	MNG/JTG

6-Acetyl-nicotinic Acid, (2c Scheme G.3) (synthesized by CAJ)

To a solution of **2b**,(0.5 gm, 1.9 mmol) in 3:1 THF/water two equivalents of KOH was added. The reaction was stirred for three hours without heat. The THF was removed by rotary evaporation and the water was washed with methylene chloride (3 x 10 mL). The organic layers were combined and dried by rotary evaporation to yield un-reacted starting material, **2b**. The aqueous layer was acidified with HCl (2 equivalents) to yield a

precipitate, which was filtered and washed with water, yielding 0.18 gm (47%) of **2c** when dried. ^{1}H NMR δ = 8.67 (s, 1H), 8.04 (dd, J = 8.1, 1H), 7.73 (dd, J = 8.1, 1H), 4.67 (s, 4H), 2.45 (s, 3H)

6-Acetyl-nicotinic Acid Thiazoline Ester, (2d Scheme G.3) (synthesized by CAJ)

To a solution of **2c** (0.180gm, 1.08 mmol) in 5 mL methylene chloride and 5 mL tetrahydrofuran, one equivalent of 2-mercaptothizaoline (0.119 gm, 1 mmol) one equivalent of DCC (dicyclohexylcarboimide) (0.206 gm, 1 mmol) and one-twentieth equivalent of DMAP (4-(dimethylamino)-pyridine) (0.0061 gm, 0.05 mmol) was added. The reaction was stirred at room temperature under nitrogen for 5 hours, at which point the solution was a deep yellow color. A white precipitate formed and the reaction was filtered to remove the DCU (dicyclohexylcarbourea). The crude product was purified by column chromatograph (2:1 hexanes: ethyl acetate), yield 0.040 gm of yellow solid (thick oil) **2d** (15%). ^{1}H NMR δ = 8.85 (s, 1H), 8.03 (s, 2H), 8.09 (dd, J = 8.1, 0.6 Hz, 1H), 4.60 (t, J = 6.9 Hz, 2H), 3.52 (t, J = 6.9 Hz, 2H), 2.72 (s, 3H)

Schiff Base Ligand. **(5a Scheme G.3)** Table 2 entries A-G. To a solution of ketone, **2a,** (0.26 gm, 1.3 mmol) in 4 mL of methanol 0.49 equivalents of benzidine **3** (0.124 gm, 0.67 mmol) was added. The reaction was stirred at reflux for four hours. The reaction was then reduced by rotary evaporation and re-suspended in a minimal amount of 9:1 $CHCl_3$:MeOH solution. Hexanes were then carefully layered on top and crystals formed overnight. The liquid layer was filtered off and the remaining crystals were the desired product **5a**. Yield 0.075 gm, 0.14 mmol, 20 %.

Schiff Base Ligand. (5a Scheme G.3) Table 2 entries H-L. To a solution of ketone, **2a,** (0.203 gm, 1.05 mmol) in 4 mL of solvent 0.2 equivalents of benzidine **3** (0.038 gm, 0.2 mmol) was added. To the reaction a catalytic amount of acid was added (5 drops of concentrate acid, notes column). The reaction was stirred at reflux for four hours. Within 30 minutes the transparent solution had become opaque with a precipitate. After four hours the reaction was removed from the heat and allowed to cool to room temperature. The reaction was filtered and washed with methanol; the solid was the desired product. Yield 0.095 gm, 0.17 mmol, 85 %.

3 ^{1}H NMR δ = 7.34 (d, J = 8.7 Hz, 4H), 6.73 (d, J = 8.1 Hz, 4H), 3.65 (s, 2H); ^{13}C NMR δ = 145.3, 127.5, 115.7.

5a ^{1}H NMR δ = 9.26 (s, 2H), 8.36 (s, 4H), 7.64 (d, J = 8.1 Hz, 4H), 6.94 (d, J = 8.4 Hz, 4H), 4.44 (q, J =7.1 Hz, 4H), 2.43 (s, 6H), 1.43 (t, J = 7.1 Hz, 6H); ^{13}C NMR δ = 166.78, 165.05, 159.62, 150.05, 149.80, 137.18, 136.31, 127.25, 126.76, 120.85, 119.73, 61.47, 16.52, 14.20, there are fewer than predicted ^{13}C resonances. Based on the purity of 5a according to ^{1}H spectra, it is assumed that several ^{13}C resonances have coincidentally identical shifts ; ESI-MS m/z: MH^{+}(calc. 535.23 , obs. 535.3, 100%), MNa^{+}(calc. 557.22 , obs. 557.2 25%).

The crystal was mounted on a quartz fiber with paratone oil. Data in the frames corresponding to an arbitrary hemisphere of data (ω scans, 10 sec frames) were

intergrated using SAINT[64] [SAINT, SAX Area Detector Intergration Program, Bruker AXS, Inc., Madison, **1995**] Data were corrected for Lorentz and polarization effects. The data were further analyzed using XPREP[65] [G. M. Sheldrick, SHELXTL, Bruker AXS, Inc., WI, USA, **1997**]. An empirical absorption correction based on the measurement of redundant and equivalent reflections and an ellipsoidal model for the absorption surface were applied using SADABS.[66] The structure solution and refinement were performed using SHELXTL (refined on F2).[67] All non-hydrogen atoms were refined anisotropically. Hydrogen atoms were included but not refined on all appropriate atoms.

Crystal size 0.49 x 0.33 x 0.002 mm; T = -120°C; monoclinic, $P2_1/c$ (#14), a = 27.95 (1) Å, b = 6.230 (2) Å, c = 7.747 (3) Å, β = 93.870 (6)°, ; V = 1346.0 (8) Å^3, Z = 2, μ = .088 mm^{-1}, F(000) = 564 ρ_{calcd} = 1.319 g mL^{-1}, $2\Theta_{max}$ = 52.272°,. Of the 5980 reflections, which were collected, 1909 were unique (Rint = 0.0319); equivalent reflections were merged. Empirical absorption correction: Tmax = 0.999, Tmin = 0.660. Final R1 = 0.0468 for 1466 data for I>2σ(I) (241 Parameters, 0 restraints); for all 1906 data, *w*R2 = 0.122, GOF = 1.059.

Table G.2 – Condensation results for Ligand **5a**

Reaction	Ketone **2a**	Benzidine 3	solvent	time	heat	notes	yield (%) **5a**	
A	2	1	Methanol	4 hours	Reflux		20	Crude
B	2	1	Ethanol	4 hours	Reflux		25	Crude
C	2	1	Toluene	8 hours	Reflux		0	Crude
D	2	1	Ethanol	4 hours	Reflux	3Å MS	25	Crude
E	2	1	Ethanol	4 hours	Reflux	3Å MS, Cat. HCl	10	Crude
F	2	1	Ethanol	4 hours	Reflux	Cat. HCl	45	Crude
G	5	1	Ethanol	4 hours	Reflux	Cat. HCl	65	Crude

H	5	1	Ethanol	4 hours	Reflux	Cat. Acetic	75	Clean
I	5	1	Ethanol	4 hours	Reflux	Cat. Formic	60	Clean
J	5	1	Methanol/Hexanes	8 hours	Reflux	Cat. Acetic	50	Clean
K	5	1	Ethanol	16 hours	Reflux	Cat. Acetic	85	Clean
L	5	1	Ethanol	16 hours	Reflux	Cat. Acetic	88	Clean

Schiff Base Ligand Benzyl ester benzidine core (5b Scheme G.5) To a solution of ketone, **2b,** (0.200 gm, 0.783 mmol) in 4 mL of Ethanol 0.2 equivalents of benzidine **3** (0.029 gm, 0.157 mmol) was added. To the reaction a catalytic amount of acetic acid (5 drops) was added. The reaction was allowed to stir at reflux for four hours. Within 30 minutes the transparent solution had become opaque with precipitate. After four hours the reaction was removed from the heat and cooled to room temperature. The reaction was filtered and washed with methanol, the solid was the desired product. Yield 0.054 gm, 0.082 mmol, 52 %.

5b ^{1}H NMR δ = 9.26 (s, 2H), 8.36 (s, 2H), 8.02 (s, 2H), 7.75 (d, J = 8.4 Hz, 2H), 7.5(m, 5H), 6.94 (d, J = 8.4 Hz, 4H), 5.44 (s, 4H), 2.43 (s, 6H); ^{13}C NMR δ = 166.82, 165.0, 159.85, 149.95, 149.83, 137.35, 136.41, 135.46, 128.66, 128.26, 127.32, 120.96, 119.77, 115.39, 67.14, 16.53; ESI-MS m/z: MH^{+}(calc. 659.27 , obs. Inconclusive)

Schiff Base Ligand. (5c Scheme G.3) To a solution of ligand **5a** (0.100 gm, 0.187 mmol) in 4 mL of DMSO ,10 equivalents of 1M KOH (2 mL of sol.) was added. The reaction was heated for 16 hours at 95°C, then reduced by rotary evaporation and the product was precipitated with acetone. The reaction was centrifuged and the supernate

was decanted and dried down by rotary evaporation. The dried solution was resuspended in minimal 1:1 DMSO:water then precipitated with acetone again. The pellets were combined and washed with excess acetone and then dried. Yield 0.01 gm, 0.01 mmol, 10 %.

Schiff Base Ligand Ethyl ester terphenyl core (6a Scheme G.3) To a solution of ketone **2a** (0.25 gm, 1.2 mmol) in 4 mL of ethanol, 0.2 equivalents of 4-4"-terphenyldiamine **4** (0.127 gm, 0.689 mmol) was added. To the reaction a catalytic amount of acetic acid (5 drops) was added. The reaction was stirred at reflux for four hours. Within 30 minutes the transparent solution had become opaque with precipitate. After four hours the reaction was removed from the heat and cooled to room temperature as product precipitated. The reaction was filtered and washed with methanol, then dried, and the solid was the desired product. Yield 0.170 gm, 0.278 mmol, 40 %. ^{1}H NMR δ = 9.23 (s, 2H), 8.34 (s, 4H), 7.68 (s, 4H), 7.65 (d, J = 7.2 Hz, 4H), 6.91 (d, J = 7.2 Hz, 4H), 4.41 (q, J =7.1 Hz, 4H), 2.41 (s, 6H), 1.40 (t, J = 7.1 Hz, 6H); ^{13}C NMR δ = 166.78, 165.05, 159.62, 150.05, 149.80, 137.18, 136.31, 127.25, 126.76, 120.85, 119.73, 61.47, 16.52, 14.20 there are fewer than predicted ^{13}C resonances. Based on the purity of 5a according to ^{1}H spectra, it is assumed that several ^{13}C resonances have coincidentally identical shifts; ESI-MS m/z: MH^{+} (calc. 611.27 , obs. 611.2, 15%).

4 ^{1}H NMR δ = 7.34 (d, J = 8.7 Hz, 4H), 6.73 (d, J = 8.1 Hz, 4H), 3.65 (s, 2H)

Schiff Base Ligand Benzyl terphenyl core (6b Scheme G.3) To a solution of ketone **2b** (0.376 gm, 1.47 mmol) in 4 mL of solvent 0.2 equivalents of 4-4"terphenyldiamine **4** (0.084 gm, 0.323 mmol) was added. To the reaction a catalytic amount of formic acid (5 drops) was added. The reaction was allowed to stir at reflux for four hours. Within 30 minutes the transparent solution had become opaque with precipitate. After four hours the reaction was removed from the heat and allowed to cool to room temperature. The reaction was filtered and washed with methanol and hexanes through a plug of silica gel. Yield 0.15 gm, 63 %. ^{1}H NMR δ = 9.26 (s, 2H), 8.36 (s, 4H), 7.70 (s, 4H), 7.67 (d, J = 8.1 Hz, 4H), 6.93 (d, J = 8.4 Hz, 4H), 4.44 (q, J =7.1 Hz, 4H), 2.43 (s, 6H), 1.43 (t, J = 7.1 Hz, 6H); ^{13}C NMR δ = 166.78, 165.05, 159.62, 150.05 149.80, 138.2 137.18, 136.31, 127.6, 127.25, 126.76, 120.85, 119.73, 61.47, 16.52, 14.20, there are fewer than predicted ^{13}C resonances. Based on the purity of 5a according to ^{1}H spectra, it is assumed that several ^{13}C resonances have coincidentally identical shifts; ESI-MS m/z: MH_2^{2+} (calc. 368.15, obs. 368.2, 100%), MH^+(calc. 735.3, obs. 735.4 10%).

Schiff Base Ligand. (6c Scheme G.3) To a solution of ligand, **6b**, (0.6 gm, 2 mmol) in 3:1 THF/water two equivalents of KOH was added. The reaction was stirred for five hours without heat. The THF was removed by rotary evaporation and the water was washed (3 x 10 mL) with DCM. Organic layers combined and dried down to yield un-reacted starting material, **6b**. The aqueous layer was acidified with HCl (2 equivalents) to yield a precipitate, the solid was filtered and washed with water, yielding 0.141 gm (23.5%) of **6c** when dried. Carried on to 6d without characterization.

Schiff Base Ligand. (**6d Scheme G.3**) To a solution of ligand, **6c** (0.180 gm, 1.08 mmol) in 5 mL DCM and 5 mL THF, one equivalent of 2-mercaptothiazoline (0.119 gm, 1.08 mmol) one equivalent of EDCI (0.192 gm, 1 mmol) and one twentieth equivalent of DMAP (6.2 gm, 0.05 mmol) was added. The reaction was stirred at room temperature under nitrogen for 5 hours, at which point the solution was a deep yellow color. A white precipitate formed, the reaction was filtered to remove the EDUI. The crude product was purified by column chromatograph (2:1 hexanes: Ethyl acetate). Yields 0.05 gm of yellow solid (thick oil) 6d (28%). Characterization is currently being done.

BIBLIOGRAPHY

Chapter I

1. Johansson, G., *Acta Chem. Scand.* **1960,** 14, 771-773.

2. Anderson, J. S., Constitution of the Poly-acids. *Nature* **1937,** 140, 850.

3. Casey, W. H., Large Aqueous Aluminum Hydroxide Molecules. *Chem. Rev.* **2006,** 106, 1.

4. Pope, M. T., *Heteropoly and isopoy Oxometalates*. 1983.

5. Lorenzo-Luis, P. A.; Gili, P., Polyoxometalates with an Anderson-Evans structure. *Recent Res. Devel. Inorg. Chem.* **2000,** 2, 185-196.

6. Long, D.-L.; Burkholder, E.; Cronin, L., Polyoxometalate clusters, nanostructures and materials: From self-assembly to designer materials and devices. *Chem. Soc. Rev.* **2007,** 36, 105.

7. Jeannin, Y. P., The Nomenclature of Polyoxometalates: How To Connect a Name and a Structure. *Chem. Rev.* **1998,** 98, 51.

8. Gouzerh, P.; Proust, A., Main-Group Element, Organic, and Organometallic Derivatives of Polyoxometalates. *Chem. Rev.* **1998,** 98, 77.

9. Weinstock, I. A., Homogeneous-Phase Electron-Transfer Reactions of Polyoxometalates. *Chem. Rev.* **1998,** 98, 113.

10. Kozhevnikov, I. V., Catalysis by Heteropoly Acids and Multicomponent Polyoxometalates in Liquid-Phase Reactions. *Chem. Rev.* **1998,** 98, 171.

11. Sadakane, M.; Steckhan, E., Electrochemical Properties of Polyoxometalates as Electrocatalysts. *Chem. Rev.* **1998,** 98, 219.

12. Müller, A.; Peters, F.; Pope, M. T.; Gatteschi, D., Polyoxometalates: Very Large ClusterssNanoscale Magnets. *Chem. Rev.* **1998,** 98, 239.

13. Klemperer, W. G.; Wall, C. G., Polyoxoanion Chemistry Moves toward the Future: From Solids and Solutions to Surfaces. *Chem. Rev.* **1998,** 98, 297.

14. Yamase, T., Photo- and Electrochromism of Polyoxometalates and Related Materials. *Chem. Rev.* **1998,** 98, 307.

15. Rhule, J. T.; Hill, C. L.; Judd, D. A.; Schinazi, R. F., Polyoxometalates in Medicine. *Chem. Rev.* **1998,** 98, 327.

16. Katsoulis, D. E., A Survey of Applications of Polyoxometalates. *Chem. Rev.* **1998,** 98, 359.

17. Cronin, L.; Beugholt, C.; Krickermeyer, E.; Schmidtamann, M.; Bögge, H.; Kögerler, P.; Luong, T. K. K.; Müller, A., "Molecular Symmetry Breakers" Generating Metal-Oxide-Based Nanoobject Fragments as Synthons for Complex Structures: $[\{Mo_{128}Eu_4O_{388}H_{10}(H_2O)_{81}\}_2]_{20}$, a Giant-Cluster Dimer. *Angew. Chem. Int. Ed.* **2002,** 41, 2805.

18. Müller, A.; Krickermeyer, E.; Bögge, H.; Schmidtamann, M.; Peters, F., Organizational Forms of Matter: An Inorganic Super Fullerene and Keplerate Based on Molybdenum Oxide. *Angew. Chem. Int. Ed.* **1988,** 37, 3359.

19. Müller, A.; Beckmann, E.; Bögge, H.; Schmidtamann, M.; Dress, A., Inorganic Chemistry Goes Protein Size: A Mo_{368} Nano-Hedgehog Initiating Nanochemistry by Symmetry Breaking. *Angew. Chem. Int. Ed.* **2002,** 41, 1162.

20. Müller, A.; Beugholt, C.; Bögge, H.; Schmidtamann, M., Influencing the Size of Giant Rings by Manipulating Their Curvatures: $Na_6[Mo_{120}O_{366}(H_2O)_{48}H_{12}\{Pr(H_2O)_5\}_6]\bullet(\ 200H_2O)$ with Open Shell Metal Centers at the Cluster Surface. *Inorg. Chem.* **2000,** 39, 3112.

21. Müller, A.; Serain, C., Soluble Molybdenum Blues- "des Pudels Kern". *Acc. Chem. Res.* **2000,** 33, 2.

22. Müller, A.; Shan, S. Q. N.; Bögge, H.; Schmidtamann, M.; Kögerler, P.; Hauptfleisch, B.; Leiding, S.; Wittler, K., Thritry Electrons "trapped" in a Sperical Matrix: A Molybdenum Oxide-Based Nanostructured Keplerate Reduced by 36 Electrons. *Angew. Chem. Int. Ed.* **2000,** 39, 1614.

23. Honda, D.; Ikegami, S.; Inoue, T.; Ozeki, T.; Yagasaki, A., Protonation and Methylation of an Anderson-Type Polyoxoanion $[IMo_6O_{24}]^{5-}$. *inorg. Chem.* **2007,** 46, 1464.

24. Murugesu, M.; Clérac, R.; Wernsdorfer, W.; Anaon, C. E.; Powell, A. K., Hierarchical Assembly of $\{Fe_{13}\}$ Oxygen-Bridged Clusters into a Close-Packed Superstructure. *Angew. Chem. Int. Ed.* **2005,** 44, 6678.

25. Goodwin, J. C.; Sessoli, R.; Gatteschi, D.; Wernsdorfer, W.; Powell, A. K.; Heath, S. L., Towards nanostcutred Arrays of Single Molecular Magnets: new Fe_{19} oxyhydroxide clusterd displaying high ground state spins and hysteresis. *J. Chem. Soc. Dalton Trans.* **2000**, 1835.

26. Pohl, I. A. M.; Westin, L. G.; Kritikos, M., Preparation, Structure, and Properties of a New Giant Manganese Oxo-Alkoxide Wheel, $[Mn_{19}O_{12}(OC_2H_4OCH_3)_{14}(HOC_2H_4OCH_3)_{10}]\bullet HOC_2H_4OCH_3$. *Chem. - Eur. J.* **2001,** 7, 3439.

27. Evans, H. T., Jr, The Molecular Structure of the Hexamolybdotellurate Ion in the Crystal Complex with Telluric Acid, $(NH_4)_6ITeMo_6Oz_4]$. $Te(OH)_6.7H_2O$. *Acta Cryst.* **1974,** B30, 2095.

28. Nordin, J. P.; Sullivan, D. J.; Phillips, B. L.; Casey, W. H., Mechanism for fluoride-promoted dissoultion of bayerite [ß-$Al(OH_3)$(s)] and boehmite [g-AlOOH]: 19F -NMR Spectroscopy and aqueous Surface Chemistry. *Geochimica et Cosmochimica Acta* **1999,** 63, (21), 3513.

29. Johansson, G., The Crystal Strucutres of $[Al_2(OH)_2(H_2O)_8](SO_4)_2 \bullet 2H_2O$ and $[Al_2(OH)_2(H_2O)_8](SeO_4)_2 \bullet 2H2O$. *Acta Chem. Scand.* **1962,** 16, 403.

30. Casey, W. H.; Phillips, B. L., Kinetics of oxygen exchange between sites in the $GaO_4Al_{12}(OH)_{24}(H_2O)_{12}^{7+}$(aq) molecule and aqueous solution. *Geochimica et Cosmochimica Acta* **2001,** 65, (5), 705.

31. Filowitz, M.; Ho, R. K. C.; Klemperer, W. G.; Shum, W., 17O Nuclear Magnetic Resonance Spectroscopy of Polyoxometalates. 1. Sensitivity and Resolution. *Inorg. Chem.* **1979,** 18, 93.

32. Kortz, U.; Jeannin, Y. P.; Tézé, A.; Hervé, G.; Isber, S., A Novel Dimeric Ni-Substituted beta-Keggin Silicotungstate: Structure and Magnetic Properties of $K_{12}[\{\beta\text{-}SiNi_2W_{10}O_{36}(OH)_2(H_2O)\}_2]\bullet 20H_2O$. *Inorg. Chem.* **1999,** 38, 3670.

33. Tézé, A.; Cadot, E.; Béreau, V.; Hervé, G., About the Keggin Isomers: Crystal Structure of $[N(C_4H_9)_4]_4$-gamma-$[SiW_{12}O_{40}]$, the gamma-Isomer ofthe Keggin Ion. Synthesis and ^{183}W NMR Characterization of the Mixed gamma-$[SiMo_2W_{10}O_{40}]$n-(n = 4 or 6). *Inorg. Chem.* **2001,** 40, 2000.

34. Rowsell, J.; Nazar, L. F., Speciation and Thermal Transformation in Alumina Sols: Structures of the Polyhydroxoaluminum Cluster $[Al_{30}O_8(OH)_{56}(H_20)_{26}]^{18+}$ and its ∂-Keggin Moiete. *J. Am. Chem. Soc.* **2000,** 122, 3777-3778.

35. Son, J.-H.; Kwon, Y.-U., Crystal Engineering through Face Interactions between Tetrahedral and Octahedral Building Blocks: Crystal Structure of [E-$Al_{13}O_4(OH)_{24}(H_2O)_{12}]_2[V_2W_4O_{19}]3(OH)_2$•$27H_2O$. *Inorg. Chem.* **2004,** 43, 1929.

36. Allouche, L.; Gerardin, C.; Loiseau, T.; Ferey, G.; Taulelle, F., Al_{30} : Giant Aluminum Polycation. *Angew. Chem. Int. Ed.* **2000,** 39, 511-514.

37. Xin, F.; Pope, M. T.; Long, G. J.; Russo, U., Polyoxometalate Derivatives with Multiple Organic Groups. 2. Synthesis and Structures of Tris(organotin) a, b-Keggin Tungstosilicates. *Inorg. Chem.* **1996,** 35, 1207.

38. Evans, H. T., Jr, The Crystal Structures of Ammoium and Potassium Molydotellurates. *J. Am. Chem. Soc.* **1948,** 70, (3), 1291.

39. Heath, S. L.; Jordan, P. A.; Johnson, I. D.; Moore, G. R.; Powell, A. K.; Helliwell, M., Comparative X-ray and ^{27}Al NMR Spectroscopic Studies of the Speciation of Aluminum in Aqueous Systems: Al(III) Complexes of $N(CH_2CO_2H)_2(CH_2CH_2OH)$. *J. Inorg. Biochem.* **1995,** 59, 785-794.

40. Seichter, W.; Mogel, H.-J.; Brand, P.; Salah, D., Crystal Structure and Formation of the Aluminum Hydroxide Cloride $[Al_{13}(OH)_{24}(H_2O)_{24}]Cl_{15}$ • 13 H_2O. *Eur. J. Inorg. Chem.* **1998**, 795-797.

41. Rather, E.; Gatlin, J. T.; Nixon, P. G.; Tsukamoto, T.; Kravtsov, V.; Johnson, D. W., A Simple Organic Reaction Mediates the Crystallization of the Inorganic Nanocluster $[Ga_{13}(\mu_3\text{-}OH)_6(\mu_2\text{-}OH)_{18}(H_2O)_{24}](NO_3)_{15}$. *J. Am. Chem. Soc.* **2005,** 127, 3242-3243.

42. Goodwin, J. C.; Teat, S. J.; Heath, S. L., How do clusters grow? The Synthesis and Structure of Polynuclear Hydroxide Gallium(III) Clusters. *Angew. Chem. Int. Ed.* **2004,** 43, 4037-4041.

43. Rujiwatra, A.; Mander, G. J.; Kepert, C. J.; Rosseinsky, M. J., *Cryst. Growth Des.* **2005,** 5, 183.

44. Casey, W. H.; Olmstead, M. M.; Phillips, B. L., A New Aluminum Hydroxide Octamer, $[Al_8(OH)_{14}(H_2O)_{18}](SO_4)_5$•$16H_2O$. *Inorg. Chem.* **2005,** 44, 4888.

45. Takada, K.; Onoda, M.; Argyriou, D. N.; Choi, Y.-N.; Izumi, F.; Sakurai, H.; Takayama-Muroachi, E.; Sasaki, T., Order and Disorder Aspects of Interlayer guests in Superconducting Hydrous Sodium Cobalt Oxides. *Chem. Mater.* **2007,** 19, (14), 3519.

46. Wery, A. S. J.; Gutiérrez-Zorrilla, J. M.; Luque, A.; Ugalde, M.; Román, P.; Lezama, L.; Rojo, T., Synthesis, Crystal Structure, and Vibrational and Electron Spin Resonance Study of tert-Butylammonium [H_9-n$CrMo_6O_{24}$] •mH2O (n=2, m=2; n=3, m=8). Effects of Degress fo Protonation and Hydration. *Acta Chem. Scand.* **1998,** 52, 1194.

47. Orpen, G. A.; Brammer, L.; Allen, F. H.; Kennard, O.; Watson, D. G.; Taylor, R., Tables of Bond Lengths Determined by X-Ray and Neutron Diffraction 2. Organometallic Compouns and Coordination complexes of the D-Block and F-Block Metals. *J. Chem. Soc. Dalton Trans.* **1989**, S1.

48. Shannon, R. D., Revised Effective Ionic Radii and Systematic Studies of Interatomie Distances in Halides and Chaleogenides. *Acta Cryst.* **1976,** A32, 751.

49. CSD *2006*, Cambridge Cryastallographic Data Centre.

50. Hasenknopf, B.; Delmont, R.; Herson, P.; Gouzerh, P., Anderson-Type Heteroplymolybdates Containing Tris(alkoxo) Ligands: Synthesis adn Structure Characterization. *Eur. J. Inorg. Chem.* **2002**, 1081.

51. Khan, M. I.; Tabussum, S.; Doedens, R. J.; Golub, V. O.; O'Connor, C. J., Synthesis, structure and magnetic properties of a novel ferromagnetic cluster [FeV_6O_6{$(OCH_2CH_2)_2N(CH_2CH_2OH)$}$_6$]$Cl_2$. *Inorg. Chem. Commun.* **2004,** 7, 54.

52. Khan, M. I.; Tabussum, S.; Doedens, R. J.; Golub, V. O.; O'Connor, C. J., Functionalized Metal Oxide Clusters: Synthesis, Characterization, Crystal Structures, and Magnetic Properties of a Novel Series of Fully Reduced Heteropolyoxovanadium Cationic Clusters Decorated with Organic Ligandss[MVIV $_6O_6${$(OCH_2CH_2)_2N(CH_2CH_2OH)$}$_6$]X (M) Li, X) Cl•LiCl; M) Na, X) Cl•H2O; M) Mg, X) 2Br•H2O; M) Mn, Fe, X) 2Cl; M) Co, Ni, X) 2ClâH2O). *Inorg. Chem.* **2004,** 43, 5850.

53. Favette, S.; Hasenknopf, B.; Vaissermann, J.; Gouzerh, P.; Roux, C., Assebly of a polyoxometalate into an anisotropic getl. *Chem. Commun.* **2003**, 2664.

54. Kurata, T.; Hayashi, Y.; Uehara, A.; Isobe, K., Synthesis of a reduced Tridecavanadate Dimer Linked by eight Hydrogen Bonds. *Chem. Letters* **2003,** 32, (11), 1040.

55. An, H.; Guo, Y.; Li, Y.; Wang, E.; Lü, J.; Xu, L.; Hu, C., A novel organic–inorganic hybrid with Anderson type polyanions as building blocks: [$(Gly)_2Cu$][$Na(H_2O)_4Cr(OH)_6Mo_6O_{18}$] 9.5$H_2O$ (Gly=glycine). *Inorg. Chem. Commun.* **2004,** 7, 521.

56. An, H.; Li, Y.; Wang, E.; Xiao, D.; Sun, C.; Xu, L., Self-Assembly of a Series of Extended Architectures Based on Polyoxometalate Clusters and Silver Coordination Complexes. *Inorg. Chem.* **2005,** 44, 6062.

57. He, Q.; Wang, E., Hydrothermal synthesis and crystal structure of a new molybdenum(VI) areseate(III), $Co^{III}(en)_3H_3O[(Co^{II}O_6)Mo_6{}^{VI}O_{18}(As_3{}^{III}O_3)_2]\cdot 2H_2O$. *Inorg. Chem. Acta* **1999,** 295, 244.

58. Chen, Y.; Zhu, H.; Liu, Q.; Chen, C., Sodium Triethanolamine Complex with Extended 3-D Network Structure. *Chem. Letters* **1999**, 585.

59. Chen, Y.; Liu, Q.; Deng, Y.; Zhu, H.; Chen, C.; Fan, H.; Liao, D.; Gao, E., Vanadium, Molybdenum, and Sodium Triethanolamine Complexes Derived from a Assembly System Containing Tetrathiometalate and Triethanolamine. *Inorg. Chem.* **2001,** 40, 3725.

60. Zhang, Q.-Z.; Yu, Y.-Q.; Chen, S.-M.; He, X.; Yan, Y.; Liu, J.-H.; Chen, L.-J.; Xia, C.-K.; Xu, X.-J.; Wu, X.-Y.; Lu, C.-Z., *Chinese J. Struct. Chem.* **2004,** 23, 1269.

61. He, Q.; Wang, E., Hydrothermal synthesis and crystal structure of a new copper(II) molybdenum(IV) areseate(III), $C(c_5H_5NH)_2(H_3O)_2[(Co_{II}O_6)Mo_6VIO_{18}(As_3{}^{III}O_3)_2]$. *Inorg. Chem. Commun.* **1999**, 399.

62. Cui, Y.; Chen, J.-T.; Huang, J.-S., Syntheses, Crystals structures and magnetic properties of Heterometallic copper-lanthanide clusters $[Cu_{12}Ln_6(\mu_3\text{-}OH)_{24}(\mu\text{-}O_2CR)_{12}(H_2O)_{18}(\mu_{12}\text{-}ClO_4)]^{5+}$ (Ln = La, Nd; R = CH_2Cl, CCl_3). *Inorg. Chem. Acta* **1999,** 293, 129.

63. Shivaiah, V.; Nagaraju, M.; Das, S. K., Formation of a Spiral-Shaped Inorganic-Organic Hybrid Chain, $[Cu^{II}(2,2'\text{-bipy})(H_2O)_2Al(OH)_6Mo_6O_{18}]n$ n-: Influence of Intra- and Interchain Supramolecular Interactions. *Inorg. Chem.* **2003,** 42, 6604.

64. Affronte, M.; Cornia, A.; Lascialfari, A.; Borsa, F.; Gatteschi, D.; Hinderer, J.; Horvatic, M.; Jansen, A. G. M.; Julien, M.-H., Observation of Magnetic Level Repulsion in Fe6:Li Molecular Antiferromagnetic Rings. *Phys. Rev. Lett.* **2002,** 88, (16), 167201.

65. An, H.; Lan, Y.; Li, Y.; Wang, E.; Hao, N.; Xiao, D.; Duan, L.; Xu, L., novel chain-like polymer constructed from heteropolyanions covalently linked by lanthanide cations: $(C_5H_9NO_2)_2[La(H_2O)_7CrMo_6H_6O_{24}]$ • $11H_2O$(Proline=$C_5H_9NO_2$). *Inorg. Chem. Commun.* **2004,** 7, 356.

66. Li, F.; Xu, L.; Wei, Y.; Wang, X.; Wang, W.; Wang, E., Arsenicum-centered Molybdenum–Vanadium polyoxometalates bearing transition metal complexes: Hydrothermal syntheses, crystal structures and magnetic properties. *J. Mol. Struct.* **2005,** 753, 61.

67. Janas, Z.; Jerzykiewicz, L. B.; Sobota, P.; Utko, J., Synthesis and crystal structures of the heptamagnesium cationic and mixed magnesium(II)/nickel(II) molecular 2-tetrahydrofurfuroxo aggregates. *New J. Chem.* **1999,** 23, 185.

68. Ochsenbein, S. T.; Murrie, M.; Rusanov, E.; Stoeckli-Evans, H.; Sekine, C.; Güdel, H. U., Synthesis, Structure, and Magnetic Properties of the Single-Molecule Magnet $[Ni_{21}(cit)_{12}(OH)_{10}(H_2O)_{10}]^{16-}$. *Inorg. Chem.* **2002,** 41, 5133.

69. Kaziev, G. Z.; Dutov, A. A.; Quinones, S. H.; Belsky, V. K.; Stash, A. I.; A., I., *Russ. Coord. Chem.* **2004,** 30, 83.

70. Ouahab, L.; Golhen, S.; Yoshida, Y.; Saito, G., *J. Cluster Sci.* **2003,** 14, 193.

71. Jones, L. F.; Brechin, E. K.; Collison, D.; Raftery, J.; Teat, S. J., New Routes to High Nucleartiy Clusters: Flouride-Based Octametallic and Tridecametallic Clusters of Manganese. *Inorg. Chem.* **2003,** 42, 6971.

72. Harden, N. C.; Bolcar, M. A.; Wernsdorfer, W.; Abboud, K. A.; Streib, W. E.; Christou, G., Heptanuclear and Decanuclear Manganese Complexes with the Anion of 2-Hydroxymethylpyridine. *Inorg. Chem.* **2003,** 42, 7067.

73. An, H.; Xiao, D.; Wang, E.; Li, Y.; Xu, L., A series of new polyoxoanion-based inorganic-organic hybrids: $(C_6NO_2H_5)[(H_2O)_4(C_6NO_2H_5)Ln(CrMo_6H_6O_{24})]$ •4H2O (Ln = Ce, Pr, La and Nd) with a chiral layer structure. *New J. Chem.* **2005,** 29, 667.

74. Goel, S. C.; Matchett, M. A.; Chiang, M. Y.; Buhro, W. E., A Very large Calcium Dialkoxide Molecular Aggregate haveing a CdI_2 Core Geometry: $Ca_9(OCH_2CH_2OMe)_{18}(HOCH_2CH_2OMe)_2$. *J. Am. Chem. Soc.* **1991,** 113, 1844.

75. Boulmaaz, S.; Papiernik, R.; Hubert-Pfalzgraf, L. G.; Vaissermann, J.; Daran, J.-C., Synthesis and molecular structure of $Cd_9(OC_2H_4OMe)_{18}$,$2HOC_2H4OMe$, the first cadmium aggregate based on oxygen donor ligands. *Polyhedron* **1992,** 11, (11), 1331.

76. Kahn, M. I.; Chang, Y.; Chen, Q.; Hope, H.; Parking, S.; Goshorn, D. P.; Zubieta, J., (Organoaronato)polyoxovandaium Clusters: Properties and Structures of the $V^{(v)}$ clusters. *Angew. Chem. Int. Ed.* **1992,** 31, (9), 1197.

77. Shivaiah, V.; Das, S. K., Polyoxometalate-Supported Transition Metal Complexes and Their Charge Complementarity: Synthesis and Characterization of $[M(OH)_6Mo_6O_{18}\{Cu(Phen)(H_2O)_2\}_2][M(OH)_6Mo_6O_{18}\{Cu(Phen)(H_2O)Cl\}_2]\cdot 5H_2O$ (M) Al3+, Cr3+). *Inorg. Chem.* **2005,** 44, 8846.

78. Abbati, G. L.; Cornia, A.; Fabretti, A. C.; Malavasi, W.; Schenetti, L.; Caneschi, A.; Gatteschi, D., Modulated Magnetic Coupling in Alkoxoiron(III) Rings by Host-Guest Interactions with Alkali Metal Cations. *inorg. Chem.* **1997,** 36, 6443.

79. Saalfrank, R. W.; Bernt, I.; Uler, E.; Hampel, F., Template-Mediated Self Assembly of Six- and Eight-Member Iron Coronates. *Angew. Chem. Int. Ed.* **1997,** 36, 2428.

80. Bolcar, M. A.; Aubin, S. M. J.; Folting, K.; Hendrickson, D. N.; Christou, G., A new Manganese Cluster topology capable of yielding high spin species: mixed-valence $[Mn_7(OH)_3Cl_3(hmp)_9]^{2+}$ with $S \geq 10$. *Chem. Commun.* **1997,** 1485.

81. Abbati, G. L.; Cornia, A.; Fabretti, A. C.; Caneschi, A.; Gatteschi, D., A Ferromagnetic Ring of Six Manganese(III) Ions with a S = 12 Ground State. *Inorg. Chem.* **1998,** 37, 1430.

82. Golhen, S.; Ouahab, L.; Grandjean, D.; Molinié, P., Preparation, Crystal Structures, and Magnetic and ESR Properties of Molecular Assemmblies of Ferrocenium Derivatives and Paramagnetic Polyoxometalates. *Inorg. Chem.* **1998,** 37, 1499.

83. Saalfrank, R. W.; Prakash, R.; Maid, H.; Hampel, F.; Heinemann, F. W.; Trautwein, A. X.; Böttger, L. H., Synthesis and Characterization of Metal-Centered, Six-Membered, Mixed-Valent, Heterometallic Wheels of Iron, Manganese, and Indium. *Chem. - Eur. J.* **2006,** 12, 2428.

84. Marcoux, P. R.; Hasenknopf, B.; Vaissermann, J.; Gouzerh, P., Developing Remote Metal Binding Sites in Heteropolymolybdates. *Eur. J. Inorg. Chem.* **2003,** 2406.

85. Zhang, J.-J.; Sheng, T.-L.; Xia, S.-Q.; Leibeling, G.; Meyer, F.; Hu, S.-M.; Fu, R.-B.; Xiang, S.-C.; Wu, X.-t., Syntheses and Characterizations of a Series of Novel Ln6Cu24 Clusters with Amino Acids as Ligands. *Inorg. Chem.* **2004,** 43, 5472.

86. Saalfrank, R. W.; Nakajima, T.; Mooren, N.; Scheurer, A.; Maid, H.; Hampel, F.; Trieflinger, C.; Daub, J., Syntheses and Properties of Metal-Centered Mixed-Valent $[NEt_4]\{Mn^{II}\ [Mn^{II}_3Mn^{III}_3Cl_6(L)_6]\}$ Manganese Wheels. *Eur. J. Inorg. Chem.* **2005**, 1149.

87. Abbati, G. L.; Cornia, A.; Fabretti, A. C.; Caneschi, A.; Gatteschi, D., Structure and Magnetic Properties of a Mixed-Valence Heptanuclear Manganese Cluster. *Inorg. Chem.* **1998,** 37, 3759.

88. Brechin, E. K.; Clegg, W.; Murrie, M.; Parsons, S.; Teat, S. J.; Winpenny, R. E. P., Nanoscale Cages of Manganese and Nickel with "Rock Salt" Cores. *J. Am. Chem. Soc.* **1998,** 120, 7365.

89. Hayashi, Y.; Fukuyama, K.; Takatera, T.; Uehara, A., Synthesis and Structure of a New Reduced Isopolyvanadate, [V17O42]4-. *Chem. Letters* **2000**, 770.

90. Abbati, G. L.; Brunel, L.-C.; Casalta, H.; Cornia, A.; Fabretti, A. C.; Gatteschi, D.; Hassaon, A. K.; Jansen, A. G. M.; Maniero, A. L.; Pardi, L.; Paulsen, C.; Segre, U., Single-Iron versus Dipolar Origin of the Magnetic Anisotropy in Iron(III)-oxo Clusters: A Case Study. *Chem. - Eur. J.* **2001,** 7, 1796.

91. An, H.; Xiao, D.; Wang, E.; Sun, C.; Xu, L., Organic–inorganic hybrids with three-dimensional supramolecular channels based on Anderson type polyoxoanions. *J. Mol. Struct.* **2005,** 743, 117.

92. Koizumi, S.; Nihei, M.; Nakano, M.; Oshio, H., Antiferromagnetic Fe(III)6 Ring and Sinle-Molecule Magnet $Mn^{(II)}_3Mn^{(III)}_4$ Wheel. *Inorg. Chem.* **2005,** 44, 1208.

93. Liu, C.-M.; Huang, Y.-H.; Zhang, D.-Q.; Gao, S.; Jiang, F.-C.; Zhang, J.-Y.; Zhu, D.-B., *Cryst. Growth Des.* **2005,** 5, 1531.

94. Caneschi, A.; Cornia, A.; Fabretti, A. C.; Foner, S.; Gatteschi, D.; Grandi, R.; Schenetti, L., Synthesis, Crystal Structure, Magnetism, and Magnetic Anisotropy of Cyclic Clusters Comprising Six Iron(III) Ions and Entapping Alkaline Ions. *Chem. - Eur. J.* **1996,** 2, 1379.

95. Sun, Z.; Gantzel, P. K.; Hendrickson, D. N., Supercubane Mixed-Valence Tridecanuclear Manganese Complex. *Inorg. Chem.* **1996,** 35, 6640.

96. Tesmer, M.; Muller, B.; Vahrenkamp, H., Oligonuclear zinc complexes of 2-pyridylmethanol. *Chem. Commun.* **1997**, 721.

97. Oshio, H.; Hoshino, N.; Ito, T.; Nakano, M.; Renz, F.; Gütlich, P., Hihg-Sping Whell of Heptanuclear Mixed Valent Fe(ii,iii) Complex. *Angew. Chem. Int. Ed.* **2003,** 42, (2), 223.

98. Schmitt, W.; Baissa, E.; Mandel, A.; Anson, C. E.; Powell, A. K., $[Al_{15}(\mu_3\text{-}O)_4(\mu_3\text{-}OH)_6(\mu\text{-}OH)_{14}(hpdta)_3]^{3-}$ - A New Al_{15} Aggergate Which forms a Suprmolecular Zeotype. *Angew. Chem. Int. Ed.* **2001,** 40, 3578-3581.

99. Mehring, M.; Mansfeld, D.; Sanna, P.; Schürmann, M., Polynuclear Bismuth-Oxo Clusters: Insight into the Formation Process of a Metal Oxide. *Chem. - Eur. J.* **2006,** 12, 1767.

100. Lee, U.; Jang, S.-J.; Joo, H.-C.; Park, K.-M., Triguanidinium hexahydrogenhexa-molybdocobaltate(III) tetrahydrate. *Acta Cryst.* **2003,** E59, m345.

101. An, H.; Xiao, D.; Wang, E.; Sun, C.; Li, Y.; Xu, L., Synthesis and characterization of two new extended structures based on Anderson-type polyoxoanions. *J. Mol. Struct.* **2005,** 751, 184.

102. Duan, L.-M.; Xu, J.-Q.; Xie, F.-T.; Cui, X.-B.; Ding, H.; Song, J.-F., *Mendeleev Commun.* **2005**, 79.

103. Labat, G.; Boskovic, C.; Güdel, H. U., Hexakis(l4-2-amino-2-methylpropane-1,3-diolato)hexachloroheptairon(II,III) acetonitrile disolvate monohydrateq. *Acta Cryst.* **2005,** E61, m611.

104. Murrie, M.; Stoeckli-Evans, H.; Güdel, H. U., Assembly of Ni_7 and Ni_{21} Molecular Clusters by using Citric Acid. *Angew. Chem. Int. Ed.* **2001,** 40, (10), 1957.

105. Khan, M. I.; Tabussum, S.; Doedens, R. J., A novel cationic heteropolyoxovanadium(IV) cluster functionalized with organic ligands: synthesis and characterization of the fully reduced species [MnIIVIV6O6{(OCH2CH2)2N(CH2CH2OH)}6]Cl2. *Chem. Commun.* **2003**, 532.

106. Lee, U.; Jang, S.-J.; Joo, H.-C.; Park, K.-M., Anhydrous octaguanidinium hexatungstoplatinate(IV). *Acta Cryst.* **2003,** E59, m116.

107. An, H.; Xiao, D.; Wang, E.; Li, Y.; Wang, X.; Xu, L., Open-Framework Polar Compounds: Synthesis and Characterization of Rare-Earth Polyoxometalates $(C_6NO_2H_5)_2[Ln(H_2O)_5(CrMo_6H_6O_{24})]\cdot 0.5H_2O$ (Ln = Ce and La). *Eur. J. Inorg. Chem.* **2005**, 854.

108. Murugesu, M.; Habrych, M.; Wernsdorfer, W.; Abboud, K. A.; Christou, G., Single-Molecul Magnets: Mn_{25} Complex with a record S = 51/2 sping for a Molecular Species. *J. Am. Chem. Soc.* **2004,** 126, 4766.

109. Morosin, B., Molecular Configuration of Tridecazirconium oxide-methoxide complexes. *Acta. Cryst. Sect. B* **1977,** 33, 303.

110. Heath, S. L.; Powell, A. K., The Trapping of Iron Hydroxide Units by the Ligand "HEIDI"; Two new Hydroxo(oxo)iron Clusters Containing 19 and 17 Iron Atoms. *Angew. Chem. Int. Ed.* **1992,** 31, 191.

111. Morgenstern, B.; Sander, J.; Huch, V.; Hegetschweiler, Complexation of a Hetapnuclear Polyoxotantalate Anion with K+: Formation of a Supramolecular $[K_6\text{-}(\mu\text{-}OH_2)_6\text{-}(OH_2)_8]^{6+}$ Ring Structure. *Inorg. Chem.* **2001,** 40, 5307.

112. Brockman, J. T.; Huffman, J. C.; Christou, G., A High Nuclearity, Mixed-Valence Manganeses (III,IV) Complex: $[Mn_{21}O_{24}(OMe)_8(O_2CCH_2tBu)_{16}(H_2O)_{10}]$. *Angew. Chem. Int. Ed.* **2002,** 41, 2506.

113. Zaleski, C. M.; Depperman, E. C.; Denrinou-Samara, C.; Alexiou, M.; Kampf, J. W.; Kessissoglou, D. P.; Kirk, M. L.; Pecoraro, V. L., Metallacryptate Single-Molecule Magnets: Effect of Lower Molecular Symmetry on Blocking Temperature. *J. Am. Chem. Soc.* **2005,** 127, 12862.

114. Day, V. W.; Klemperer, W. G.; Pafford, M. m., Methyltriskaidecazirconates, Molecular froms of Zirconia. *Inorg. Chem.* **2005,** 44, 5397.

115. Denrinou-Samara, C.; Alexiou, M.; Zaleski, C. M.; Kampf, J. W.; Kirk, M. L.; Kessissoglou, D. P.; Pecoraro, V. L., Synthesis and Magnetic Properties of a Metallcryptate that behaves as a Single-Molecular Magnet. *Angew. Chem. Int. Ed.* **2003,** 42, 3763.

116. Smith-Jones, P. M.; Stolz, B.; Bruns, C.; Albert, R.; Reist, H. W.; Freidrich, R.; Mäcke, H. R., Gallium-67/Gallium-68-[DFO]-Octreotide—A Potential Radiopharmaceutical for PET Imaging of Somatostatin Receptor-Positive Tumors: Synthesis and Radiolabeling In Vitro and Preliminary In Vivo Studies. *J. Nuc. Med.* **1994,** 35, (2), 317.

117. Hoffend, J.; Mier, W.; Schuhmacher, J.; Schmidt, K.; Dimitrakopoulou-Strauss, A.; Strauss, L. G.; Elsehut, M.; Kinscherf, R.; Haberkorn, U., Gallium-68-DOTA-albumin as a PET blood-pool marker: experimental evaluation in vivo. *Nuc. Med. Bio.* **2005,** 32, (3), 287.

118. Kersting, B.; M. Meyer; Powers, R. E.; Raymond, K. N., Dinuclear Catecholate Helicates: Their Inversion Mechanism. *J. Am. Chem. Soc.* **1996,** 118, 7221.

119. Cohen, S. M.; Raymond, K. N., Catecholate/salicylate heteropodands: Demonstration of a catecholate to salicylate coordination change. *Inorganic Chemistry* **2000,** 39, (16), 3624-3631.

120. Johnson, D. W.; Raymond, K. N., The Self-Assembly of a Ga_4L_6 Tetrahedral Cluster Thermodynamically Driven by Host-Guest Interactions. *Inorg. Chem.* **2001,** 40, 5157-5161.

121. Gatlin, J. T.; Mensinger, Z. L.; Meyers, S. T.; Zakharov, L. N.; Keszler, D. A.; MacInnes, D.; Johnson, D. W., Heterometallic Group 13 Keggin-like Nanoclsuters. **Manuscript in preparation.**

122. Gerasko, O. A.; Mainicheva, E. A.; Naumov, D. Y.; Kuratieva, N. V.; Sokolov, M. N.; Fedin, V. P., Synthesis and Crystal Structure of Unprecedented Oxo/Hydroxo-Bridged Polynuclear Gallium(III) Aqua Complexes. *Inorg. Chem.* **2005,** 44, 4133.

123. Mainicheva, E. A.; Gerasko, O. A.; Sheludyakova, L. A.; Naumov, D. Y.; Naumova, M. I.; Fedin, V. P., Synthesis and crystal structures of supramolecular compounds of polynuclear aluminum(III) aqua hydroxo complexes with cucurbit[6]uril. *Russ. Chem. Bull., Int. Ed.* **2006,** 55, (2), 267.

124. Coronado, E.; Galán-Mascarós, J. R.; Giménez-Saiz, C.; Gómez-García, C. J.; Matínez-Ferrero, E.; Almeida, M.; Lopes, E. B., Metallic Conductivity in a Polyoxovandate Radical Salt of BEDT-TTF: Synthesis, Structure and Physical Characterization. *Adv. Mater.* **2004,** 16, 324.

125. Coronado, E.; Giménez-Saiz, C.; Gómez-García, C. J., Recent advances in polyoxometalate-containing molecular conductors. *Coord. Chem. Rev.* **2005,** 249, 1776.

126. Lapinski, A.; Starodub, V.; Golub, M.; Kravchenko, A.; Baumer, V.; Faulques, E.; Graja, A., Characterization and spectral Properties of the new organic metal $(BEDT\text{-}TTF)_6(Mo_8O_{26})(DMF_{(3)})$. *Synth. Met.* **2003,** 138, 483.

127. Alley, K. G.; Bircher, R.; Waldmann, O.; Ochsenbein, S. T.; Güdel, H. U.; Moubaraki, B.; Murray, K. S.; Fernandez-Alonso, F.; Abrahams, B. F.; Boskovic, C., Mixed-Valent Cobalt Spin Clusters: a Hexanuclear Complex and a One-Dimensional Coordination Polymer Comprised of Alternating Hepta- and Mononuclear Fragments. *Inorg. Chem.* **2006,** 45, 8950.

128. Hyeon, T., Chemical synthesis of magnetic nanoparticles. *Chem. Commun.* **2003**, 927-934.

129. Kong, D.; Li, Y.; Ouyang, X.; Prosvirin, A. V.; Zhao, H.; Ross, J. H., Jr.; Dunbar, K. R.; Clearfield, A., Syntheses, Structure, and magnetic Properties of New Types of Cu(II), Co(II), and Mn(II) organophosphonates Materials: Three-Dimersonal Framworks and a one Dimersion Chain Motif. *Chem. Mater.* **2004,** 16, 3020.

130. Murugesu, M.; Anson, C. E.; Powell, A. K., Engineering of Ferrimagnetic Cu_{12}-cluster arrays throught supramolecular interactions. *Chem. Commun.* **2002**, 1054-1055.

131. Tasiopoulos, A. J.; Vinslava, A.; Wernsdorfer, W.; Abboud, K. A.; Christou, G., Giant Single-Molecule Magnets: A $\{Mn_{84}\}$ Torus and Its Supramolecular Nanotubes. *Angew. Chem. Int. Ed.* **2004,** 43, 2117.

132. Viertelhaus, M.; Adler, P.; Clérac, R.; Anaon, C. E.; Powell, A. K., Iron(II) Formate $[Fe(O_2CH)_2]\cdot 1/3HCO_2H$: A Mesoporous Magnet Solvothermal Syntheses and Crystal Structures of the Isomorphous Framework Metal(II) Formates $[M(O_2CH)_2]\cdot n$(Solvent) (M Fe, Co, Ni, Zn, Mg). *Eur. J. Inorg. Chem.* **2005**, 692.

133. Koizumi, S.; Nihei, M.; Shiga, T.; Nakano, M.; Nojiri, H.; Bircher, R.; Waldmann, O.; Ochsenbein, S. T.; Güdel, H. U.; Fernandez-Alonso, F.; Oshio, H., A Wheel-Shaped Single-Molecule Magnet of $[Mn(II)_3Mn(III)_4]$: Quantum Tunneling of Magnetization under Static and Pulse Magnetic Fields. *Chem. - Eur. J.* **2007,** 13, 8445.

134. Saalfrank, R. W.; Scheurer, A.; Prakash, R.; Heinemann, F. W.; Nakajima, T.; Hampel, F.; Leppin, R.; Pilawa, B.; Rupp, H.; Müller, P., Synthesis, Redox, and Magnetic Properties of a Neutral, Mixed-Valent Heptanuclear Manganese Wheel with S) 27/2 High-Spin Ground State. *Inorg. Chem.* **2007,** 46, 1586.

135. Manoli, M.; Prescimone, A.; Bagai, R.; Mirshra, A.; Murugesu, M.; Parsons, S.; Wernsdorfer, W.; Christou, G.; Brechin, E. K., High-Spin Mn Wheels. *Inorg. Chem.* **2007,** 46, 6988.

136. Saalfrank, R. W.; Deutscher, C.; Maid, H.; Ako, A. M.; Sperner, S.; Nakajima, T.; Bauer, W.; Hampel, F.; Heb, B. A.; van Eikema Hommes, N. J. R.; Puchta, R.; Heinemann, F. W., Synthesis, Structure, and Dynamics of Six-Membered Metallacoronands and Metallodendrimers of Iron and Indium . *Chem. - Eur. J.* **2004,** 10, 1899.

137. Liu, Y.-B.; Duan, L.-M.; Yang, X.-M.; Xu, J.-Q.; Zhang, Q.-B.; Lu, Y.-K.; Liu, J., Hydrothermal synthesis and characterization of two new bicapped Keggin heteropoly tungstovanadated derivatives. *J. Solid State Chem.* **2006,** 179, 122.

138. Papaefstathiou, G. S.; Manessi, A.; Raptopoulou, C. P.; Terzis, A.; Zafiropoulos, T. F., Methanolysis as a Route to Gallium(III) Clusters: Synthesis and Structural Characterization of a Decanuclear Molecular Wheel. *Inorg. Chem.* **2006,** 45, 8823.

139. King, P.; Stamatatos, T. C.; Abboud, K. A.; Christou, G., Reversible Size Modification of Iron and Gallium Molecular Wheels: A Ga_{10} "Gallic Wheel" and Large Ga_{18} and Fe_{18} Wheels. *Angew. Chem. Int. Ed.* **2006,** 45, 7379.

140. Salignac, B.; Riedel, S.; Dolbecq, A.; Sécheresse, F.; Cadot, E., "Wheeling Templates" in Molecular Oxothiomolybdate Rings: Synthesis, Strcutures and Dynamics. *J. Am. Chem. Soc.* **2000,** 122, 10381.

141. Brüdgam, I.; Fuchs, J.; Hartl, H.; Palm, R., Two new Isopolyoxotungstates(VI) with Empirical Composition $Cs_2W_2O_7$•2 H_2O and $Na_2W_2O_7$ • H_2O: and Icosatetratungstate and a Polymeric Compound. *Angew. Chem. Int. Ed.* **1998,** 37, 2668.

142. Salmon, L.; Thuery, P.; Ephritikhine, M., *Polyhedron* **2004,** 23, 623.

143. Modec, B.; Brencic, J. V.; Koller, J., *Eur. J. Inorg. Chem.* **2004**, 1611.

144. Darensbourg, D. J.; Gray, R. L.; Delord, T., *Inorg. Chem. Acta* **1985,** 98, L39.

145. Onoda, A.; Yamada, Y.; Okamura, T.; Doi, M.; Yamamoto, H.; Ueyama, N., *J. Am. Chem. Soc.* **2002,** 124, 1052.

146. Wang, R.; Selby, H. D.; Liu, H.; Carducci, M. D.; Jin, T.; Zheng, Z.; Anthis, J. W.; Staples, R. J., *Inorg. Chem.* **2002,** 41, 278.

147. Beattie, J. K.; Hambley, T. W.; Klepetko, J. A.; Masters, A. F.; Turner, P., *Chem. Commun.* **1998**, 45.

148. Chen, Q.; Liu, S.; Zubieta, J., *Angew. Chem. Int. Ed.* **1988,** 27, 1724.

149. Chen, Q.; Liu, S.; Zubieta, J., *Inorg. Chem.* **1989,** 28, 4433.

150. Modec, B.; Dolenc, D.; Brencic, J. V.; Koller, J.; Zubieta, J., *Eur. J. Inorg. Chem.* **2005**, 3224.

151. Kessler, V. G.; Turova, N. Y.; Turevskaya, E. P., *Inorg. Chem. Commun.* **2002,** 5, 549.

152. Kajiwara, T.; Wu, H.; Ito, T.; Iki, N.; Miyano, S., Octalanthanide Wheels Supported by *p-tert*-Butylsulfonylcalix[4]arene. *Angew. Chem. Int. Ed.* **2004,** 43, 1832.

Chapter II

1. Seichter, W.; Mogel, H.-J.; Brand, P.; Salah, D., Crystal Structure and Formation of the Aluminum Hydroxide Cloride $[Al_{13}(OH)_{24}(H_2O)_{24}]Cl_{15} \cdot 13\ H_2O$. *Eur. J. Inorg. Chem.* **1998**, 795-797.

2. Goodwin, J. C.; Teat, S. J.; Heath, S. L., How do clusters grow? The Synthesis and Structure of Polynuclear Hydroxide Gallium(III) Clusters. *Angew. Chem. Int. Ed.* **2004**, *43*, 4037-4041.

3. Jordan, P. A.; Clayden, N. J.; Heath, S. L.; Moore, G. R.; Powell, A. K.; Tapparo, A., Defining speciation profiles of Al^{3+} complexed with small organic ligands: the Al^{3+}- heidi system. *Coord. Chem. Rev.* **1996**, *149*, 281-309.

4. Gerasko, O. A.; Mainicheva, E. A.; Naumov, D. Y.; Kuratieva, N. V.; Sokolov, M. N.; Fedin, V. P., Synthesis and Crystal Structure of Unprecedented Oxo/Hydroxo-Bridged Polynuclear Gallium(III) Aqua Complexes. *Inorg. Chem.* **2005**, *44*, 4133.

5. Casey, W. H., Large Aqueous Aluminum Hydroxide Molecules. *Chem. Rev.* **2006**, *106*, 1.

6. Mainicheva, E. A.; Gerasko, O. A.; Sheludyakova, L. A.; Naumov, D. Y.; Naumova, M. I.; Fedin, V. P., Synthesis and crystal structures of supramolecular compounds of polynuclear aluminum(III) aqua hydroxo complexes with cucurbit[6]uril. *Russ. Chem. Bull., Int. Ed.* **2006**, *55*, (2), 267.

7. Schmitt, W.; Baissa, E.; Mandel, A.; Anson, C. E.; Powell, A. K., $[Al_{15}(\mu_3\text{-}O)_4(\mu_3\text{-}OH)_6(\mu\text{-}OH)_{14}(hpdta)_3]^{3-}$ - A New Al_{15} Aggergate Which forms a Suprmolecular Zeotype. *Angew. Chem. Int. Ed.* **2001**, *40*, 3578-3581.

8. Hagrman, P. J.; Finn, R. C.; Zubieta, J., *Soild State Sci.* **2001**, *3*, 745-774.

9. Crawford, N. R. M.; Long, J. R., *Inorg. Chem.* **2001**, *40*, 3456-3462.

10. Michot, L. J.; Montarges-Pelletier, E.; Lartiges, B. S.; de la Caillerie, J.-B. d. E.; Briois, L., Formation Mechanism of the Ga_{13} Keggin Ion: A combined EXFAS and NMR Study. *J. Am. Chem. Soc.* **2000**, *122*, 6048-6056.

11. Allouche, L.; Gerardin, C.; Loiseau, T.; Ferey, G.; Taulelle, F., Al_{30} : Giant Aluminum Polycation. *Angew. Chem. Int. Ed.* **2000**, *39*, 511-514.

12. Schmitt, W.; Jordan, P. A.; Henderson, R. K.; Moore, G. R.; Anson, C. E.; Powell, A. K., Synthesis, Structure and Properties of hydrolytic Al(III) aggregates and Fe(III) analogues formed with iminodiacetate-based chelating ligands. *Coord. Chem. Rev.* **2002**, *228*, 115-126.

13. Casey, W. H.; Phillips, B. L.; Furrer, G., Aqueous Aluminum Polynuclear Complexes and Nanoclusters: A Review. In *Reviews in Mineralogy & Geochemistry*, Mineralogical Society of America: Washington D.C., **2001**; Vol. 44, pp 167-190.

14. Rowsell, J.; Nazar, L. F., Speciation and Thermal Transformation in Alumina Sols: Structures of the Polyhydroxoaluminum Cluster $[Al_{30}O_8(OH)_{56}(H_20)_{26}]^{18+}$ and its ∂-Keggin Moiete. *J. Am. Chem. Soc.* **2000**, *122*, 3777-3778.

15. Harris, W. R.; Messori, L., A comparative study of aluminum(III), gallium(III), indium(III), and thallium(III) binding to human serum transferrin. *Coord. Chem. Rev.* **2002**, *228*, 237-262.

16. Alvisiatos, A.; Barbara, P. F.; Castleman, A. W.; Chang, J.; Dixon, D. A.; Klein, M. L.; Mclendon, G. L.; MIller, J. S.; Ratner, M. A.; Rossky, P. J.; Stupp, S. I.; Thompson, M. E., From Molecules to Materials: Current Trends And Future Directions. *Adv. Mater.* **1998**, *10*, 1297-1336.

17. Bradley, S. M.; Kydd, R. A.; Yamdagni, R., Detection of a new Polymeric species formed through the Hydrolysis of Gallium(III) Salt Solutions. *J. Chem. Soc. Dalton Trans.* **1990**, 413-417.

18. Bradley, S. M.; Kydd, R. A., Comparison of the Species formed Upon Base Hydrolyses of Gallium(III) adn Iron(III) Aqueous Solutions: The Possibility of Existence of an $[FeO_4Fe_{12}(OH)_{24}(H_2O)_{12}]^{7+}$ polyxoxocation. *J. Chem. Soc. Dalton Trans.* **1993**, 2407-2413.

19. Heath, S. L.; Jordan, P. A.; Johnson, I. D.; Moore, G. R.; Powell, A. K.; Helliwell, M., Comparative X-ray and ^{27}Al NMR Spectroscopic Studies of the Speciation of Aluminum in Aqueous Systems: Al(III) Complexes of $N(CH_2CO_2H)_2(CH_2CH_2OH)$. *J. Inorg. Biochem.* **1995**, *59*, 785-794.

20. Velikorodov, A. V., *Zh. Org. Kim.* **2000**, *36*, 256-262.

21. Maleski, R. J.; Kluge, M.; Sicker, D., *Synth. Commun.* **1995**, *25*, 2327-2335.

22. Raphael, R. A.; Ravenscroft, P., *J. Chem. Soc. Perkin Trans. 1* **1988**, 1823-1825.

23. Johansson, G., *Acta Chem. Scand.* **1960**, *14*, 771-773.

24. Schonherr, S., *Anorg. Allg. Chem.* **1983**, *503*, 37-42.

Chapter III

1. Rather, E.; Gatlin, J. T.; Nixon, P. G.; Tsukamoto, T.; Kravtsov, V.; Johnson, D. W., A Simple Organic Reaction Mediates the Crystallization of the Inorganic Nanocluster $[Ga_{13}(\mu_3\text{-}OH)_6(\mu_2\text{-}OH)_{18}(H_2O)_{24}](NO_3)_{15}$. *J. Am. Chem. Soc.* **2005,** 127, 3242-3243.

2. Dieterich, D. A.; Paul, I. C.; Curtin, D. Y., Structural Studies on Nitrosobenzene and 2-Nitrosobenzoic Acid. Crystals and Molecular Structures of *cis*-Azobenzene Dioxide and *trans*-2,2'-Dicarboxyazobenzene Dioxide. *J. Am. Chem. Soc.* **1974,** 96, 6372.

3. *Cambridge Structural Database*, Cambridge Crystallographic Data Centre: 12 Union Road, Cambridge, CB2 1EZ, UK, November 2006.

4. In *Langs Handbook of Chemistry*, 15th ed.; Dean, J. A., Ed. McGraw Hill: 1999; p 8153.

5. Okabe, N.; Tamaki, K.; Suga, T.; Kohyama, Y., Aluminium Cupferronate, $[Al(C_6H_5N_2O_2)_3]$. *Acta Cryst.* **1995,** C51, 1295.

6. Casey, W. H., Large Aqueous Aluminum Hydroxide Molecules. *Chem. Rev.* **2006,** 106, 1.

7. Mainicheva, E. A.; Gerasko, O. A.; Sheludyakova, L. A.; Naumov, D. Y.; Naumova, M. I.; Fedin, V. P., Synthesis and crystal structures of supramolecular compounds of polynuclear aluminum(III) aqua hydroxo complexes with cucurbit[6]uril. *Russ. Chem. Bull., Int. Ed.* **2006,** 55, (2), 267.

8. *Merck Index*. 11th ed.; 1989.

9. Chellamani, A.; Suresh, R., Kinetics and Mechanism of Oxidation of Triphenylphosphine by hydrogen-Peroxide. *Reac. Kinet. Cat. Lett.* **1988,** 37, (2), 501.

10. Srinivasan, C.; Chellamani, A., Kinetics of Oxidation of Triarylasines by Potassium Peroxodisulfate. *Indian J. Chem. Sec. A* **1984,** 23A, 684.

11. Srinivasan, C.; Pitchumani, K., Mechanism of the Oxidation of Triphenyl Derivatives of P, As, and Sb by Peroxodiphospahte. *Can. J. Chem.* **1985,** 63, (8), 2285.

12. Hasbrouck, L. J.; Carlin, C. M.; Risley, J. M., Origin of the oxygen in the oxidation of triphenylphosphine by potassium perphosphate. *Inorg. Chem. Acta* **1997,** 258, (1), 123.

13. Copley, D. B.; Fairbrother, F.; Miller, J. R.; Thompson, A., The Oxidation of Triphenylphosphine with Hydrogen Peroxide. *Proc. Chem. Soc.* **1964**, 300.

14. Arbuzov, B. A., Oxidation of organic compounds with peracetic and perbenzoic acids. *Journal fuer Praktische Chemie* **1931,** 131, 357.

15. Glidewell, C.; Harris, G. S.; Holden, H. D.; Liles, D. C.; McKechnie, J. S., *J. Fluorine Chem.* **1981,** 18, 143.

16. Beagley, B.; El-Sayrafi, O.; Gott, G. A.; Kelly, D. G.; McAuliffe, C. A.; Mackie, A. G.; MacRory, P. P.; Pritchard, R. G., *J. Chem. Soc. Dalton Trans.* **1988**, 1095.

17. Calleri, M.; Ferguson, G., *Cryst. Struct. Commun.* **1972,** 1, 331.

18. Weitze, A.; Henshel, D.; Blaschette, A.; Jones, P. G., *Z. Anorg. Allg. Chem.* **1995,** 621, 1746.

19. Goodwin, J. C.; Teat, S. J.; Heath, S. L., How do clusters grow? The Synthesis and Structure of Polynuclear Hydroxide Gallium(III) Clusters. *Angew. Chem. Int. Ed.* **2004,** 43, 4037-4041.

20. Allouche, L.; Gerardin, C.; Loiseau, T.; Ferey, G.; Taulelle, F., Al_{30} : Giant Aluminum Polycation. *Angew. Chem. Int. Ed.* **2000,** 39, 511-514.

21. Casey, W. H.; Phillips, B. L.; Furrer, G., Aqueous Aluminum Polynuclear Complexes and Nanoclusters: A Review. In *Reviews in Mineralogy & Geochemistry*, Mineralogical Society of America: Washington D.C., 2001; Vol. 44, pp 167-190.

22. Rowsell, J.; Nazar, L. F., Speciation and Thermal Transformation in Alumina Sols: Structures of the Polyhydroxoaluminum Cluster $[Al_{30}O_8(OH)_{56}(H_20)_{26}]^{18+}$ and its ∂-Keggin Moiete. *J. Am. Chem. Soc.* **2000,** 122, 3777-3778.

23. Schmitt, W.; Baissa, E.; Mandel, A.; Anson, C. E.; Powell, A. K., $[Al_{15}(\mu_3\text{-}O)_4(\mu_3\text{-}OH)_6(\mu\text{-}OH)_{14}(hpdta)_3]^{3-}$ - A New Al_{15} Aggergate Which forms a Suprmolecular Zeotype. *Angew. Chem. Int. Ed.* **2001,** 40, 3578-3581.

24. Schmitt, W.; Jordan, P. A.; Henderson, R. K.; Moore, G. R.; Anson, C. E.; Powell, A. K., Synthesis, Structure and Properties of hydrolytic Al(III) aggregates and Fe(III) analogues formed with iminodiacetate-based chelating ligands. *Coord. Chem. Rev.* **2002,** 228, 115-126.

25. Seichter, W.; Mogel, H.-J.; Brand, P.; Salah, D., Crystal Structure and Formation of the Aluminum Hydroxide Cloride $[Al_{13}(OH)_{24}(H_2O)_{24}]Cl_{15} \bullet 13\ H_2O$. *Eur. J. Inorg. Chem.* **1998**, 795-797.

26. Heath, S. L.; Jordan, P. A.; Johnson, I. D.; Moore, G. R.; Powell, A. K.; Helliwell, M., Comparative X-ray and ^{27}Al NMR Spectroscopic Studies of the Speciation of Aluminum in Aqueous Systems: Al(III) Complexes of $N(CH_2CO_2H)_2(CH_2CH_2OH)$. *J. Inorg. Biochem.* **1995,** 59, 785-794.

27. Casey, W. H.; Olmstead, M. M.; Phillips, B. L., A New Aluminum Hydroxide Octamer, $[Al_8(OH)_{14}(H_2O)_{18}](SO_4)_5 \bullet 16H_2O$. *Inorg. Chem.* **2005,** 44, 4888.

28. Johansson, G., *Acta Chem. Scand.* **1960,** 14, 771-773.

29. Lee, A. P.; Phillips, B. L.; Olmstead, M. M.; Casey, W. H., Synthesis and Characterization of the $GeO_4Al_{12}(OH)_{24}(OH_2)_{12}^{8+}$ Polyoxocation. *Inorg. Chem.* **2001,** 40, 4485.

30. Casey, W. H.; Phillips, B. L., Kinetics of oxygen exchange between sites in the $GaO_4Al_{12}(OH)_{24}(H_2O)_{12}^{7+}$(aq) molecule and aqueous solution. *Geochimica et Cosmochimica Acta* **2001,** 65, (5), 705.

31. Gerasko, O. A.; Mainicheva, E. A.; Naumov, D. Y.; Kuratieva, N. V.; Sokolov, M. N.; Fedin, V. P., Synthesis and Crystal Structure of Unprecedented Oxo/Hydroxo-Bridged Polynuclear Gallium(III) Aqua Complexes. *Inorg. Chem.* **2005,** 44, 4133.

32. Wulfsberg, G., University Science Books: Sausalito, CA, 2000; p 59.

33. Gatlin, J. T.; Mensinger, Z. L.; Meyers, S. T.; Zakharov, L. N.; Keszler, D. A.; M; Johnson, D. W., Heterometallic Group 13 Keggin-like Nanoclsuters. **Manuscript in preparation.**

34. Anderson, J. S., Constitution of the Poly-acids. *Nature* **1937,** 140, 850.

35. Evans, H. T., Jr, The Crystal Structures of Ammoium and Potassium Molydotellurates. *J. Am. Chem. Soc.* **1948,** 70, (3), 1291.

36. Van der Sluis, P.; Spek, A. L., BYPASS: an effective method for the refinement of crystal structures containing disordered solvent regions. *Acta Cryst.* **1990,** A46, 194-201.

Chapter IV

1. Seichter, W.; Mogel, H.-J.; Brand, P.; Salah, D., Crystal Structure and Formation of the Aluminum Hydroxide Cloride $[Al_{13}(OH)_{24}(H_2O)_{24}]Cl_{15} \cdot 13\ H_2O$. *Eur. J. Inorg. Chem.* **1998**, 795-797.

2. Heath, S. L.; Jordan, P. A.; Johnson, I. D.; Moore, G. R.; Powell, A. K.; Helliwell, M., Comparative X-ray and ^{27}Al NMR Spectroscopic Studies of the Speciation of Aluminum in Aqueous Systems: Al(III) Complexes of $N(CH_2CO_2H)_2(CH_2CH_2OH)$. *J. Inorg. Biochem.* **1995,** 59, 785-794.

3. Goodwin, J. C.; Teat, S. J.; Heath, S. L., How do clusters grow? The Synthesis and Structure of Polynuclear Hydroxide Gallium(III) Clusters. *Angew. Chem. Int. Ed.* **2004,** 43, 4037-4041.

4. Rather, E.; Gatlin, J. T.; Nixon, P. G.; Tsukamoto, T.; Kravtsov, V.; Johnson, D. W., A Simple Organic Reaction Mediates the Crystallization of the Inorganic Nanocluster $[Ga_{13}(\mu_3\text{-}OH)_6(\mu_2\text{-}OH)_{18}(H_2O)_{24}](NO_3)_{15}$. *J. Am. Chem. Soc.* **2005,** 127, 3242-3243.

5. Gatlin, J. T.; Mensinger, Z. L.; Meyers, S. T.; Zakharov, L. N.; Keszler, D. A.; Johnson, D. W., Heterometallic Group 13 Keggin-like Nanoclsuters. **Manuscript in preparation.**

6. Gerasko, O. A.; Mainicheva, E. A.; Naumov, D. Y.; Kuratieva, N. V.; Sokolov, M. N.; Fedin, V. P., Synthesis and Crystal Structure of Unprecedented Oxo/Hydroxo-Bridged Polynuclear Gallium(III) Aqua Complexes. *Inorg. Chem.* **2005,** 44, 4133.

7. Casey, W. H.; Olmstead, M. M.; Phillips, B. L., A New Aluminum Hydroxide Octamer, $[Al_8(OH)_{14}(H_2O)_{18}](SO_4)_5 \cdot 16H_2O$. *Inorg. Chem.* **2005,** 44, 4888.

8. Gatlin, J. T.; Mensinger, Z. L.; Zakharov, L. N.; MacInnes, D.; Johnson, D. W., Facile Synthesis of Aluminum13 Keggin-Like Nanocluster. *Inorg. Chem.* **manuscript accepted.**

9. Bradley, S. M.; Kydd, R. A., Comparison of the Species formed Upon Base Hydrolyses of Gallium(III) adn Iron(III) Aqueous Solutions: The Possibility of Existence of an $[FeO_4Fe_{12}(OH)_{24}(H_2O)_{12}]^{7+}$ polyxoxocation. *J. Chem. Soc. Dalton Trans.* **1993**, 2407-2413.

10. Bradley, S. M.; Kydd, R. A.; Yamdagni, R., Detection of a new Polymeric species formed through the Hydrolysis of Gallium(III) Salt Solutions. *J. Chem. Soc. Dalton Trans.* **1990**, 413-417.

11. Kudynska, J.; Buckmaster, H. A.; Kawano, K.; Bradley, S. M.; Kydd, R. A., A 9 GHz cw-electron-paramagnetic resonance study of the sulphate salts of tridecameric $[Mn_xAl_{13-x}O_4(OH)_{24}(H_20)_{12}]^{(7-x)}$. *J. Chem. Phys.* **1993,** 99, 3329.

12. Oszkó, A.; Kiss, J.; Kiricsi, I., XPS investigations on the feasibility of isomorphous substitution of octahedral Al^{3+} for Fe^{3+} in Keggin ion salts. *Phys. Chem. Chem. Phys.* **1999,** 1, 2565.

13. Parker, W. O., Jr.; Millini, R.; Kiricsi, I., Metal Substitution in Keggin-Type Tridecameric Aluminum-Oxo-Hydroxy Clusters. *Inorg. Chem.* **1997,** 36, 571.

14. Nsouli, N. H.; Bassil, B. S.; Dickman, M. H.; Kortz, U.; Keita, B.; Nadjo, L., Synthesis and Structure of Dilacunary Decatungstogermanate, $[g\text{-}GeW_{10}O_{36}]^{8-}$. *Inorg. Chem.* **2006,** 45, 3858.

15. Wang, J.-P.; Zhao, J.-W.; Duan, X.-Y.; Niu, J.-Y., Syntheses and Structures of One- and Two-Dimensional Organic-Inorganic Hybrid Rare Earth Derivatives Based on Monovacant Keggin-Type Polyoxotungstates. *Cryst. Growth Des.* **2006,** 6, (2), 507.

16. Lee, A. P.; Furrer, G.; Casey, W. H., On the Acid–Base Chemistry of the Keggin Polymers: $GaAl_{12}$ and $GeAl_{12}$. *J. Colloid Interface Sci.* **2002,** 250, 269.

17. Cowan, J. J.; Bailey, A. J.; Heintz, R. A.; Do, B. T.; Hardcastle, K. I.; Hill, C. L.; Weinstock, I. A., Formation, Isomerization, and Derivatization of Keggin Tungstoaluminates. *Inorg. Chem.* **2001,** 40, 6666.

18. Carrier, X.; de la Caillerie, J.-B. d. E.; Lambert, J.-F.; Che, M., The Support as a Chemical Reagent in the Preparation of $WO_x/g\text{-}Al_2O_3$ Catalysts: Formation and Deposition of Aluminotungstic Heteropolyanions. *J. Am. Chem. Soc.* **1999,** 121, 3377.

19. Lee, A. P.; Phillips, B. L.; Olmstead, M. M.; Casey, W. H., Synthesis and Characterization of the $GeO_4Al_{12}(OH)_{24}(OH_2)_{12}^{8+}$ Polyoxocation. *Inorg. Chem.* **2001,** 40, 4485.

20. Heath, S. L.; Powell, A. K., The Trapping of Iron Hydroxide Units by the Ligand "HEIDI"; Two new Hydroxo(oxo)iron Clusters Containing 19 and 17 Iron Atoms. *Angew. Chem. Int. Ed.* **1992,** 31, 191.

21. Chiang, H. Q.; Hong, D.; Hung, C. M.; Presley, R. E.; Wager, J. F.; Park, C.-H.; Keszler, D. A.; Herman, G. S., Thin-film transistors with amorphous indium gallium oxide channel layers. *J. Vac. Sci. Technol.* **2006,** 24, 2702.

22. Presley, R. E.; Honga, D.; Chianga, H. Q.; Hunga, C. M.; Hoffmanb, R. L.; Wager, J. F., Transparent ring oscillator based on indium gallium oxide thin-film transistors. *Soild State Electronics* **2006,** 50, 500.

23. Nomura, K.; Ohta, H.; Takagi, A.; Kamiva, T.; Hirano, M.; Hosono, H., Room-temperature fabrication of transparent flexibile thin-film trasistors using amorphous oxide semicondutors. *Nature* **2004,** 432, 488.

24. Anderson, J. T.; Munsee, C.; Hung, C. M.; Phung, T. M.; Johnson, D. C.; Herman, G. S.; Wager, J. F.; Keszler, D. A., *Adv. Funct. Mater.* **in press.**

25. Meyers, S. T.; Anderson, J. T.; Hong, D.; Hung, C. M.; Wager, J. F.; Keszler, D. A., *Chem. Mater.* **in press.**

Chapter V

1. Li, C.; Lai, M. Y. D.; Leong, W. K., ToF-SIMS analysis of surface-anchored organometallic clusters. *J. Organometallic Chem.* **2005,** 690, 2861.

2. Nazmutdinov, R. R.; Zinkicheva, T. T., *Russ. J. Electrochem.* **2004,** 40, (4), 379.

3. Rostam-Khani, P.; Philipsen, J.; Jansen, E.; Eberhard, H.; Vullings, P., *Appl. Surf. Sci.* **2006,** 252, 7255.

4. Schröder-Oeynhausen, F.; Burkhardt, B.; Fladung, T.; Kötter, F.; Schnieders, A.; Wiedmann, L.; Benninghoven, A., *J. Vac. Sci. Technol.* **1998,** 16, 1002.

5. Aubriet, F.; Poleunis, C.; Bertrand, P., Investigation of the cluster ion formation process for inorganic compounds in static SIMS . *Appl. Surf. Sci.* **2003,** 203, 114.

6. Graham, D. J.; Wagner, M. S.; Castner, D. G., Information from complexity: Challenges of TOF-SIMS data interpretation. *Appl. Surf. Sci.* **2006,** 252, 6860.

7. Sein, L. T., Jr., Using Punnett Squares To Facilitate Students' Understanding of Isotopic Distributions in Mass Spectrometry. *J. Chem. Ed.* **2006,** 83, 228.

8. Li, Z.; Hirokawa, K., Ga+ Primary Ion ToF-SIMS Fragment Pattern of Metals and Inorganic Compounds. *Anal. Sci.* **2003,** 19, 1231.

9. Li, Z.; Hirokawa, K., Ga+ Primary Ion ToF-SIMS fragment pattern of inorganic compounds and Metals. *Appl. Surf. Sci.* **2003,** 220, 136.

10. Casey, W. H.; Olmstead, M. M.; Phillips, B. L., A New Aluminum Hydroxide Octamer, $[Al_8(OH)_{14}(H_2O)_{18}](SO_4)_5 \bullet 16H_2O$. *Inorg. Chem.* **2005,** 44, 4888.

11. Goodwin, J. C.; Teat, S. J.; Heath, S. L., How do clusters grow? The Synthesis and Structure of Polynuclear Hydroxide Gallium(III) Clusters. *Angew. Chem. Int. Ed.* **2004,** 43, 4037-4041.

12. CAChe *CAChe*, 6.1.1; Fujitsu Limitied, Inc.: U.S.A., 2001.

13. Garrison, B. J.; Winograd, N.; Harrison, D. E., Jr., Atomic and Molecular ejection from ion-bombarded reacted single-crystals surfaces. Oxygen on Copper(100). *Phys. Rev. B* **1978,** 18, (11), 6000.

14. Colton, R. J., Molecular seconday ion mass spectrometry (SIMS). *J. Vac. Sci. Technol.* **1981,** 78, 737.

15. Garrison, B. J.; Winograd, N.; Harrison, D. E., Jr., Formation of Small Metal Clusters by ion bombardment of Single crystal surfaces. *J. Chem. Phys.* **1978,** 69, (4), 1440.

16. Pachuta, S. J.; Cooks, R. G., Mechanisms in Molecular SIMS. *Chem. Rev.* **1987,** 87, 647.

17. Wucher, A.; Garrison, B. J., Cluster formation in sputtering: A molecular dynamics study using the MD/MC corrected Effective medium Potential. *J. Chem. Phys.* **1996,** 105, 5999.

18. Wucher, A., Internal Energy of Sputtered Metal Clusters. *Phys. Rev. B* **1994,** 49, (3), 2012.

19. Wucher, A.; Garrison, B. J., Unimolecular Decomposition in the sputtering of metal clsuters. *Phys. Rev. B* **1992,** 46, (8), 4855.

20. Anderson, J. T.; Munsee, C.; Hung, C. M.; Phung, T. M.; Johnson, D. C.; Herman, G. S.; Wager, J. F.; Keszler, D. A., *Adv. Funct. Mater.* **in press.**
21. Meyers, S. T.; Anderson, J. T.; Hong, D.; Hung, C. M.; Wager, J. F.; Keszler, D. A., *Chem. Mater.* **in press.**

22. Brauman, J. I., Least Squares Analysis and Simplification of Multi-Isotope Mass Spectra. *Anal. Chem.* **1966,** 38, 607.

Chapter VI

1. Yan, C.-H.; He, C.; Wang, L.-Y.; Wang, Z.-M.; Liu, Y.; Liao, C.-S., Self-assembly of tetrahedral M4L6 clusters from a new rigid ligand. *J. Chem. Soc., Dalton Trans.* **2002**, 134.

2. Rice, C. R.; Baylies, C. J.; Clayton, H. J.; Jeffery, J. C.; Paul, R. L.; Ward, M. D., Novel multidentate pyridyl/thiazolyl ligands containing terpyridine units: formation of dinuclear and trinuclear double helicate complexes. *Inorganica Chimica Acta* **2003,** 351, 207-216.

3. Rice, C. R.; Worl, S.; Jeffery, J. C.; Paul, R. L.; Ward, M. D., New multidentate ligands for supramolecular coordination chemistry: double and triple helical complexes of ligands containing pyridyl and thiazolyl donor units. *J. Chem. Soc., Dalton Trans.* **2001**, (5), 550-559.

4. Bell, Z. R.; McCleverty, J. A.; Ward, M. D., New Multidentate Pyrazolyl-Pyridine Ligands — Syntheis and Structures. *Aust. J. Chem.* **2003,** 56, 665.

5. Paul, R. L.; Bell, Z. R.; Fleming, J. S.; Jeffery, J. C.; McCleverty, J. A.; Ward, M. D., Self-Assembly of Anion-Binding Supramolecular Cage Complexes. *Heteroatom Chemistry* **2002,** 13, (6), 567.

6. Saalfrank, R. W.; Bernt, I.; Chowdhry, M. M.; Hampel, F.; Vaughan, G. B. M., Ligand-to-Metal Ratio Controlled Assembly of Tetra- and Hexanuclear Clusters Towards Single-Molecule Magnets. *Chem. Eur. J.* **2001,** 7, 2765.

7. Saalfrank, R. W.; Demleitner, B.; Glaser, H.; Maid, H.; Bathelt, D.; Hampel, F.; Bauer, W.; Teichert, M., Enantiomerisation of Tetrahedral Homochiral $[M_4L_6]$ Clusters: Synchronised Four Bailar Twists and SixAtropena ntiomerisation Processes Monitored by Temperature-Dependent Dynamic 1H NMR Spectroscopy. *Chem. Eur. J.* **2002,** 8, 2679.

8. Saalfrank, R. W.; Glaser, H.; Demleitner, B.; Hampel, F.; Chowdhry, M. M.; Schünemann, V.; Trautwein, A. X.; Vaughan, G. B. M.; Yeh, R.; Davis, A. V.; Raymond, K. N., Self-Assembly of Tetrahedral and Trigonal Antiprismatic Clusters $[Fe_4(L_4)_4]$ and $[Fe_6(L_5)_6]$ on the Basis of Trigonal Tris-Bidentate Chelators. *Chem. Eur. J.* **2002,** 8, 493.

9. Saalfrank, R. W.; Reimann, U.; Göritz, M.; Hampel, F.; Scheurer, A.; Heinemann, F. W.; Büschel, M.; Daub, J., Metal- and Ligand-Directed One-Pot Syntheses, Crystal Structures, and Properties of Novel Oxo-Centered Tetra- and Hexametallic Clusters. *Chem. Eur. J.* **2002,** 8, 3614.

10. CAChe *Cache Quantum*, 6.1.1; Fujitsu Limited: 2001.

11. Bell, Z. e. R.; Jeffery, J. C.; McCleverty, J. A.; Ward, M. D., Assembly of a Truncated-Tetrahedral Chiral $[M_{12}(\mu\text{-}L)_{18}]^{24+}$ Cage. *Angew. Chem. Int. Ed.* **2002,** 41, 2515.

12. Biradha, K.; Seward, C.; Zaworotko, M. J., Helical Coordination Polymers with Large Chiral Cavities. *Angew. Chem. Int. Ed.* **1999,** 38, 492.

13. Paul, R. L.; Couchman, S. M.; Jeffery, J. C.; McCleverty, J. A.; Reeves, Z. R.; Ward, M. D., Effects of metal co-ordination geometry on self-assembly: a dinuclear double helicate complex and a tetranuclear cage complex of a new bis-bidentate bridging ligand. *J. Chem. Soc., Dalton Trans.* **2000**, 845.

14. Saalfrank, R. W.; Löw, N.; Trummer, S.; Sheldrick, G. M.; Teichert, M.; Stalkec, D., Octanuclear Bis(triple-helical) Metal(II) Complexes. *Eur. J. Inorg. Chem.* **1998**, 559.

15. Saalfrank, R. W.; Schmidt, C.; Maid, H.; Hampel, F.; Bauer, W.; Scheurer, A., Enantimericaly Pure Copper (II) Cubanes $[Cu_4L_2(OMe)_4]$ from Chiral Bis-1,3-diketones H_2L through Diastereoselective Self-Assembly. *Angew. Chem. Int. Ed* **2006,** 45, 315.

Appendix B

1. SAINT, S. A. D. I. P., Bruker AXS, Inc., Madison, 1995.

2. G. M. Sheldrick, S., Bruker AXS, Inc., WI, USA, 1997 *SHELXTL*.

3. G. M. Sheldrick, B. A., Inc., WI, USA, 1996, SADABS.

Appendix D

1. Chen, Z.; Zhou, Y.; Weng, L.; Zhang, H.; Zhao, D., Hydrothermal synthesis of two layered indium oxalates with 12-membered apertures. *J. Solid State Chem.* **2003,** 173, 435.

2. Rather, E.; Gatlin, J. T.; Nixon, P. G.; Tsukamoto, T.; Kravtsov, V.; Johnson, D. W., A Simple Organic Reaction Mediates the Crystallization of the Inorganic Nanocluster $[Ga_{13}(\mu_3\text{-}OH)_6(\mu_2\text{-}OH)_{18}(H_2O)_{24}](NO_3)_{15}$. *J. Am. Chem. Soc.* **2005,** 127, 3242-3243.

3. Van der Sluis, P.; Spek, A. L., BYPASS: an effective method for the refinement of crystal structures containing disordered solvent regions. *Acta Cryst.* **1990,** A46, 194-201.

Appendix G

1. Steed, J. W.; Atwood, J. L. *Supramolecular Chemistry*; Wiley, 2000.

2. Garrett, R. H.; Grisham, C. M. *Biochemistry*; 2nd ed.; Saunders College Publishing: Orlando, Flordia, 1999.

3. Lehn, J. M. *Rep. Prog. Phys.* **2004**, *67*, 249.

4. Chambron, J.-C.; Collin, J.-P.; Heitz, V.; Jouvenot, D.; Kern, J.-M.; Mobian, P.; Pomeranc, D.; Sauvage, J.-P. *Eur. J. Org. Chem.* **2004**, 1627.

5. Leigh, D. A.; Lusby, P. J.; Teat, S. J.; Wilson, A. J.; Wong, J. K. Y. *Angew. Chem. Int. Ed.* **2001**, *40*, 1538.

6. Kaiser, G.; Jarrosson, T.; Otto, S.; Ng, Y.-F.; Bond, A. D.; Sanders, J. K. M. *Angew. Chem. Int. Ed.* **2004**, *43*, 1959.

7. Hogg, L.; Leigh, D. A.; Lusby, P. J.; Morelli, A.; Parsons, S.; Wong, J. K. Y. *Angew. Chem. Int. Ed.* **2004**, *43*, 1217.

8. Hasenknopf, B.; Lehn, J.-M.; Boumediene, N.; Leize, E.; Dorsselaer, A. V. *Angew. Chem. Int. Ed.* **1998**, *37*, 3265.

9. Ibukuro, F.; Fujita, M.; Yamaguchi, K.; Sauvage, J.-P. *J. Am. Chem. Soc.* **1999**, *121*, 11014.

10. Feyter, S. D.; Abdel-Mottaleb, M. M. S.; Schuurmans, N.; Verkuijl, B. J. V.; Esch, J. H. v.; Feringa, B. L.; Schryver, F. C. D. *Chem. Eur. J.* **2004**, *10*, 1124.

11. Saalfrank, R. W.; Trummer, S.; Reimann, U.; Chowdhry, M. M.; Hampel, F.; Waldmann, O. *Angew. Chem. Int. Ed.* **2000**, 3492.

12. Saalfrank, R. W.; Glaser, H.; Demleitner, B.; Hampel, F.; Chowdhry, M. M.; Schünemann, V.; Trautwein, A. X.; Vaughan, G. B. M.; Yeh, R.; Davis, A. V.; Raymond, K. N. *Chem. Eur. J.* **2002**, *8*, 493.

13. Yoshizawa, M.; Kusukawa, T.; Fujita, M.; Sakamoto, S.; Yamaguchi, K. *J. Am. Chem. Soc.* **2001**, *123*, 10454-10459.

14. Yoshizawa, M.; Takeyama, Y.; Kusukawa, T.; Fujita, M. *Angew. Chem. Int. Ed.* **2002**, *41*, 1347.

15. Sanmartín, J.; Bermejo, M. R.; García-Deibe, A. M.; Rivas, I. M.; Fernández, A. R. *J. Chem. Soc., Dalton Trans.* **2000**, 4174.

16. Muller, I.; Spillmann, S.; Franck, H.; Pietschnig, R. *Chem. Eur. J.* **2004**, *10*, 2207.

17. Saalfrank, R. W.; Maid, H.; Mooren, N.; Hampel, F. *Angew. Chem. Int. Ed.* **2002**, *41*, 304.

18. Bell, Z. e. R.; Jeffery, J. C.; McCleverty, J. A.; Ward, M. D. *Angew. Chem. Int. Ed.* **2002**, *41*, 2515.

19. Yan, C.-H.; He, C.; Wang, L.-Y.; Wang, Z.-M.; Liu, Y.; Liao, C.-S. *J. Chem. Soc., Dalton Trans.* **2002**, 134.

20. Holliday, B. J.; Mirkin, C. A. *Angew. Chem. Int. Ed.* **2001**, *40*, 2022.

21. Gavrilova, A. L.; Bosnich, B. *Chem. Rev.* **2004**, *104*, 349.

22. Fujita, M. *Chem. Soc. Rev.* **1998**, *27*, 417.

23. Field, J. E.; Combariza, M. Y.; Vacheta, R. W.; Venkataraman, D. *Chem. Commun.* **2002**, 2260.

24. Comba, P.; Schiek, W. *Coord. Chem. Rev.* **2003**, *238-239*, 21.

25. Saalfrank, R. W.; Uller, E.; Demleitner, B.; Bernt, I. *Structure & Bonding* **2000**, *96*, 149.

26. Fekner, T.; Gallucci, J.; Chan, M. K. *Org. Lett.* **2004**, *6*, 989.

27. Boswell, C. A.; Sun, X.; Niu, W.; Weisman, G. R.; Wong, E. H.; Rheingold, A. L.; Anderson, C. J. *J. Med. Chem.* **2004**, *47*, 1465.

28. Aime, S.; Cavallotti, C.; Gianolio, E.; Giovenzana, G. B.; Palmisano, G.; Sisti, M. *Org. Lett.* **2004**, *6*, 1201.

29. Lu, T.; Zhuang, X.; Li, Y.; Chen, S. *J. Am. Chem. Soc.* **2004**, *126*, 4760.

30. Jiang, P.; Guo, Z. *Coord. Chem. Rev.* **2004**, *248*, 205.

31. Baret, P.; Einhorn, J.; Gellon, G.; Pierre, J.-L. *Synthesis* **1998**, 431.

32. CAChe; 6.1.1 ed.; Fujitsu Limited, 2001.

33. Dong, G.; Pang, K.-l.; Duan, C.-y.; Cheng, H.; Meng, Q.-j. *Inorg. Chem.* **2002**, *41*, 5978-5985.

34. Hu, Y.-Z.; Zhang, G.; Thummel, R. P. *Org. Lett.* **2003**, *5*, 2251.

35. CSD In *Cambridge Structure Database System*; Cambridge Cryastallographic Data Centre.

36. CAJ and Eric Synthesis note

37. Isobe, T.; Ishikawa, T. *J. Org. Chem.* **1999**, *64*, 6984.

38. James S. Fleming; Karen L. V. Mann; Charles-Antoine Carraz; Elefteria Psillakis; Jeffery, J. C.; McCleverty, J. A.; Ward, M. D. *Angew. Chem. Int. Ed.* **1998**, *37*, 1279.

39. Paul, R. L.; Bell, Z. R.; Jeffery, J. C.; Harding, L. P.; McCleverty, J. A.; Ward, M. D. *Polyhedron* **2003**, *22*, 781.

40. Gong, J.; Gibb, B. C. *Org. Lett.* **2004**, *6*, 1353.

41. Åkermark, B.; Bjernemose, J.; Börje, A.; Chmielewski, P. J.; Paulsen, H.; Simonsen, O.; Stein, P. C.; Toftlund, H.; Wolny, J. A. *J. Chem. Soc., Dalton Trans.* **2004**, 1215.

42. Colasson, B. X.; Sauvage, J.-P. *Inorg. Chem.* **2004**, *43*, 1895.

43. Brooker, S.; Iremonger, S. S.; Plieger, P. G. *Polyhedron* **2003**, *22*, 665.

44. Shepherd, R. E. *Coord. Chem. Rev.* **2003**, *247*, 147.

45. Biradha, K.; Seward, C.; Zaworotko, M. J. *Angew. Chem. Int. Ed.* **1999**, *38*, 492.

46. Saalfrank, R. W.; Maid, H.; Hampel, F.; Peters, K. *Eur. J. Inorg. Chem.* **1999**, 1859.

47. Tavacoli, S.; Miller, T. A.; Paul, R. L.; Jeffery, J. C.; Ward, M. D. *Polyhedron* **2003**, *22*, 507.

48. Stiriba, S.-E.; Frey, H.; Haag, R. *Angew. Chem. Int. Ed.* **2002**, *41*, 1329.

49. Schmittel, M.; Kalsani, V.; Fenskeb, D.; Wiegrefea, A. *Chem. Commun.* **2004**, 490.

50. Uppadine, L. H.; Gisselbrechtb, J.-P.; Lehn, J.-M. *Chem. Commun.* **2004**, 718.

51. Nitschke, J. R.; Lehn, J.-M. *Proc. Natl. Acad. Sci. USA* **2003**, *100*, 11970.

52. Hasenknopf, B.; Lehn, J.-M.; Boumediene, N.; Emmanuelle Leize; Dorsselaer, A. V. *Angew. Chem. Int. Ed.* **1998**, *37*, 3265.

53. Hogarth, G.; Humphrey, D. G.; Kaltsoyannis, N.; Kim, W.-S.; Lee, M.-y. V.; Norman, T.; Redmond, S. P. *J. Chem. Soc., Dalton Trans.* **1999**, 2705.

54. Zhu, H.-L.; Tong, Y.-X.; Chen, X.-M. *J. Chem. Soc., Dalton Trans.* **2000**, 4182.

55. Charbonniere, L. J.; Williams, A. F.; Piguet, C.; Bernardinelli, G.; Rivara-Minten, E. *Chem. Eur. J.* **1998**, *4*, 485.

56. Piguet, C.; Edder, C.; Rigault, S.; Bernardinelli, G.; Bünzli, J.-C. G.; Hopfgartner, G. *J. Chem. Soc., Dalton Trans.* **2000**, 3999.

57. Schalley, C. A.; Lutzen, A.; Albrecht, M. *Chem. Eur. J.* **2004**, *10*, 1072.

58. Albrecht, M. *Chem. Rev.* **2001**, *101*, 3457-3497.

59. Fujita, M. *Structure & Bonding* **2000**, *96*, 177.

60. Johnson, D. W.; Xu, J.; Saalfrank, R. W.; Raymond, K. N. *Angew. Chem. Int. Ed.* **1999**, *38*, 2882.

61. Telfer, S. G.; Yang, X.-J.; Williams, A. F. *J. Chem. Soc., Dalton Trans.* **2004**, 699.

62. Paul, R. L.; Bell, Z. R.; Fleming, J. S.; Jeffery, J. C.; McCleverty, J. A.; Ward, M. D. *Heteroatom Chemistry* **2002**, *13*, 567.

63. Saalfrank, R. W.; Bernt, I.; Hampel, F. *Chem. Eur. J.* **2001**, *7*, 2770.

64. SAINT, S. A. D. I. P., Bruker AXS, Inc., Madison, 1995.

65. G. M. Sheldrick, B. A., Inc., WI, USA, 1996, Xprep

66. G. M. Sheldrick, B. A., Inc., WI, USA, 1996, SADABS.

67. G. M. Sheldrick, S., Bruker AXS, Inc., WI, USA, 1997 *SHELXTL*.